

Synthesis and Characterization of Metal Complexes of Different Antibiotics and their Biological Activities

A Dissertation Submitted to University of Dhaka
for the Partial Fulfillment of the Requirements of
the Degree of Doctor of Philosophy (PhD)

Submitted by

Registration No. 139/2017-2018 and 12/2022-2023(Re-Reg.)



Department of Chemistry

Faculty of Science

University of Dhaka

Dhaka-1000

Bangladesh

May 2023

DECLARATION

Experiments described in this thesis were carried out by the author of this thesis in the Department of Chemistry, University of Dhaka and Centre for Advanced Research in Sciences (CARS), University of Dhaka, Dhaka-1000, Bangladesh.

This work has not been presented and will not be presented for any other degree.

Shuchismita Dey

PhD student

Department of Chemistry

University of Dhaka

Dhaka-1000

Bangladesh

SUPERVISORS' APPROVAL

This is to certify that the research work in this Thesis entitled “Synthesis and Characterization of Metal Complexes of Different Antibiotics and their Biological Activities” described by Shuchismita Dey, is an original work and has been carried out under our supervision in the Department of Chemistry, University of Dhaka and Centre for Advanced Research in Sciences (CARS), University of Dhaka, Dhaka-1000, Bangladesh for the degree of Doctor of Philosophy (PhD). No part of this thesis has previously been submitted to any University/Institute for any degree.

Dr. Md. Abdus Salam
Professor
Department of Chemistry
University of Dhaka
Dhaka 1000, Bangladesh.

Dr. Md. Zakir Sultan
Principal Scientist
Centre for Advanced Research in Sciences (CARS)
University of Dhaka
Dhaka 1000, Bangladesh.

Dedicated

to

My Parents,

My Husband

&

My Son

ACKNOWLEDGEMENTS

I am greatly indebted to my honorable supervisor **Prof. Dr. Md. Abdus Salam**, Department of Chemistry, University of Dhaka, for his excellent supervision, inspiring guidance, enthusiastic encouragement and affectionate surveillance throughout the execution of my research work.

I am highly pleased to express my best regards and sincere gratitude to respected co-supervisor **Dr. Md. Zakir Sultan**, Principal Scientist, Centre for Advanced Research and Sciences (CARS), University of Dhaka for his wise suggestions, helpful attitude, moral support, and advices throughout the completion of this work.

I wish to express my gratitude to **Prof. Dr. Md. Qamrul Ehsan**, Chairman, Department of Chemistry, University of Dhaka for his cooperation for the completion of the work.

I am also grateful to **Prof. Dr. Ishtiaque M. Syed**, Director, Centre for Advanced Research in Sciences (CARS), University of Dhaka for his kind support to conduct the research work.

I am most grateful to **Prof. Dr. Golam Mohammed Bhuiyan**, Director, Bose Centre for Advanced Study and Research in Natural Sciences for funding this work.

I sincerely express my gratitude to **Prof. Dr. Md Aftab Ali Shaikh**, Chairman of the Bangladesh Council of Scientific and Industrial Research for his cooperation in the analysis of my samples.

I am also indebted to my respected teachers of the Department of Chemistry, University of Dhaka namely **Prof. Dr. Azizur Rahman**, Ex-Chairman, **Prof. Dr. Tofayel Ahmed**, Ex-Chairman, **Prof. Dr. Md. Anwarul Islam**, Ex-Chairman, **Prof. Dr. Shahida Sultana**, Ex-Chairman, **Prof. Dr. Omar Ahmed**, **Prof Dr. Abu Bin Hasan Susan**, **Prof. Dr. Md. Ahsan Habib**, **Prof. Dr. Abdus Salam** for their valuable suggestions and kind support during this work.

I would like to thank the authority of Southeast University, Dhaka, Bangladesh for approving my study leave to pursue the Doctoral studies at Dhaka University, Bangladesh.

I am thankful to **Dr. Ishrat Jahan Bulbul** and the authority of Incepta Pharmaceuticals Ltd., Bangladesh for providing the working standard of different antibiotics to complete this research work.

I would like to thank the scientists, officers, and staff of CARS, Department of Chemistry, BCSIR and the Dept. of Mechanical Engineering, BUET for their support to carry out the research work as well as sample analyses.

Finally, I am indebted to my parents, my beloved husband **Prof. Dr. Arun Kanti Guha**, and my son **Divyendu Guha** for their moral support, suggestions, and patience during this study. My sincere gratitude is also to all the other family members and well-wishers for their encouragement.

Shuchismita Dey

CONTENTS

	Page
Contents	i-v
List of Figures	vi-x
List of Tables	xi-xiii
List of Schemes	xiv
Abstract	xv-xvii
<i>Chapter One: Introduction</i>	1-58
1.1. Antibiotics	2
1.1.1. History	3
1.1.2. Classification	8
1.1.3. Mechanism of action of antibiotics	9
1.1.4. Antibiotic resistance	11
1.1.4.1. Socio-economic impact of antibiotic resistance	15
1.1.4.2. Remedy and measures to be taken for antibiotic resistance	16
1.2. Metal Complexes	18
1.2.1. Chelation	20
1.2.2. Metal complexes with bioactivity	21
1.2.3. Complexation of antibiotics with metals leads to the development of new drugs with modified bioactivity	33
1.3. Selection of Antibiotics and Metals	35
1.3.1. Ceftibuten dihydrate	35
1.3.2. Cefpodoxime proxetil	37
1.3.3. Cefuroxime axetil	38
1.3.4. Gemifloxacin mesylate	41
1.3.5. Copper(II) and its significance in complexation	43
1.3.6. Nickel(II) and its significance in complexation	45
1.3.7. Silver(I) and its significance in complexation	46

1.4.	Objectives	47
1.5.	Literature Review	48
1.6.	Present Work	55
 Chapter Two: Materials and Methods		59 - 74
2.1.	Synthetic Route of Ceftributen Dihydrate with Cu(II), Ni(II) and Ag(I) Metal Ions	60
2.2.	Synthetic Route of Cefpodoxime Proxetil with Cu(II), Ni(II) and Ag(I) Metal Ions	62
2.3.	Synthetic Route of Cefuroxime Axetil with Cu(II), Ni(II) and Ag(I) Metal Ions	64
2.4.	Synthetic Route of Gemifloxacin Mesylate with Cu(II), Ni(II) and Ag(I) Metal Ions	66
2.5.	Characterization Methods	68
2.5.1.	Physical Properties	68
2.5.1.1	Color	68
2.5.1.2.	Physical state	68
2.5.1.3.	Melting point determination	69
2.5.1.4.	Solubility	69
2.5.2.	Spectroscopic Methods	69
2.5.1.1.	UV-Visible	69
2.5.2.2.	FT-IR	70
2.5.2.3.	¹ H NMR	70
2.5.3.	Thermal Analysis Method	71
2.5.3.1.	DSC	71
2.5.3.2.	TGA	72
2.5.3.3.	DTG	72
2.5.3.4.	DTA	72
2.5.4.	Elemental Analyzer	73
2.5.5.	Biological Activities	73
2.5.5.1.	Antibacterial Assay	74
2.5.5.2.	Antifungal Screening	74

Chapter Three: Results and Discussion	75 -179
3.1. Physical Properties of Ceftibuten Dihydrate with Cu(II), Ni(II) and Ag(I) Metal Ions	76
3.2. UV-Vis Spectrum Analysis of Ceftibuten Dihydrate with Ag(I) Metal Ions	77
3.3. FT-IR Studies of Ceftibuten Dihydrate with Cu(II), Ni(II) and Ag(I) Metal Ions	78
3.4. Thermal Analyses of Ceftibuten Dihydrate with Cu(II), Ni(II) and Ag(I) Metal Ions	85
3.5. Elemental Analyses of Ceftibuten Dihydrate with Cu(II), Ni(II) and Ag(I) Metal Ions	94
3.6. Proposed Structure of Ceftibuten Dihydrate with Cu(II), Ni(II) and Ag(I) Metal Ions	95
3.7. Biological Activities of Ceftibuten Dihydrate with Cu(II), Ni(II) and Ag(I) Metal Ions	95
3.8. Physical Properties of Cefpodoxime Proxetil with Cu(II), Ni(II) and Ag(I) Metal Ions	100
3.9. UV-Vis Spectra Analyses of Cefpodoxime Proxetil with Cu(II), Ni(II) and Ag(I) Metal Ions	101
3.10. FT-IR Studies of Cefpodoxime Proxetil with Cu(II), Ni(II) and Ag(I) Metal Ions	102
3.11. Interpretation of ¹H NMR Of Cefpodoxime Proxetil with Cu(II), Ni(II) and Ag(I) Metal Ions	108
3.12. Thermal Analyses of Cefpodoxime Proxetil with Cu(II), Ni(II) and Ag(I) Metal Ions	114
3.13. Elemental Analyses of Cefpodoxime Proxetil with Cu(II), Ni(II) and Ag(I) Metal Ions	122
3.14. Proposed Structure of Cefpodoxime Proxetil with Cu(II), Ni(II) and Ag(I) Metal Ions	123

3.15.	Biological Activities of Cefpodoxime Proxetil with Cu(II), Ni(II) and Ag(I) Metal Ions	124
3.16.	Physical Properties of Cefuroxime Axetil with Cu(II) and Ni(II) Metal Ions	128
3.17.	UV-Vis Spectra Analyses of Cefuroxime Axetil with Cu(II) and Ni(II) Metal Ions	129
3.18.	FT-IR Studies of Cefuroxime Axetil with Cu(II) and Ni(II) Metal Ions	131
3.19.	Interpretation of ¹H NMR of Cefuroxime Axetil with Cu(II) and Ni(II) Metal Ions	136
3.20.	Thermal Analyses of Cefuroxime Axetil Cu(II) and Ni(II) Metal Ions	140
3.21.	Elemental Analyses of Cefuroxime Axetil with Cu(II) and Ni(II) Metal Ions	145
3.22.	Proposed Structure of Cefuroxime Axetil with Cu(II) and Ni(II) Metal Ions	146
3.23.	Biological Activities of Cefuroxime Axetil with Cu(II) and Ni(II) Metal Ions	147
3.24.	Physical Properties of Gemifloxacin Mesylate with Cu(II), Ni(II) and Ag(I) Metal Ions	150
3.25.	UV-Vis Spectra Analyses of Gemifloxacin Mesylate with Cu(II), Ni(II) and Ag(I) Metal Ions	151
3.26.	FT-IR Studies of Gemifloxacin Mesylate with Cu(II), Ni(II) and Ag(I) Metal Ions	152
3.27.	Interpretation of ¹H NMR of Gemifloxacin Mesylate with Cu(II), Ni(II) and Ag(I) Metal Ions	163
3.28.	Thermal Analyses of Gemifloxacin Mesylate with Cu(II), Ni(II) and Ag(I) Metal Ions	167
3.29.	Elemental Analyses of Gemifloxacin Mesylate with Cu(II), Ni(II) and Ag(I) Metal Ions	175

3.30. Proposed Structure of Gemifloxacin Mesylate with Cu(II), Ni(II), and Ag(I) Metal Ions	176
3.31. Biological Activities of Gemifloxacin Mesylate with Cu(II), Ni(II) and Ag(I) Metal Ions	176
<i>Chapter Four: Conclusion</i>	180-183
References	184-205
List of Publications	206

List of Figures

Figure No.	Title	Page No.
1.1.	The Structure of Salvarsan	4
1.2.	Active metabolite of prontosil <i>in vivo</i>	5
1.3.	The general structure of Penicillin	6
1.4.	Mechanism of action of antibiotics <i>via</i> different target sites of antibacterial agent	10
1.5.	Mechanisms of antimicrobial resistance	12
1.6.	Graphical representation of antibacterial resistance	17
1.7.	Pictorial representation and chemical structure of hemoglobin and chlorophyll	19
1.8.	Structure of vitamin B ₁₂	20
1.9.	Approved and trialed analogs of anticancer drug, cisplatin	23
1.10.	Molecular mechanism of anticancer drug, cisplatin	24
1.11.	The general structure of Schiff base (Ligand)	26
1.12.	Chemical structure of some copper complexes of Schiff's bases Possessing anticancer activity	27
1.13.	Examples of chelating agents: Dithiocarbamate derivatives and quinolone derivatives. 8-OHQ, 8-hydroxyquinoline; CQ, Clio-quinol; PDTc, Pyrrolidine dithiocarbamate; DSF, disulfiram; DTC, diethyldithiocarbamate	28
1.14.	Chemical structure silver complexes of different ligands	30
1.15.	Mechanism of the antimicrobial activity of silver	30
1.16.	Structure of gold-based anticancer drug	31
1.17.	Tamoxifen and its ferrocene derivatives	34
1.18.	Chemical structure of paclitaxel and its ferrocene derivatives. (Type I and Type II)	34
1.19.	Sequential steps of working mechanism of β -lactam antibiotics	40

1.20.	Pictorial representation of the working mechanism of β -lactam antibiotics	40
1.21.	Sequential steps of the bactericidal activity of fluoroquinolone antibiotics	42
1.22.	Pictorial representation of the bactericidal activity of fluoroquinolone antibiotics	43
1.23.	Chemical structure of Ru(III) and In(III) complexes used as anti-cancer drugs	49
1.24.	Chemical structure of bivalent metal complexes of benzothiazole Schiff base	50
1.25.	Ag-complexation of sulfadiazine	51
1.26.	The chemical structure of Ag(I) and Au(III) complexes of moxifloxacin	52
1.27.	Chemical structure of the bismuth-norfloxacin complex	53
1.28.	Images of the working standard of four different antibiotics	56
2.1.	A set of equipment, used for the synthesis of antibiotic-metal complexes	60
3.1.	Images of parent antibiotic, antibiotic-metal complexes, and their solution	76
3.2.	UV-Vis spectra of ceftibuten dihydrate and its Ag(I)-complex	77
3.3.	FT-IR spectrum of the precursor antibiotic, ceftibuten dihydrate	79
3.4.	FT-IR spectrum of Cu(II)-complex of ceftibuten dihydrate	80
3.5.	FT-IR spectrum of Ni(II)-complex of ceftibuten dihydrate	81
3.6.	FT-IR spectrum of Ag(I)-complex of ceftibuten dihydrate	82
3.7.	Proposed structure of cephradine-metal complexes by Sultana <i>et al.</i>	85
3.8.	Thermogram (TG) of precursor antibiotic, ceftibuten dihydrate (CFT)	86
3.9.	Thermogram (TG) of Cu(II)-complex of ceftibuten dihydrate	86
3.10.	Thermogram (TG) of Ni(II)-complex of ceftibuten dihydrate	87
3.11.	Thermogram (DSC) of precursor antibiotic, ceftibuten dihydrate.	88

3.12.	Thermogram (DSC) of copper coordinated ceftibuten dehydrate antibiotic	89
3.13.	Thermogram (DSC) of nickel coordinated ceftibuten dihydrate antibiotic	89
3.14.	Thermogram (TG/DTG/DTA) of Ag-complex of ceftibuten dihydrate antibiotic	92
3.15.	Proposed structure of metal complexes of ceftibuten dihydrate	95
3.16.	Proposed structure of salicylidine-cephradine	97
3.17.	The antibacterial activity of CFT antibiotic and its metal complexes, signified by inhibition zone diameter	98
3.18.	Images of the metal complexes of CFP antibiotic and their solution in DMSO	100
3.19.	UV-Vis spectrum of cefpodoxime proxetil and its Cu(II)-complex	101
3.20.	FT-IR spectrum of the antibiotic, Cefpodoxime proxetil (CFP)	102
3.21.	FT-IR spectrum of Cu(II)-complex of precursor antibiotic cefpodoxime proxetil (CFP)	103
3.22.	FT-IR spectrum of Ni(II)-complex of precursor antibiotic cefpodoxime proxetil (CFP)	104
3.23.	FT-IR spectrum of Ag(I)-complex of precursor antibiotic cefpodoxime proxetil	105
3.24.	Structure of ceftiofur hydrochloride	107
3.25.	¹ H NMR spectrum of cefpodoxime proxetil (free ligand) antibiotic	108
3.26.	¹ H NMR spectrum of Cu(II)-complex of precursor antibiotic, cefpodoxime proxetil(CFP)	111
3.27.	¹ H NMR spectrum of Ni(II) complex of precursor antibiotic, cefpodoxime proxetil (CFP)	112
3.28.	¹ H NMR spectrum of Ag(I) complex of precursor antibiotic cefpodoxime proxetil (CFP)	113
3.29.	Thermogram (TG/DTG/DTA) of the precursor antibiotic, cefpodoxime proxetil (CFP)	115

3.30.	Thermogram (TG/DTG/DTA) of Cu(II)- complex of cefpodoxime proxetil	117
3.31.	Thermogram (TG/DTG/DTA) of Ni(II)- complex of cefpodoxime proxetil	118
3.32.	Thermogram (TG/DTG/DTA) of Ag(I)- complex of cefpodoxime proxetil	120
3.33.	Proposed structure of metal complexes of cefpodoxime proxetil (CFP)	124
3.34.	An agar plate showing antimicrobial activity signified <i>via</i> inhibition zone diameter	126
3.35.	Cefuroxime axetil (CFU) and its metal complexes	128
3.36.	Electronic spectrum of CFU antibiotic	129
3.37.	Electronic spectra of coordination complexes of CFU antibiotic	130
3.38.	FT-IR spectrum of the precursor antibiotic, cefuroxime axetil (CFU)	131
3.39.	FT-IR spectrum of Cu(II)-complex cefuroxime axetil (CFU) antibiotic	132
3.40.	FT-IR spectrum of Ni(II)- complex of the cefuroxime axetil antibiotic	134
3.41.	¹ H NMR spectrum of the parent antibiotic, cefuroxime axetil (CFU)	137
3.42.	¹ H NMR spectrum of Cu(II)-complex of cefuroxime axetil (CFU)	138
3.43.	¹ H NMR spectrum of Ni(II)-complex of cefuroxime axetil	139
3.44.	TG/DTG/DTA curves of Cu(II)-complex of cefuroxime axetil (CFU)	141
3.45.	TG/DTG/DTA curves of Ni(II)-complex of cefuroxime axetil (CFU)	143
3.46.	Proposed structure of metal complexes cefuroxime axetil antibiotic	147
3.47.	An agar plate showing the antibacterial activity of CFU antibiotic and its metal complexes	148
3.48.	Gemifloxacin mesylate and its Cu(II), Ni(II) and Ag(I) complexes	150
3.49.	Electronic (UV) spectra of parent antibiotic (gemifloxacin mesylate) and its metal complexes	151

3.50.	Foremost coordination mode of quinolone antibiotics	153
3.51.	Chemical structure of gemifloxacin mesylate	154
3.52.	The general structure of fluoroquinolone ligand binding to the metal ions in (a) 1:1 and (b) 1:2 (metal: ligand) molar ratio	155
3.53.	Proposed structure of lomefloxacin metal complexes	155
3.54.	Proposed structure of norfloxacin metal complexes	156
3.55.	Proposed structure of metal complexes of gatifloxacin	156
3.56.	FT-IR spectrum of the precursor antibiotic, gemifloxacin mesylate	158
3.57.	FT-IR spectrum of Cu(II)-complex of gemifloxacin mesylate	159
3.58.	FT-IR spectrum of Ni(II)-complex of gemifloxacin mesylate	159
3.59.	FT-IR spectrum of Ag(I)-complex of gemifloxacin mesylate	160
3.60.	¹ H NMR spectrum of precursor antibiotic, gemifloxacin mesylate	163
3.61.	¹ H NMR spectrum of Cu(II)-complex of gemifloxacin mesylate	165
3.62.	¹ H NMR spectrum of Ni(II)-complex of gemifloxacin mesylate	166
3.63.	¹ H NMR spectrum of Ag(I)-complex of gemifloxacin mesylate	167
3.64.	TG/DTG/DTA curve of the precursor antibiotic, gemifloxacin mesylate (GMX)	168
3.65.	TG/DTG/DTA curves of Cu(II)-complex of gemifloxacin mesylate	170
3.66.	TG/DTG/DTA curves of Ni(II)-complex of gemifloxacin mesylate	171
3.67.	TG/DTG/DTA curves of Ag(I)-complex of gemifloxacin mesylate	172
3.68.	The proposed structure of gemifloxacin-metal complexes	176
3.69.	A representative agar plate showing the activity of gemifloxacin mesylate and its metal complexes	178

List of Tables

Table No.	Title	Page No.
1.1.	Classification of antibiotics based on mechanism of action	11
1.2.	Examples of some phytobiotics derived from herbs, spices, and aromatic plants	15
1.3.	A brief summary of clinically approved Pt(II)-based anticancer drugs.	23
1.4.	Antimicrobial activity of metal complexes of different antibiotics	32
1.5.	Clinical development of quinolone antibiotics with time	41
3.1.	Physical properties of the parent antibiotic (CFT) and its metal complexes	76
3.2.	UV-Vis spectral data of ceftibuten dihydrate and its Ag(I) complex	78
3.3.	Characteristic vibrational frequencies (cm^{-1}) of CFT antibiotic and antibiotic metal complexes	84
3.4.	TG-DSC results of CFT antibiotic and its metal(II)-coordinated complexes	91
3.5.	Thermal (TGA, DTG, and DTA) results of Ag(I) complex of ceftibuten dihydrate antibiotic	93
3.6.	Elemental analysis (C, H, N, and S) data of metal complexes of ceftibuten dihydrate	94
3.7.	Antibacterial activity of precursor antibiotic, ceftibuten dihydrate and its metal complexes	98
3.8.	Physical properties of the parent antibiotic (CFP) and its metal complexes	100
3.9.	UV-Vis spectral data of cefpodoxime proxetil and its Cu(II) complex	101
3.10.	Characteristic FT-IR bands in cm^{-1} of Cu(II), Ni(II), and Ag(I)-CFP-complexes	106
3.11.	Assignments of ^1H NMR bands of cefpodoxime proxetil (CFP) in DMSO-d_6	109
3.12.	Assignments of characteristic ^1H NMR bands of Cu(II)-CFP in comparison to CFP (parent	111

	antibiotic)	
3.13.	Assignments of characteristic ^1H NMR bands of Ni(II)-CFP in comparison to CFP (Parent antibiotic)	112
3.14.	Assignments of ^1H NMR bands of Ag(I)-CFP in comparison to CFP (Parent antibiotic)	113
3.15.	Thermal (TG/DTG/DTA) results of parent antibiotic, cefpodoxime proxetil (CFP)	116
3.16.	Thermal (TG/DTG/DTA) results of Cu(II) and Ag(I)-complexes of cefpodoxime proxetil (CFP)	121
3.17.	Elemental analysis data of the metal complexes of cefpodoxime proxetil (CFP).	122
3.18.	Bactericidal activities of CFP antibiotic and its metal complexes, represented as inhibition zone diameter values/mm	126
3.19.	Physical properties of the parent antibiotic (CFU) and its metal complexes.	128
3.20.	UV-Vis spectral data of cefuroxime axetil along with its complexes	130
3.21.	Characteristic vibrational frequencies (cm^{-1}) of CFU antibiotic and its metal complexes	135
3.22.	Assignments of ^1H NMR bands of CFU antibiotic and its metal complexes	140
3.23.	Thermo-analytical (TGA, DTG, and DTA) results of Cu(II) complex of cefuroxime axetil	144
3.24.	Thermo-analytical (TGA, DTG, and DTA) results of Ni(II) complex of cefuroxime axetil	145
3.25.	Elemental analyses data of metal complexes of cefuroxime axetil (CFU).	146
3.26.	The antimicrobial activities of the CFU antibiotic and its Cu-complex, represented as inhibition zone diameter values/mm	149
3.27.	Physical properties of the parent antibiotic (GMX) and its metal complexes.	150
3.28.	UV-Vis spectral data of gemifloxacin mesylate and its complexes	152

3.29.	Main vibrational frequencies (cm^{-1}) of gemifloxacin mesylate (GMX) and its metal complexes	161
3.30.	Significant ^1H NMR signals of gemifloxacin mesylate (GMX) in DMSO-d_6	164
3.31.	Thermo-analytical results of the precursor antibiotic, gemifloxacin mesylate (GMX)	169
3.32.	Thermo-analytical (TG/DTG/DTA) results of metal complexes of gemifloxacin mesylate (GMX)	174
3.33.	Elemental analyses (C, H, N, S) data of the newly synthesized metal complexes	175
3.34.	The antimicrobial activity of gemifloxacin mesylate (GMX) and its metal complexes, represented as inhibition zone diameter values/mm	179

List of Schemes

Scheme No.	Caption	Page No.
1.1	The timeline of antibiotic development. The name of the different antibiotics and the year they were discovered are shown on the timeline	8
1.2	Classification of antibiotics	9
2.1	Reaction route to prepare ceftibuten-metal complexes	61
2.2	Synthetic route of metal complexes of cefpodoxime proxetil	63
2.3	Synthetic scheme of metal complexation of cefuroxime axetil	65
2.5	Synthetic route to prepare complexes of Gemifloxacin mesylate	67
3.1	Different options for coordination of carboxylate group	161

Abstract

Antibiotics are the most important invention in the field of medicine which is crucial in fighting against infectious diseases. Metal complexes also known as coordination complexes contain a central metal atom or ion around which ligands bearing neutral or negative charge have bonded. Metal coordination compounds of antibiotics with improved bioactivity can play a vital role in searching for new antibiotics to combat drug-resistant life-threatening infectious bacteria. In this work, the complexations of four different antibiotics with biologically important metals Cu, Ni, and Ag were done. The antibiotics were ceftibuten dihydrate (CFT), cefpodoxime proxetil (CFP), cefuroxime axetil (CFU), and gemifloxacin mesylate (GMX). The physical properties of all the newly prepared metal complexes were studied. Different types of spectroscopic methods (UV-Vis, FT-IR, and NMR), elemental analysis as well as diverse thermo-analytical techniques (TG, DTG, DTA, and DSC) were used to characterize the synthesized metal complexes. Paper disc diffusion assay was used for *in vitro* antimicrobial study of the antibiotic ligands and their metal complexes. In FT-IR spectra of all the metal complexes of CFT, a separation value of the carboxylate group frequency, $\Delta\nu > 200 \text{ cm}^{-1}$ was found. Also, significant changes in the frequencies of the 3^o nitrogen atom of the *beta*-lactam ring as well as a broad band in the range of 3200 – 3600 cm^{-1} were observed. The obtained FT-IR data suggested that metal ions were involved in coordination through carboxylate oxygen, the *beta*-lactam ring nitrogen atom of CFT antibiotic and water molecule. The different degradation patterns in the TG curve of the metal complexes from the precursor antibiotic were also supportive of the characterization of new metal complexes. On the other hand, CFP antibiotic acts as a tridentate ligand where the β -lactam carbonyl group, 2^o amide carbonyl group, and 1^o amine group are involved in the metal-coordination process. FT-IR study of CFP antibiotic and its metal complexes

revealed the shifting of frequency of the β -lactam carbonyl group and appearing of new absorption bands in the range $575\text{-}605\text{ cm}^{-1}$ and $430\text{-}480\text{ cm}^{-1}$ which are due to the formation of new metal-oxygen and metal-nitrogen bonds. Significant changes in the chemical shift value of characteristic proton ($-\text{NH}_2$ and $-\text{NH}-$) which are directly involved in coordination as well as the protons nearer to the binding site also occurred due to complexation. A broad band in the frequency range $3200\text{-}3600\text{ cm}^{-1}$ in IR spectra and a weight loss of around 7% at the temperature of $150\text{ }^\circ\text{C}$ in TG curves of the metal complexes are indicative of coordinated water in the metal complexes. The CFU antibiotic also formed metal complexes through the participation of the oxygen atom of the β -lactam ($\text{C}=\text{O}$) group and the oxygen atom of the amide group. All analytical results including physical properties, FT-IR data, ^1H NMR data, thermo-analytical results, and also EA data confirmed the successful interaction of metal ions to ligand antibiotics. GMX is a quinolone-type antibiotic. Like other quinolones, it interacts with metal ions through the carboxyl group and carbonyl group of the nearest position. The absence of carboxyl stretching frequency (1714 cm^{-1}) and the presence of two new bands in IR spectra of the GMX-metal complexes indicated the participation of the $-\text{COOH}$ group in complexation with the metal ions. Moreover, the absence of a signal of proton at 11.0 ppm in the ^1H NMR spectrum of the complexes suggested the nonparticipation of $-\text{COOH}$ group in the coordination process. The antibiotic-metal complexes were found to be thermally more stable than the precursor antibiotic. The EA data also give evidence for the formation of new metal complexes with 1:2 metal-to-ligand stoichiometries. The bactericidal activity of antibiotics may increase upon chelation with metal ions. This is due to the increased lipo-solubility of the metal complexes as compared to ligands. In this work, a total of 12 bacterial strains and two fungal strains were used for biological study. Among all the newly synthesized metal complexes, the Ag(I)-CFT , Ag(I)-GMX , Cu(II)-CFT and Cu(II)-CFU complexes showed excellent and

enhanced activity compared to the precursor antibiotic against most of the microbes. The Ag(I)-CFP and Ni(II)-CFP complexes show similar but significant activity as the parent CFP antibiotic against most of the microbes. However, Ag(I)-CFP showed increased activity against *Styphylococcus aureus* and *Enterobacter faecium*, and a decreased activity was observed by Cu(II)-CFP complex. The Cu(II)-CFT complex was found to be 15 times more active against *S. aureus* and 1.6 times more active against *S. typhi*. On the contrary, an enhanced activity against *Candida sp.* and *E. coli 0157* was observed by Cu(II)-GMX and Ni(II)- GMX, respectively.

Chapter One

Introduction

1.1. Antibiotics

Antibiotics are chemical compounds that can kill bacteria or inhibit the growth of bacteria. They may be either bactericidal or bacteriostatic. Compounds that kill bacteria are bactericidal and compounds that obstruct the growth of bacteria are bacteriostatic. Originally antibiotics were called antibiosis that means 'against life' which was introduced by a French bacteriologist named Vulleimin. Later on, they were renamed antibiotics by Salman Wakeman, an American microbiologist [1, 2]. Formerly, antibiotics were produced from living organisms and defeated other microorganisms. Most of the antibiotics were produced from soil microbes. Soils are home to a huge variation and various inhabitants of microbes. Soil microbes were the principal source of producing antibiotics and still linger to hold their importance. Several classes of antibiotics such as beta-lactams, aminoglycosides, tetracyclines, macrolides, and streptomycin are produced from soil bacteria and fungi [3, 4]. Industrially, fermentation is the process that is used to produce antibiotics. Oceans are another largest source of microbes and microbial metabolites. But recently (last 15-20 years) marine biosphere was investigated in search of new compounds from marine organisms and around 30,000 compounds of the new interesting structures have been isolated. So, the ocean is a promising source of antibiotic research [5]. Antibiotics are widely used to prevent bacterial infections in humans, plants, and animals either by killing or preventing them from reproducing. Antibiotics can be taken in several ways. They

can be taken either orally (pills, capsules) or topically (cream, ointment) and intravenously. Three forms of antibiotics are available, natural (aminoglycosides), synthetic (quinolones), and semi-synthetic (cephalosporins).

1.1.1. History

More than 2500 years ago, ancient civilizations including the Chinese, Egyptians, and Greeks used molds, and plant extracts to treat several infections. But the mechanism of action was unknown then [6].

Salvarsan (1909) was the first man-made antibiotic prepared by Alfred Berthem in Paul Ehrlich's lab. Paul Ehrlich was a medical student and had the passion to invent new drugs for the treatment of diseases that causes death. That's why he constituted a team including chemist Alfred Berthem and bacteriologist Sahachiro Hata and took initiatives for the treatment of syphilis, an incurable disease with the hope to get a magic drug that kills microbes responsible for disease without maltreatment of human host. To serve this purpose, Ehrlich selected an organic compound containing arsenic as a starting material and prepared a series of the related organo-arsenic compound with the help of chemist Alfred Bertram. Finally, Sahachiro Hata (1909), a bacteriologist noticed that salvarsan (compound 606) was the best one for curing syphilis [7,8]. In 1910, it was marketed by a German chemical company named Hoechst. Neosalvarsan (compound 914), a modified form of salvarsan was then introduced to minimize the side effects as well as reduce toxicity. Salvarsan was the most effective, widely prescribed drug

for curing syphilis before the marketing of the natural antibiotic penicillin (1943). The working mechanism of salvarsan is yet unknown and recently Nicholson *et al.* [9] reported that salvarsan is truly a combination of two cyclic As-As bonded species depicted in Figure 1.1.

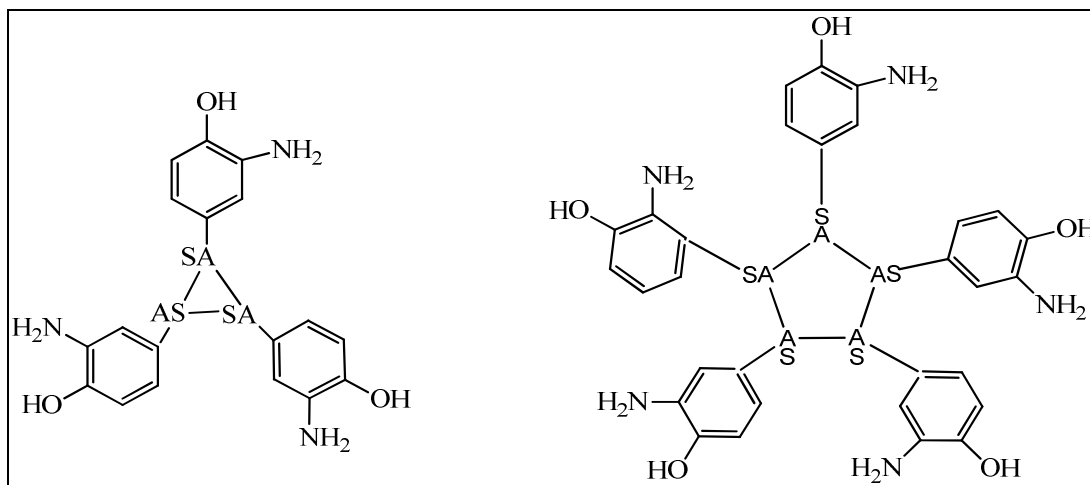


Figure 1.1. The structure of Salvarsan.

As an extension of the Ehrlich concept, in 1932, Domagk *et al.* studied a large No. of azo dyes and found *in vitro* antibacterial activity of an azo dye named prontosil. It was found to be the first successful drug and the first of many sulpha drugs to treat the bacterial infection causing blood poisoning. Prontosil acts as an antibacterial agent belonging to the sulphonamide group which opened a new door in medicine at that time [10].

Later on, prontosil has been replaced by other sulpha-drugs like sulfathiazole, sulfadiazine, etc. Prontosil was found to be metabolized into the active ingredient sulphanilamide *in vivo* as shown in Figure 1.2.

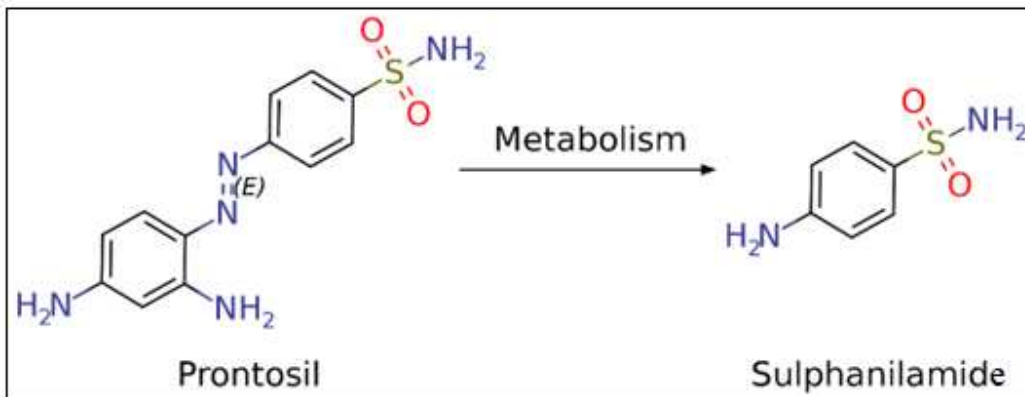


Figure 1.2. Active metabolite of prontosil-*in vivo*.

Sulfa drugs were found to have limited use after the invention of natural antibiotic penicillin in 1942. Alexander Fleming, a Scottish scientist was the first who accidentally discovered penicillin in 1928. However, the isolation of penicillin in pure form is a very difficult task and it needs around 14 years for purification as well as successful clinical use [11]. In 1939, at Oxford University, Howard Florey along with his co-workers Norman Heatley and Ernst Chain successfully purified penicillin, work out for industrial production, and used it clinically. They published their findings in 1940 [12]. Alexander Fleming, Ernst Chain, and Howard Florey together received the Nobel Prize in Medicine for their

contribution to the invention of penicillin in 1945. Dorothy Hodgkin, an English chemist confirmed the chemical structure of penicillin (Figure 1.3) by using X-ray crystallography and received a Nobel prize in chemistry (1964) along with other contributions in Chemistry.

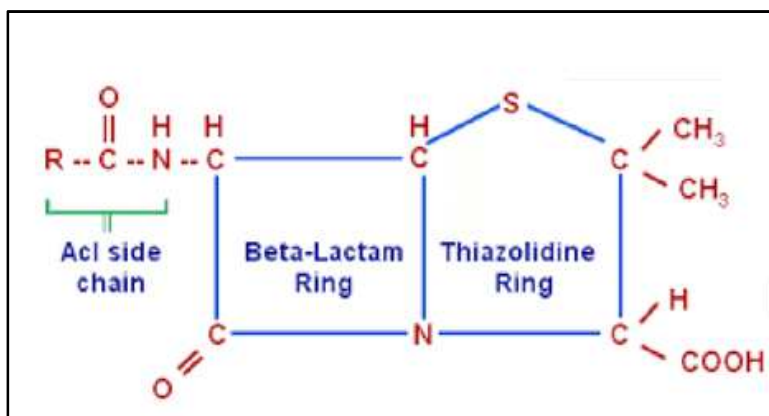


Figure 1.3. The general structure of penicillin.

There is a thiazolidine ring close to a β -lactam ring in penicillin and the β -lactam ring is responsible for its bacterial action. Penicillin was found to be effective against two pathogens *staphylococci* and *streptococci*. After that, penicillin was successfully synthesized in the laboratory by a chemist named John C. Sheehan at MIT, USA in 1957 [13]. Because of the narrow spectrum activity of natural penicillin (penicillin G), researchers developed many derivatives of penicillin with broad-spectrum activity [14]. The period from 1940-1950 was marked as a golden time of antibiotic discovery. More than 15 antibiotics that were discovered

at that time are clinically used even today. Selman Waksman, a microbiologist and biochemist had a lot of contributions in the field of discovery of antibiotics [15]. He, along with his co-workers discovered a number of antibiotics from soil microbes including streptomycin and neomycin which are effective against tuberculosis, caused by Gram-negative bacterial strains. Since 1970, the discovery rate of new antibiotics has declined. Before the discovery of antibiotics, thousands and millions of lives had been lost due to several types of bacterial infections. So, the invention of antibiotics opened a new era in medicine and increased the lifespan of a human being by 23 years [16]. The development of antibiotics with time is presented in **Scheme 1.1**. The time period (1950-1970) was regarded as the golden age of antibiotic discovery. Almost half of the discovered antibiotics were invented at that time period. Unfortunately, the last antibiotic was marketed in 1987. But there are a few antibiotics in the pipeline for clinical use [16]. Moreover, antibiotic resistance has occurred and many common antibiotics are ineffective against microbial infection. Currently, available antibiotics could not effective against a long range of pathogens. So, this is the time to develop more potent drugs with improved bio-activity.

And a major investment is indeed essential to combat the increasing trend of drug-resistant infectious diseases.

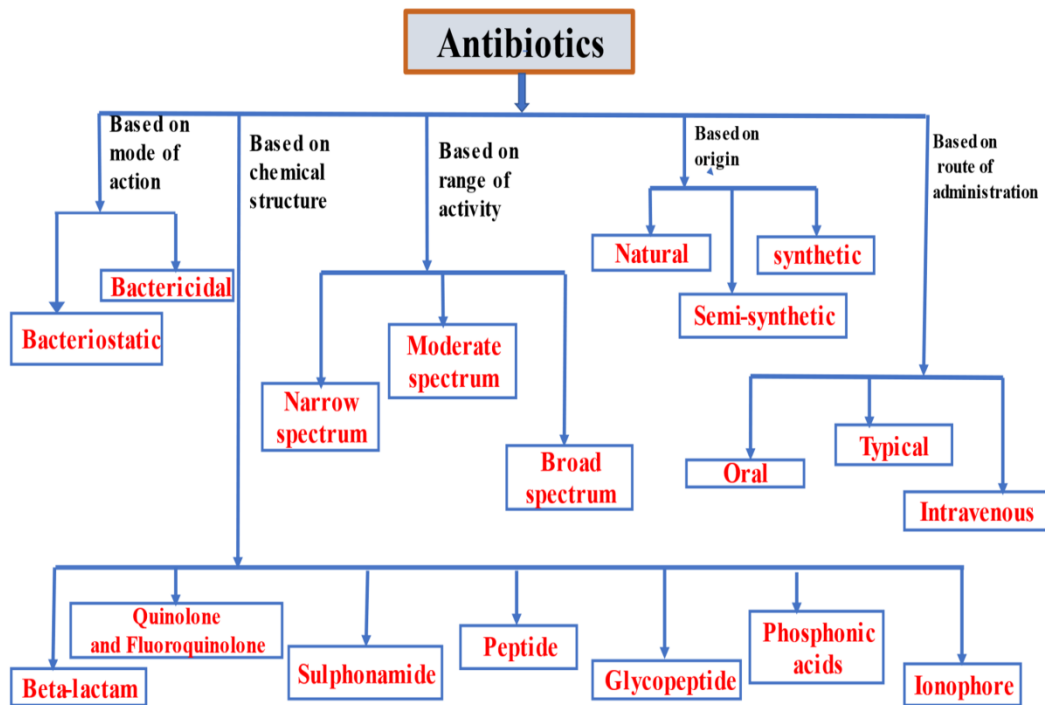
Before 1930	1930-1939	1940-1949	1950-1959	1960-1969	
Penicillin discovered (1928)	Sulfonamides discovered (1932) Gramicidin discovered (1939)	Penicillin introduced (1942) Streptomycin discovered (1943) Bacitracin discovered (1943) Cephalosporins discovered (1945) Chloramphenicol discovered (1947) Chlortetracycline discovered (1947) Neomycin discovered (1949)	Oxytetracycline discovered (1950) Erythromycin discovered (1952) vancomycin discovered (1956) Kanamycin discovered (1957)	Methicillin introduced (1960) Ampicillin introduced (1961) Spectinomycin reported (1961) Gentamicin discovered (1963) Cephalosporins introduced (1964) Vancomycin introduced (1964) Doxycycline introduced (1966) Clindamycin reported (1967)	
	Rifampicin introduced (1971) Tobramycin discovered (1971) Cephameycins discovered (1972) Minocycline introduced (1972) Cotrimoxazole introduced (1974) Amikacin introduced (1976)		Azithromycin introduced (1993) Quinupristin/dalfopristin introduced (1999)		
		Amoxicillin-clavulanate introduced (1984) Imipenem/cilastin introduced (1987) Ciprofloxacin introduced (1987)		Linezolid introduced (2000) Cefditoren introduced (2002) Daptomycin introduced (2003) Telithromycin introduced (2004) Tigecycline introduced (2005)	

Scheme 1.1. The timeline of antibiotic development. The name of the different antibiotics and the year they were discovered are shown on the timeline. (Adopted from cvm.msu.edu, 2011) [17, 18].

1.1.2. Classification

There are several ways to classify antibiotics, which are depicted in the following

Scheme 1.2 [2, 19].



Scheme 1.2. Classification of antibiotics.

1.1.3. Mechanism of action of antibiotics.

Antibiotics also be of different types depending on the diverse working mechanisms, i.e., how do antibiotics work against microbes?

Antibiotics work against microbes *via* different modes of action including cell wall synthesis inhibition, protein synthesis inhibition, and interference with nucleic acid synthesis. Sometimes antibiotics show antimetabolite activity by preventing the formation of folic acid and also act as cell membrane inhibitors

[20, 21]. The molecular target sites of antibacterial agents are presented in Figure 1.4.

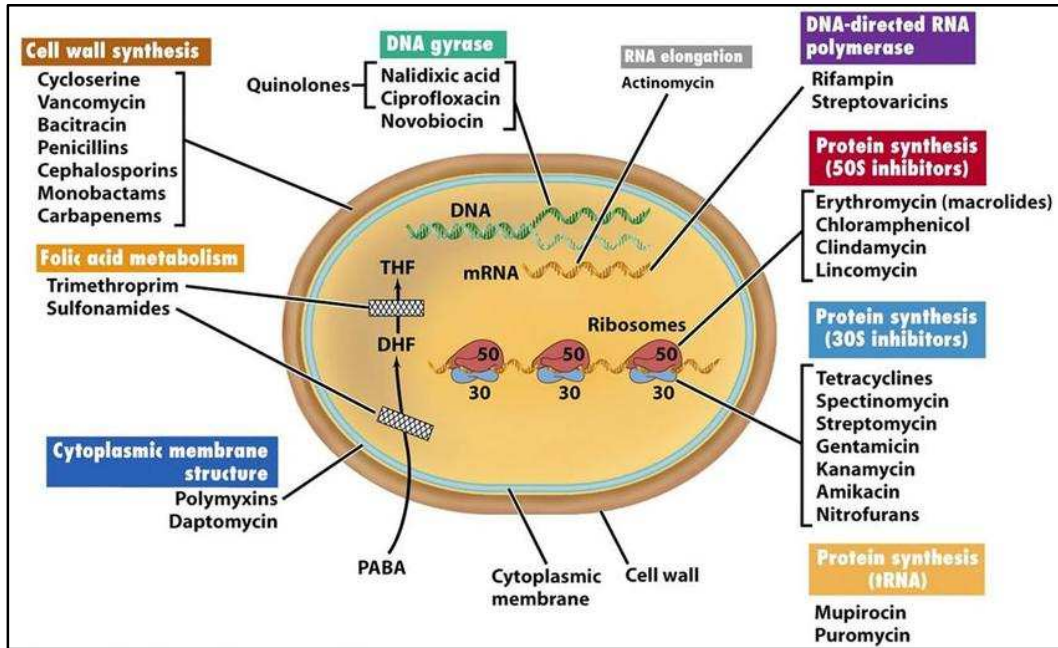


Figure 1.4. Mechanism of action of antibiotics *via* different target sites of antibacterial agent (Adopted from the literature [22]).

There are different types of antibiotics according to different modes of action which are listed in Table 1.1.

Table 1.1. Classification of antibiotics based on mechanism of action.

Mechanism of action	Type	Antibiotics
Blocking of cell wall synthesis	Bactericidal	β -lactam antibiotics Penicillin derivatives Cephalosporin derivatives
Blocking of protein synthesis		
30 S ribosome site	Bacteriostatic	Tetracyclinederivatives Aminoglycosides
50 S ribosome site	Bactericidal	Macrolides, Chloramphenicol
Blocking of nucleic acid synthesis		
DNA	Bactericidal	Quinolones, Fluoroquinolones
RNA	Bactericidal	Bacitracin
Antimetabolite		Sulphonamides

1.1.4. Antibiotic resistance

The principle of antimicrobial therapy is that one living microorganism kills another microbe without doing any harm to the host. Alexander Fleming and Paul Domagk in their Nobel Lecture first warned about antibiotic resistance, which may cause serious public health threats globally. Actually, it has occurred when an antibacterial agent failed to defeat the microorganism for which the drug is

prescribed. As a result, in the presence of an antibacterial agent, the drug-resistant bacteria are not killed and undergo replication continuously. Actually, the germs themselves adapt some defense strategy against antibiotics. The resistance mechanism by which germs survive includes modification of the drug target, inactivation of the drug through producing enzymes, replacement of the drug target, and reducing the cell permeability [23]. Formation of bio-film is another way of causing antibiotic resistance. In that case, the antibiotics themselves could not reach the target microorganisms within the biofilm and causing antibiotic resistance against those microorganisms [24].

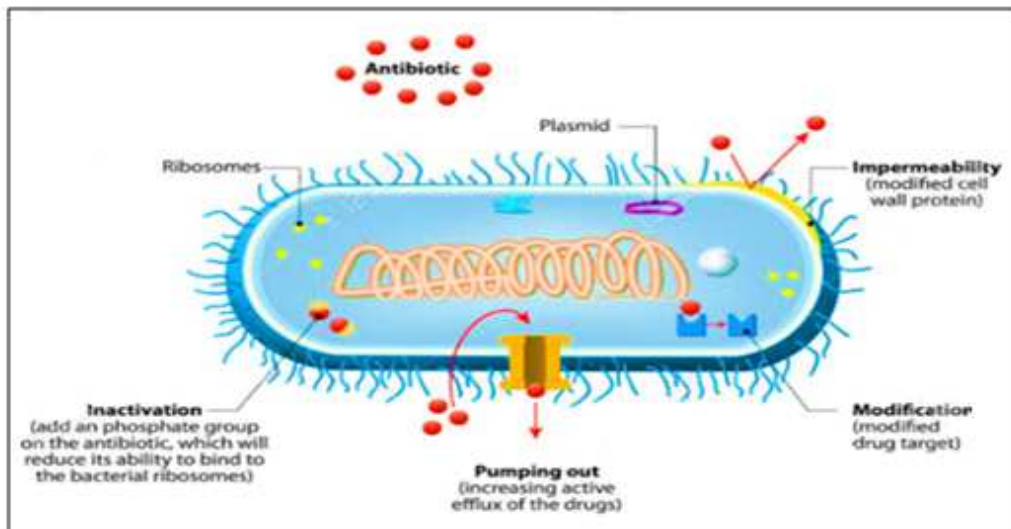













Figure 1.5. Mechanisms of antimicrobial resistance (Adopted from literature [22]).

Resistant infections are very dangerous and sometimes impossible to treat and create serious public health problems. In recent statics, it was found that around

7,00,000 people died worldwide in each year due to antibiotic resistance and it will be 10,00,000 by 2050 [WHO report]. Issues responsible for spreading antibiotic resistance include overuse of many common antibiotics by both human and animals, improper prescribing of antimicrobial drugs by physicians because of low cost and low toxicity, misuse of broad-spectrum antibiotics that is unnecessary. Self-treatment practice is another major issue of causing antibiotic resistance especially in low-income countries. As a result, the antibiotics are found to be ineffective for the organisms causing infections [25]. Besides, treatment against bacterial infection, antibiotics can also be used in non-therapeutic purposes in agricultural production as growth promoters since 1950 [26]. The introduction of antibiotics as a feed additive in animal feed and plant increases the rate of growth and decrease morbidity and mortality by preventing and controlling bacterial diseases in animals and plant [27]. The efficacy of growth is occurred due to the interaction of antibiotics with intestinal microbes present in animals. There is no doubt about the use of antibiotics as a growth promotor is the money-making and efficient production of livestock. The excessive use of antibiotics in animal feed may develop antimicrobial resistant organisms [28]. But there raised a problem, the transfer of a drug-resistant gene from animals to humans *via* the food chain. Today, the problem of antibiotic - resistant is a serious threat to public health worldwide. The World Health Organization (WHO) has made several reports on risk assessment of using

antibiotics as growth promoters in livestock [29-36]. After that many developed countries banned the use of most antibiotics as food additives and permitted fewer antibiotics in animal feed [37]. To overcome the resistance issue, many scientists worked on safer alternative approaches to replace antibiotics as food additives. Sandra *et al.* (2015) introduced the use of herbs, spices and plant extracts with promising biological properties known as phytobiotics, as potential feed additives [37, 38]. In fact, phytobiotics are products of plant origin which are added in animal feed to increase the performance of animal health and nutrition. Examples of some phytobiotics used as an alternative of antibiotic growth promoters in animal nutrition are listed in Table 1.2. Phytobiotics include non-woody flowering plants having medicinal properties, spices and essential oils extracted from different parts (flower, leaves, root, seed) of plant materials, used as natural growth promoters (NGPs) for poultry production. Phytobiotics can improve the growth and performance of animal health through improving digestion, nutrient assimilation and stimulating the immune response [39]. Day by day, the use of phytobiotics as feed additives in poultry production gain popularity due to increasing bacterial resistance [40]. Thus, phytobiotics could serve as better replacement of synthetic antibiotic growth promoter to enhance the production and health performance of poultry regarding food security [41].

Table 1.2. Example of some phytoadditives derived from herbs, spices and aromatic plants (Adopted from literature [42]).

	Phytoadditive		Major Component and Potency
	Gedi (<i>Abelmoschus manihot</i> L. Medik) leaves	Parts of plant (leaves)	flavonoid, phenolic compound, antioxidant activity
	Lemon basil (<i>Ocimum x citriodorum</i>) leaves		caffeic acid, flavonoid, antioxidant and antimicrobial activity
	Leilem (<i>Clerodendrum minahassae</i> L.) leaves		flavonoid, phenolic compound, antioxidant activity
	Bitter leaves (<i>Vernonia amygdalina</i>)		flavonoid, phenolic compound, antioxidant activity
	Cucumber (<i>Cucumis sativus</i>) seeds	Parts of plant (seeds)	lipid lowering, antioxidant activity
	Pumpkin (<i>Cucurbita moschata</i>) seeds		phenolic compound, antioxidant activity
	Cinnamon (<i>Cinnamomum verum</i>)		Cinnamic acid and cinnamaldehyde, antioxidant activity
	Nutmeg (<i>Myristica fragrans</i>)	Spices	Essential oils
	Candlenut (<i>Aleurites moluccanus</i>)		polyphenols content
	Celery (<i>Apium graveolens</i>)	Aromatic plants	natural antioxidants (especially vitamins, flavonoids, and unsaturated fatty acids)
	Lemongrass (<i>Cymbopogon citratus</i>)		antioxidant activity

1.1.4.1. Socio-economic impact of antibiotic resistance

The discovery of antibiotic in the 20th century played an important role in the field of modern medicine and various infections could be easily handled at that time which saved thousand and millions of human lives [43]. Antibiotics are also used in the agricultural sector and livestock production as growth promoters [26]. Today antibiotic resistance is a global crisis rather than a national one. Though the crisis occurs naturally, misuse and widespread use of antibiotics catalyze the

crisis. As a result, post-surgical infections even common infections are difficult to treat and sometimes impossible which increases the mortality rate and decreases working skills. Around two million infections and 30,000 deaths occur each year only in the USA due to resistant bacterial species [44]. Healthcare cost also increases due to long time hospital stays that cause a negative impact on the economy. The high cost of healthcare leads to poverty and material deprivation. Ultimately it influences a country's GDP and affects the global economy. The populations of underdeveloped and developing countries face the problem the most [45]. Like other developing countries in Bangladesh, the scenario of AMR is simply frustrating [46]. It may perhaps act as a 'silent epidemic' throughout the world [47].

1.1.4.2. Remedy and measures to be taken for antibiotic resistance

Antibiotic resistance is a threat to human health, food production, and development. Today it's a great challenge for us to mitigate the drug-resistant issue. The public and non-public sectors must have to be involved to prevent and control the spread of infections caused by drug-resistant bacteria. The following measures can be taken to challenge the threat.

- Natural products have a long history to treat infections [48]. Increase the dependency on natural products like ginger, garlic, and tulsi with active ingredients.

- Proper sanitization habit is mandatory.
- Development of new antibiotics with improved bioactivity is an urgent need. But it's not an easy task. It needs time and money. Chemical modification of common antibiotics with unique properties can serve as a better alternative.
- Always depends on the advice of a health professional not self-medication.
- Always complete a full course of antibiotics and do not take any antibiotics if not urgent.

Finally, public awareness can lower the risk of spreading antibiotic resistance.

As a whole, antibiotic resistance: - causes, socio-economic impact, and strategies to overcome the issue could be summarized in Figure 1.6 [49].

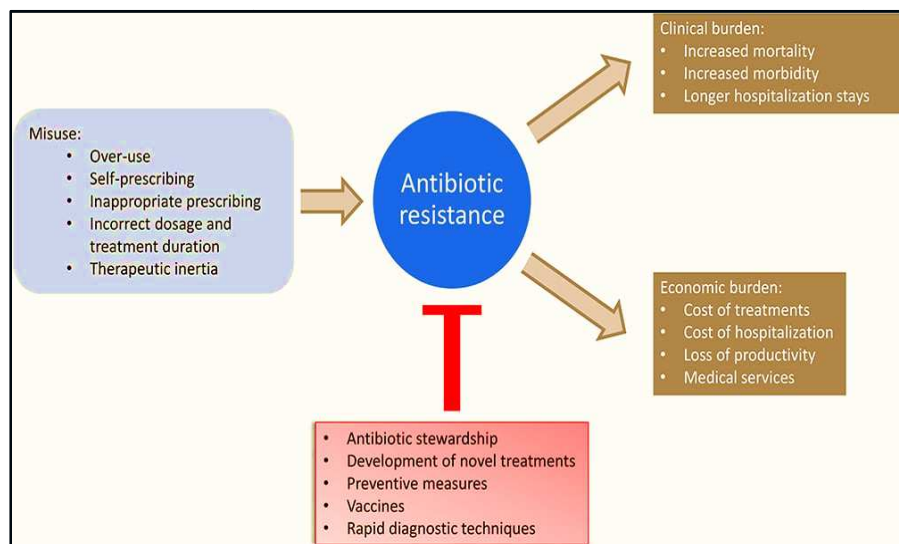


Figure 1.6. Graphical representation of antibiotic resistance.

1.2. Metal Complexes

The concept of modern coordination chemistry was first introduced by Alfred Werner who was an inorganic chemist, received the Nobel Prize in chemistry in 1913 for proposing the correct structure of a transition metal complex [50].

Metal complexes also known as coordination complexes contain a central metal atom or ion around which neutral or negatively charged species known as ligands have bonded. They may be neutral or charged complex. In metal complexes, the interaction of ligand to metal ion occurred through the formation of a dative bond which is a Lewis acid-base type interaction. Usually, metal ions with vacant valence shell orbitals can act as Lewis acids and accept electron pairs from ligands, and form dative bonds. Many coordination compounds are found to play crucial role in living systems. For example, hemoglobin is an iron complex found in the RBC of living cells and acts as an oxygen carrier from respiratory organs to the rest of the human body. On the other hand, chlorophyll is also a magnesium complex found in green plants and involves in photosynthesis. Hemoglobin and chlorophyll both have remarkably similar chemical structures (Figure 1.7 and Figure 1.8). Vitamin B₁₂ is another coordination complex of cobalt surrounded by corrin ligands. Apart from these, many naturally occurring enzymes like catalase and carboxypeptidase are metal complexes that regulate many biological processes of the human body.

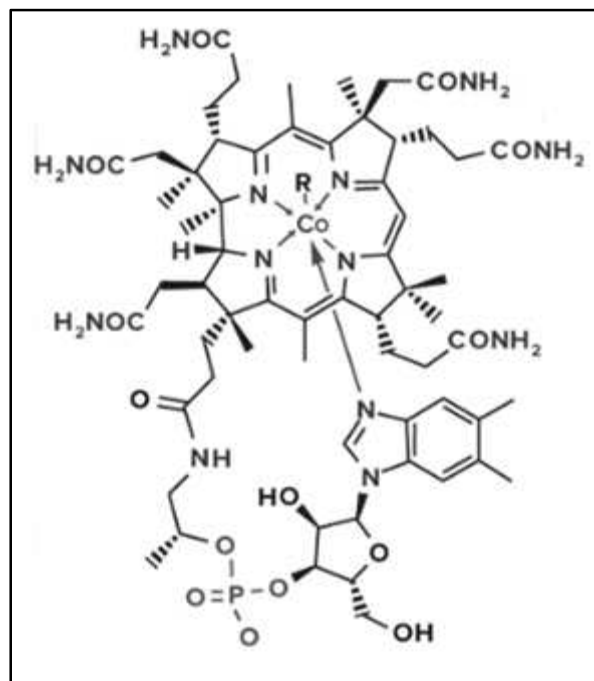


Figure 1.8. Chemical structure of vitamin B₁₂.

1.2.1. Chelation

Chelation is a process by which a metal complex is formed between a central metal ion and polydentate ligands where the ligand donor atoms are attached to the central metal ion *via* dative bond formation. Usually, the ligands are organic moieties containing more than one donor atom, known as a chelate. Chelating agents have a variety of applications in medicine. Chelate compounds are more stable than non-chelate compounds.

1.2.2. Metal complexes with bioactivity

The recent progress of metal complexes in the field of pharmaceutical chemistry is emerging. Almost all metal ions form complexes (coordination compounds). Metals especially transition metals possess several oxidation states and different types and numbers of coordinated ligands are involved in complexation resulting in different coordinative geometry after complexation which in turn provides a variety of properties. These properties make them interesting and useful for the medicament of various deadly infectious diseases like diabetes, carcinomas, cardiovascular diseases, neurological disorder, and even cancer [51]. Many bioactive ligands act as drug candidates and sometimes failed in clinical trials due to poor solubility. Metal ions play a vital role to improve the solubility of drugs. The lipophilicity of a drug candidate is an important factor to determine the bioactivity. However, chelation decreases the positive charge of metal ion through the delocalization of ligand electron to the central metal atom and thus increases the lipophilicity of the complex which in turn increases the permeability of the complex through bacterial membrane. As a result, the antimicrobial activity of the complex would be increased. For example, tetracycline after complexation with iron(III) and Cu(II) shows enhanced antimicrobial activity than precursor ligand. Moreover, the toxicity of a bioactive ligand would be decreased through complexation. For example, the toxicity of a drug, ketonazole would be decreased through complexation with metal ion.

Metal complexes with their unique electronic and stereochemical features make them attractive alternatives to common resistant drugs. Many metal complexes are now being widely used in medicine. For example, platinum complex, cis-platin [52] is a successful anticancer drug, gold complex, auranofin is used as an antirheumatic agent [53], ebselen, an anti-inflammatory agent is a selenium complex, polaprezinc is a zinc complex and bismuth complex [54] is used to resolve different gastrointestinal problems. Drug-screening results also revealed the antitumor activity of auranofin. In fact, metal-based drugs have shown remarkable success as therapeutic agents since the advent of cisplatin by Dr. Rosenberg in 1960. In 1978, the US food and drug administration (FDA) approved cisplatin in the treatment of testicular cancer. Later on, this drug is used as a combination of chemotherapy in the treatment of lung, ovarian, bladder, breast, and cervical cancer. It is still used in the treatment of cancer successfully. However, researchers still trying to develop cisplatin analogs to reduce toxic side-effects. Examples of some common and approved analogs are carboplatin, oxaliplatin, picoplatin, Nedaplatin, Iproplatin, lobaplatin, Heptoplatin, and satraplatin, *etc.* whose chemical structures are given in Figure 1.9 [55-58]. Table 1.3 also listed an overview of those clinically approved Pt-based anticancer drugs [58].

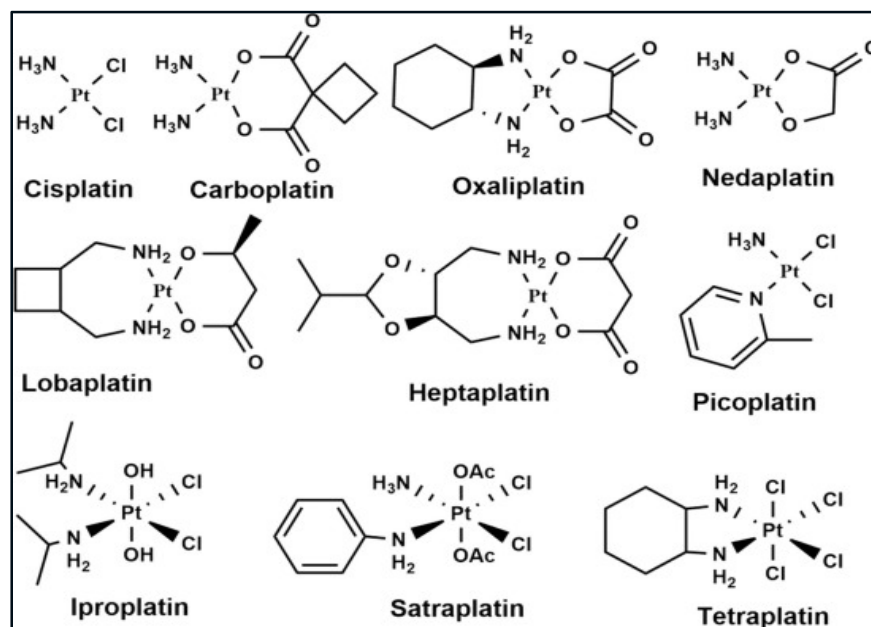


Figure 1.9. Approved and trialed analogs of anticancer drug, cisplatin.

Table 1.3. A brief summary of clinically accepted Pt (II)-based anticancer drugs.

Drug	Approved year	Approved country	Uses
Cisplatin	1978	Worldwide	Testicular, Ovarian, and Bladder cancer
Carboplatin	1989	Worldwide	Ovarian, Breast, Lung & Bladder cancer
Nedaplatin	1995	Japan	Oesophageal and Head and neck cancer
Oxaliplatin	1996	Worldwide	Colon cancer
Heptaplatin	1999	Korea	Gastric cancer
Lobaplatin	2010	China	Metastatic breast cancer

An outline of the molecular mechanism of cisplatin in the medicament of human cancer is presented in Figure 1.10 [56].

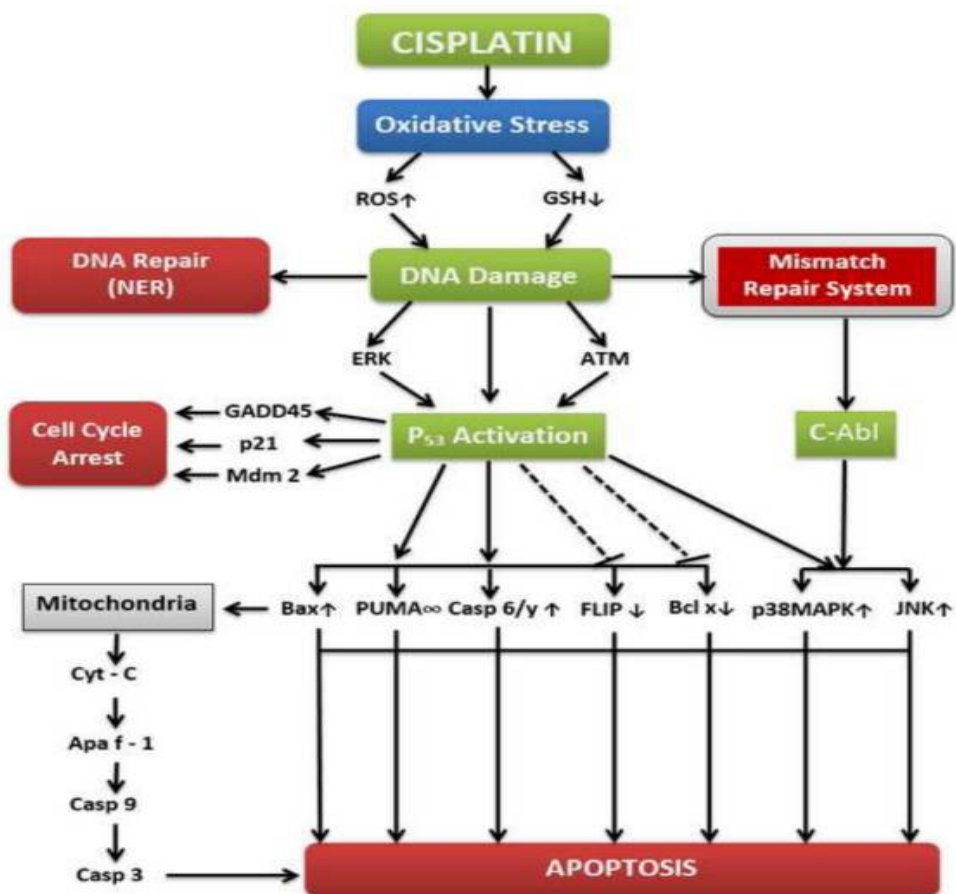


Figure 1.10. Molecular mechanism of anticancer drug, cisplatin.

To overcome the dependency on platinum-based chemotherapy as well as to develop non-platinum anticancer agents, researchers were trying to introduce new metal-based anticancer agents. Fe, Ru, and Pd complexes were also reported to have anticancer activity [59].

But however, the coordination chemistry of gold, silver, and copper is also interesting. These metals are known to have medicinal values since ancient times [60]. For example, copper was used to reduce inflammation, and iron was used to treat anemia. In addition, traces of Cu metal are essential for proper body functioning. It works with iron in the body to form red blood cells and helps to maintain the nervous system and immune system healthy. But an excess or deficiency of this trace metal causes several diseases like Alzheimer, Wilson's and Menkes' diseases [61]. Both silver and copper metal are found to have antimicrobial activity and they are used as effective metal surface coating especially in food industry [62]. Moreover, many binary and ternary Cu(II)-complexes of aromatic molecules with N, S and O donor atoms are known to possess significant biological activity and act as potential therapeutic agents [63]. For example, binary Cu(II)-complexes of pyridyl-2-carboxamidrazone [64] and 6-(2-Chlorobenzyl amino) purine [65] are found to have noteworthy anticancer activity. A number of ternary Cu(II) complexes of mixed ligand of the type $[\text{CuLL}']^+$ were synthesized and found to show significant biological activities ranging from anti-inflammatory to anticancer *etc.* [66]. On the other hand, Schiff bases, a well-known ligand in coordination chemistry, formed through condensation of primary aliphatic or aromatic amine and carbonyl compound. The general chemical formula of Schiff base is $\text{R}^1\text{R}^2\text{C}=\text{NR}^3$ where R^3 = alkyl or aryl

and contains an imine functional group (-C=N-) which is crucial for its biological activities.

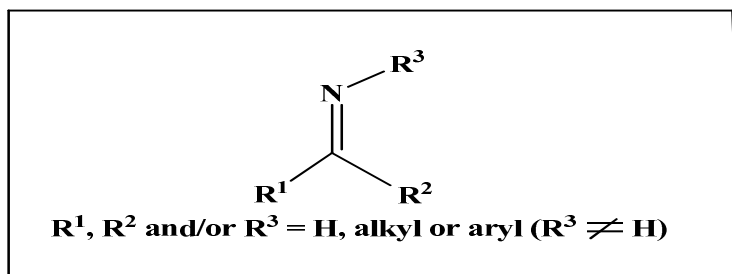


Figure 1.11.The general structure of Schiff base (Ligand).

It has found versatile use in industry and as an intermediate of organic synthesis [67]. It has also been found to have applications in medicinal chemistry and the pharmaceutical field because of its diverse biological activities like antifungal, anticancer, anti-inflammatory, anti-urease, antitubercular, and antioxidant activities [68-71]. Almost all d-block metals including lanthanides can form coordination complexes of therapeutic importance with Schiff bases. Schiff base-metal complexes are found to have better bioactivity than free ligands [72]. Examples of some of Schiff's base-Cu(II) complexes are given in Figure 1.12 [69].

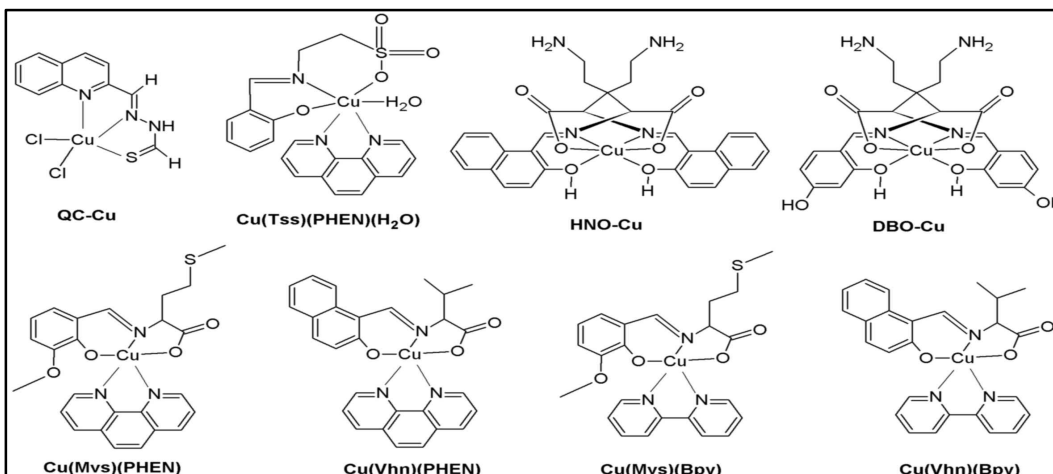


Figure 1.12. Chemical structure of some copper complexes of Schiff's base possessing anticancer activity. QC, quinoline-2-carboxaldehyde; TSS, taurine salicylic Schiff-base; HNO, 2-hydroxy-1-nathaldehyde-L-ornithine; DBO, 2,4-dihydroxybenzaldehyde-L-ornithine; PHEN, 1, 10-phenanthroline; Bpy, 2,2'-bipyridine; Mvs, L-methionine-o-vanillin Schiff base; Vhn, valine-2-hydroxy-1-naphthaldehyde Schiff base.

Apart from Schiff bases, many ligands like derivatives of dithiocarbamate and quinoline successfully bind to copper metal and the copper complexes are found to possess significant anticancer activity. The chemical structure of dithiocarbamate derivatives and quinoline derivatives are shown in Figure 1.13. [69].

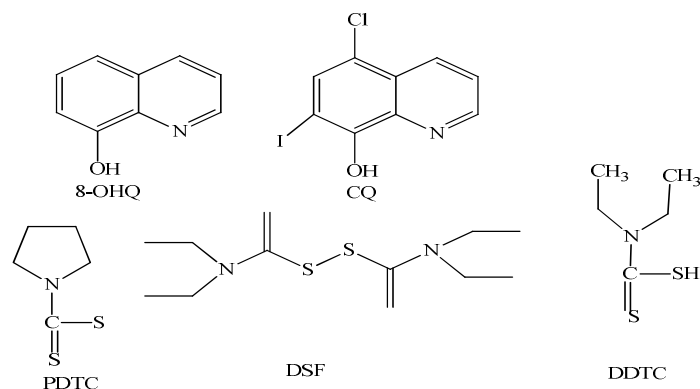


Figure 1.13. Examples of chelating agents: Dithiocarbamate derivatives and quinolone derivatives. 8-OHQ, 8-hydroxyquinoline; CQ, Clioquinol; PDTc, Pyrrolidine dithiocarbamate; DSF, disulfiram; DDTC, Diethyldithiocarbamate.

Several research groups worked on the synthesis, characterization and biological studies of copper complex of the chelating agents which are mentioned above (Figure 10). They have found that the copper complexes behave as potent proteasome inhibitors and act as anticancer agents [73-76]. So, it seems that the copper complexes of Schiff base, dithiocarbamate derivatives and quinolone derivatives could be substitute of successful anticancer drugs like cisplatin, carboplatin etc. regarding the toxic side-effects and resistance properties.

Before the introduction of antibiotics, silver may be the most effective in curing infections [60]. Silver, due to its antimicrobial activity has been used for stomach pain and wound healing by ancient Greek. It is widely used in wound dressing, antiseptic cream for external infections and as an antibiotic coating on medical

devices. It is also used in water cleaning systems and as a disinfection agent. Silver compound, AgNO_3 has been found to use in ophthalmologic and skin care treatment. AgNO_3 has also been used in dentistry as a dental amalgam. Colloidal silver was also reported to be effective in the treatment of ulcers, cancers, arthritis, tuberculosis, etc. [77]. Though Ag is a non-essential element for humans it has remarkable antimicrobial and anticancer activities. Compared to other metals like gold, bismuth iron, platinum, ruthenium, and arsenic, silver is found to have better cytotoxic activity with minimum toxicity. That's why researchers have focused their attention on the coordinated complexes of silver. Silver and its complexes with chelating agent have found applications to develop novel therapeutic agents because of low toxic side effects [78-79]. Many ligands containing donor atoms like nitrogen, oxygen, Sulphur, and phosphorous form complexes with Ag^+ ions, and those complexes are found to have promising activity against cancer cell lines [79-81]. The chelating agents which are used to form such complexes are Schiff base, N-heterocyclic carbenes (NHCs), phosphines, carboxylates, NSAIDs, and 5-fluorouracil, etc. The silver coordinated complexes of different ligands are found to possess improved biological activity than free ligands and most of the silver complexes reported recently serve as anticancer agents with low toxicity compared with cisplatin [82-83]. Examples of some silver complexes of different ligands are presented in Figure 1.14.

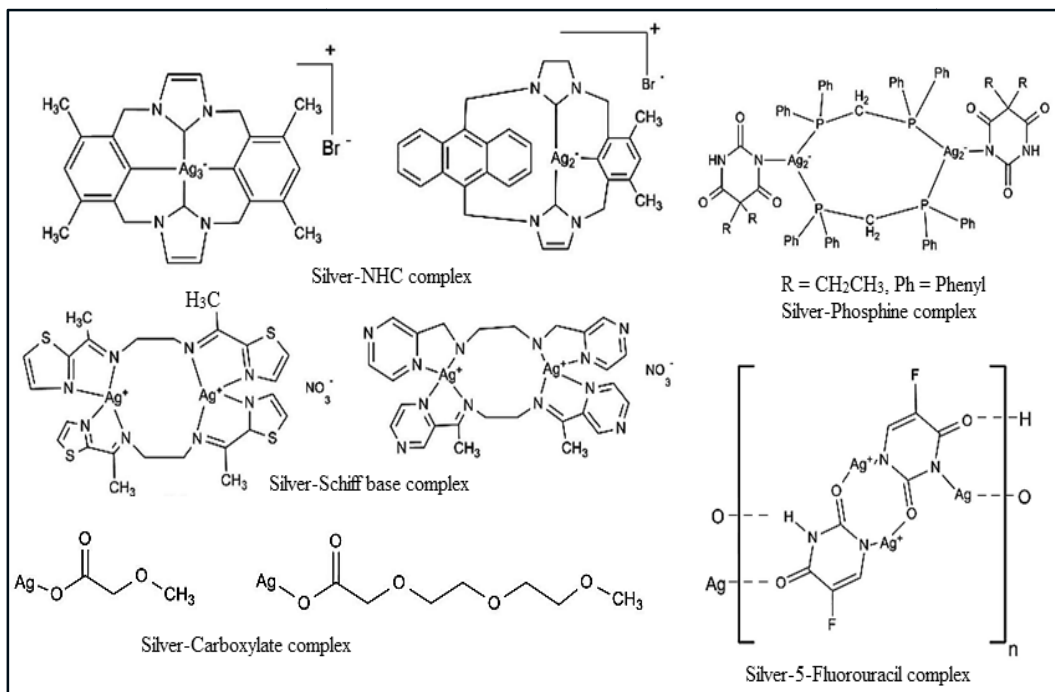


Figure 1.14. Chemical structure of silver complexes of different ligands.

The bactericidal activity of silver (Figure 1.15) originated through the binding of silver ions with bacterial cell walls, bacterial DNA, and bacterial proteins [84].

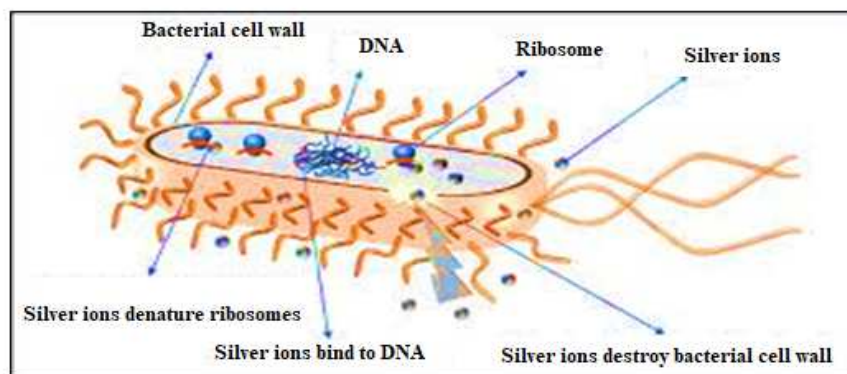


Figure 1.15. Mechanism of the antimicrobial activity of silver.

The journey of gold-based drugs has been started in ancient times especially in India, China, and Egypt to treat tuberculosis, infection, and inflammation [85, 86]. Gold can exist in a number of oxidation states (-I to +V). Gold was used 1st (1890) in modern medicine when Robert Koch synthesized potassium gold(I) cyanide salt, $K[Au(CN)_2]$, and proved to be effective to treat tuberculosis [85]. Later, in 1985, auranofin, a gold-based drug was used effectively as an anti-rheumatic agent to cure rheumatoid arthritis. As gold is inert in the human body, so modern research applied gold as a valid transport agent of anticancer drugs to the target site through blood without problems with normal cells [87]. Current research also investigates gold compounds as anticancer agents with low toxicity and as antimicrobial agents [88, 89]. Examples of some gold-based drugs are shown in Figure 1.16 [90].

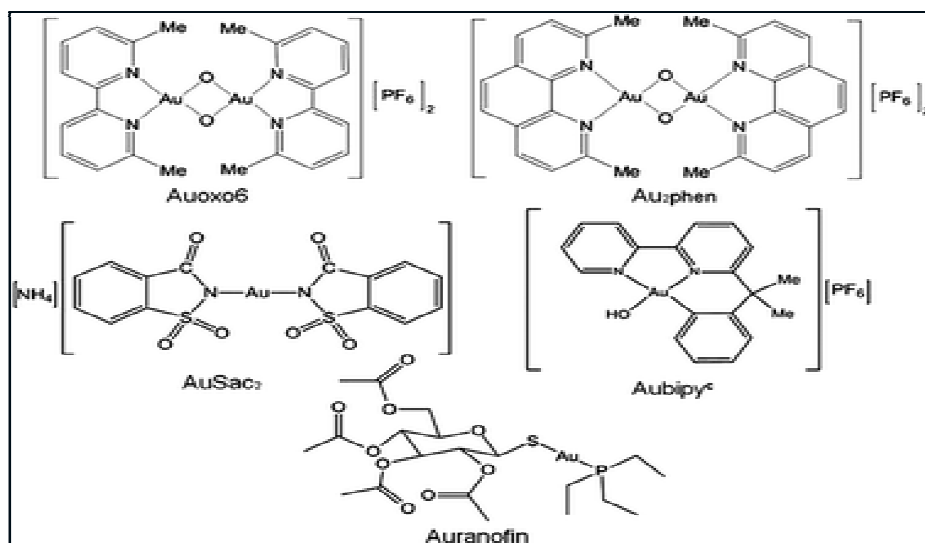


Figure 1.16. Structure of gold-based anticancer drugs.

1.2.3. Complexation of antibiotics with metals leads to the development of new drugs with improved bioactivity

Owing to antibiotic resistance, there is a dire need for new antibiotics with promising biological activities. So, the discovery of new antibiotics with therapeutic properties can resolve the problem. But it is time consuming and needs enough expenditure to discover a new antibiotic. In this regard, antibiotic-metal complexes could serve as a better alternative to new drugs. Many research groups worked on the silver complexation of several classes of antibiotics like β -lactam, aminoglycoside, quinolone, and tetracycline and reported the enhancement of the antimicrobial activity of antibiotics through coordination with silver ions [91-94]. The results are tabulated in Table 1.4 [95].

Table 1.4. Antimicrobial activity of metal complexes of different antibiotics.

Antibiotics		Organism	Culture condition	Effects	Ref.
β -lactams	Ampicillin	<i>E. Coli</i>	Lab.	10-fold increase in antimicrobial activity,	[91]
Quinolones	Ofloxacin	<i>E. Coli</i>	Lab.	10-fold increase in antimicrobial activity.	[91, 92]
	Nalidixic Acid Norfloxacin		Animal models	MIC value decreased 10 – 25%	
Amino-glycosides	Gentamicin	<i>C. difficile</i>	Lab.	MIC value decreased 4-fold	[91]
		<i>E. Coli</i>	Lab. Animal model	A 100-fold increase in antimicrobial activity	[91, 92]

	Tobramycin	<i>E. Coli</i>	Lab.	MIC decreased 10-fold (E.coli)	
		<i>P. aeruginosa</i>		3-fold increase in antimicrobial activity	[92, 93]
	Kanamycin	<i>E. coli</i>	Lab.	MIC value decreased more than 10-fold	[92]
	Streptomycin				
Vancomycin		<i>E. coli</i>	Lab. & Animal model	10-fold increase in antimicrobial activity	[91]
Chlor- amphenicol		<i>E. coli</i>	Lab.	MIC value decreased 1.5- fold	[92]
Rifampicin		<i>A. baumannii</i>	Lab.	MIC value decreased 5- 10-fold	[94]
Tetracycline		<i>E. coli</i>	Lab.	MIC value decreased 2- fold	[91]

Chemotherapeutic resistance is a major health problem today. The use of cisplatin as an anticancer drug established the involvement of metal complexes as potential therapeutic agents. However, platinum group metals like Ru, Rh, Pd, Os, and Ir-complexes are also studied to find out new potent inorganic drugs [59]. Moreover, several researchers [98, 99] proposed the introduction of organometallic parts by conjugation to existing antibiotics to overcome the drug resistance crisis. For example, ferrocene is an organometallic compound that is used in conjugation with existing drugs. The lipophilic nature of ferrocene makes them to pass through cell membranes effectively. Tamoxifen as well as hydroxytamoxifen both are used to treat breast cancer. Top *et al.* worked on the ferrocene derivatives of

these drugs (Figure 1.17) and reported enhanced activity compared to the organic precursor [100-101].

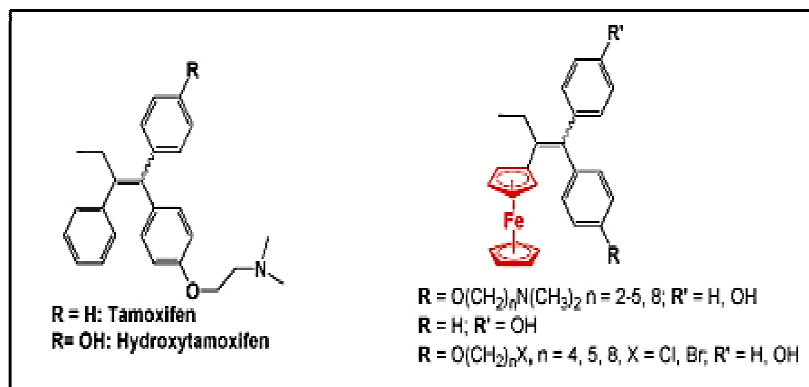


Figure 1.17. Tamoxifen and its ferrocene derivatives [99].

Paclitaxel is another anticancer drug used to treat ovarian and breast cancer.

Rychlik *et. al.* studied the ferrocene derivatives of paclitaxel (Figure 1.18).

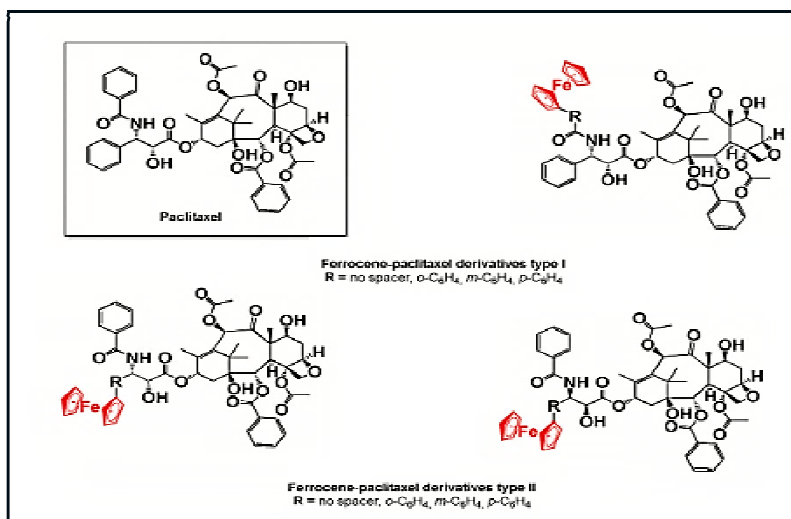


Figure 1.18. Chemical structure of paclitaxel and its ferrocene derivatives (Type I and II) [102].

They have reported that the position of ferrocene moiety determines the effectiveness of the drug. It was found that the spatial positioning of ferrocene moiety mostly influenced the activity of paclitaxel [102]. Type I derivative shows the most activity in the order of no aromatic spacer >*m*-substituted >*p*-substituted> *o*-substituted. Type II derivative did not show any significant activity.

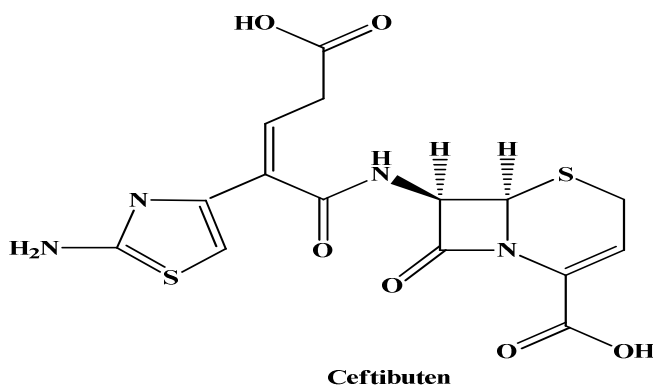
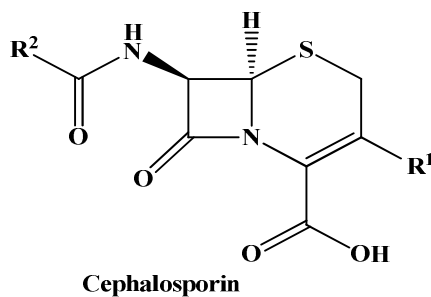
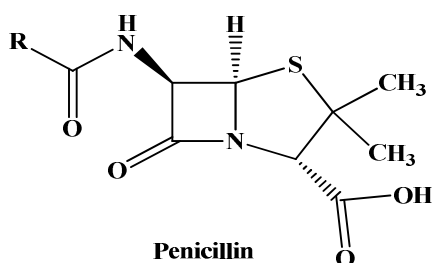
1.3. Selection of Antibiotics and Metals

The development of new drugs with therapeutic importance is ubiquitous in the pharmaceutical industry to mitigate the drug-resistant issue. Synthesis of new antimicrobial compounds through the complexation of different antibiotics with different essential and non-essential metals can meet the demand. In this regard, four different antibiotics belonging to two different classes namely cephalosporin and fluoroquinolone and three metals copper, nickel and silver were chosen for this study.

1.3.1. Ceftibuten dihydrate (CFT)

Ceftibuten dihydrate is a semi-synthetic derivative of a third-generation cephalosporin antibiotic. Cedax is the trade name of this antibiotic and chemically is designated as (+)-(6R,7R)-7-[(Z)-2-(2-amino-4-thiazolyl)-4-carboxycrotonamido]-8-oxo-5-thia-1-azabicyclo[4.2.0]oct-2-ene-2-carboxylic acid dihydrate. $C_{15}H_{18}N_4O_8S_2$ is its chemical formula and 446.5 is molecular

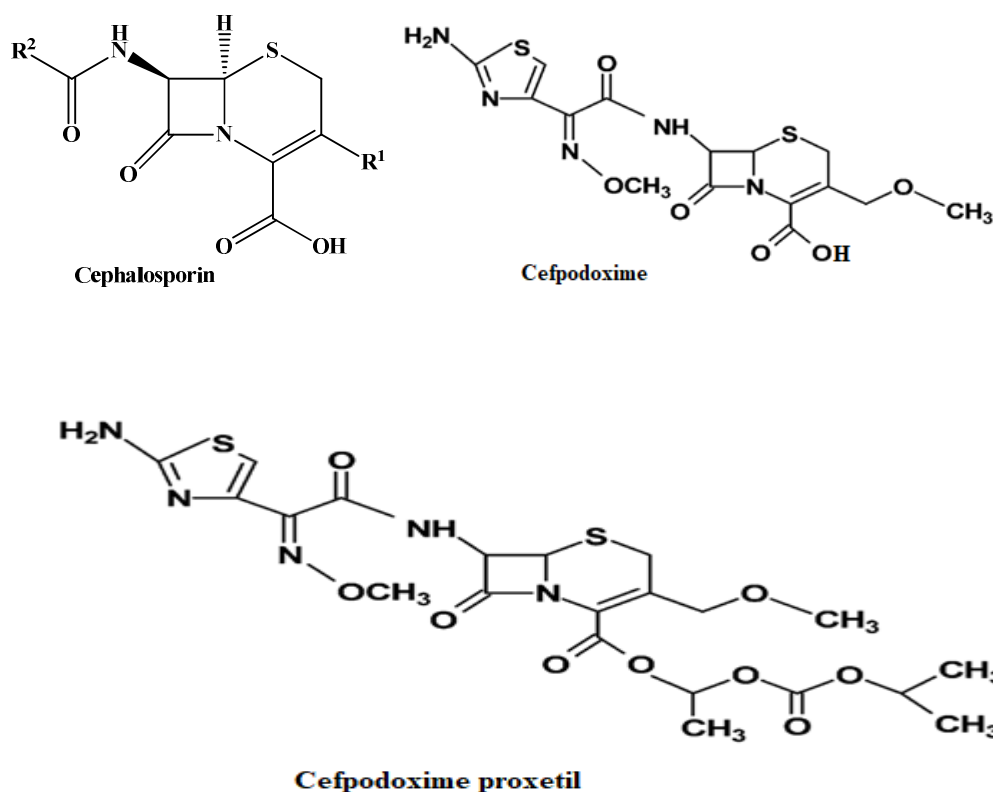
weight [103]. Like penicillin, it is also a β -lactam antibiotic containing a thiazolidine ring attached to the β -lactam ring which is accountable for biological activity.



It is bactericidal and kills the bacteria *via* the β -lactam ring. Actually the β -lactam ring fixes to penicillin-binding protein and thus hinders the formation of the bacterial cell wall. In the absence of a cell wall, a bacterium is vulnerable and ultimately falls to death [104]. Like other cephalosporins antibiotics, it is effective in the treatment of urinary tract infections (UTIs), ear infections, pneumonia, strep throat, and gastroenteritis and is most effective against respiratory tract infections [105].

1.3.2. Cefpodoxime proxetil (CFP)

Cefpodoxime proxetil is an ester prodrug of cefpodoxime which is taken orally and found to be metabolized to the active ingredient cefpodoxime in the gastrointestinal tract. Like ceftibuten, it is also a semi-synthetic derivative of a third-generation cephalosporin antibiotic.

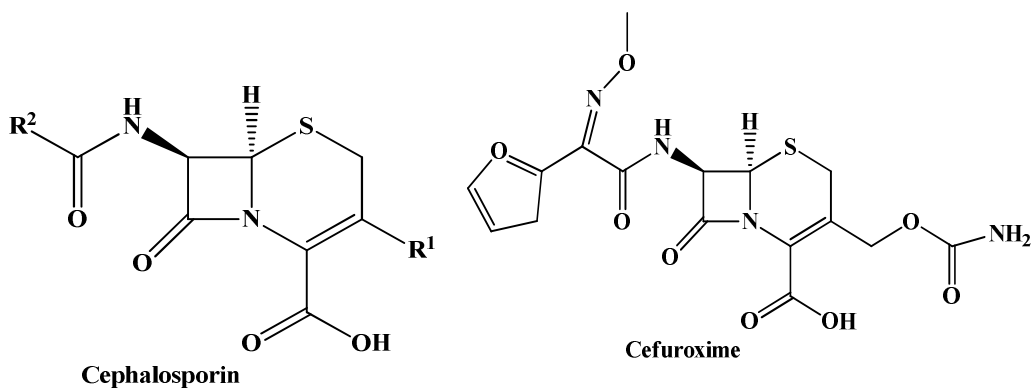


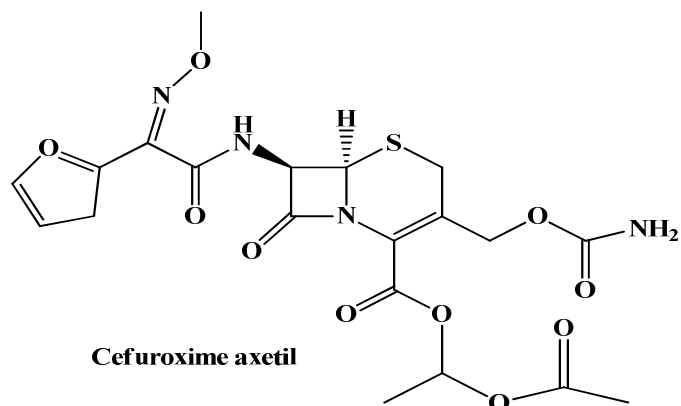
Molecular formula of this drug is C₂₁H₂₇N₅O₉S₂ along with a molecular weight of 557.6 g/mol [106]. It kills bacteria through binding to penicillin-binding protein which in turn prevents the formation of the cell layer and results in the lysis of the

bacterial cell. In a study, it was found that, it is effective, especially for pediatric patients against a variety No. of common infectious diseases [107].

1.3.3. Cefuroxime axetil (CFU)

Cefuroxime axetil is also an ester prodrug of cefuroxime and Ceftin is its brand name. It is a semi-synthetic derivative of a 2nd generation oral cephalosporin antibiotic. Its IUPAC name is 1-[(6R,7R)-3-[(carbamoyloxy)methyl]-7-[(2Z)-2-(furan-2-yl)-2-(methoxyimino)acetamido]-8-oxo-5-thia-1-azabicyclo[4.2.0]oct-2-ene-2-carboxyloxy]ethyl acetate along with molecular formula $C_{20}H_{22}N_4O_{10}S$ and molecular weight 510.5 g/mol [108].





It has a broad-spectrum activity effective against a large No. of microbes. As this antibiotic belongs to the cephalosporin family, its bactericidal activity results from the prevention of the formation of cell walls. Without the cell layer, the bacteria will be helpless and fall under the pressure of molecular water which results in cell lysis [109]. Cefuroxime axetil is stable to β -lactamases enzyme and it is active against a number of beta-lactamase-producing strains including gonococci and Haemophilus influenzae and used to cure respiratory infections.

The three antibiotics namely ceftibuten dihydrate, cefpodoxime proxetil and cefuroxime axetil belong to group cephalosporin, a class of β -lactam antibiotics. The bactericidal activity of β -lactam antibiotics can be represented as in the following way (Figure 1.19 and Figure 1.20).

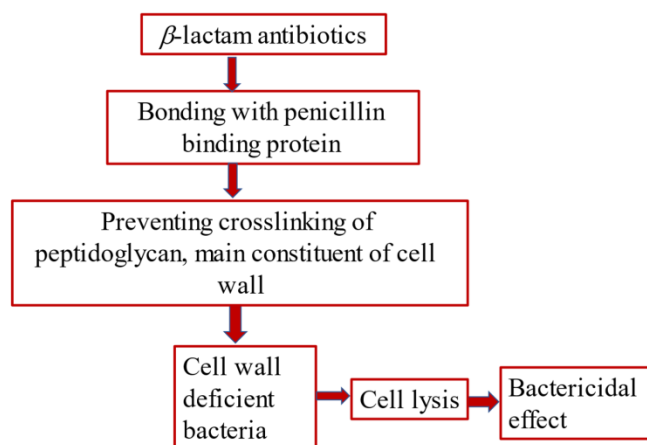


Figure 1.19. Sequential steps of working mechanism of β -lactam antibiotics.

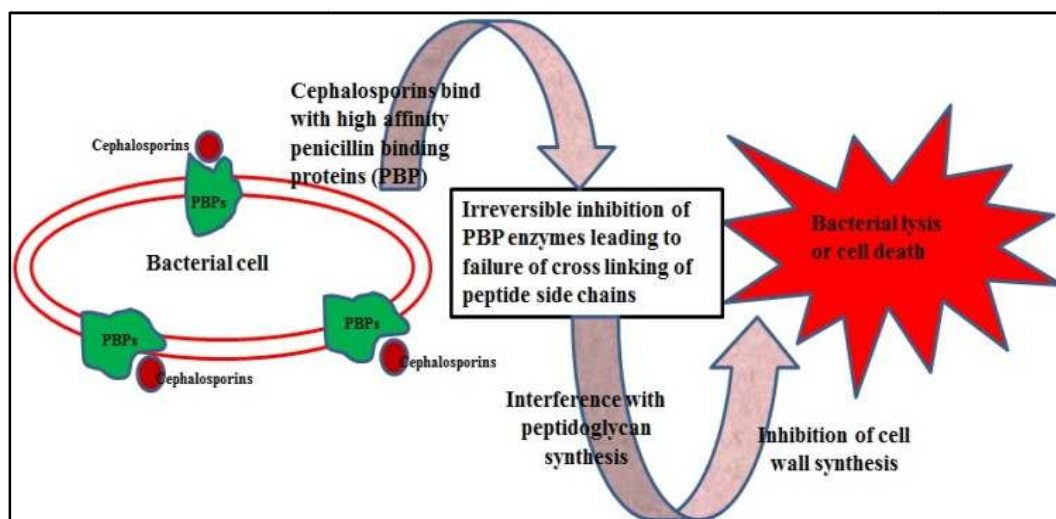
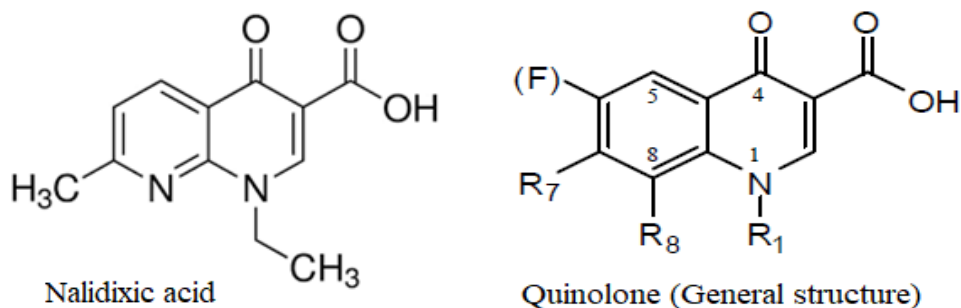


Figure 1.20. Pictorial representation of the working mechanism of β -lactam antibiotics (Adopted from the literature [110]).

1.3.4. Gemifloxacin mesylate (GMX)

Gemifloxacin mesylate, belonging to the quinolone family, is an orally taken synthetic fourth-generation fluoroquinolone-type antibiotic. Nalidixic acid (1960) was the 1st member of the series. Later on, several modifications were made to increase the spectrum of antimicrobial activity.

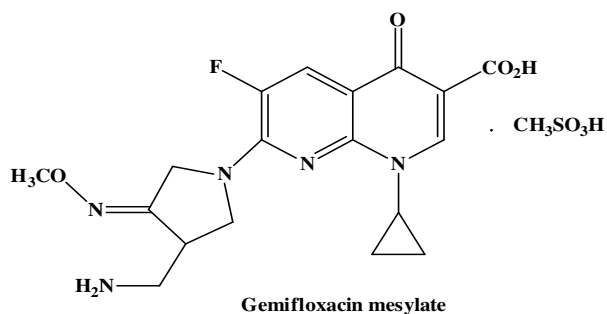


The clinical development of quinolone antibiotics with example are presented in Table 1.5.

Table 1.5. Clinical development of quinolone antibiotics in time.

Generation	Time	Drug Examples
1 st	1970-1980	Cinoxacin, Pipemidic acid, Flumequine
2 nd	1980-1990	Norfloxacin, Enoxacin, Ciprofloxacin
3 rd	1990-2000	Levofloxacin, Gatifloxacin, Sparfloxacin
4 th	2000-	Moxifloxacin, Clinafloxacin, Gemifloxacin

GMX has a long range of activity against microorganisms. IUPAC name of this antibiotic is 7-[(4Z)-3-(aminomethyl)-4-methoxyiminopyrrolidin-1-yl]-1-cyclopropyl-6-fluoro-4-oxo-1,8-naphthyridine-3-carboxylic acid; methanesulfonic acid along with molecular formula $C_{19}H_{24}FN_5O_7S$ and M.W. 485.5.



It is bactericidal and kills bacteria causing several infectious diseases like pneumonia, chronic bronchitis, and urinary infections. The bactericidal activity of fluoroquinolone antibiotic can be represented in Figure 1.21 and Figure 1.22.

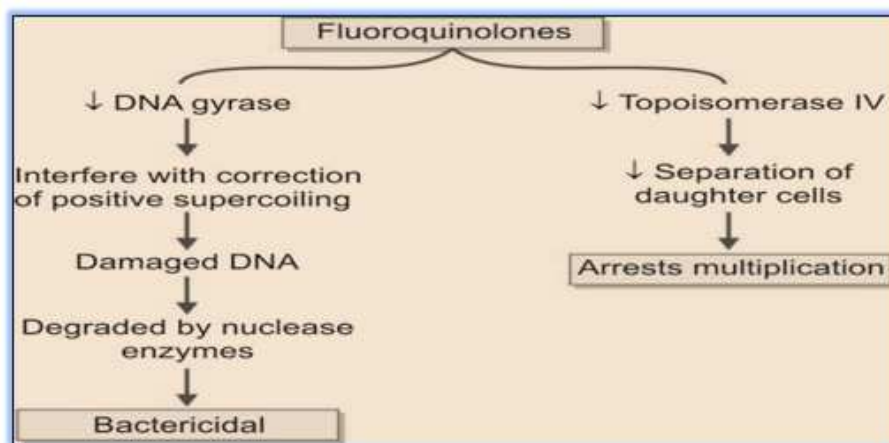


Figure 1.21. Sequential steps of bactericidal activity of fluoroquinolone antibiotics [111].

Gemifloxacin mesylate works by binding itself to enzymes DNA gyrase and topoisomerase IV which in turn hinders the replication, recombination, and transcription of bacterial DNA. As a result, bacterial growth would be stopped.

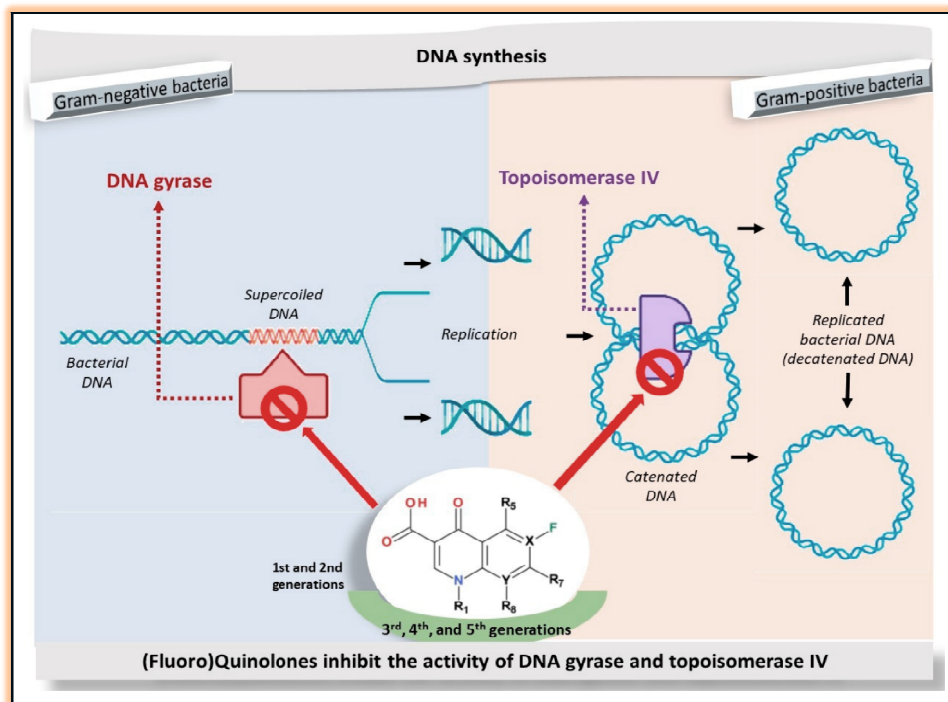


Figure 1.22. Pictorial representation of the bactericidal activity of fluoroquinolone antibiotics [112].

1.3.5. Copper(II) and its significance in complexation

Metals are an integral part of the human body, constitute 2.5% of total body weight and play crucial and critical roles to regulate the body's biological function. The human being needs around 20 elements for proper functioning. Out

of them, ten are metals and ten are non-metals. The metals are Na, K, Ca, Mg, Mn, Fe, Co, Cu, Zn, and Mo [113].

Copper(Cu) has atomic no. 29, a member of transition (d-block) metals, present in group 11 in the periodic table. Cu is a redox transition metal, that transfers electrons within the biologically active molecule. It is found to present as + 1 (Cuprous) and + 2 (Cupric) oxidation states. Cu is involved in various physiological processes. Copper works together with iron to form red blood cells and aids the body in iron absorption. Moreover, it makes the nervous system, immune system, blood vessels and bones healthy. An excess or deficiency of Cu relates to several diseases like cardiovascular arrests, Osteoporosis and most of them are neurological disorders including Alzheimer's, Wilson and Menkes disease [114]. Copper has a long history in the field of medicine from ancient times. Cu was found to use to purify water, wound care, and eye infections. Actually, copper has effective antimicrobial properties, defeating microbes through oxidation. Moreover, Cu containing d electrons can form coordination complexes with promising therapeutic properties. These properties make interest medicinal chemists and inorganic biochemists to use metal ions in searching of new drugs to fight against microbes causing deadly infection. In a study [115], the authors focused on the development of various Cu-complexes with potential therapeutic use. It was found that copper complexes provide diverse biological

properties including antibacterial, anti-inflammatory, enzyme inhibitory, and even cytostatic properties [116]. Generally, chelation changes considerably the biological activities of ligands and makes the complex more liposoluble than the ligand itself. As a result, the complex easily gets access to pass through the cell membrane and shows improved bioactivity than ligands [116]. In this regard, metallodrug can also be a substitute for a new drug to cure cancer, neuro problems and other serious deadly infectious diseases.

1.3.6. Nickel(II) and its significance in complexation

The Atomic No. of nickel (Ni) is 28, belonging to group 10 in the periodic table. Ni is found in nature as Ni(II) rather than Ni(0), Ni(I) and Ni(II) because of the stability factor [117]. Nickel is also an essential micronutrient for human beings to regulate the proper functioning of biological processes. It is found as a metalloenzyme especially urease which acts as a catalyst in the hydrolytic decomposition of urea to gaseous products carbon dioxide and ammonia. It also functions in the body as a hormone regulator, assists iron absorption, and helps to metabolize lipids [118]. Long-time exposure to nickel has some adverse effects. It may cause allergic actions, lung infections, cardiac problems even cancer risk [119]. The Coordination chemistry of nickel is interesting. The common geometries of Ni-complexes are square planer, octahedral, trigonal bipyramidal, and tetrahedral. Nickel complexes have versatile applications in industries

including medicine, automobile, etc. [120]. In a study, it was found that Ni-dithiocarbamate complexes showed promising biological properties ranging from antibacterial to anticancer [121]. Many Ni- complexes serve as efficient catalysts in industrial applications [122].

1.3.7. Silver and its significance in complexation

Silver (Ag) is an element of group 11 in the periodic table. Its atomic No. is 47 and be identified as a d-block transition metal. Common oxidation states of Ag are +1, +2 and +3. The most stable oxidation state is +1 [123]. Germicidal properties of silver(I) are well known since ancient times. Silver was found to use in wound dressing, coating for medical devices, ointment and urinary catheters to prevent external infection [124]. Recently Ag was found to use in the clothing sector and household appliances for its antimicrobial activity. Coordination compounds of silver with different ligands containing donor atoms like N, S and O possess a wide range of biological properties including antibacterial, antifungal, anti-inflammatory, etc. [125]. Still, many research works are going on silver-based compounds and around 300 compounds are in clinical trials [126]. One example is silver sulfadiazine also called Silvadene acts as an effective antibiotic against burn wounds. In a recent study on metal (Ag) complexes of ampicillin antibiotic, it was found that the activity is increased against *K. pneumonia*, *A. baumannii* and *P. aeruginosa* and decreased against *E. coli* and *S. aureus* due to

complexation [127]. Therefore, the production of new compounds with therapeutic importance by complexation of Ag(I) with different ligands is a dire need to combat drug-resistant crises [128].

1.4. Objectives

Presently, antibiotic resistance is a burning issue worldwide which creates a serious threat to public health [162]. The discovery rate of new antibiotics is slow while antibiotic resistance is rising [WHO report]. Therefore, the development of more potent antimicrobial agents to eradicate infections caused by drug-resistant bacteria is ubiquitous for mankind. Metal coordination compounds of antibiotics with improved bioactivity can play a vital role in searching for new antibiotics to fight against life-threatening infections caused by drug-resistant bacteria [136]. In most cases, the effectiveness of antibiotics is increased [151, 157] and toxicity is reduced [163] through chelation. This work aims to search for new potent antibiotics keeping the following objectives in mind.

- ✓ To establish an easy and suitable synthetic route.
- ✓ To synthesize new metal complexes of common antibiotics with improved bioactivity.
- ✓ To initiate a new approach in the treatment of various infectious diseases.
- ✓ To mitigate drug resistance issues caused by overuse, misuse and improper use of antibiotics.

1.5. Literature Review

The discovery of a new drug with potent activity is really challenging. It covers a number of processes including target selection and validation, compound screening, hit identification, lead production and optimization, and then clinical development [129]. Several scientific disciplines like chemistry, biochemistry, biology, and pharmacology are involved in this process [130]. But it is time-consuming, expensive and needs around 10-15 years to introduce a new drug into the market for mankind. Research and development on existing drugs, on the other hand comparatively less expensive and hassle-free, which may introduce new drugs with improved bioactivity. Now, it is a very emerging field with bright future in pharmaceutical chemistry which includes acquiring knowledge of traditional medicine [131], drug-drug interaction [132], metal-ligand interaction [133], and isolation of bioactive constituents from natural products [134]. Moreover, several strategies on existing drugs including drug re-profiling, drug repurposing or repositioning were taken by medicinal scientists to develop new drugs which may be effective in other diseases [135]. Recent advances in medicinal chemistry try to develop new antimicrobial agents focusing on metal complex-based antimicrobial compounds [136-37]. Metals due to their unique characteristics including variable oxidation states, redox potential, coordination modes, number, ligand design and coordinative geometry after complexation offer

a diversity of biological properties. These properties make them interesting as well as attractive to medicinal chemists and successful candidates to fight against several life-threatening diseases even cancer [138]. Many successful findings on metal-based antimicrobial compounds are available in the literature. For example, platinum-based drugs, cisplatin, and analogs of cisplatin like carboplatin, oxaliplatin, nedaplatin, and lobaplatin were approved and successfully used as anticancer therapy [139]. Moreover, ruthenium and iridium metal-based complexes were found to have anticancer activity.

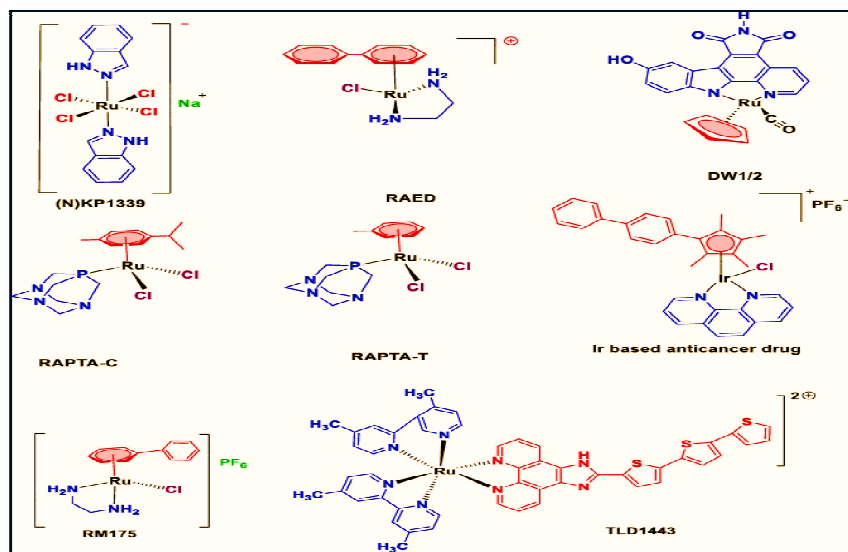


Figure 1.23. Chemical structure of Ru(III) and Ir(III) complexes used as anticancer drugs [140].

Several studies reported the increased biological activity of various ligands, is due to complexation with transition (II) metals like Cu, Ni, Co, Fe, Bi, and Pd [141]. For example, Cu and Ni complexes of thiocarbamoyl dihydro pyrazole possess high inhibitory activity towards *Candida strain* and palladium pyrazolinethiocarbamoyl possesses a higher effect on *Entamoeba histolytica* than the free ligand [142]. Co is also an essential trace element in the human body. Vamsikrishn *et al.* (2016) reported on the synthesis and *in vitro* biological activity of metal complexes of the type $M(L1)_2$ and $M(L2)_2$, where $M = Cu(II)$, $Ni(II)$ and $Co(II)$ and $L1$ & $L2$ are benzothiazole Schiff bases. The complexes showed enhanced antibacterial activity than the ligand precursor [143].

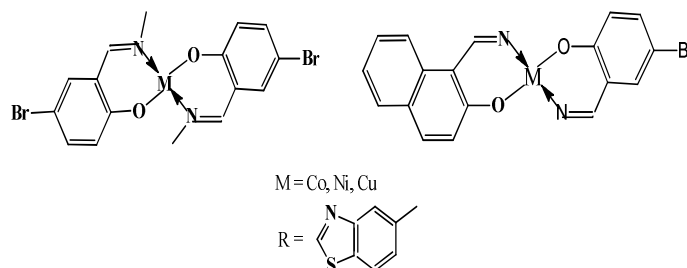


Figure 1.24. Chemical structure of bivalent metal complexes of benzothiazole Schiff base [143].

Now-a-days, metal complex-based antibiotic shows promising result against bacterial infections. Metallodrugs were also found to have enhanced biological activity toward microbes. Sulfadiazine is a synthetic bacteriostatic antibiotic

belonging to the sulfonamide group. Silver sulfadiazine, an antibiotic-metal complex showed excellent efficacy to treat and prevent infections of severe burns [144].

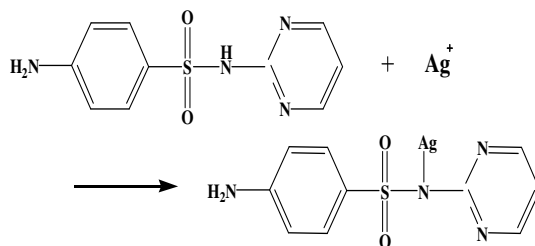


Figure 1.25. Ag-complexation of silver sulfadiazine.

Moxifloxacin is a fourth-generation fluoroquinolone antibiotic, which was developed to treat RTI infections and pneumonia. Seku *et al.* successfully synthesized and characterized the Au(III) and Ag(I) complexes of moxifloxacin and studied antimicrobial activity. Both the Ag(I) and Au(II) complexes showed more potent activity towards microbes than the free ligand, moxifloxacin [145]. However, Leitao *et al.* reported the *in vitro* biological activity of the Ag-complex of camphor amine [146].

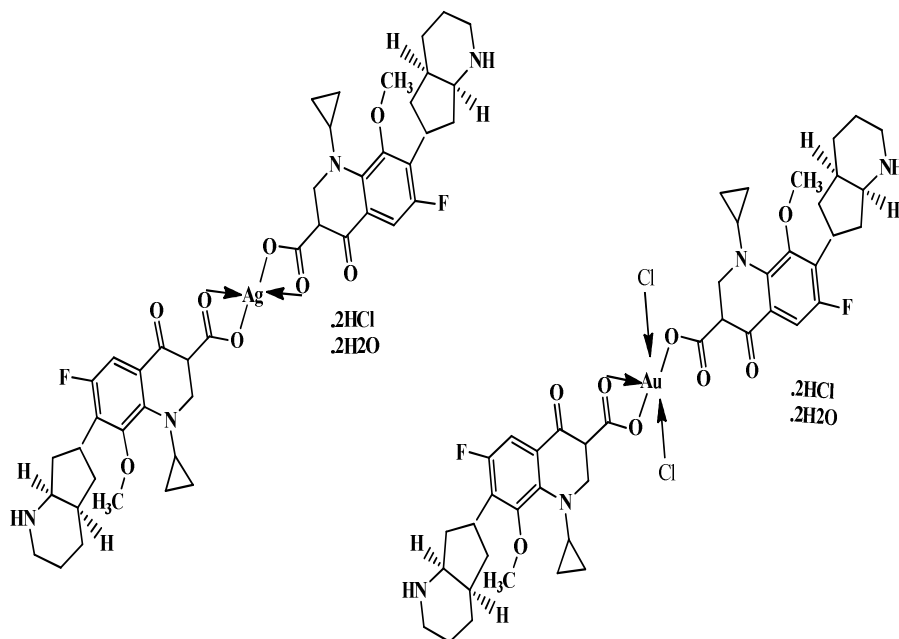


Figure 1.26. The chemical structure of Ag(I) and Au(III) complexes of moxifloxacin.

Norfloxacin is also a quinolone antibiotic. It was reported by Sadeek *et al.* that Y(III) and Pd(II) complexes of norfloxacin showed increased antibacterial activity than the parent antibiotic [147]. Another group of researchers reported higher antimicrobial activity of bismuth norfloxacin complex than norfloxacin itself [148].

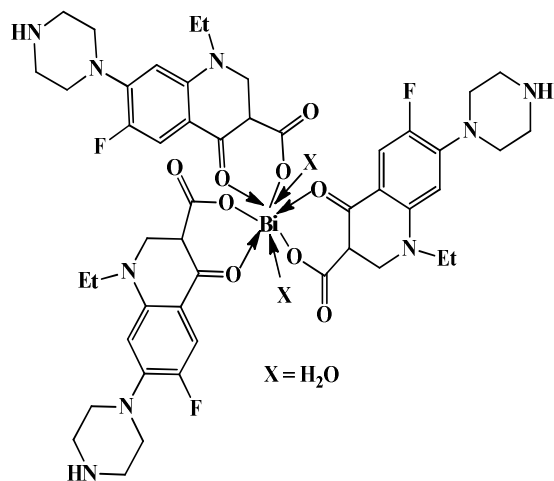


Figure 1. 27. Chemical structure of the bismuth-norfloxacin complex.

They have clarified the result based on Tweedy's chelation theory and overtone concept. Upon chelation, with metals, the polarity of the complexes reduced as well as the lipo-solubility of complexes is increased due to the charge transfer of metal ions to ligands. Actually, the lipo-solubility of complexes is the determining factor in controlling antimicrobial activity. The increased lipo-solubility of the complexes made them easier to pass through lipid membranes and arrest themselves in the enzymes metal binding site of microorganisms. As a result, protein synthesis is hampered and ultimately stopped bacterial growth [149]. Tetracycline is an orally taken bacteriostatic antibiotic belonging to the family tetracyclines which is used to cure several diseases like malaria, syphilis, and RTI infection, etc. Based on experimental results, Guerra *et al.* reported the increased potency of Pd(II) complex of tetracycline is about sixteen times that of the parent

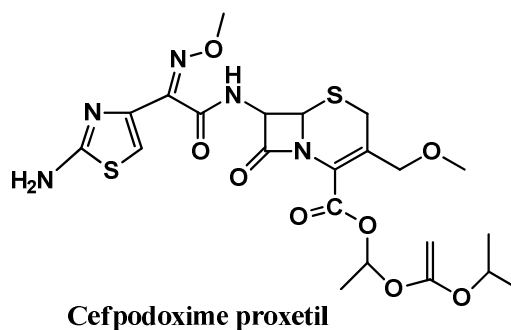
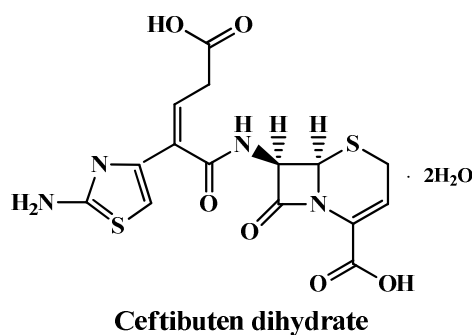
ligand [150]. Many other researchers worked on the complexation of different antibiotics of the cephalosporin and quinolone family [151-154]. Penicillin G is a semi-synthetic, beta-lactam antibiotic of the cephalosporin family and ciprofloxacin is a quinolone antibiotic. Both antibiotics are commonly used to cure human infections and cattle feed additives. Due to the over-use of antibiotics, there is an increasing trend of emerging multidrug-resistant microorganisms. To overcome the failing trend of antibiotics, researchers have proposed combination therapy, a mixture of antibiotics with metal and it may be a good solution to treat resistant bacteria [155]. Kumar *et al.* [156] reported enhanced activity of the Fe(III) complex of penicillin G and Ni(II) complex of ciprofloxacin compared to the parent antibiotic. In other studies, Anacona *et al.* worked on metal complexation of cephalosporin antibiotics, cefotaxime and cefoperazone and found the enhanced activity of complexes than parent drug against microbes [157, 158]. Two different research groups, Nleonu *et al.* (2020) and Khalil *et al.* (2020) worked on the complexation of ciprofloxacin and derivatives of ciprofloxacin. They reported the increased bioactivity of metal (Cu, Fe, Zn) complexes of ciprofloxacin than ligand antibiotic against *S. aureus* and Cu(II) complexes of ciprofloxacin derivatives displayed enhanced antibacterial activity against both Gram-positive and Gram-negative bacteria [159,160]. Very recently, Sharfalddin *et al.* (2021) studied on metal (Cu, Zn, Co, Ni, Fe) complexation of thiamphenicol, a derivative of chloramphenicol act as a broad antimicrobial drug.

They have synthesized, characterized and finally elucidate biological activities. The Cu and Zn complexes showed good anticancer activity [161]. In this regard, antibiotic-metal complexes may serve as a better alternative to cure infections caused by drug-resistant bacteria.

1.6. Present Work

In this work, the complexations of four different antibiotics with biologically important metals Cu, Ni and Ag were done. The three antibiotics, namely ceftibuten dihydrate, cefpodoxime proxetil and cefuroxime axetil belong to the cephalosporin type, and another antibiotic, gemifloxacin mesylate belongs to the fluoroquinolone type based on chemical structure.

A. Cephalosporin type:



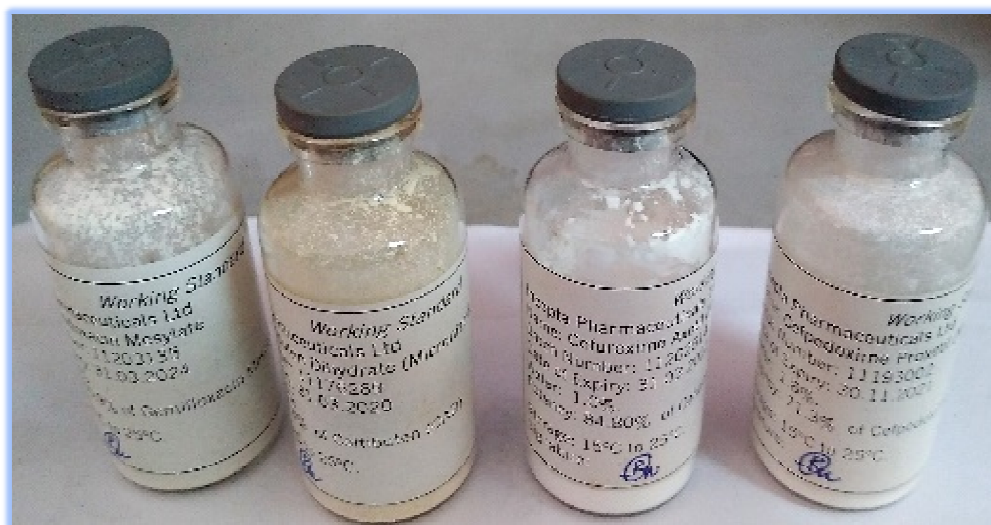
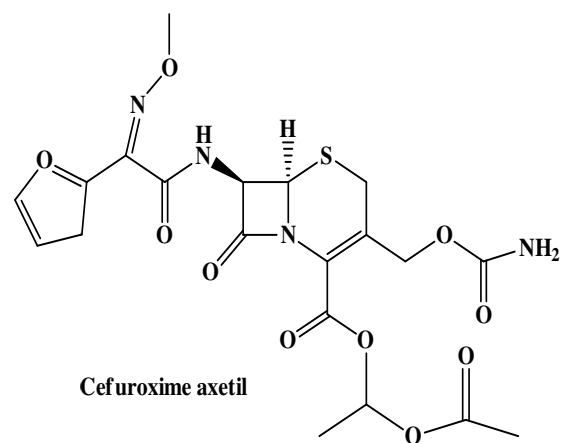


Figure 1. 28. Image of working standard of four different antibiotics.

mesylate were reported previously. In the case of cefuroxime axetil, complexation was done by the mechanochemical method. Herein, the synthesis of metal complexes of cefuroxime axetil is done in a different approach, the solvolytic method.

Chapter Two

Materials and Methods

2.1. Synthetic Route of Ceftibuten Dihydrate with Cu(II), Ni(II) and Ag(I) Metal Ions

The drug, ceftibuten dihydrate (potency 98.6%) was a gift from a recognized pharmaceutical of Bangladesh, Incepta Pharmaceuticals Ltd., Dhaka. Metal salts (Merck, Germany) were of analytical grade and procured from local suppliers. $\text{CuSO}_4 \cdot 5\text{H}_2\text{O}$, $\text{NiCl}_2 \cdot 6\text{H}_2\text{O}$ and AgNO_3 were employed as a source of Cu^{2+} , Ni^{2+} and Ag^+ , respectively. Water was double-distilled in the lab. All other chemicals and organic solvents were also collected from local suppliers and extra purification was not required.

A modified method of preparation of metal complexes of ceftibuten dihydrate was used as described earlier [164]. The reaction was done in a 250 mL round bottom flask placing in an oil bath over a hot plate with a magnetic stirrer.



Figure 2.1. A set of equipment, used for the synthesis of antibiotic-metal complexes.

corresponding metal salt (0.224 mmol) was taken in a beaker and made solution in water. After that, the salt solution was poured into a round-bottom flask containing the parent drug solution. The reaction mixture was then refluxed at the same temperature with continuous stirring. The reaction time was taken about 4 hours. In every case, a colored precipitate was obtained. Then the mixture was reserved for about 24 hours without disturbing for settling down the precipitated complex. The solvent was removed using rotavapor under reduced pressure. The precipitated complex was then washed several times with distilled water and n-hexane for purification so as to remove unreacted materials. Drying of the precipitated complex was done in an oven at 40 °C and then kept in a desiccator at room temperature. The complexes were stable in air and moisture.

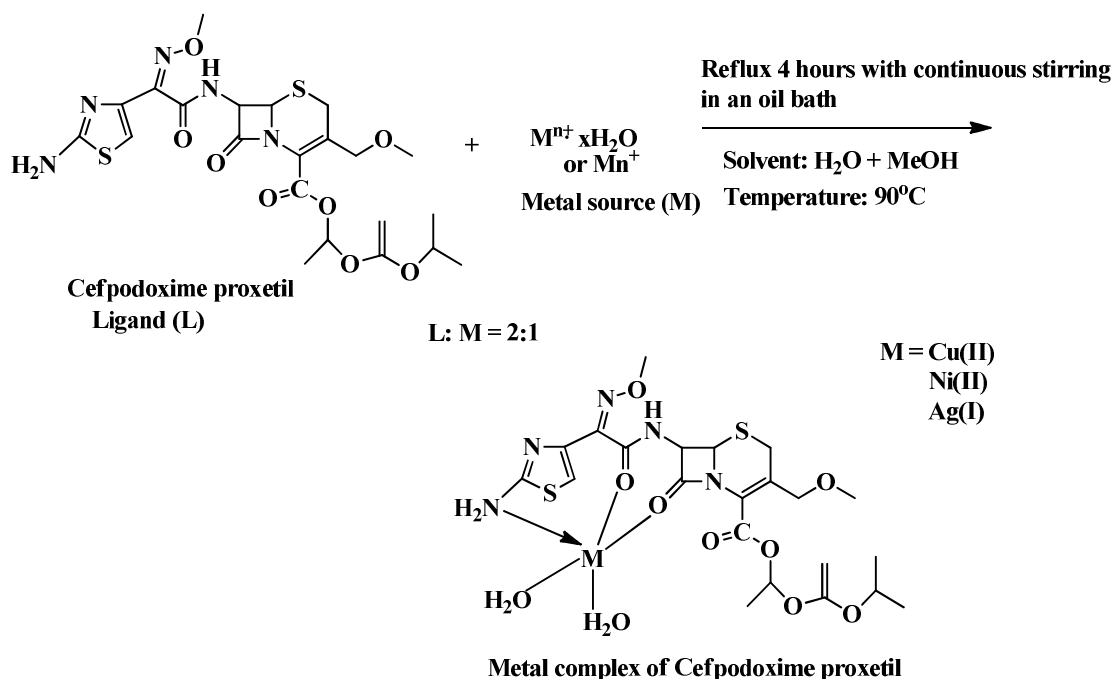
2.2. Synthetic Route of Cefpodoxime Proxetil with Cu(II), Ni(II) and Ag(I) Metal Ions

Cefpodoxime proxetil (potency 71.3%) is another 3rd generation cephalosporin antibiotics earned as a kind gift from a well-known pharmaceutical, Incepta Pharmaceuticals Ltd. Dhaka, Bangladesh. Metal salts, reagents and solvents (Merck, Germany), required for the synthesis were bought from local suppliers and further purification was not required.

Cefpodoxime proxetil is poorly water-soluble but freely soluble in methanol. In this case, complexation was done in a 1:1 mixture of water and methanol as a

reaction medium at 90 °C. The mole ratio of the parent drug (L) and metal salts (M) was adjusted to 2:1 (L:M).

The synthetic method to prepare metal [Cu(II), Ni(II) and Ag(I)] complexes of cefpodoxime proxetil is given in Scheme 2.2.



Scheme 2.2. Synthetic route of metal complexes of cefpodoxime proxetil.

Firstly a 250 mL round bottom flask was charged with the drug, cefpodoxime proxetil (200 mg, 0.358 mmol) and made soluble in MeOH. Then the volume of the drug solution was made doubled using distilled water. After that required amount of respective metal salt (0.179 mmole) solution was prepared in a beaker

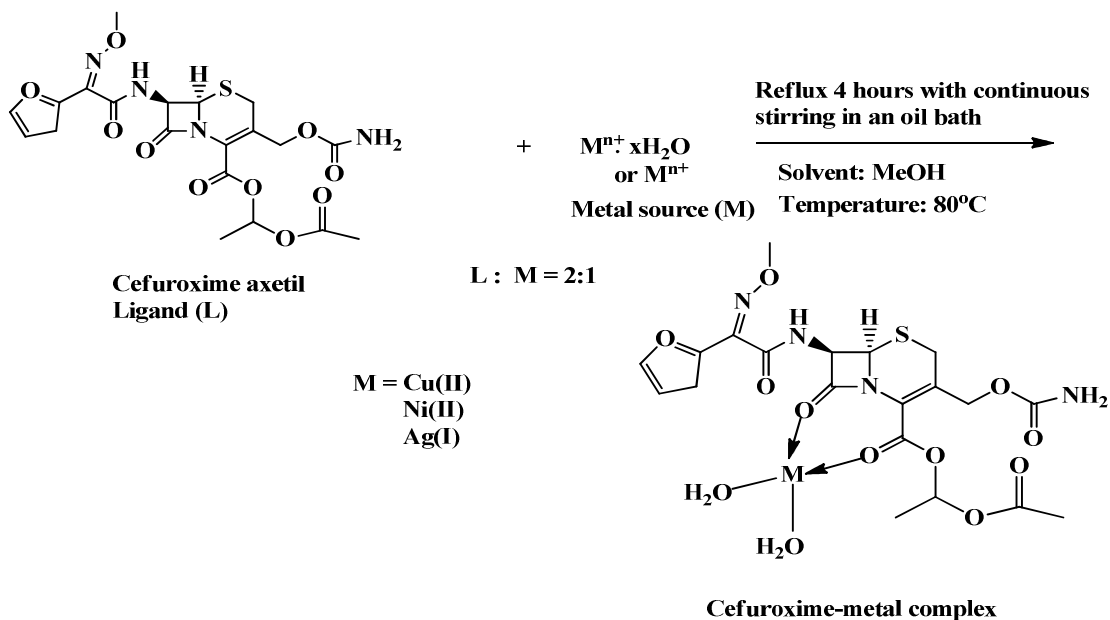
using water. The salt solution was then added in the round bottom flask which was fitted to the water condenser. The reaction mixture was then refluxed in an oil bath at 90 °C for about 4 hours. In every case, a colored precipitate was obtained. To purify the solid complex, the precipitate was washed several times with water and n-hexane.

2.3. Synthetic Route of Cefuroxime Axetil with Cu(II), Ni(II), and Ag(I) Metal Ions

Cefuroxime axetil (potency 88.4%) is also an antibiotic of the cephalosporin family, received as a gift from the same pharmaceutical, Incepta Pharmaceuticals Ltd., Dhaka, Bangladesh. The same metal salts were used to provide metal ions (Cu^{2+} , Ni^{2+} and Ag^+) for complexation. All other reagents and organic solvents (Merck, Germany) were procured from local suppliers and used without further purification.

Cefuroxime axetil is also a poorly water-soluble drug but freely soluble in methanol. Interaction of cefuroxime axetil with metal salts was performed in methanol as the reaction medium. The reflux temperature was fixed at 80 °C and the complexation time was about 4.0 hours. The mole ratio of the parent drug (L) and metal salts (M) was adjusted to 2:1 (L:M).

The synthetic route for the formation of metal [Cu(II), Ni(II) and Ag(I)] complexes of cefuroxime axetil antibiotic is shown in Scheme 2.3.



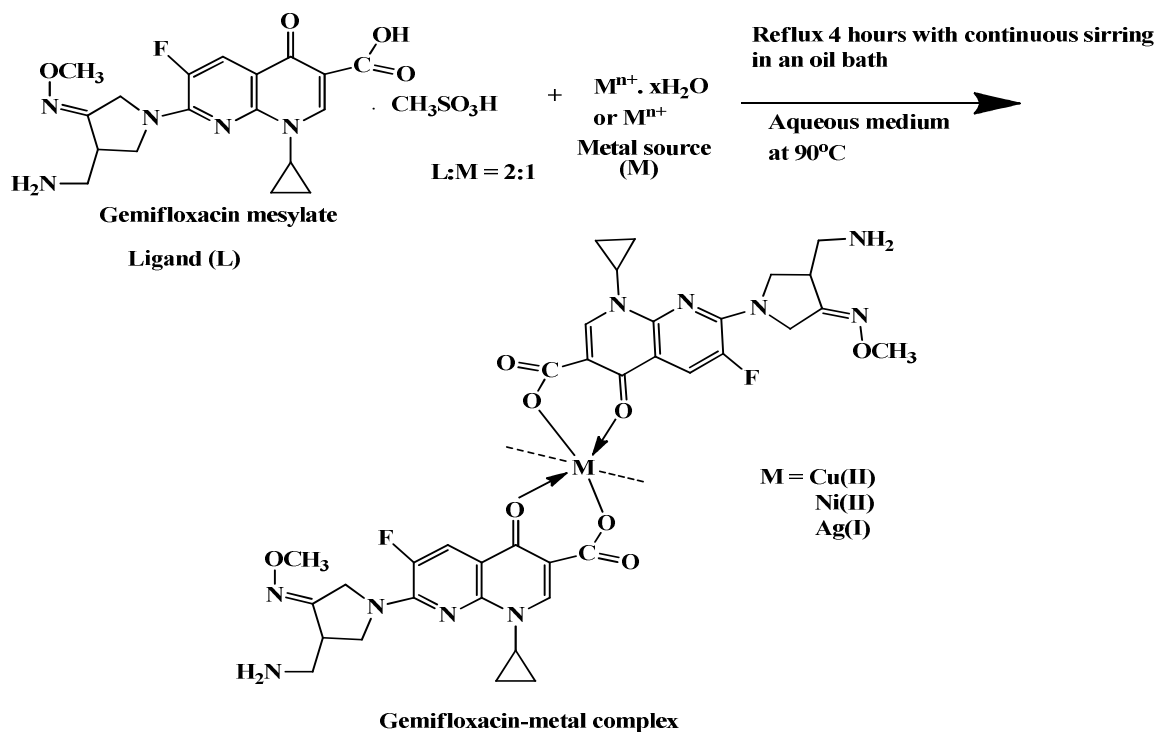
Scheme 2.3. Synthetic scheme of metal complexation of cefuroxime axetil.

First, the antibiotic (200 mg, 0.39 mmol) was taken in a 250 mL round bottom flask to serve the purpose. Methanol was added to prepare the drug solution. Then required amount of respective metal salt (0.196 mmol) was taken and made solution with MeOH. After that, the salt solution was added to the drug solution and refluxed for about 4.0 hours. The total volume of the reaction mixture was about 100 mL. In each case, a colored precipitate was obtained. The solvent was removed by rotavapor. The solid complex was then washed multiple times with water and n-hexane to purify and dried in an oven at 40 °C. The dried purified solid complexes were reserved in the refrigerator for further use.

2.4. Synthetic Route of Gemifloxacin Mesylate with Cu(II), Ni(II) and Ag(I) Metal Ions

Gemifloxacin mesylate (potency 100%) is a synthetic antibiotic of the fluoroquinolone family, received as a kind gift from a familiar pharmaceutical, Incepta Pharmaceuticals Ltd. Dhaka, Bangladesh. All the necessary reagents, organic solvents and metal salts (Merck, Germany) for complexation were bought from local providers and used as if they were provided.

Gemifloxacin mesylate is a freely water-soluble drug. Water was chosen as the reaction medium for complexation. The temperature was fixed at 90 °C and the complexation time for about 4.0 hours. The mole ratio of the parent drug (L) and metal salts (M) was adjusted to 2:1 (L:M). The synthetic route which was followed to prepare gemifloxacin-metal complexes is presented in Scheme 2.4. The complexation reaction was carried out in a 250 mL round bottom flask, fitted with a reflux condenser which was placed in an oil bath over a hot plate with a magnetic stirrer. Initially, an aqueous solution of the drug (200 mg, 0.41 mmol) was taken in the round bottom flask. Then an aqueous solution of respective metal salt (0.205 mmol) was added to the drug solution taken in the round bottom flask.



Scheme 2.4. Synthetic route to prepare complexes of gemifloxacin mesylate.

The reaction mixture was then refluxed at 90 °C for about 4 hours. In every case a colored solid precipitate was gained and kept overnight for settling down the product. Rotavapor was used to remove the solvent under reduced pressure. The solid complex was then washed multiple times with distilled water and n-hexane to purify so as to remove unreacted materials. Lastly, the solid complex was dried in an oven at 40 °C and reserved in the refrigerator for further use.

2.5. Characterization Methods

The newly formed metal complexes of the antibiotics were then characterized by various physico-chemical properties, spectral investigation and thermal techniques.

2.5.1. Physical Properties

The physical properties of any sample are those which are observable and measurable without changing the chemical composition of a sample. Common physical properties are color, odor, physical state, solubility, melting point, boiling point, etc. These properties can be used to describe a sample and differentiate one sample from another sample.

2.5.1.1. Color

The color of the newly formed solid complexes was determined by visual observation. The color of a sample arises when visible light interacts with the surface of a sample. The amount of light that is reflected by the sample surface determines the color of the sample.

2.5.1.2. Physical state

It is one of the most fundamental physico-chemical characteristics of a sample. At ordinary temperature and pressure, a sample can exist in three forms: solid, liquid, and gas.

2.5.1.3. Melting point determination

The melting point of a solid is the temperature at which a solid sample changes its state, from solid to liquid. A pure sample always melts at a sharp temperature while an impure sample melts over a long range of temperatures. Moreover, different samples melt at different temperatures. Therefore, an unknown sample can be identified by its melting point. A digital instrument (Model: WRS-1B, China) was used to determine the melting point of newly formed solid complexes of different antibiotics.

2.5.1.4. Solubility

The term 'solubility' refers to a property of a sample (solute) that enables the sample to form a solution in a given solvent that may either be polar or nonpolar. Usually, temperature and pressure can affect the solubility of a solid product.

2.5.2. Spectroscopic Methods

Spectroscopy is the branch of chemistry that deals with the interaction of radiation with matter, resulting in electromagnetic spectra as a function of frequency or wavelength. Interpreting spectra, the molecular structure of a compound can be determined.

2.5.2.1. UV-Visible

UV-Vis spectrophotometry is a common analytical tool in analytical chemistry. It quantifies the amount of absorbed or radiated light as a function of wavelength. It is used to quantify conjugation as well as transition metal ions in coordination

complexes. UV-Visible spectral analysis was done for four different antibiotics precursor and their metal complexes. A double-beam Shimadzu UV-Visible spectrophotometer, model UV-1800 PC, range 200 – 800 nm, was used to record the UV-Visible spectrum. DMSO was used to prepare the stock solution and distilled water was used to achieve the correct dilution.

2.5.2.2. FT-IR

Fourier Transform Infrared Spectroscopy (FT-IR) is a widely used analytical technique to detect the functional groups present in a molecule. Every functional group has characteristic IR absorption frequency. It is concerned with the vibrational frequency of molecules. FT-IR spectrum of all precursor antibiotics and their solid complexes were taken between 4000 cm^{-1} - 400 cm^{-1} using an FT-IR spectrophotometer (Model: 8400s, Shimadzu, Japan). KBr pellet was prepared to serve the purpose. It records an IR spectrum as a function of % transmittance vs. wavelength of absorbed radiation.

2.5.2.3. ^1H NMR

NMR stands for Nuclear Magnetic Resonance. NMR spectroscopy is a spectral method by which the interaction of Radio Frequency (RF) (3 kHz – 300GHz) radiation with certain atomic nuclei occurs. The NMR spectrum gives information about the structure of molecules. Interpreting the three-distinguishing feature in ^1H NMR, namely the chemical shift value of each absorption peak, the integration value of each peak, and the splitting pattern of each absorption peak can give an

idea of the structure of molecules. Bruker AMX 500 MHz spectrophotometer was engaged to determine ^1H NMR spectra of precursor antibiotics and their complexes. DMSO- d_6 was used as an NMR solvent and TMS as an internal standard.

2.5.3. Thermal Analysis Method

In thermal analysis, a group of techniques including DSC, TGA, DTG, and DTA is used to determine the changes in properties of materials with the change in temperature. The properties are melting point, boiling point, vaporization, sublimation, thermal stability, enthalpy, crystallization, etc.

2.5.3.1. DSC

DSC is a thermal analysis method in which the heat difference between the sample and reference is measured to increase the temperature of a substance as a function of temperature. This technique is widely used in the pharmaceutical and polymer industry. A DSC instrument (Model: DSC 131, EVO, Setaram Instrumentation, France) was involved to record the DSC thermogram. The samples were taken in an aluminum-sealed pan and the temperature range was set from 20 °C to 700 °C. During recording, the rate of flow of N_2 gas 20 mL/min and the rate of increasing temperature 10 °C/min was adjusted.

2.5.3.2. TGA

Thermogravimetric analysis (TGA) is a method of measuring mass loss with increasing temperature over time. Mass loss due to oxidative degradation, pyrolysis, and combustion are common phenomena in TGA. TGA 50H (Shimadzu, Japan) instrument was used to perform TGA studies of precursor antibiotics and their complexes. TGA was done by taking samples in an aluminum pan in the temperature range 25-800 °C. 10 mL/min N₂ gas flow rate and 10 °C/ min heating rate were adjusted during the recording of thermograms.

2.5.3.3. DTG

The differential form of thermogravimetry (DTG) also known as derivative thermogravimetry is also a method of thermal analysis. In DTG, the mass loss rate upon heating is monitored against temperature changes. Compare to TGA, the peak temperature of sample mass loss is obtained in DTG. DTG was performed in a simultaneous TG-DTA instrument (TGA-50H, Shimadzu, Japan).

2.5.3.4. DTA

Differential thermal analysis is another method of thermal study. DTA was performed along with TGA in a simultaneous TG-DTA analyzer (TGA-50H, Shimadzu, Japan). A platinum pan was used as a sample holder and the temperature was raised to 1000 °C where a 10 °C/min heating rate was maintained

in a nitrogen atmosphere for the inert environment. In DTA, the temperature difference between the sample and reference material is monitored against temperature or time. The DTA thermogram thus gives information about melting, crystallization, and phase changes.

2.5.4. Elemental Analyzer

The % of element composition was determined using C, H, N, S analyzer (Vario Micro V 1. 6. 1 GmbH, Germany) with a TCD detector.

2.5.5. Biological Activities

Biological activities of all precursor antibiotics and newly formed coordination complexes of the antibiotics were performed by the Kirby-Bauer paper disc diffusion technique [165-167]. Mueller Hinton agar was chosen as the best medium to prepare the plates for bacteria, and potato dextrose agar (PDA) was used as fungal media. Before use, the plates were dried in an incubator at 30 - 37 °C. Then the plates were inoculated with the test microorganism. The paper discs (diameter 6 mm) were then saturated with samples and referenced drugs, and placed in the previously seeded agar culture plates of tested microorganisms. A maximum of 5 discs were placed in an agar (9 cm) plate. The discs should be placed 10-15 mm distant from the edge of a petri dish. The plates were then incubated at around 37 °C. The time taken was about 24 hours for the antibacterial

assay and about 7 days to determine antifungal activity. After that inhibition zone diameter was measured in mm and recorded.

2.2.5.1. Antibacterial Assay

A long range of Gram-positive and Gram-negative bacteria were used to determine the antibacterial activity of parent antibiotics and corresponding metal complexes. The bacterial strains are *Bacillus cereus*, *Escherichia coli*, *Pseudomonas aeruginosa*, *Staphylococcus aureus*, *Salmonella typhi*, *Vibrio cholera*, *Klebsiella pneumoniae*, *Citrobacter freundii*, *Enterobacter faecalis*, *Enterobacter faecium*.

2.5.5.2. Antifungal Screening

Two fungal strains, *Candida sp.* and *Aspergillus niger* were chosen to determine antifungal activity of the synthesized metal complexes of the antibiotics.

Chapter Three

Results and Discussion

3.1 Physical Properties of Ceftibuten Dihydrate with Cu(II), Ni(II) and Ag(I) Metal Ions

The physical properties of Cu(II), Ni(II), and Ag(I)-complexes of ceftibuten dihydrate are presented in Table 3.1.

Table 3.1. Physical properties of the parent antibiotic and its metal complexes.

Sl No.	Code	Compound	Color	State	M.P. °C	Solubility in	
						DMSO	Hot Water
1	CFT	Ceftibuten dihydrate	Pale yellowish brown	Amorphous	180	Soluble	Soluble
2	CFT-Cu	Copper(II) complex	Deep brown	Crystalline	272	Soluble	Soluble
3	CFT-Ni	Nickel(II) complex	Light brown	Crystalline	305	Soluble	Soluble
4	CFT-Ag	Silver(I) complex	Blackish	Crystalline	265	Soluble	Soluble

Images of the parent antibiotic and its complexes are shown in Figure 3.1.



Figure 3.1. Images of parent antibiotic, antibiotic-metal complexes, and their solution.

3.2 UV-VIS Spectrum Analysis of Ceftibuten Dihydrate with Ag(I) Metal Ion

UV-Vis spectroscopy is an important analytical tool to determine the structure of an organic and inorganic compound. The number of absorption bands, the intensity of each absorption band, and the wavelength of each absorption band in the UV-Vis spectrum provides information about the structure of a compound [168]. The formation of a new metal complex can be verified by comparing the UV-vis spectrum of the parent antibiotic with the corresponding antibiotic-metal complex. Any changes, either the bathochromic shift (shifted to higher values) or the hypsochromic shift (shifted to lower values) of absorption bands revealed the formation of a new metal complex. Changes in the intensity of absorption bands also occurred due to complexation. Sometimes, new absorption bands appeared when a metal binds to a ligand molecule [169]. The electronic (UV) spectra of the parent antibiotic, ceftibuten dihydrate, and its silver complex are displayed in Figure 3.2.

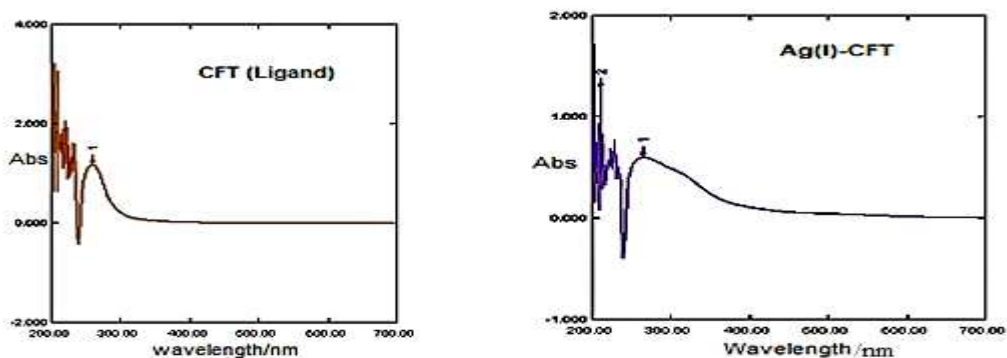


Figure 3.2. UV-Vis spectra of ceftibuten dihydrate and its Ag(I)-complex

The analytical results are given in Table 3.2.

Table 3.2. UV-Vis spectral data of ceftibuten dihydrate and its Ag(I) complex.

Compound	Wavelength of transition(nm)	Assignments
CFT (Parent antibiotic)	281, 209	π - π^* , n- π^*
Ag(I)-CFT	265, 211	π - π^* , n- π^*

The electronic absorption bands for the parent antibiotic appeared at 281 and 209 nm while the Ag-complex showed at 265 and 211 nm. The shifting of absorption bands occurred due to complexation [170].

3.3. FT-IR Studies of Ceftibuten Dihydrate with Cu(II), Ni(II) and Ag(I) Metal Ions

FT-IR is a largely used competent analytical technique to determine the structure of a molecule. IR radiation is associated with molecular vibration and the absorbed radiation perfectly determines the nature of bonds present in a molecule [171]. The FT-IR spectrum of the precursor antibiotic, ceftibuten dihydrate is given in Figure 3.3. Ceftibuten dihydrate is a cephalosporin antibiotic belonging to third-generation. In the case of the antibiotics of the cephalosporin family, it is evident that several coordination sites are available for complexation. Interaction of metal to the ligand can occur through the oxygen atom of the carbonyl group of

the beta-lactam ring, the nitrogen atom of the beta-lactam ring, the oxygen atom of the carbonyl group of the amide side chain, and the carboxylate group [151].

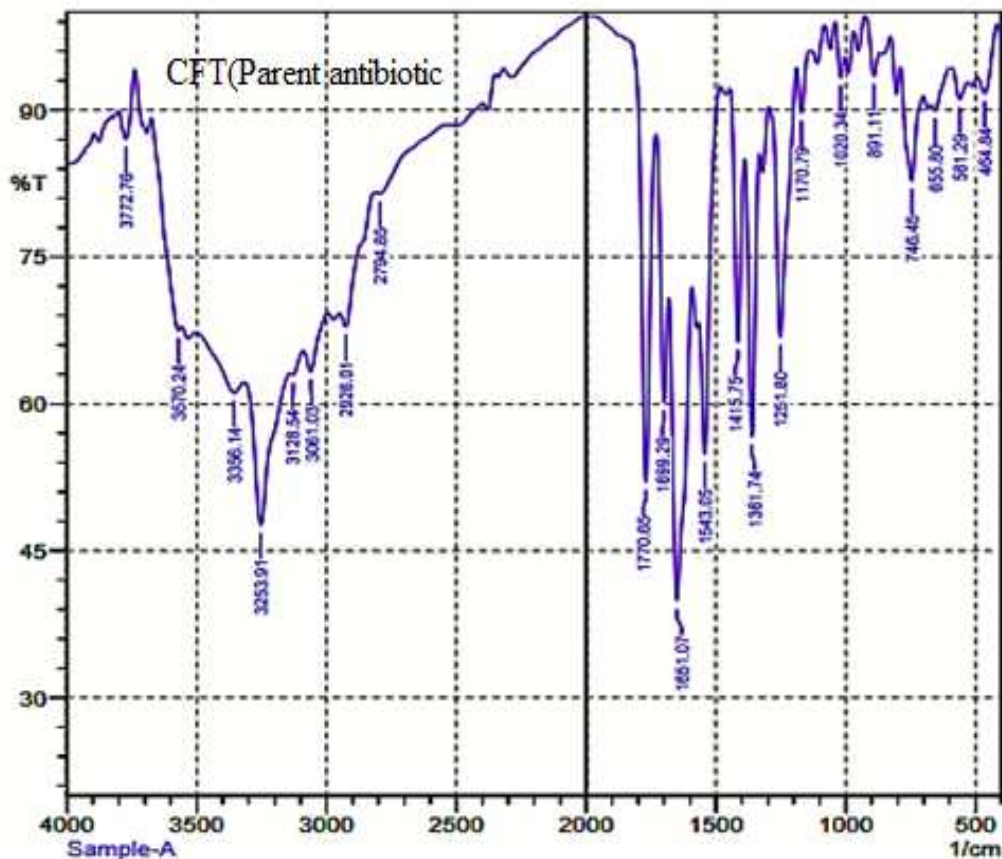


Figure 3.3. FT-IR spectrum of precursor antibiotic ceftibuten dihydrate.

The free ligand (CFT) possesses several characteristic absorption bands of different functional groups. The strong band observed at 1770 cm^{-1} and 1651 cm^{-1} in the free ligand are due to the beta-lactam carbonyl group and the carboxyl group. Also, there is a strong band at 1361 cm^{-1} which is due to $\nu(\text{C-N})$, the

nitrogen atom of the beta-lactam ring. The spectra of the Cu(II), Ni(II), and Ag(I) complexes are given in Figures 3.4, 3.5 and 3.6, respectively.

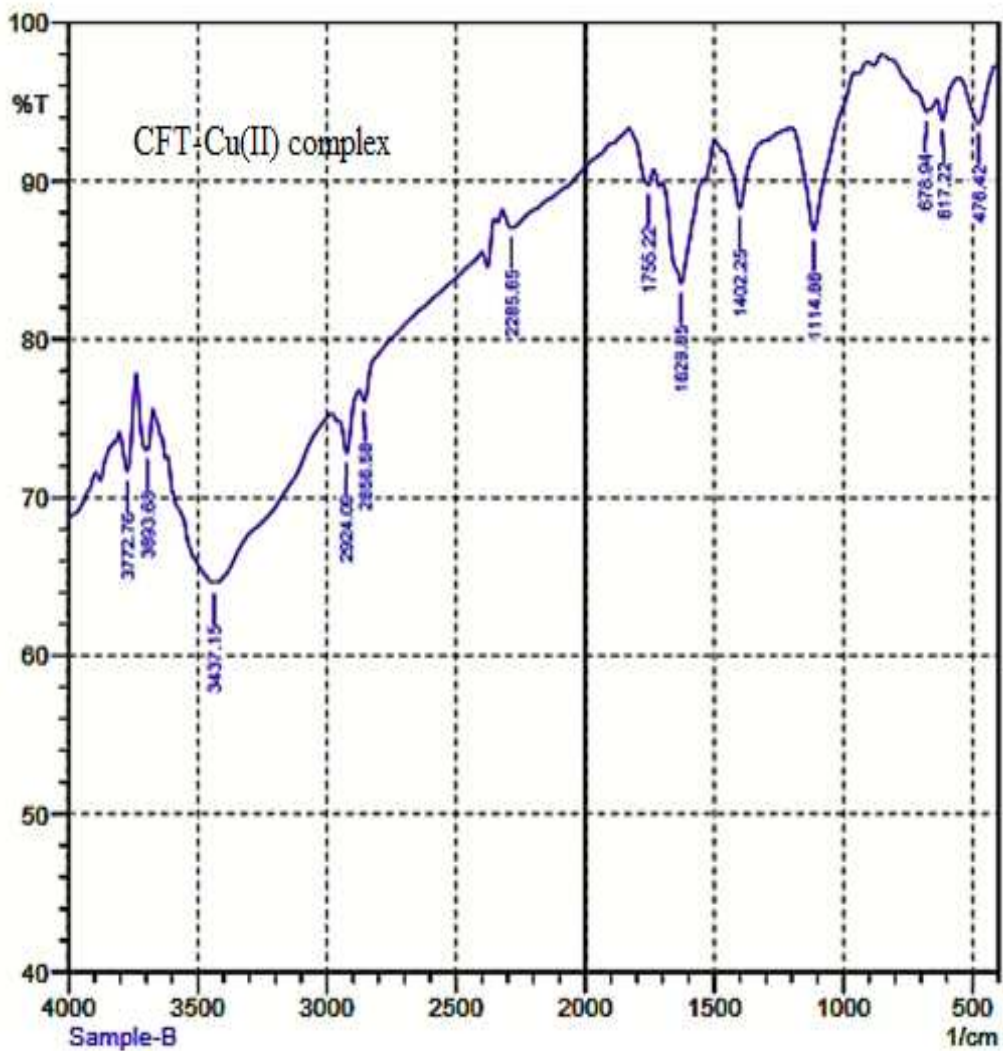


Figure 3.4. FT-IR spectrum of Cu(II) complex of ceftibuten dihydrate.

Noteworthy changes in the vibrational frequency of characteristic absorption bands of the free ligand as well as the disappearance of any absorption band give

evidence for complex formation. Moreover, the appearance of new bands regarding M-O and M-N vibration confirmed the complexation with metals.

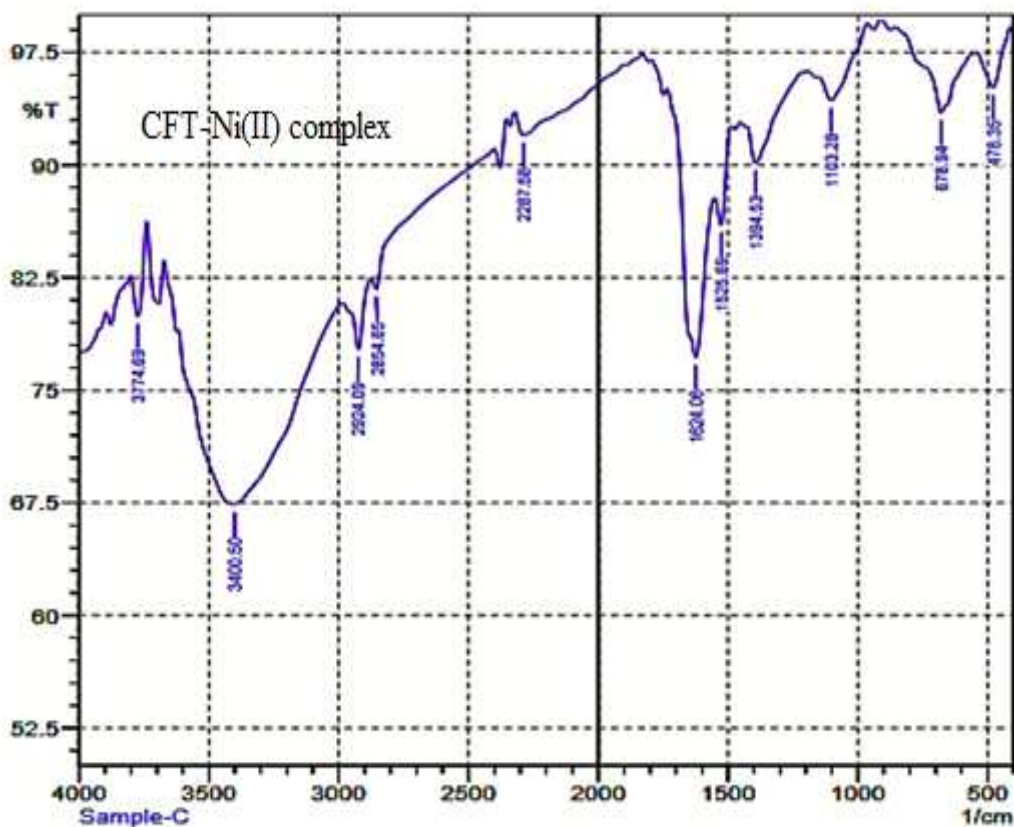


Figure 3.5. FT-IR spectrum of Ni(II)-complex of ceftibuten dihydrate.

In the case of free ligand (CFT), because of the zwitterionic nature of the cephalosporin antibiotic, there are two peaks found at 1651 and 1415 cm^{-1} for asymmetric and symmetric stretching vibrations of the carboxylate group and the coordination mode of the carboxylate ion depends on the shifting of the asymmetric and the symmetric stretching vibration of the carboxylate group.

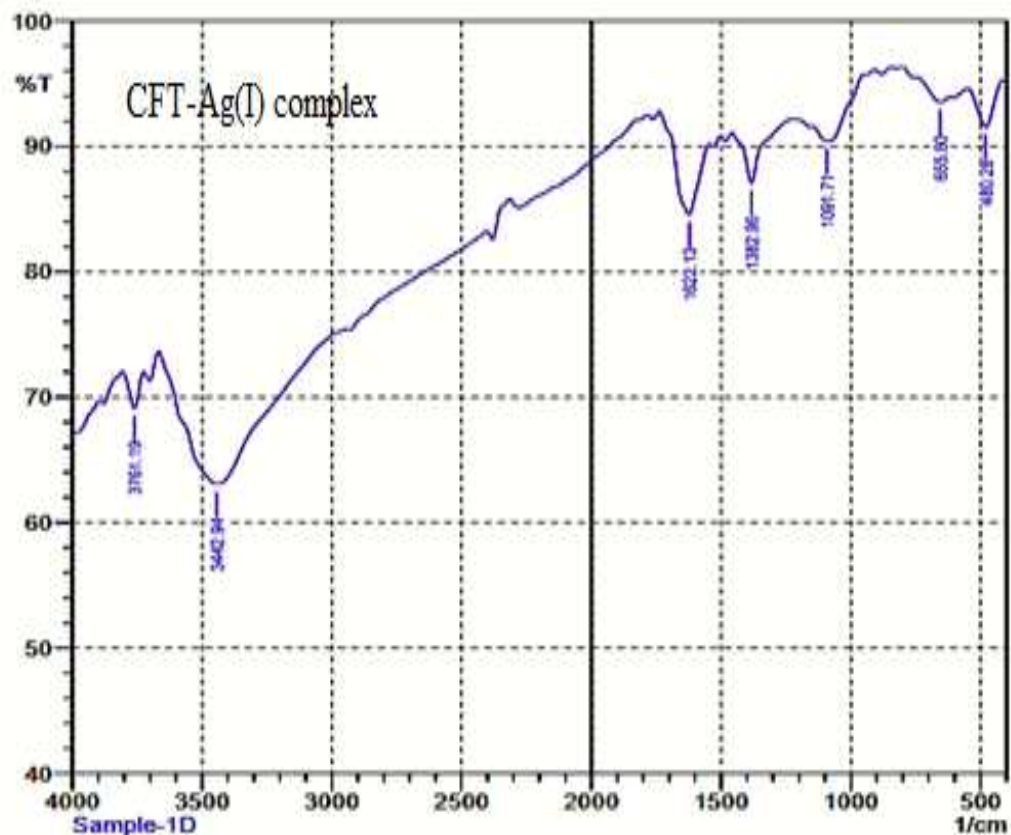


Figure 3.6. FT-IR spectrum of Ag(I)-complex of ceftibuten dihydrate.

In all three complexes, the band due to the beta-lactam carbonyl group (C=O) is not significant, indicating the non-involvement of the lactam carbonyl group in complex formation [172,173]. Upon complexation with Cu(II) ion, the peaks of the carboxylate group's asymmetric and symmetric stretching vibrations shifted to 1629 and 1402 cm^{-1} , respectively. The difference between the value of asymmetric and symmetric stretching vibration ($\Delta\nu = \nu_{\text{asym}} - \nu_{\text{sym}}$) indicates the coordination mode of the carboxylate group [174]. If the separation value ($\Delta\nu$) is

in between 200-300 cm^{-1} , the coordination mode is unidentate and $\Delta\nu < 100 \text{ cm}^{-1}$ indicates the bidentate coordination mode of the carboxylate group. In Cu(II)-complex of ceftibuten dihydrate, the separation value, $\Delta\nu > 200 \text{ cm}^{-1}$ was found and indicates the monodentate binding mode of the carboxylate group. Likewise, in Ni(II) and Ag(I) complexes of ceftibuten dihydrate, the separation value ($\Delta\nu$) of greater than 200 cm^{-1} was found, which suggests the similar (unidentate) coordination mode of the carboxylate group [157, 175]. A strong band at 1361 cm^{-1} is observed in the free ligand due to the presence of a *tert*- nitrogen atom (C-N) of the beta-lactam ring. A considerable change in the frequency of the *tert*-N atom has occurred after complexation, which is due to the participation of *tert*-N in complexation [176]. In Cu(II)-complex, the ν (C-N) appeared at 1114 cm^{-1} , while at 1103 cm^{-1} for Ni(II)-CFT and at 1091 for Ag(I)-CFT, respectively. Moreover, a new band appeared in all three complexes in the region of 470-480 cm^{-1} , which is due to the formation of the M-N bond [176, 177]. The FT-IR data of all complexes along with the precursor antibiotic are summarized in Table 3.3. All these suggest the coordination of metal ions through one of the oxygen atoms (unidentate) of the carboxylate group and the nitrogen atom of the beta-lactam ring [177, 178]. In all three complexes, a broad-band has appeared in the region of 3100 ~ 3600 cm^{-1} which is due to the presence of coordinated water in the complexes [178, 179].

Table 3.3. Characteristic vibrational frequencies (cm^{-1}) of CFT antibiotic and antibiotic-metal complexes.

Compound	ν (OH)	ν (3°N)	ν (COO)	ν (COO)	$\Delta\nu$	$\nu(\text{M-N})^*$
	H_2O	lactam	asym	sym		
CFT(Ligand)	3259, s	1361	1651	1415	236	-
CFT-Cu(II)	3437, br	1114	1629	1402	227	476
CFT-Ni(II)	3400, br	1103	1624	1398	222	478
CFT-Ag(I)	3442, br	1091	1622	1382	240	480

(M-N)* indicates M-N coordinate bonding.

In a study on the complexation of the cephradine antibiotic, Sultana *et al.* (177, 178) proposed the complexation of metal ions to the antibiotic through the N atom of the beta-lactam ring and one of the carboxylate oxygens forming a five membered ring (Figure 3.7). The shifting of the frequency of the tertiary nitrogen atom as well as the asymmetric and symmetric frequency of the carboxylate group give strong evidence for the coordination of metal ions to the nitrogen atom of the beta-lactam ring and carboxylate ion.

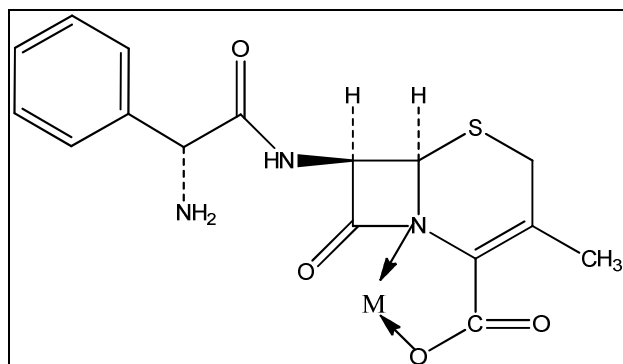


Figure 3.7. Proposed structure of cephradine-metal complex by Sultana *et al.* [176, 177].

3.4. Thermal Analyses of Ceftributen Dihydrate with Cu(II), Ni(II), and Ag(I) Metal Ions

Thermal studies belonging to DSC and TG analyses were done for Cu(II)- and Ni(II)- complexes of ceftributen dihydrate. Thermal studies describe how the properties of materials like thermal stability, enthalpy, sublimation, and melting point change with temperature change. The TG curves of precursor antibiotic, ceftributen dihydrate and its Cu(II) and Ni(II) complexes are given in Figures 3.8, 3.9, and 3.10, respectively.

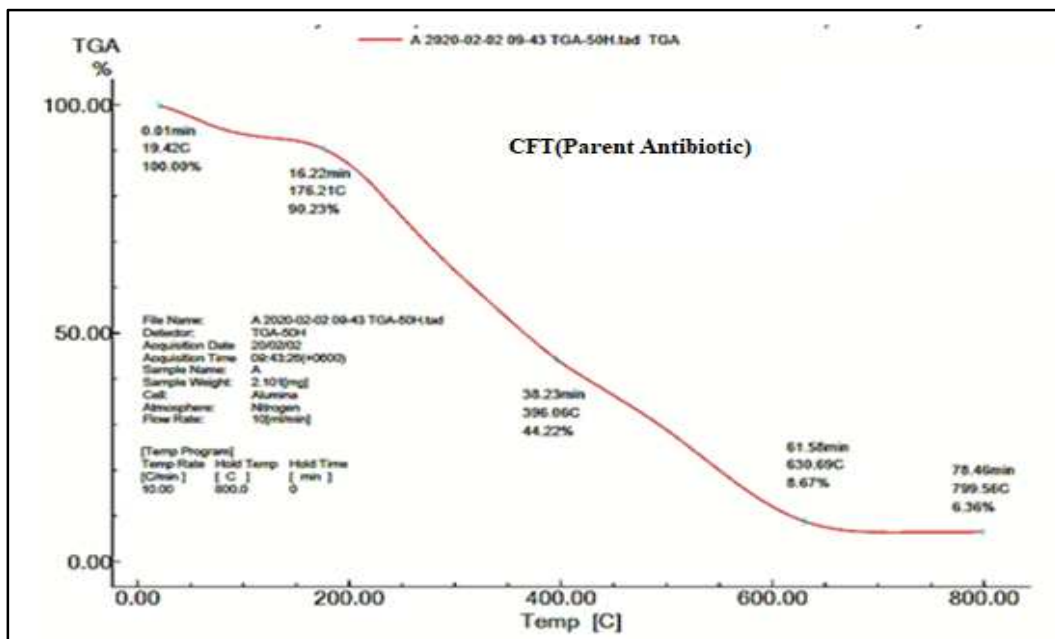


Figure 3.8. Thermogram (TG) of precursor antibiotic, ceftibuten dihydrate (CFT).

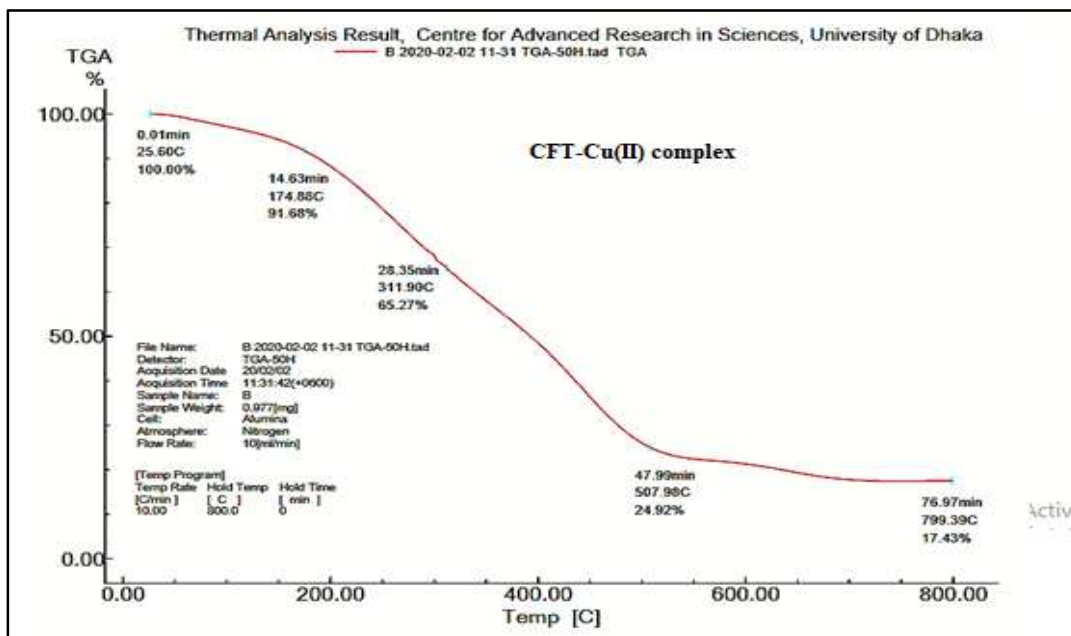


Figure 3.9. Thermogram (TG) of Cu(II)-complex of ceftibuten dehydrate.

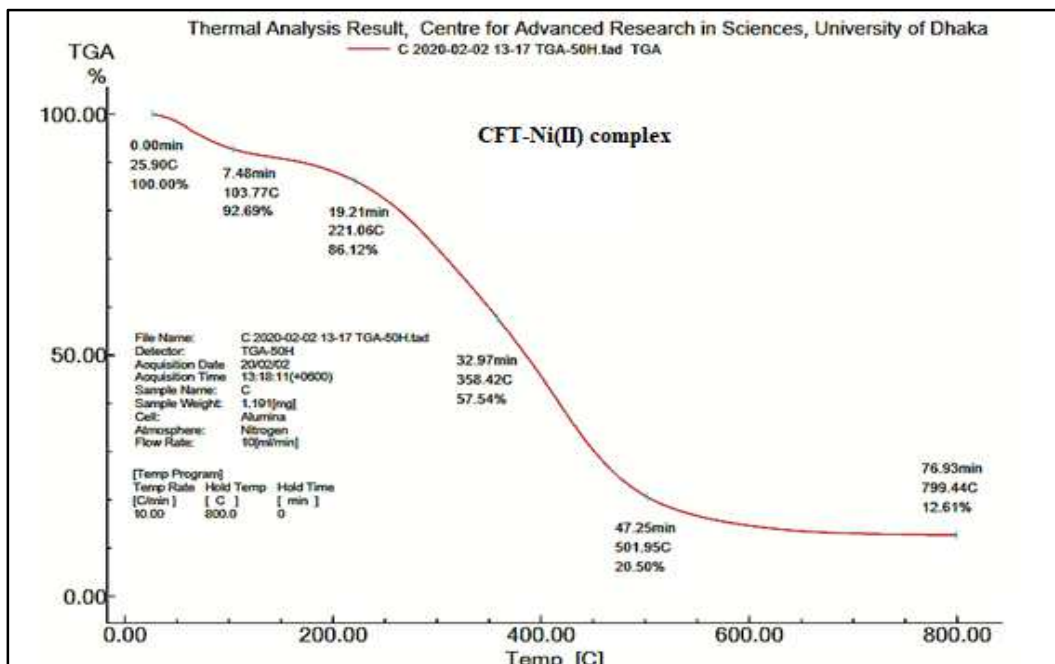


Figure 3.10. Thermogram (TG) of Ni(II)-complex of ceftibuten dehydrate.

In the TG curve of the parent antibiotic and its metal complexes, a multistep degradation process was observed and the degradation pattern of the complexes was completely different from their parent antibiotic, which implies the feedback of metal-ligand interaction [180]. The degradation of the complexes started with the loss of lattice water, then coordinated water. After that, the degradation of anhydrous species occurred, finally metal oxide was found as residue [181]. In the case of the pure antibiotic, ceftibuten dihydrate, 9.77% mass loss was found at 176.21 °C, followed by 55.78% at 396 °C, 91.33% mass loss at 630 °C and lastly 93.64% at 800 °C. The CFT-Cu(II) complex degraded 8.32% at 175 °C, followed by 34.75% at 312°C, 75% at 508 °C and finally 83% lost at 800 °C. On the other

hand, the CFT-Ni(II) complex decomposed 10.78% at 171 °C, 41.29% at 394 °C, 79.93% at 609 °C and finally 83.34% at 800 °C. It is found that 17% of total mass remained for Cu and Ni(II) coordinated-CFT antibiotic, even after heating up to 800 °C. That means the complexes possessed greater thermal stability than the precursor antibiotic.

The DSC curves of ceftibuten dihydrate antibiotic and its metal-coordinated complexes are given in Figures 3.11, 3.12, and 3.13, respectively. The DSC curve of the parent antibiotic represents an endothermic peak at 98 °C which implies the dehydration step and an exothermic peak at 242.7 °C, indicating the melting point of the pure drug.

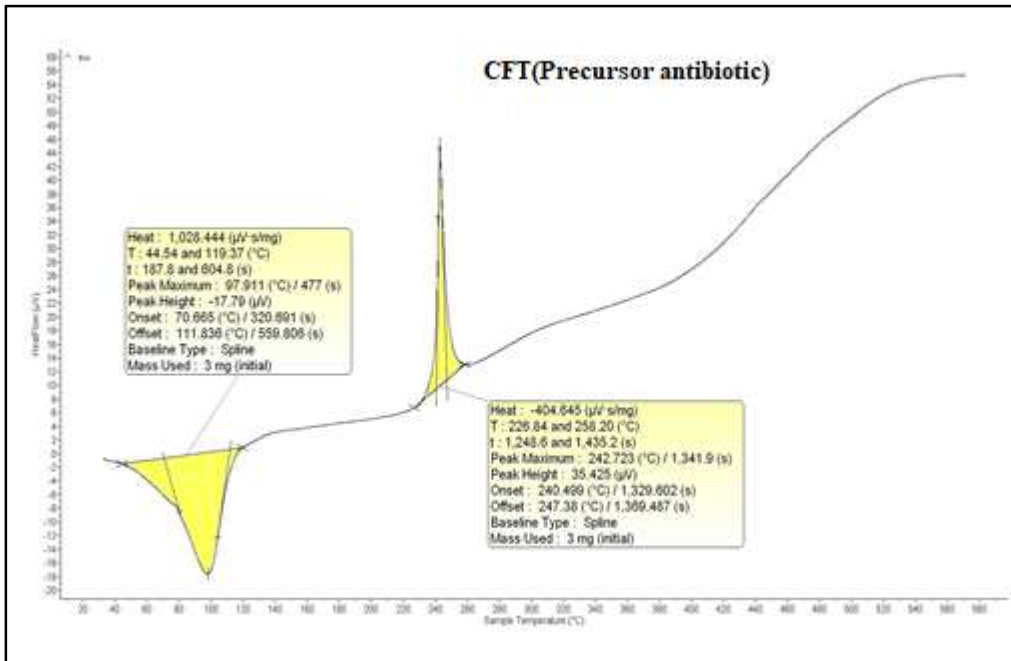


Figure 3.11. Thermogram (DSC) of precursor antibiotic, ceftibuten dihydrate.

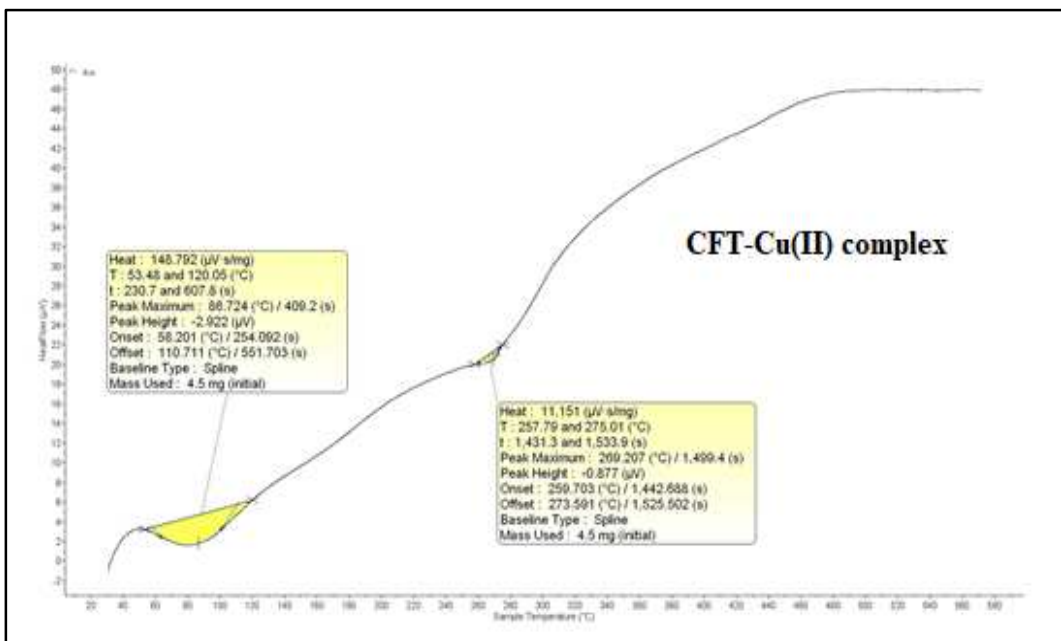


Figure 3.12. Thermogram (DSC) of copper coordinated ceftibuten dihydrate antibiotic.

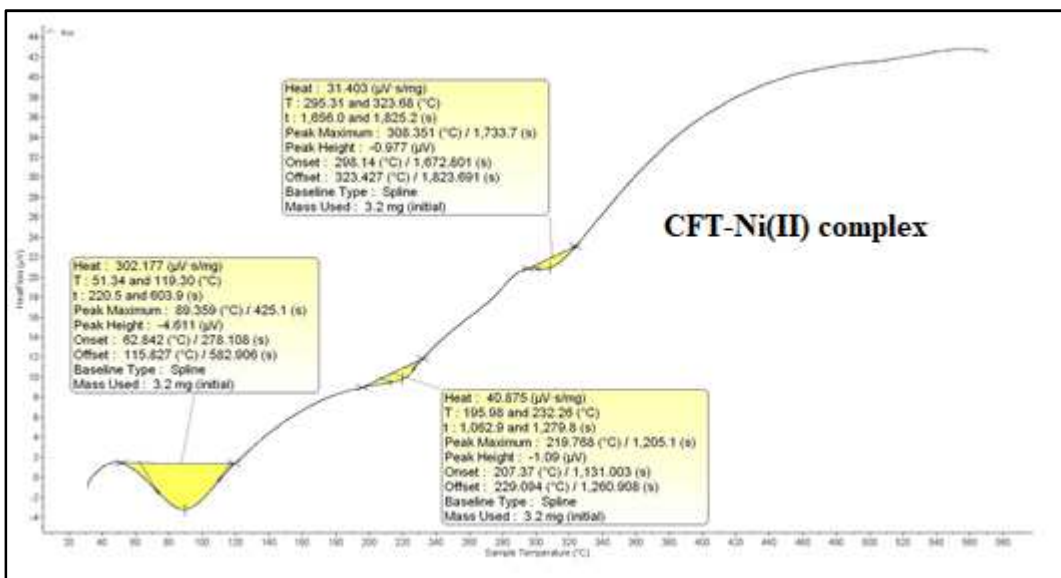


Figure 3.13. Thermogram (DSC) of nickel coordinated ceftibuten dihydrate antibiotic.

The DSC curve of Cu(II)-coordinated complex of CFT antibiotic showed two endothermic peaks, one peak at 87 °C which is due to the removal of water, and another peak at 269.2 °C which represents the melting temperature of the complex. On the other hand, three endothermic peaks are found in the DSC curve of Ni(II)-coordinated complex of CFT antibiotic. The peak at 89 °C is associated with the dehydration step followed by the peak at 220 °C which represents some reductions or phase transition. Another endothermic peak at 308 °C was found which is considered as the melting temperature of the complex. The melting points of the complexes Cu(II)-CFT (269.2 °C) and Ni(II)-CFT (308 °C), are different from the melting point of pure antibiotic, CFT (242.7 °C). These indicated the formation of new metal-coordinated complexes of CFT antibiotic. Similar thermal results were reported by different groups of researchers in the case of metal(II) complexation of different ligands [182-184]. The thermal results (TG, DSC) are concise in Table 3.4.

Table 3.4. TG-DSC results of CFT antibiotic and its metal(II)-coordinated complexes.

Compound	Stage	Temp. of TGA (°C)	Mass loss (%)	DSC Temp. (°C)	
				Endo	Exo
Ceftibuten dihydrate (CFT)	1 st	20-176	10	98	
	2 nd	176-396	46		242.7
	3 rd	396-630	36		
	4 th	630-800	7.31		
	Total loss			100	
Cu(II)-CFT	1 st	25-175	8.3	87	
	2 nd	175-312	26.3	269.2	
	3 rd	312-508	40.3		
	4 th	508-800	7.5		
	Total loss			82.57	
Residue			17.43		
Ni(II)-CFT	1 st	26-104	7.31	89	
	2 nd	104-221	6.57	219	
	3 rd	221-358	28.6	305	
	4 th	358-502	37.04		
	5 th	502-800	7.89		
Total loss			87.39		
Residue			12.61		

Ali *et al.* reported the same trend of decomposition of fluconazole-metal complexes, starting with the loss of water molecule followed by decomposition of ligand moiety, leaving metal oxide as residue. The DSC data of all the complexes of fluconazole also agreed well with the TG data [182]. On the other hand, a simultaneous TG/DTG/DTA analyses was done for the Ag(I)-complex of ceftibuten dihydrate. The Ag(I)-complex also showed a multi-stage degradation profile, where mass loss was observed with temperature. The thermogram (TG/DTG/DTA) is given in Figure 3.14 and the results are concise in Table 3.5.

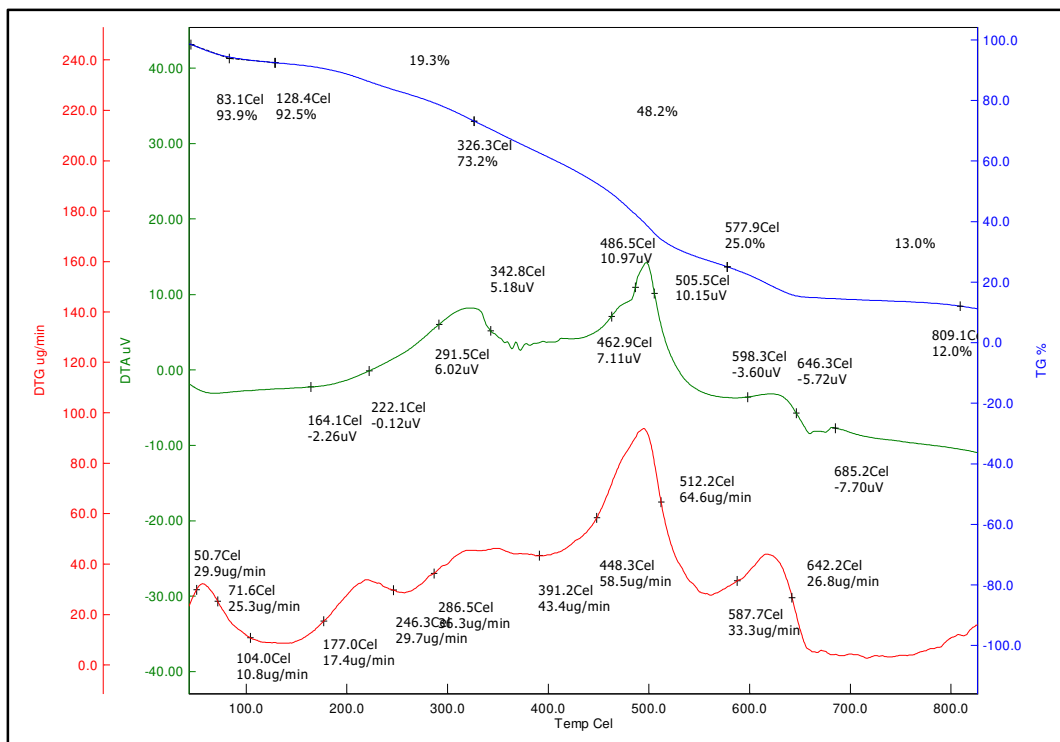


Figure 3.14. Thermogram (TG/DTG/DTA) of Ag-complex of ceftibuten dihydrate antibiotic.

In the TG curve, Ag(I)-CFT exhibited a loss of 7.5% of total mass at the temperature range of 25-128 °C in the 1st step which is due to the loss of crystalline water. After that, 19.3% and 48.2% mass loss were found at the temperature range of 128-326 and 326-578 °C, respectively. Finally, 13% mass loss was found at the temperature range 578-809 °C, leaving 12% residual mass (AgO). The DTG curve of Ag(I)-CFT showed two sharp peaks at around 310 °C and 495 °C which may be attributed to the degradation of the anhydrous complex. The DTA result showed two endothermic peaks at 140 °C (dehydration) and 266 °C (melting temperature). It also exhibited two sharp peaks at around 500 °C and 620 °C which were due to the decomposition of the complex. These indications are well in agreement with the DTG data.

Table 3.5. Thermal (TGA, DTG, and DTA) results of Ag(I) complex of ceftibuten dihydrate antibiotic.

Compound	Step	Temp. range (°C)	Mass loss (%)	DTG _{max} (T _{DTG})	DTA (T _{DTA})	
					Endo	Exo
Ag(I)-CFT	1 st	25 - 128	7.5	65		60.5
	2 nd	128 - 326	19.3	193, 316	140.5, 266	
	3 rd	326 - 578	48.2	402, 495	419, 549	480
	4 th	578 - 809	13	622, 665		614
Total loss			88			
Residue			12			

3.5. Elemental Analyses of Ceftributen Dihydrate with Cu(II), Ni(II) and Ag(I) Metal Ions

The elemental analyses of the metal complexes of ceftributen dihydrate antibiotic were performed and the results are given in Table 3.6. The results are well-fitted with the proposed molecular formula and agreed with 1:1 ligand to metal stoichiometry.

Table 3.6. Elemental analyses (C, H, N, and S) data of metal complexes of ceftributen dihydrate.

Compound (Mol. Formula)	Elemental Analysis							
	Carbon %		Hydrogen %		Nitrogen %		Sulfur %	
	Calc.	Found	Calc.	Found	Calc.	Found	Calc.	Found
Ni(II)-CFT [Ni(CFT)Cl ₂] 4H ₂ O	27.79	27.62	4.04	3.98	8.64	8.38	9.89	9.55
Ag(I)-CFT [Ag(CFT)NO ₃]6H ₂ O	24.86	24.79	4.17	4.32	9.66	9.81	8.85	8.72

3.6. Proposed Structure of Metal Complexes of Ceftibuten Dihydrate

The physical properties, spectral characterization, and thermal investigation confirmed the formation of new metal complexes with 1:1 metal-to-ligand stoichiometry. Based on analytical results, the following structure (Figure 3.15) of metal complexes is proposed.

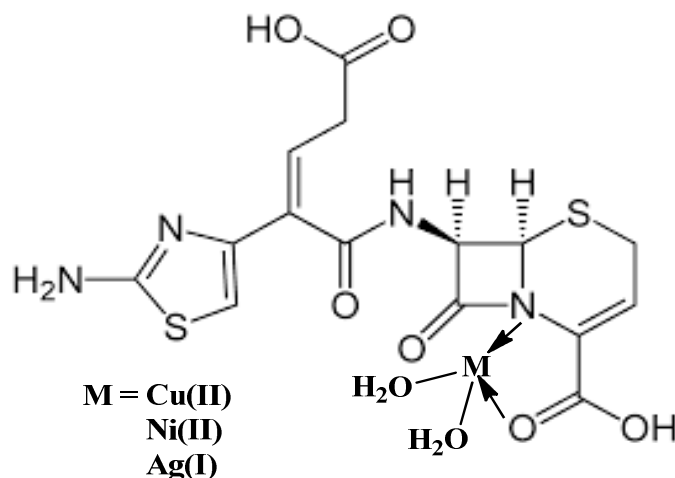


Figure 3.15. Proposed structure of metal complexes of ceftibuten dihydrate.

3.7. Biological Activities of Ceftibuten Dihydrate with Cu(II), Ni(II) and Ag(I) Metal Ions

Ceftibuten dihydrate is a cephalosporin antibiotic of third-generation. Cephalosporin is a largely used, mostly prescribed group. Because of overuse and

misuse of antibiotics, many antibiotics of the cephalosporin group have become resistant to various microbes. So, it is essential to find out new derivatives of cephalosporins with increased activity. It was reported that upon complexation with metals, many cephalosporin antibiotics like ceftriaxone [185], cefaclor [186], cefalexin [187], and cefotaxime [157] showed increased activity against several microbes. In the case of cefotaxime antibiotic, Anacona *et al.* [157] claimed the highest activity of Cu(II)-complex of cefotaxime against *S. aureus* being about 27% higher than the precursor antibiotic. In another study, Zaman *et al.* (2016) [185] worked on the complexation of several cephalosporin antibiotics namely ceftriaxone, ceftazidime, and cefepime. Fe, Cu, and Zn were used for complexation and the bacterial strains which were used to determine activity are *Staphylococcus*, *Achinobacter*, and *E. coli*. They found that most of the complexes showed increased activity against the tested microbes. Chohan *et al.* [186] reported the enhanced biological activity of the Co(II) and Ni(II)-complex of cefaclor. On the other hand, cephradine, one of the first generation cephalosporins showed significant activity against various microbes. Cephradine on complexation with metals like Cu, Mg, Ca, Cr, Co and Zn showed decreased activity against some microbes [175, 176]. But whenever complexation was done with transition metals and the ligand derived from cephradine and salicylaldehyde showed enhanced biological activity than cephradine itself [187]. Based on

experimental evidence, the proposed structure of the mixed ligand complex by Bukhari *et al.* is given in Figure 3.27 [187].

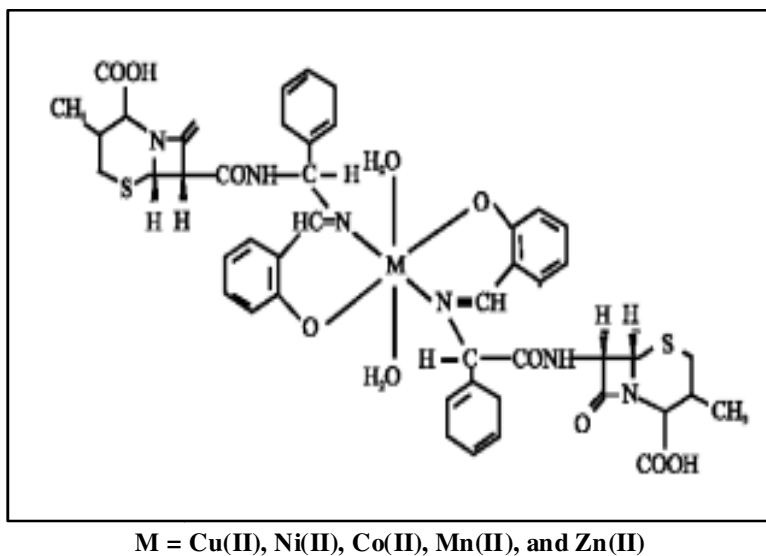


Figure 3.16. Proposed structure of salicylidine-cephradine metal complex.

In our study, the paper disc diffusion method is used to determine the antibacterial activity. Measuring the diameter of the inhibition zone in mm, the results are concise in Table 3.7. One of the representative agar plates showing antibacterial activity is given in Figure 3.17.

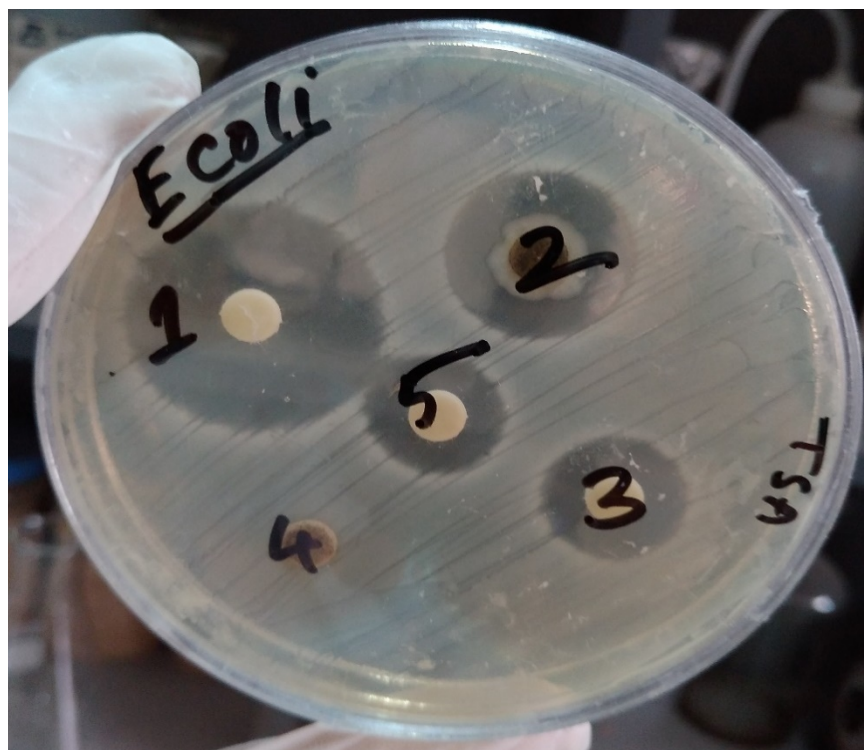


Figure 3.17. Antibacterial activity of CFT antibiotic and its metal complexes signified by inhibition zone diameter.

Table 3.7. Antibacterial activity of precursor antibiotic, ceftibuten dihydrate, and its metal complexes.

Microbial species	Inhibition zone (mm)			
	CFT (Ligand)	Cu(II)-CFT	Ni(II)-CFT	Ag(I)-CFT
<i>B. subtilis</i>	30	25	23	-
<i>S. aureus</i>	0	15	0	11
<i>S. typhi</i>	9	15	0	24
<i>E. coli</i>	23	0	0	30

From the given results, it is found that Cu(II)-CFT and Ag(I)-CFT showed excellent activity against *S. aureus* and *S. typhi* while Ni(II)-CFT possessed no activity against the microbes. The Ag(I)-CFT also showed increased activity toward *E. coli* while the Cu(II)-CFT and Ni(II)-CFT showed no activity toward *E. coli*. Upon chelation, the antibacterial activity of the complexes is increased [188]. The fact is that the lipo-solubility of the chelates is increased by the partial sharing of the positive charge of metal ions to ligand molecules and thus increases the permeation ability of the complexes through the lipid layers of the bacterial membrane. As a result, the cell wall protein formation would be stopped and the bacteria will die [188, 189]. Hence the activity of the parent antibiotic would be increased due to increased permeation of the antibiotic upon chelation.

3.8. Physical Properties of Cefpodoxime Proxetil with Cu(II), Ni(II) and Ag(I) Metal Ions

The physical properties of Cu(II), Ni(II), and Ag(I) complexes of cefpodoxime proxetil are presented in Table 3.8.

Table 3.8. Physical properties of the parent antibiotic and its metal complexes.

Sl No.	Code	Compound	Color	State	M. P. °C	% yield	Solubility in DMSO
1	CFP	Cefpodoxime proxetil	White to pale yellow	Amorphous	143	-	Soluble
2	CFP-Cu	Copper(II)-Complex	Blackish	Crystalline	219	70	Soluble
3	CFP-Ni	Nickel(II)-complex	Pale orange	Crystalline	234	62	Soluble
4	CFP-Ag	Silver(I)-complex	Dark brown	Crystalline	177	72	Soluble

Images of the parent antibiotic, antibiotic-metal complexes, and their solution are displayed in Figure 3.18.



Figure 3.18. Images of the metal complexes of CFP antibiotic and their solution in DMSO.

3.9. UV-Vis Spectrum Analysis of Cefpodoxime Proxetil with Cu(II) Metal Ion

The UV-vis spectrum of cefpodoxime proxetil antibiotic and its Cu(II)-complex are shown in Figure 3.19 and the spectral data are given in Table 3.9.

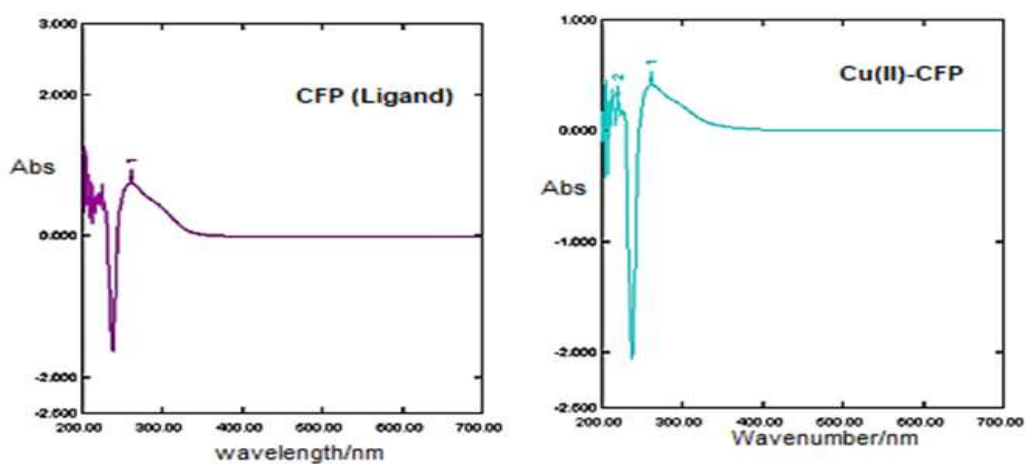


Figure 3. 19. UV-Vis spectrum of cefpodoxime proxetil and its Cu(II)-complex.

Table 3.9. UV-Vis spectral data of cefpodoxime proxetil and its Cu(II) complex.

Compound	Wavelength of electronic transition (nm)
CFP (parent antibiotic)	261, 238
Cu(II)-CFP	262, 236, 228

In the case of the complexation of cefpodoxime proxetil, shifting of absorption bands and a new band appeared due to the formation of coordination bonds with metal ions [190, 191].

3.10. FT-IR Studies of Cefpodoxime Proxetil with Cu(II), Ni(II) and Ag(I) Metal Ions

The bonding mode of metal ion to precursor antibiotic (ligand) can be ascertained by comparing the FT-IR spectra of the free ligand with corresponding metal complexes. The FT-IR spectrum of the CFP ligand is presented in Figure 3.20.

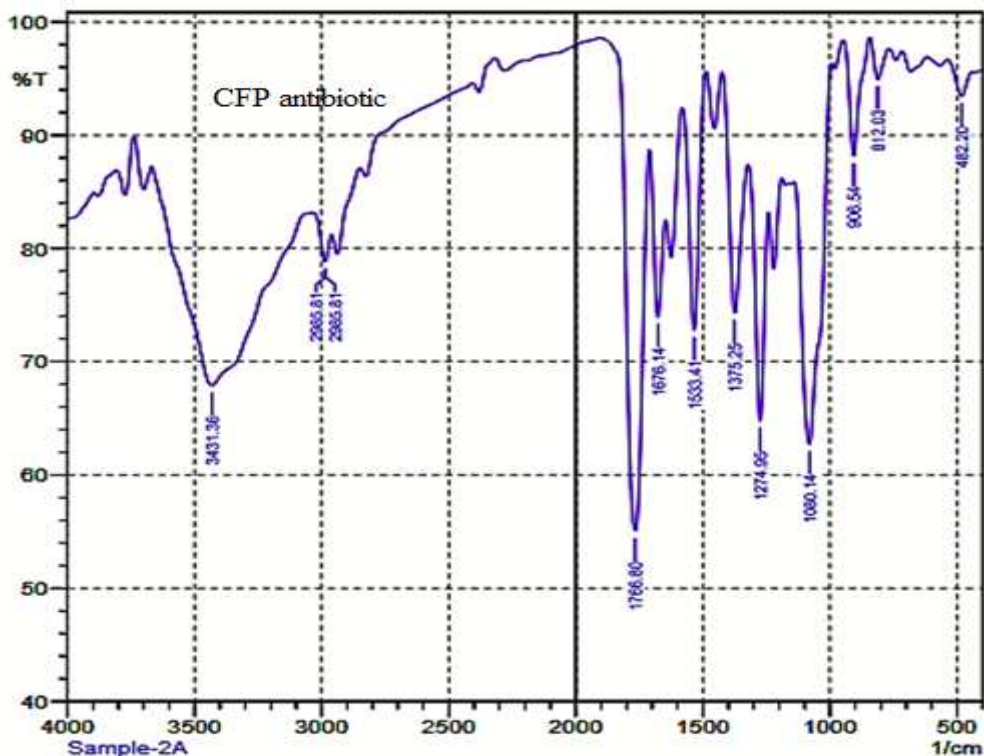


Figure 3.20. FT-IR spectrum of the antibiotic, Cefpodoxime proxetil (CFP).

Cefpodoxime proxetil (CFP) is an ester prodrug of cefpodoxime, belonging to the cephalosporin group, and contains a beta-lactam ring. Several coordination sites are available in the CFP ligand to interact with metals, but due to steric strain, it is not possible for metals to interact with all coordination sites. The FT-IR spectra of the metal complexes of the CFP ligand are presented in Figures 3.21-3.23, respectively.

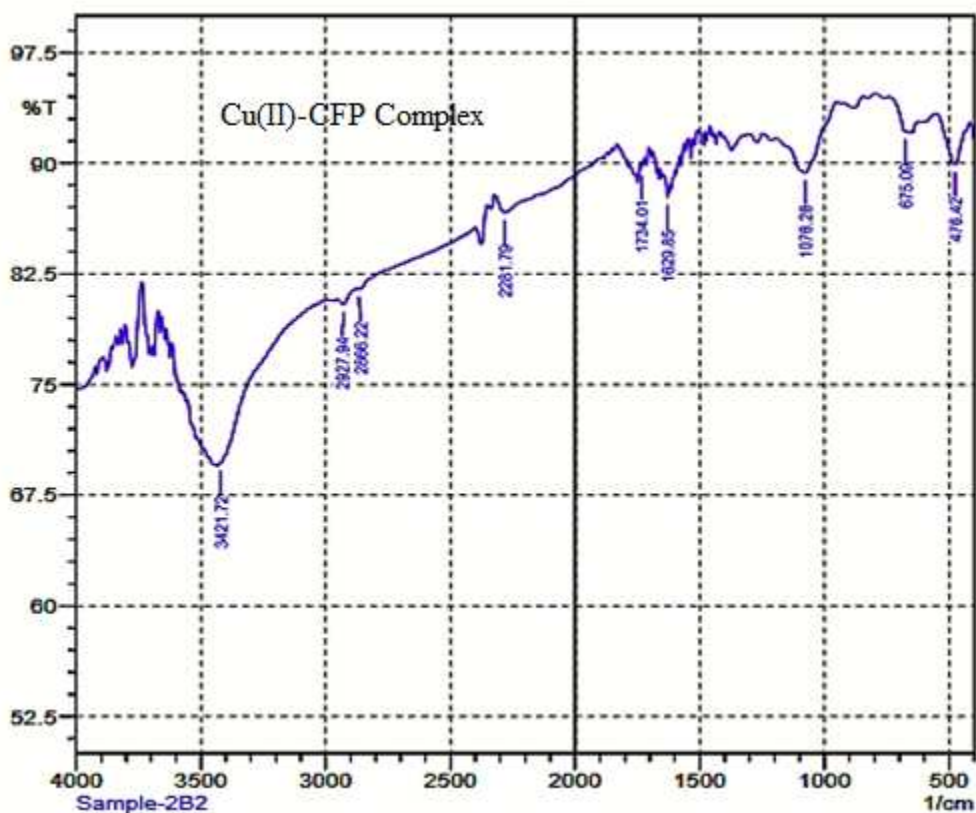


Figure 3.21. FT-IR spectrum of Cu(II)-complex of precursor antibiotic cefpodoxime proxetil (CFP).

In the FT-IR spectrum of the CFP ligand, it is observed that the lactam (C=O) appeared at 1766 cm^{-1} while the amide (C=O) and ester (C=O) overlapped at 1676 cm^{-1} . Upon complexation with metals, these bands shifted toward lower frequency. In the FT-IR spectrum of Cu(II)-CFP (Figure 3.21), the band of the lactam carbonyl group appeared at 1734 cm^{-1} while it was found at 1766 cm^{-1} (Figure 3.20) in the parent antibiotic. On the other hand, the band of the 2° amide (C=O) shifted to 1629 cm^{-1} upon complexation with Cu(II) metal, which was found at 1676 cm^{-1} in the precursor ligand (Figure 3.20). These changes are indicative of the involvement of the lactam carbonyl group and the amide carbonyl group in complexation with Cu(II) metal [192, 193].

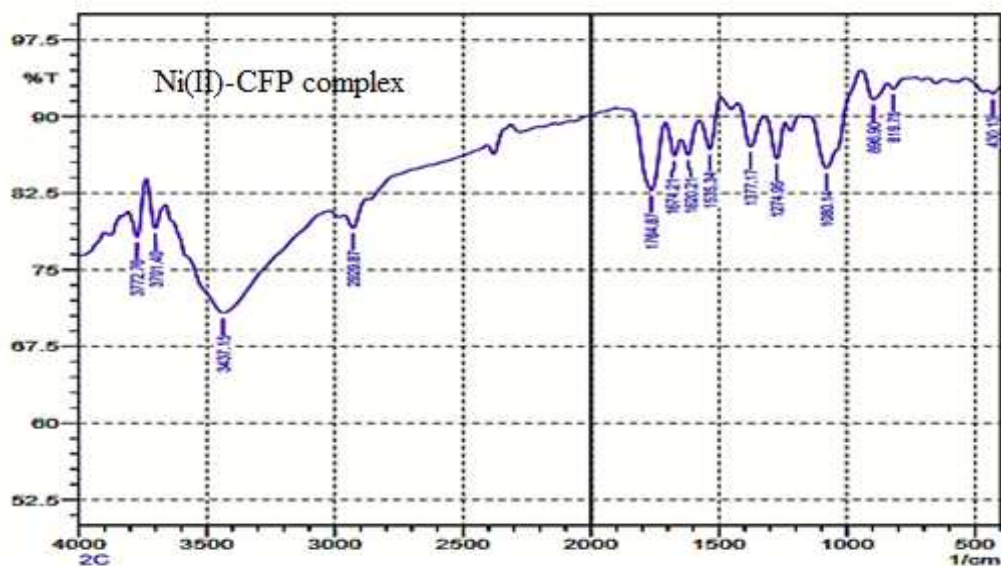


Figure 3.22. FT-IR spectrum of Ni(II)-complex of precursor antibiotic cefpodoxime proxetil (CFP).

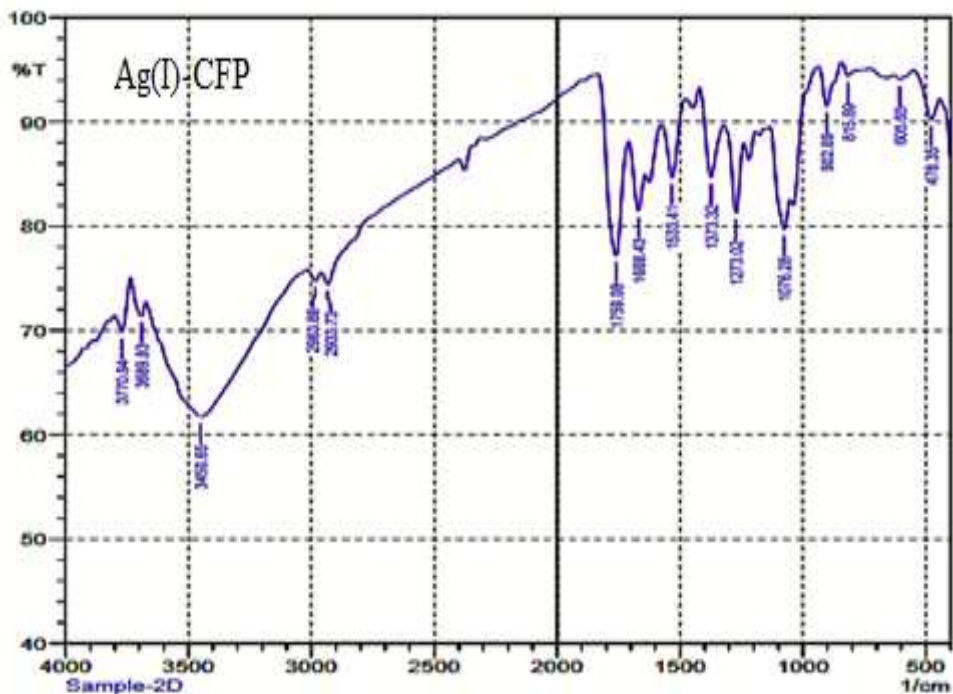


Figure 3.23. FT-IR spectrum of Ag(I)-complex of precursor antibiotic cefpodoxime proxetil.

The band of the lactam carbonyl group shifted to 1761 cm^{-1} in Ni(II)-CFP, and 1759 cm^{-1} in Ag(I)-CFP, indicative of the participation of the lactam carbonyl group in complexation [192]. On the other hand, in the case of the Ni(II)-CFP complex, the band of the 2° amide (C=O) group appeared at 1674 cm^{-1} merged with a prominent shoulder at 1620 cm^{-1} while in Ag(I)-CFP complex the amide carbonyl peak appeared at 1668 cm^{-1} merged with a prominent shoulder at 1615 cm^{-1} . Moreover, the presence of absorption bands in the region of $575\text{--}605\text{ cm}^{-1}$ in the FT-IR spectra of the complexes is due to the $\nu(\text{M-O})$, which also supports

the coordination of metal to the amide carbonyl group and lactam carbonyl group [194]. The M-N stretching vibration appeared at the 430-480 cm^{-1} range in the spectra of the complexes suggesting the involvement of the amine ($-\text{NH}_2$) group of the thiazole ring in complexation with metals [194]. The FT-IR spectral data of metal complexes of cefpodoxime proxetil were found almost similar to the free ligand, CFP [157], and have some characteristic bands which are given in Table 3.10.

Table 3.10. Characteristic FT-IR bands in cm^{-1} of Cu(II), Ni(II), and Ag(I)-CFP-complexes.

Complexes	ν_{CO} (lactam)	ν_{CO} (amide)	M- O*	M-N*
Cu(II)-CFP	1734	1629	655	476
Ni(II)-CFP	1764	1674 with a prominent shoulder at 1620	630	430
Ag(I)-CFP	1759	1668 with a prominent shoulder at 1615	605	478

M-N* indicates metal nitrogen coordinate bonding

M-O* indicates metal oxygen coordinate bonding

Ceftiofur hydrochloride, one of the third-generation cephalosporins (Figure 3.24). In the case of metal complexation of ceftiofur hydrochloride, Tendon *et al.* reported the coordination of metal ions (Fe, Cu, Ni, Ca, and Mn) through the

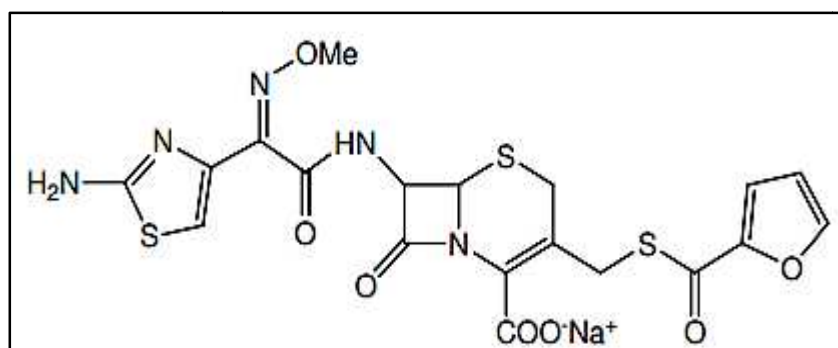


Figure 3.24. Structure of ceftiofur hydrochloride.

lactam carbonyl, amidic carbonyl group and the amino group of the thiazole ring based on the shifting of frequency of the lactam carbonyl group as well as the amidic carbonyl group and appearance of the new band at 430-480 cm^{-1} [192]. Alternatively, the N atom in the $\text{C}=\text{N}-\text{OCH}_3$ group may also participate in complexation with metal ions, but the simultaneous coordination of the $\text{C}=\text{N}-\text{OCH}_3$ group along with the lactam carbonyl and amide carbonyl group is not possible due to steric strain [157, 195]. The peaks for $\text{C}=\text{N}$ and $\text{C}-\text{N}$ stretching vibrations were found at 1533 cm^{-1} and 1375 cm^{-1} in the FT-IR spectrum of the CFP ligand. These peaks were not changed in the spectra of the complexes, indicating the nonparticipation of lactam nitrogen and thiazole nitrogen atom in coordination with metals [192]. These observations suggested the involvement of

the -NH₂ group in the coordination process. Moreover, the bands appearing at 3431 cm⁻¹ and 2985 cm⁻¹ in the CFP ligand designated N–H stretching and aromatic C–H stretching, respectively. A broad band in the range of 3200 - 3600 cm⁻¹ appeared in the FT-IR spectra of all the complexes revealing the presence of coordinated water in the complexes [196].

3.11. Interpretation of ¹H NMR of Cefpodoxime Proxetil with Cu(II), Ni(II), and Ag(I) Metal Ions

The ¹H NMR data of the antibiotic, cefpodoxime proxetil are listed in Table 3.11 and the spectrum is shown in Figure 3.25.

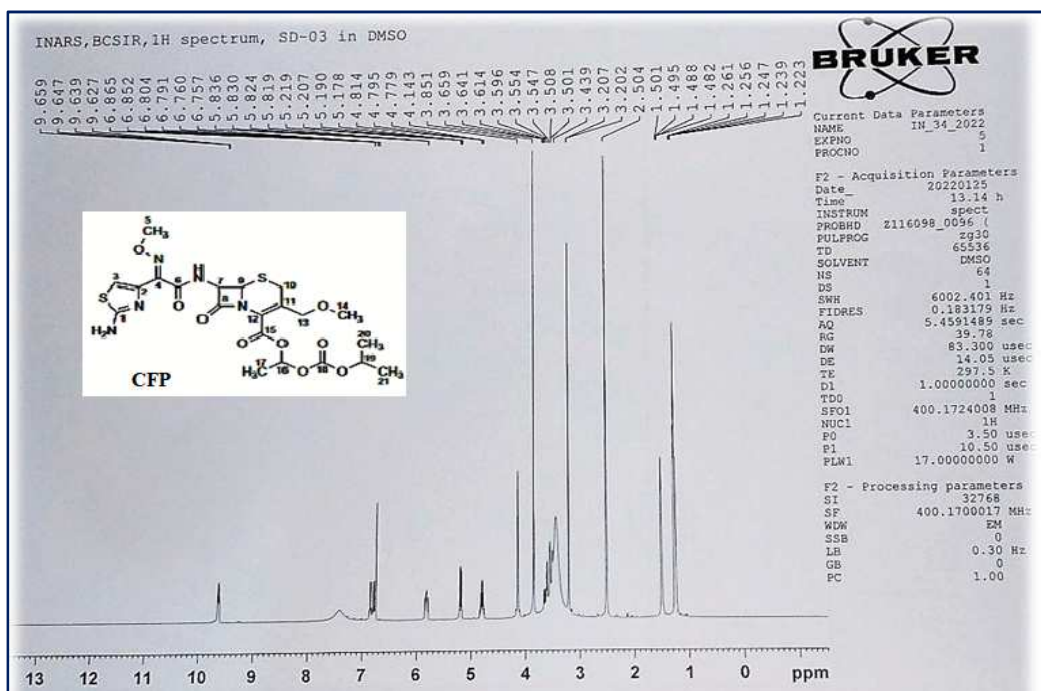


Figure 3.25. ¹H NMR spectrum of cefpodoxime proxetil (free ligand) antibiotic.

Table 3.11. Assignments of ^1H NMR bands of cefpodoxime proxetil (CFP) in DMSO- d_6 .

Chemical shift, δ ppm (Ligand)	No. of protons	Multiplicity	Assignments (proton at carbon No.)
1.22– 1.26	6	Multiplet	20, 21 (2 CH ₃)
1.48–1 .50	3	Multiplet	17 (CH ₃ CH)
3.20	3	Singlet	14 (OCH ₃)
3.54– 3.56	2	Multiplet	10 (S-CH ₂)
3.85	3	Singlet	5 (N-O-CH ₃)
4.14	2	Multiplet	13 (CH ₂ -O)
4.77– 4.81	1	Multiplet	19 [CH(CH ₃) ₂]
5.18 – 5.21	1	Multiplet	9 (N-CH-)
5.82 – 5.84	1	Multiplet	7 (CO-CH)
6.75	1	Singlet	3 (S-CH=)
6.85	1	Multiplet	16 (O-CH-)
7.35	2	br, s	NH ₂
9.63	1	Multiplet	NH

From the FT-IR study, it is concluded that CFP acted as a tridentate ligand and bonded to the metal ions through the beta-lactam carbonyl group (C-8), the carbonyl group of 2^o amide (C-6), and the amine (1^o) group nearer to C-1. However, owing to the complexation with metal ions, the signal of protons nearer to the binding site (C-7, C-9) shifted as a result of extended conjugation upon

coordination. Moreover, the NH₂ protons and NH (2° amide) proton which are directly involved in complexation also changed their chemical shift values [124, 197]. In the CFP ligand, the proton signals of C-7 (CO-CH) and C-9 (N-CH-) appeared as multiplet in the δ 5.81–5.83 ppm and δ 5.17–5.21 ppm regions. The signal of NH (2° amide) appeared at δ 9.62 ppm and the NH₂ (1° amine) protons signal appeared at δ 7.35 ppm as a broad singlet.

The ¹H NMR spectra of Cu(II), Ni(II), and Ag(I) complexes are given in Figures 3.26, 3.27, and 3.28, respectively. The characteristic NMR signals which were changed due to complexation are listed in Tables 3.12, 3.13, and 3.14.

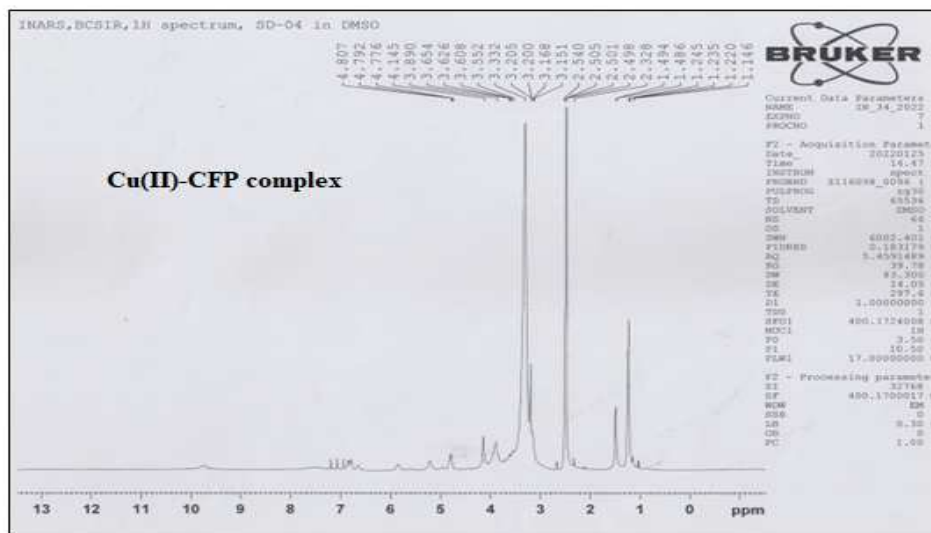


Figure 3.26. ^1H NMR spectrum of Cu(II)-complex of precursor antibiotic, cefpodoxime proxetil (CFP).

Table 3.12. Assignments of characteristic ^1H NMR bands of Cu(II)-CFP in comparison to CFP (parent antibiotic).

Chemical shift, δ ppm (CFP)	Chemical shift, δ ppm (Cu- CFP)	No. of protons	Assignments (protonated carbon No.)
5.18	5.25	1	C-9, (N-CH)
5.82	5.9	1	C-7, (CO-CH)
7.35	7.5	2	NH_2
9.63	9.8	1	NH

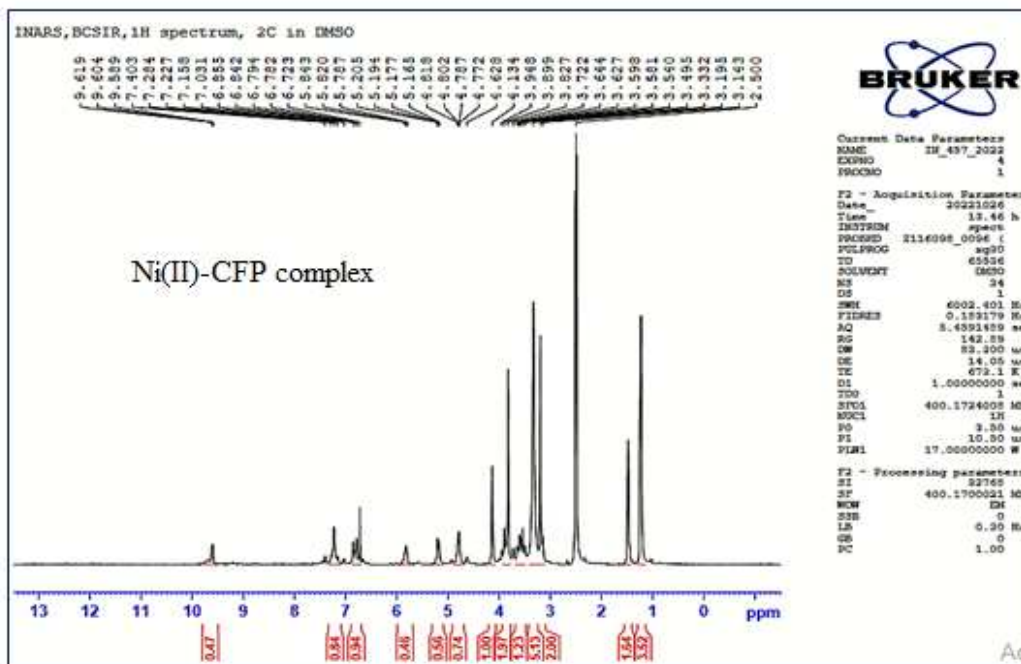


Figure 3.27. ^1H NMR spectrum of Ni(II) complex of precursor antibiotic, cefpodoxime proxetil (CFP).

Table 3.13. Assignments of characteristic ^1H NMR bands of Ni(II)-CFP in comparison to CFP (Parent antibiotic).

Chemical shifts, δ ppm, CFP	Chemical shifts, δ ppm, NI(II)-CFP	No. of protons	Assignments (proton at carbon No.)
5.18	5.16	1	C-9 (N - CH)
5.82	5.78	1	C-7 (CO - CH)
7.35	7.4	2	NH ₂
9.63	9.58	1	NH

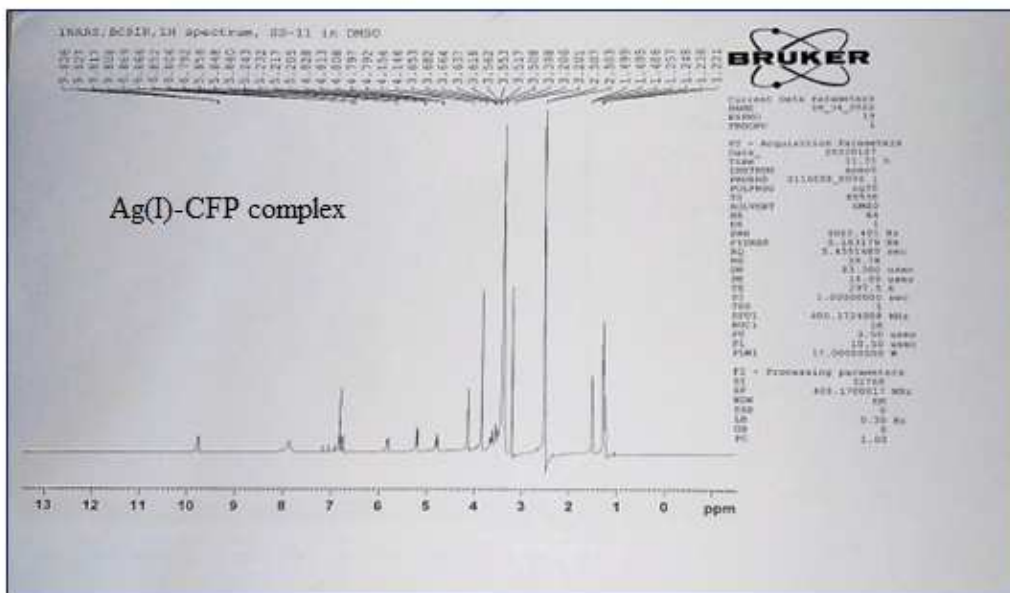


Figure 3.28. ^1H NMR spectrum of Ag(I) complex of precursor antibiotic cefpodoxime proxetil (CFP).

Table 3.14. Assignments of ^1H NMR bands of Ag(I)-CFP in comparison to CFP (Parent antibiotic).

Chemical shift, δ ppm (CFP)	Chemical shift, δ ppm, Ag(I)-CFP	No. of protons	Assignments (proton at carbon No.
5.18	5.20	1	C - 9 (N-CH)
5.82	5.84	1	C - 7 (CO-CH)
7.35	7.9	2	NH ₂
9.63	9.81	1	NH

3.12. Thermal Analyses of Cefpodoxime Proxetil with Cu(II), Ni(II), and Ag(I) Metal Ions

The thermal behavior of the antibiotic, cefpodoxime proxetil and its metal complexes were studied by using a simultaneous TG-DTA instrument where the temperature was raised to 1000 °C and a heating rate of 10 °C/min was maintained. TG along with DTG gives important information about the thermal behavior of the complexes. The whole thermal decomposition events as well as the stability of the complexes can be identified from a TG/DTG curve [178, 198]. The maximum temperature (T_{DTG}), where the weight loss is most apparent along with the corresponding weight loss of every step of the decomposition of the antibiotic and is listed in Table 3.15. The TG/DTG/DTA diagram of the precursor antibiotic, CFP is given in Figure 3.29.

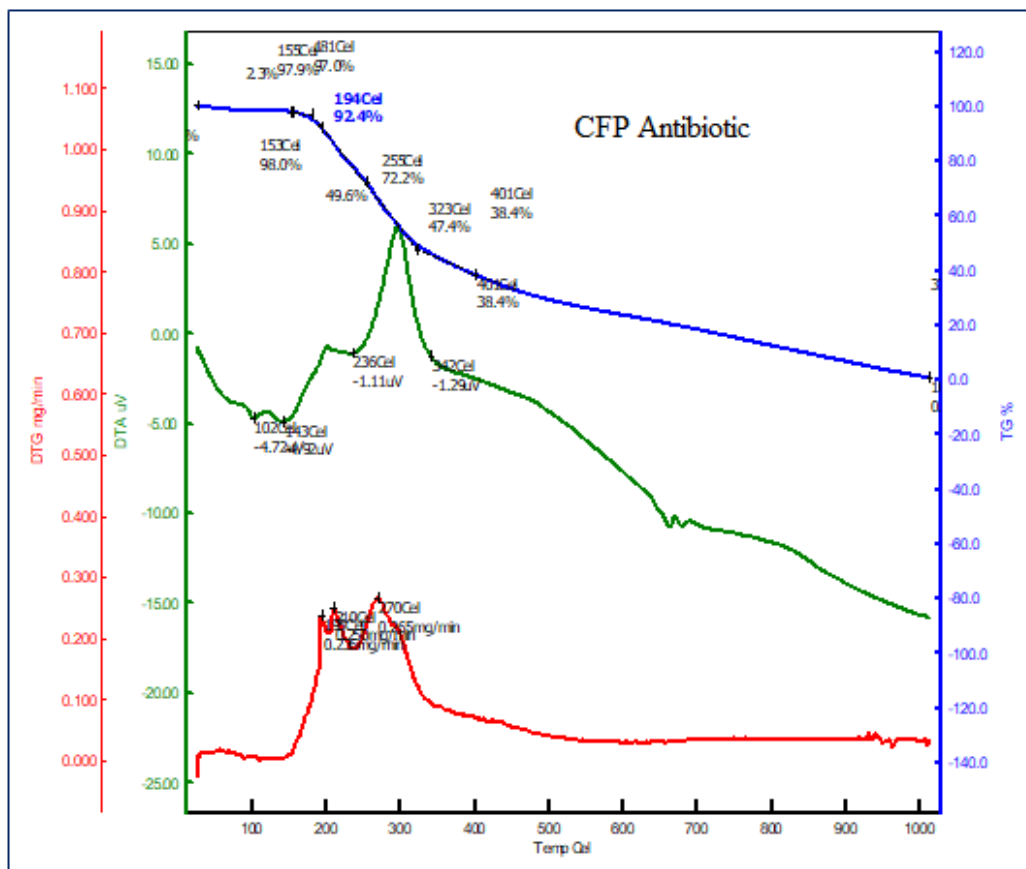


Figure 3.29. Thermogram (TG/DTG/DTA) of the precursor antibiotic, cefpodoxime proxetil (CFP).

The TG curve of the ligand showed that CFP decomposed in three steps. The 1st step corresponded to a weight loss of 7.6% at the temperature range of 25–194 °C which was followed by a weight loss of 45% at the temperature range of 194–333 °C. In the third step, a weight loss of 47% was found at the temperature range of

334-1000 °C. The ligand was fully decomposed and no residual mass was found. The DTG and DTA results were also comparable with the TG data. The DTA curve showed an endothermic peak at 143 °C corresponds to the melting temperature of the ligand.

Table 3.15. Thermal (TG/DTG/DTA) results of parent antibiotic, cefpodoxime proxetil (CFP).

Compound	Decomp. Step	Temperature range (°C)	Weight loss (%)	DTG _{max} (T _{max})	DTA (T _{DTA})	
					Endo	Exo
CFP	1 st	25 - 194	7.6		102, 143	192
(Parent antibiotic)	2 nd	194 – 333	45	195, 210, 240, 270	236	210, 289
	3 rd	334 - 1000	47.4			
	Total loss		100			
	Residue		-			

The metal complexes of CFP also showed a multistage degradation profile where mass changes occurred with increasing temperature. The thermograms of Cu(II),

Ni(II), and Ag(I) are given in Figures 3.30, 3.31, and 3.32, respectively. The thermal results are summarized in Table 3.16.

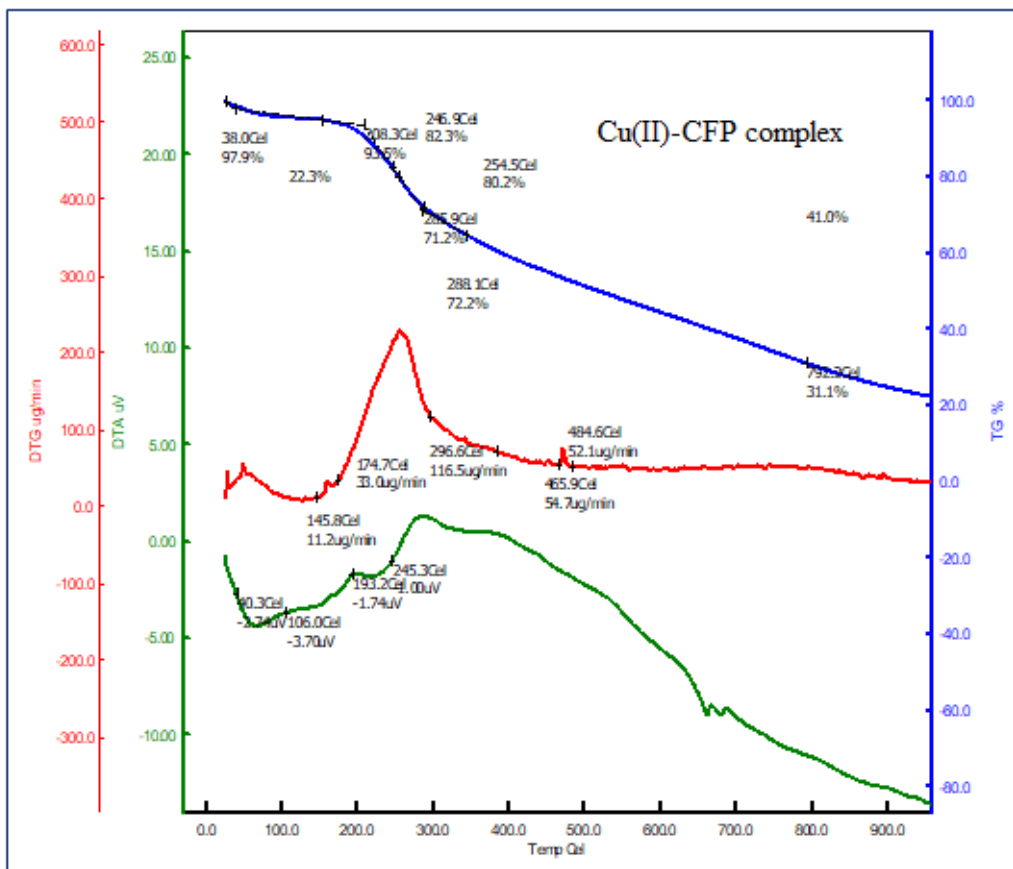


Figure 3.30. Thermogram (TG/DTG/DTA) of Cu(II)-complex of cefpodoxime proxetil.

The TG curve of Cu(II)-CFP (Figure 3.30) was composed of three decomposition steps. The 1st step of degradation occurred at 25-208 °C with maxima at 159 °C corresponds to a weight loss of 6.5%, which may be due to the loss of coordinated

water. In the 2nd step, a weight loss of 22.3% was found in the temperature range of 208 – 286 °C with a maximum at 235 °C. The third step of decomposition occurred with a maximum at 474 °C, in the temperature range of 286–792 °C, accompanied by a weight loss of 40.1%, leaving 31.1% as residue at 800 °C. This implies that the Cu(II)-CFP is thermally more stable than CFP ligand. The T_{DTA} values in the DTA curve were well in agreement with TG and DTG results. The DTA curve showed an endothermic peak at 219 °C, corresponding to the melting temperature of the complex, different from the melting temperature of the ligand (143 °C), indicating the formation of a new metal complex.

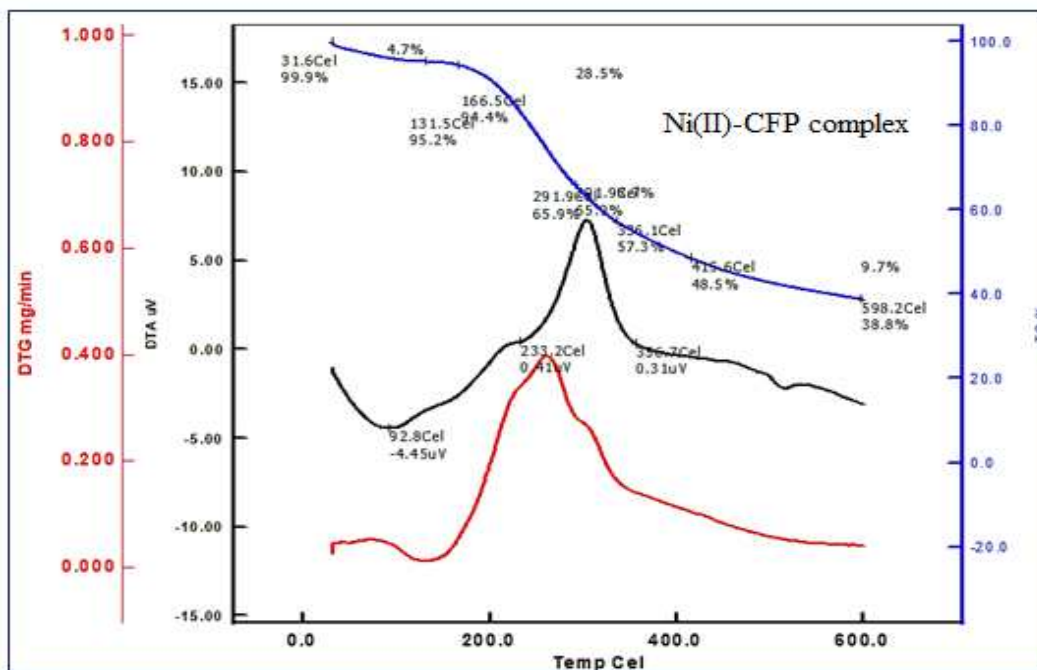


Figure 3.31. Thermogram (TG/DTG/DTA) of Ni(II)-complex of cefpodoxime proxetil.

On the other hand, the thermal decomposition of Ni(II)-CFP complex (Figure 3.31) proceeded by following four steps. The 1st step of decomposition occurred at the temperature range 31-166.5 °C, corresponds to 5.5% weight loss, which may be associated with the release of lattice water and coordinated water. In the 2nd step 28.5% weight loss was observed at the temperature range 292-336 °C and 8.6% weight loss was found in the 3rd step at the temperature range 336-600 °C, which were associated with the degradation of anhydrous complex. Finally, 18.5% weight loss was observed at the temperature range 336-600 °C, leaving metal oxide as residue. The T_{DTG} values in DTG curve were comparable with TG results. In the DTA curve of Ni(II)-CFP, there found an endothermic peak at 93 °C which was due to dehydration and another endothermic peak at 233 °C was found which corresponds to melting temperature of the complex.

The TG curve of Ag(I)-CFP (Figure 3.32) exhibited four decomposition steps in the temperature ranges 25-156, 156-237, 237-362, and 362-1000 °C. The degradation pattern of the complex was completely different from the ligand (CFP), indicating the successful interaction of metal to the ligand. The 1st step of decomposition occurred with three maxima at 62, 109, and 146 °C corresponding to a weight loss of 6.9%, associated with the loss of coordinated water. This was also supported by FT-IR data.

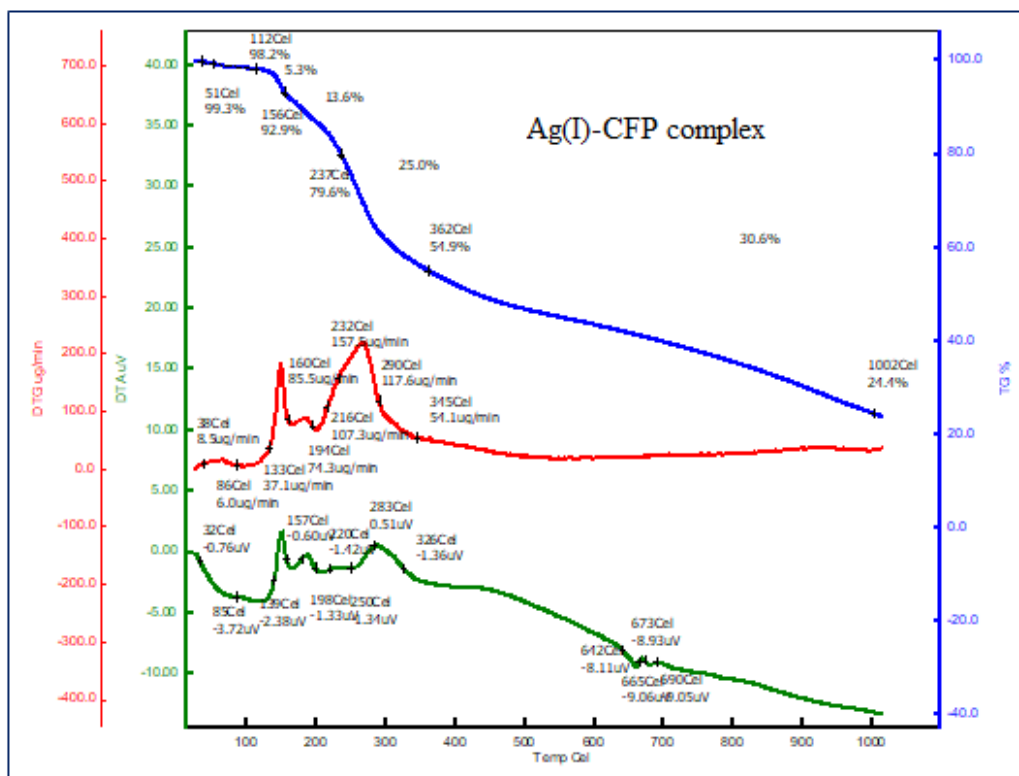


Figure 3.32. Thermogram (TG/DTG/DTA) of Ag(I)-complex of cefpodoxime proxetil.

In the 2nd step, a weight loss of 13.3% was observed with two maxima at 177 and 205 °C in the DTG curve. The third and fourth steps of decomposition proceeded with 24.7 and 30.5% of weight loss, respectively, associated with the degradation of the anhydrous complex. Finally, 24.4% residual mass was obtained even after heating to 1000 °C which indicated the significant thermal stability of the

complex. The DTA curve showed endothermic peaks at 112, 177, 205, and 266 °C. The endothermic peak at 177 °C in the DTA curve corresponds to the melting point of the complex.

Table 3.16. Thermal (TG/DTG/DTA) results of Cu(II) and Ag(I) - complexes of cefpodoxime proxetil (CFP).

Complex	Decomp. step	Temp. range (°C)	Weight loss (%)	DTG _{max} (T _{DTG})	DTA (T _{DTA})	
					Endo	Exo
Cu(II)- CFP	1 st	25–208	6.5	159	93, 149	
	2 nd	208–286	22.3	235	219	
	3 rd	286–792	40.1	474.5		
	Total loss		68.9			
Residue		31.1				
Ag(I)- CFP	1 st	25–156	6.9	109, 146		
	2 nd	156–237	13.3	177, 205	177, 205	148, 209
	3 rd	237–362	24.7	317.5	266, 343	283
	4 th	362–1000	30.5			
Total loss		75.6				
Residue		24.4				

Similar results were found in the metal complexation of penicillin G and ciprofloxacin, where decomposition starts with the loss of lattice water [156]. The last mass loss observed strictly corresponded to the mass loss of two antibiotic molecules, leaving 15% and 14% residue in case metal complexes of penicillin G and ciprofloxacin, respectively.

3.13. Elemental Analyses of Cefpodoxime Proxetil with Cu(II), Ni(II), and Ag(I) Metal Ions

The elemental analysis data supported the formation of new metal complexes with a 1:1 ligand-to-metal stoichiometry. The data are tabulated in Table 3.17.

Table 3.17. Elemental analysis data of the metal complexes of cefpodoxime proxetil.

Complex	Elemental analysis							
	Carbon %		Hydrogen %		Nitrogen %		Sulphur %	
	Calc.	Found	Calc.	Found	Calc.	Found	Calc.	Found
[Cu(CFP)(H ₂ O) ₂] SO ₄ .2H ₂ O	31.95	31.63	4.47	4.40	8.88	8.76	12.18	12.06
[Ni(CFP)(H ₂ O)]	39.76	39.40	4.61	4.11	11.04	11.85	10.11	10.37
[Ag(CFP)(H ₂ O) ₂] .2H ₂ O	34.19	34.59	4.78	4.71	9.49	9.46	8.69	8.48

3.14. Proposed Structure of Metal Complexes of Cefpodoxime Proxetil with Cu(II), Ni(II), and Ag(I) Metal Ions

Cefpodoxime proxetil (CFP) is a beta-lactam cephalosporin antibiotic of 3rd generation. As a ligand, CFP has several potential donor atoms and due to steric strain, it is not possible to form complexes with the participation of more than three donor atoms [151]. In an attempt to find out the coordination mode of CFP, firstly the metal complexes of cefpodoxime proxetil were successfully synthesized and then different spectral techniques like UV-Vis, FT-IR, NMR spectroscopy, and thermal investigation were done to establish the structure of the metal complexes. Based on all analytical results, it was concluded that coordination of CFP to the metal ions occurred through the oxygen atom of beta-lactam (C=O), the oxygen atom of 2^o amide (C=O), and the amine group of the thiazole ring. The proposed structure of metal complexes of CFP is given in Figure 3.33.

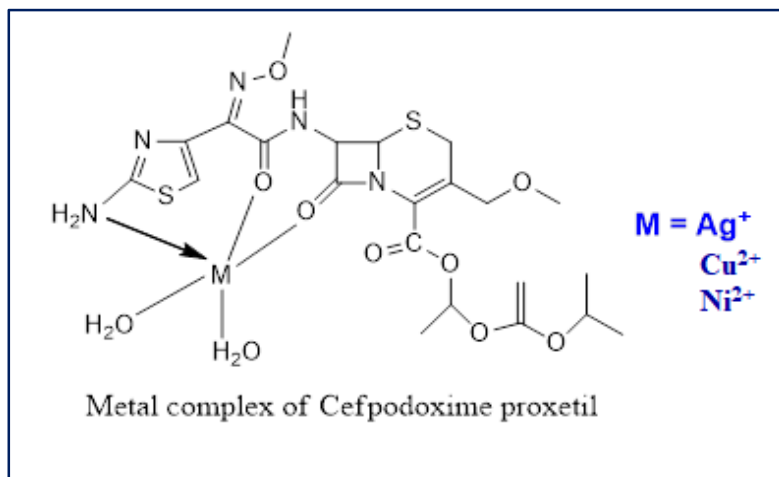


Figure 3.33. Proposed structure of metal complexes of cefpodoxime proxetil (CFP).

3.15. Biological Activities of Cefpodoxime Proxetil with Cu(II), Ni(II), and Ag(I) Metal Ions

Cefpodoxime proxetil (CFP), belonging to the cephalosporin antibiotic of 2nd generation is a bactericidal antibiotic. Like other antibiotics of the cephalosporin group, the bactericidal activity of CFP results from the inhibition of cell wall synthesis through the inhibition of enzymes in the cell wall, which are responsible for the framework of the bacterial cell membrane [199]. As a result, bacterial growth would be stopped and leading to the lysis of the bacterial cell. The bactericidal activity of CFP can be enhanced through the formation of

coordination bonds with metal ions. The increased activity of several cephalosporin antibiotics through complexation with metals has been reported previously [164, 186, 187]. It is also noticed that there is no effect on the antibacterial activity of cephalexin [173] and cefazolin [172] upon chelation with cadmium ions and copper ions, respectively. Sometimes the antimicrobial activity of antibiotics can be decreased through complexation with metal ions [200].

The Paper disc diffusion method was used to study the *in vitro* bactericidal activity against a long range of bacterial strains including both Gram-positive and Gram-negative. The bacterial strains used in this investigation were *B. cereus*, *E. coli* 0157, *E. coli*, *P. aeruginosa*, *S. aureus*, *Listeria*, *S. typhi*, *V. cholerae*, *K. pneumoniae*, *C. freundii*, *E. faecalis*, *E. faecium*. Tendon *et al.* observed the increased bactericidal activity of ceftiofur hydrochloride through complexation with metal ions [192]. Most of the synthesized metal complexes showed better bactericidal activity than the parent drug. One of the representative agar plates showing the antimicrobial activity of metal complexes of cefpodoxime proxetil is given in Figure 3.34 and the results of the bactericidal activity of CFP antibiotic and its metal complexes are concise in Table 3.18.



Figure 3.34. An agar plate showing antimicrobial activity signified *via* inhibition zone diameter in mm.

Table 3.18. Bactericidal activities of CFP antibiotic and its metal complexes, represented as inhibition zone diameter values/mm.

Compound	Bacterial strains											
	1*	2*	3*	4*	5*	6*	7*	8*	9*	10*	11*	12*
CFP	25	17	16	20	12	23	20	10	19	18	15	18
Cu(II)-CFP	13	10	6	13	6	14	10	6	8	8	6	6
Ni(II)-CFP	24	17	15	19	11	21	19	10	19	17	13	16
Ag(I)-CFP	25	16	15	20	17	22	19	10	18	16	14	20

1* = *B. cereus*, 2* = *E. coli* 0157, 3* = *E. coli*, 4* = *P. aeruginosa*, 5* = *S. aureus*,
6* = *Listeria*, 7* = *S. typhi*, 8* = *V. cholerae*, 9* = *K. pneumoniae*, 10* = *C. freundii*,
11* = *E. faecalis*, 12* = *E. faecium*.

From the results, it is observed that the bactericidal activity of the CFP antibiotic decreased upon complexation with Cu(II) metal ion while the bactericidal activity of Ni(II)-CFP and Ag(I)-CFP were comparable with the parent antibiotic (CFP). The Ni(II)-CFP showed a similar activity as the parent ligand, i.e. had no effect upon complexation with Ni(II) ion. Interestingly, the bactericidal activity of CFP increased against *S. aureus* and *E. faecium* upon complexation with Ag(I) metal ion. Generally, antibiotics on complexation with metals increase the liposolubility of the complex and thus enhance the permeation ability of the complex through the lipid layer of the bacterial cell membrane, which results in the increased bactericidal activity of the antibiotics on metal complexation. Several factors like steric, electronic, pharmacokinetic and mechanism of action are associated with metal complexation for the bactericidal activity of the complexes [200, 201].

3.16. Physical Properties of Cefuroxime Axetil with Cu(II) and Ni(II) Metal Ions

Cefuroxime axetil (CFU) is also an orally taken cephalosporin antibiotic of 2nd generation. It is an ester prodrug of cefuroxime. Like other cephalosporins, it contains a beta-lactam ring which is responsible for its bactericidal activity. The physical properties of Cu(II) and Ni(II) complexes of cefuroxime axetil are presented in Table 3.19.

Table 3.19. Physical properties of the parent antibiotic and its metal complexes.

Sl No.	Code	Compound	Color	State	M. P. °C	% yield	Solubility in DMSO
1	CFU	Cefuroxime axetil	White	Amorphous	204	-	Soluble
2	CFU-Cu	Copper(II)-complex	Dirty green	Amorphous	272	85	Soluble
3	CFU-Ni	Nickel(II)-complex	Deep brown	Crystalline	304	82	Soluble

Images of the parent antibiotic, antibiotic-metal complexes, and their solutions are displayed in Figure 3.35.



Figure 3.35. Cefuroxime axetil and its metal complexes.

3.17. UV-VIS Spectra Analyses of Cefuroxime Axetil with Cu(II) and Ni(II) Metal Ions

The electronic spectra of the cefuroxime axetil antibiotic and its metal complexes are shown in Figure 3.36 and 3.37, respectively. In the case of coordination complexes, the electronic transition involves the metal ion itself and the ligands. So, the possible types of transitions are the d-d transition and the charge transfer transition. The charge transfer transition may be either LMCT (ligand-to-metal charge transfer) or MLCT (metal-to-ligand charge transfer). Usually, d-d transitions are weak relative to charge transfer transition [202]. Shifting of the absorption band, appearance, and disappearance of the absorption band is indicative of complex formation.

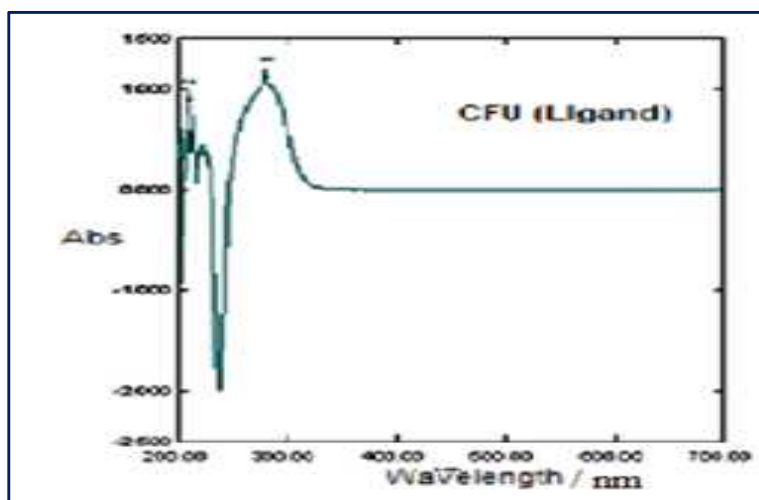


Figure 3.36. Electronic spectrum of the cefuroxime axetil antibiotic.

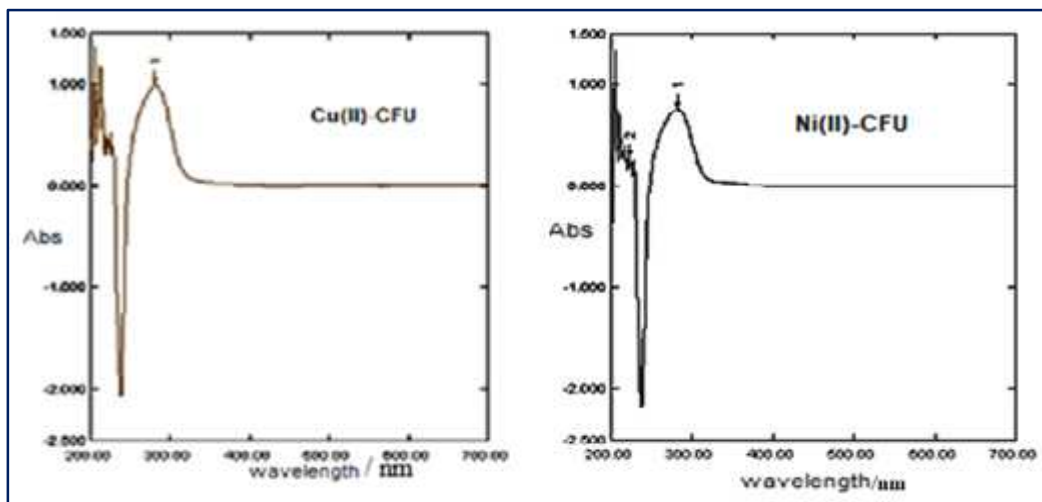


Figure 3.37. Electronic spectra coordination complexes of cefuroxime axetil antibiotic.

The spectral data are given in Table 3.20.

Table 3.20. UV-Vis spectral data of cefuroxime axetil along with its complexes.

Compound	Wavelength of electronic transition (nm)
CFU (parent antibiotic)	281, 209, 238
Cu(II)- complex	281, 237
Ni(II)-complex	282, 223, 237

3.18. FT-IR Studies of Cefuroxime Axetil with Cu(II), Ni(II) and Ag(I) Metal Ions

FT-IR gives important information regarding the functional groups present in the molecule. As a ligand, the CFU antibiotic possesses several characteristic functional groups: beta-lactam (C=O), 2^o amide, and an ester functional group. The FT-IR spectrum of CFU antibiotic (ligand) is presented in Figure 3.38.

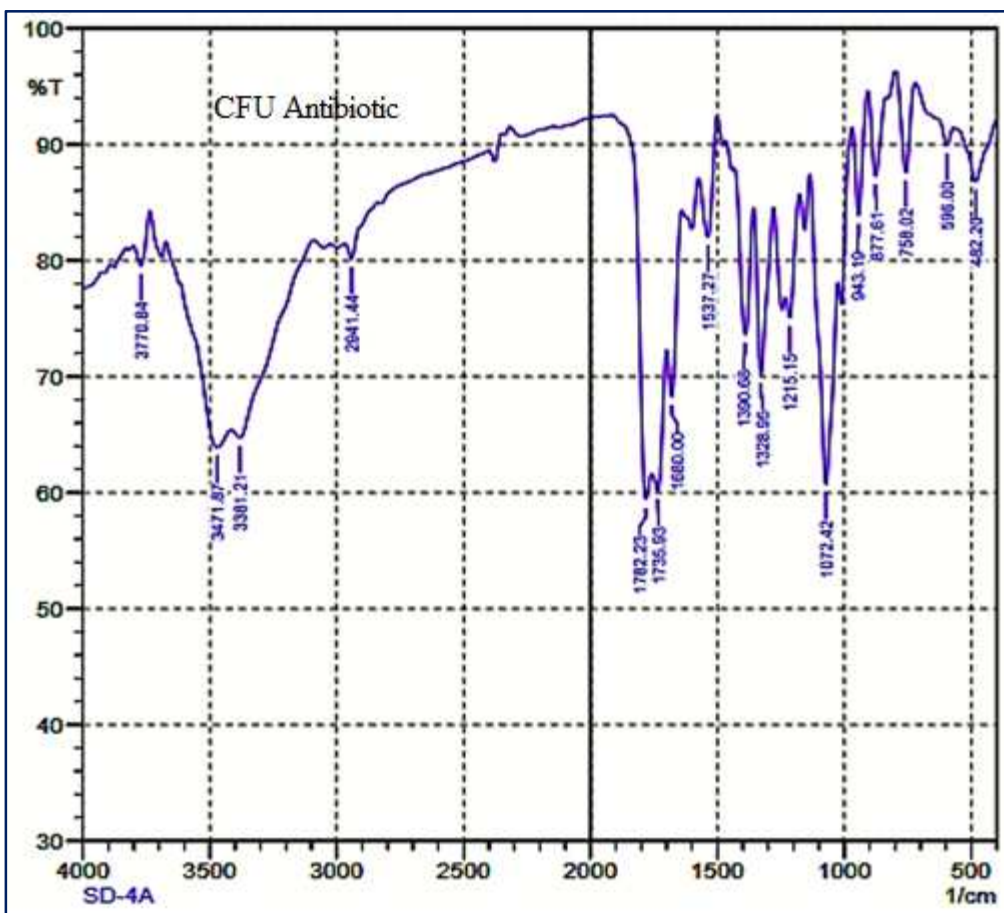


Figure 3.38. FT-IR spectrum of the precursor antibiotic, cefuroxime axetil (CFU).

The binding mode of the metal ions to the ligand donor atoms can be predicted by analyzing the FT-IR spectra of the ligand molecule as well as its corresponding metal complexes [203]. The FT-IR spectrum of Cu(II)–CFU is given in Figure 3.39.

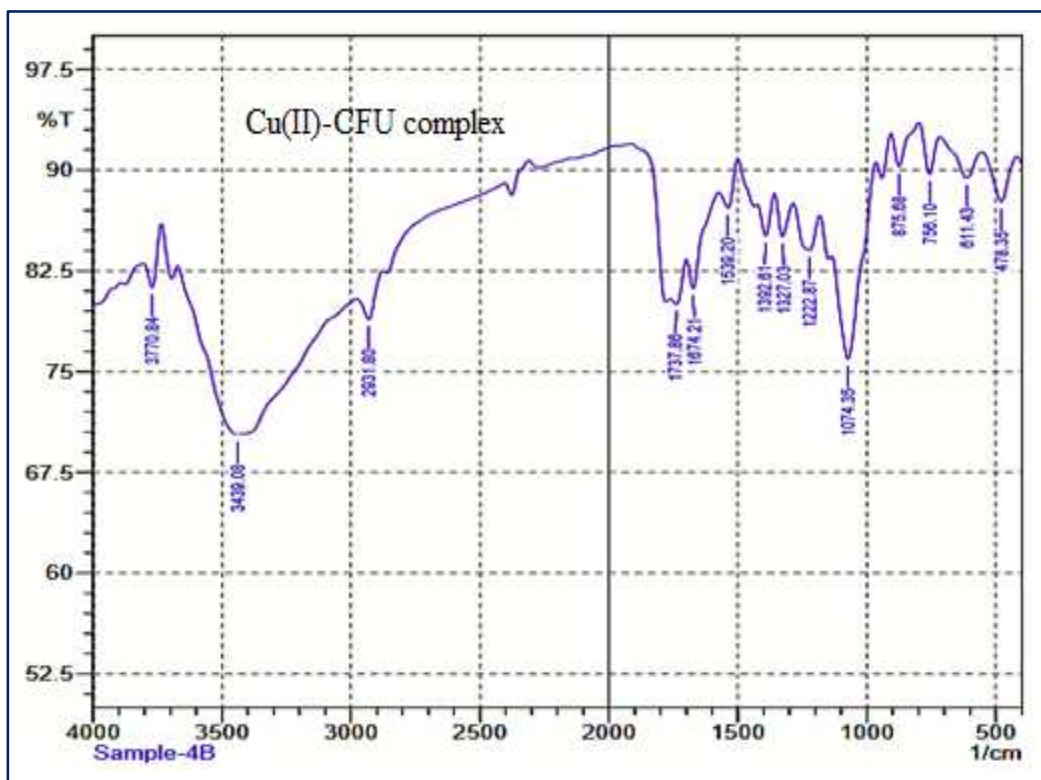


Figure 3.39. FT-IR spectrum of Cu(II)-complex cefuroxime axetil (CFU) antibiotic.

In the FT-IR spectrum of the CFU antibiotic, the lactam (C=O) band appeared at 1782 cm^{-1} and the amide (C=O) band appeared at 1680 cm^{-1} . A band found at 1735 cm^{-1} merged with the lactam (C=O) band, is due to the ester (C=O) group. In the region of $3300 - 3600\text{ cm}^{-1}$, two peaks were found for asymmetric (N-H)

and symmetric (N-H) stretching vibrations of primary amine. The peaks were found at 3471 and 3380 cm^{-1} , respectively. Significant changes in the main vibrational frequencies, characteristic of different functional groups is observed due to complexation. The relevant bands shifted to lower frequency due to interaction with the metal ions. In the case of Cu(II)-CFU, the lactam (C=O) and the amide (C=O) band appeared at 1743 and 1622 cm^{-1} , respectively. A broad peak in the region of 3000 – 3700 cm^{-1} was found, which is due to the formation of the coordination bond with water. A new peak was found at 611 cm^{-1} , absent in the free ligand, due to the formation of the Cu–O bond in the complex. All these suggested the coordination of cefuroxime antibiotic to the Cu(II) metal ion through the oxygen atom lactam (C=O) group, the oxygen atom of the amide (C=O) group, and the oxygen atom of the water molecule. The FT-IR spectrum of Ni(II)-CFU is presented in Figure 3.40.

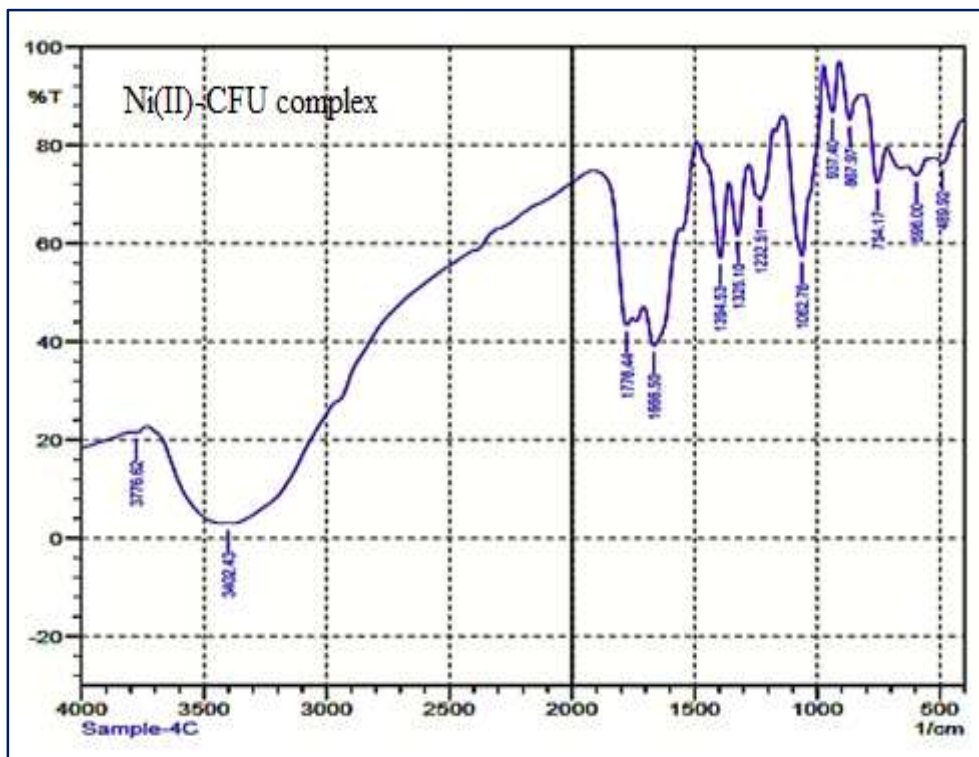


Figure 3.40. FT-IR spectrum of Ni(II)-complex of the cefuroxime axetil antibiotic.

In the case of the Ni(II)-CFU complex, the lactam (C=O) and the amide (C=O) bands appeared at 1778 cm^{-1} and 1665 cm^{-1} , respectively. A broad band in the region of $3000 - 3700\text{ cm}^{-1}$, pointing toward 3402 cm^{-1} was found which is due to the formation of the coordination bond with the water molecule. A new peak originated at 656 cm^{-1} which is assigned to the formation of Ni-O bond in the complex. Moreover, the C=N stretching vibration of the C=N-O-CH₃ group appear at 1537 cm^{-1} which is almost unaffected in the metal complexes due to the

non-involvement of the group in the complexation. The FT-IR data of the cefuroxime antibiotic and its corresponding metal complexes are listed in Table 3.21.

Table 3.21. Characteristic vibrational frequencies (cm^{-1}) of CFU antibiotic and its metal complexes.

Compound	$\nu(\text{C}=\text{O})$	$\nu(\text{C}=\text{O})$	$\nu(\text{N}-\text{H})$	$\nu(\text{OH})$	$\nu(\text{M}-\text{O})$
	lactam	2 ^o amide	1 ^o amine		
CFU antibiotic (Ligand)	1782	1680	3471	-	-
Cu(II)-CFU	1737	1674	-	3439	611
Ni(II)-CFU	1778	1666	-	3402	656

*M–O indicates the Metal–Oxygen coordinate bonding

Several groups of researchers worked on the synthesis and characterization of different cephalosporin antibiotics. Based on IR investigation, they have proposed different modes of coordination of metal ions to different cephalosporin antibiotics. In the case of the metal complexation of ceftifur hydrochloride, Tendon *et al.* [192] reported the formation of a metal complex through the coordination of the lactam (C=O) group and the 2^o amide (C=O) group based on significant changes in the vibrational frequency of both functional groups.

Cefadroxil is another cephalosporin antibiotic, Zayed *et al.* [204] proposed that the metal (Cu, Ni) complexation occurs through beta-lactam nitrogen, beta-lactam carbonyl, and the carboxylate group. Anacona's group investigated the metal complexation of a large No. cephalosporin antibiotic. Based on IR studies they noticed that the complexation of cefixime [205], ceftriaxone [206], and cephalothin [207] through the carboxylate group and the beta-lactam carbonyl group while the coordination of cefazolin [172] and cefalexin [173] occur through the amide carbonyl and the carboxylate group.

3.19. ¹H NMR Interpretation of Cefuroxime Axetil with Cu(II) and Ni(II) Metal Ions

The ¹H NMR spectrum of the parent antibiotic, cefuroxime axetil (CFU) is given in Figure 3.41. From FT-IR studies it is evident that the parent antibiotic (CFU) bonded to the metal ions through beta-lactam (C=O) and the 2° amide (C=O) group. However, owing to the complexation with metal ions, the signals of the protons nearer to the metal binding site changed their chemical shift values. In the CFU ligand, the proton signals nearer to the beta-lactam carbonyl and the 2° amide carbonyl group appeared at δ 5.88 ppm (CO-CH) and δ 5.25 ppm (N-CH). Also, the signal of the N-H (2° amide) proton which is directly involved in complexation appears at δ 9.8 ppm.

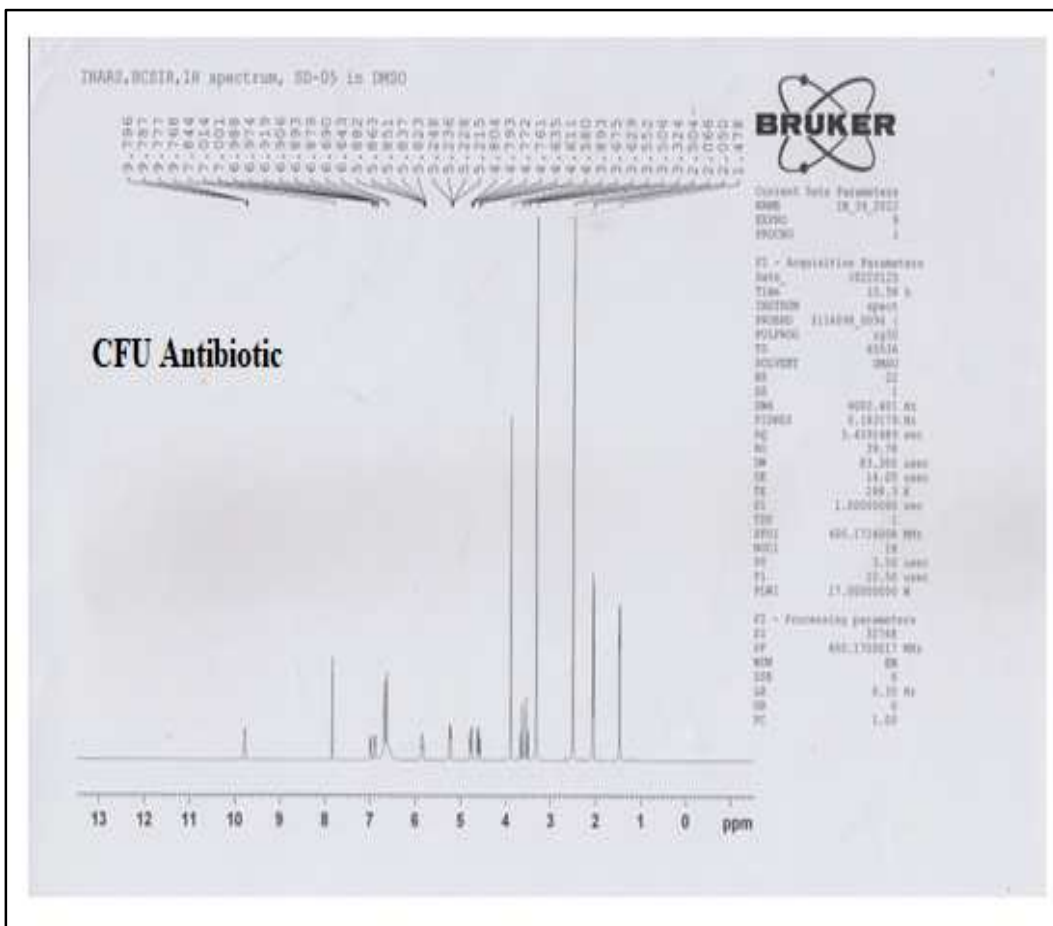


Figure 3.41. ^1H NMR spectrum of the parent antibiotic, cefuroxime axetil (CFU).

The ^1H NMR spectra of Cu(II)- and Ni(II)-complexes of cefuroxime axetil are given in Figures 3.42 and 3.43, respectively.

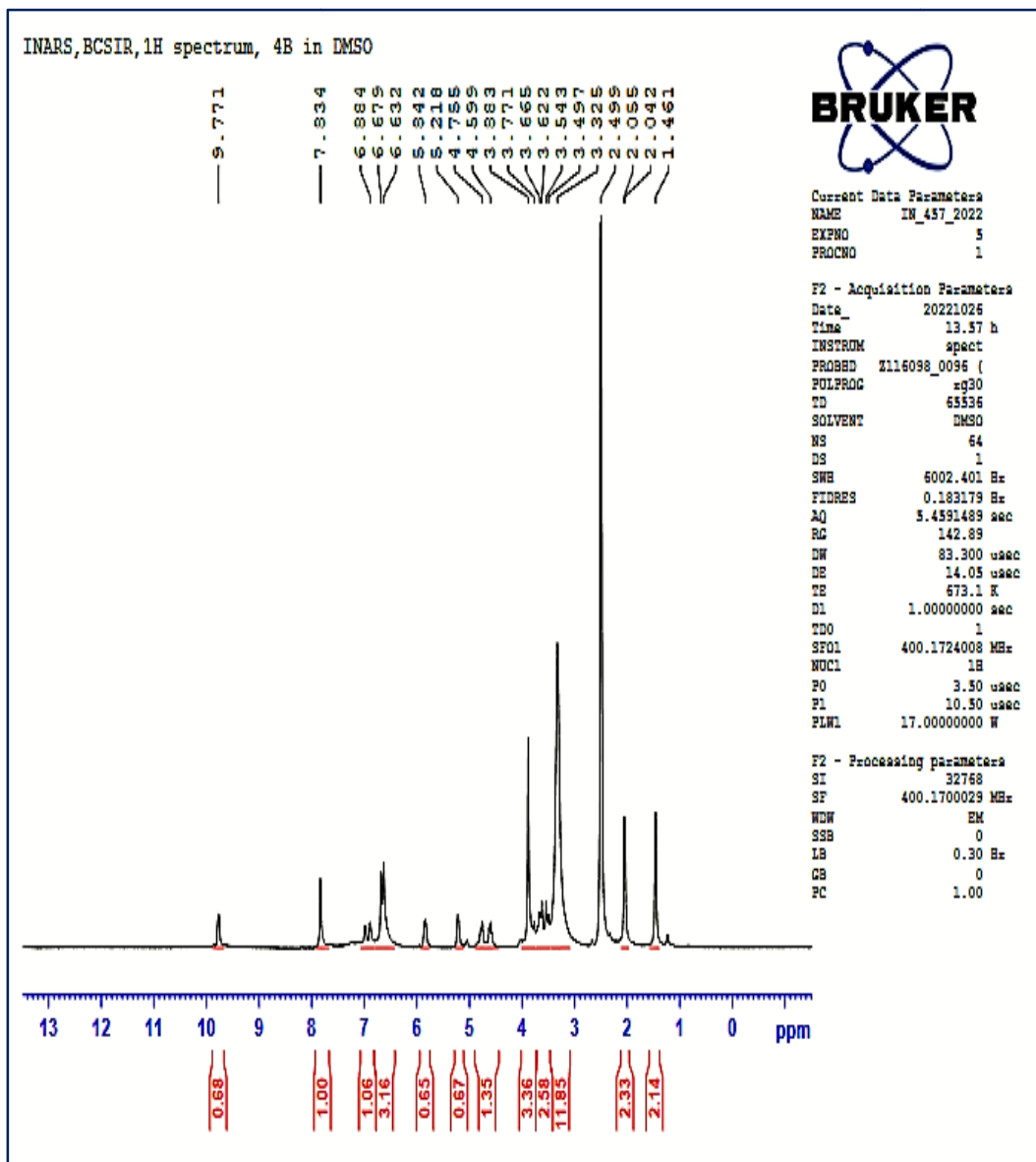


Figure 3.42. ^1H NMR spectrum of Cu(II)-complex of cefuroxime axetil (CFU).

In the case of Cu(II)-CFU complex (Figure 3.42), the signals of the protons (N-CH and CO-CH) nearer to the metal binding site appeared at δ 5.21 ppm and δ

The characteristic NMR signals nearer to the metal binding site, which was changed due to complexation are concise in Table 3.22.

Table 3.22. Assignments of ^1H NMR bands of CFU antibiotic and its metal complexes.

Chemical shift, δ ppm (CFU)	Chemical shift, δ ppm (Cu- CFU)	Chemical shift, δ ppm (Ni-CFU)	Assignments
9.8	9.77	9.73	1H, NHCO
5.88	5.84	5.79	1H, CO-CH
5.25	5.21	5.10	1H, N-CH

3.20. Thermal Analyses of Cefuroxime Axetil with Cu(II) and Ni(II) Metal Ions

Thermal analyses of metal complexes of the parent antibiotic, CFU were done in an inert atmosphere of N_2 using a simultaneous TG–DTA instrument. The TG/DTG/DTA curves of Cu(II)-CFU and Ni(II)-CFU are shown in Figures 3.44 and 3.45, respectively. TG along with DTG gives important information about the whole thermal decomposition events as well as the thermal stability of the complexes. The maximum temperature values of decomposition associated with the corresponding weight loss at a certain temperature range are listed in Tables 3.23 and 3.24.

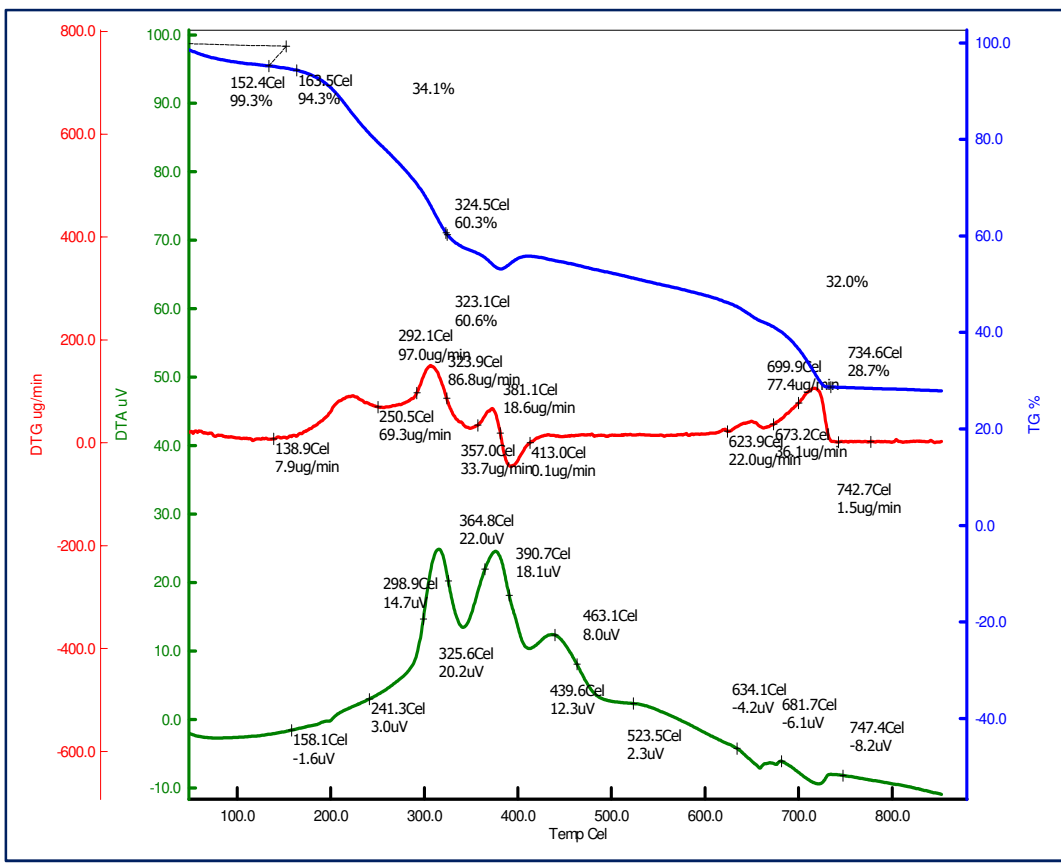


Figure 3.44. TG/DTG/DTA curves of Cu(II)-complex of cefuroxime axetil (CFU).

It was found that the degradation pattern of the complexes is completely different from each other suggesting the formation of new complexes results from the successful interaction of metal to ligand. The Cu(II)-complex was found to be thermally stable upto the temperature at 150 °C and a residual mass of 28.7% remained even after heating to 900 °C. The whole decomposition event was completed in three main degradation steps. The first step of decomposition

corresponds to weight loss of 6.7% which is associated with the loss of coordinated water molecule. In the second step, a weight loss of 34% was found in the temperature range of 163-324 °C, with a maximum temperature of T_{DTG} at 201 and 307 °C. The final step of decomposition occurred at the temperature range of 324-734 °C, associated with a weight loss of 32%. In the DTA curve of the complex, a melting endotherm at 269.5°C was observed, different from the melting temperature (210 °C, lit. value) of the parent antibiotic. Three more sharp endothermic peaks at 344 °C, 414 °C, and 493 °C were found, which are due to the decomposition of anhydrous complex. The DTA data are well in agreement with the DTG data.

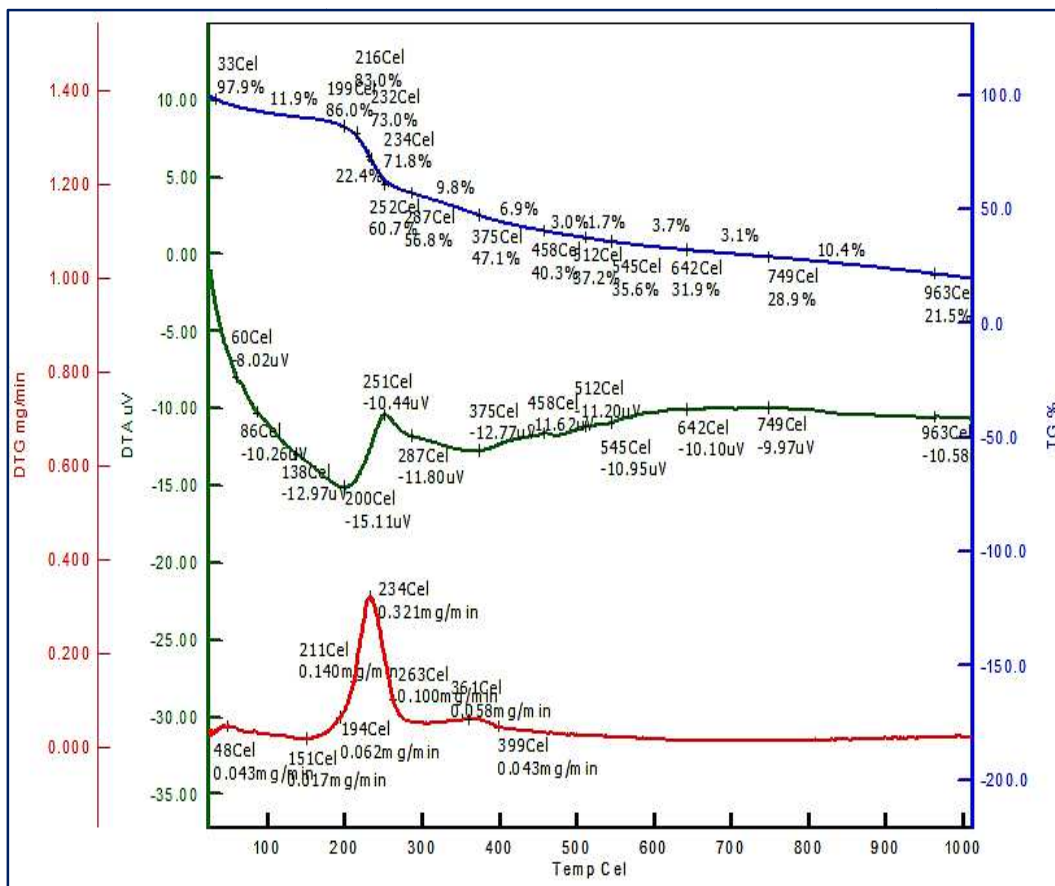


Figure 3.45. TG/DTG/DTA curves of Ni(II)-complex of cefuroxime axetil (CFU).

The thermal stability of Ni(II)-CFU complex was also comparable with Cu(II)-CFU complex and a residual mass of 21.5% remained even at 963 °C. The whole thermal decomposition process of Ni(II)-CFU (Figure 3.45) was completed in five steps. The 1st degradation step corresponds to weight loss of 14% at the temperature range of 33-200 °C, which may be associated with dehydration. The

2nd and 3rd degradation steps occurred at the temperature range of 252-512 °C and 512-750 °C, corresponding to a weight loss of 25.3 and 23.5%, respectively. These steps are associated with the degradation of the anhydrous complex. The final step of decomposition happened with 15.7% weight loss at the temperature range of 512-963 °C, leaving metal oxide as residue. An endothermic peak at 375 °C in the DTA curve refers the melting point of the complex. The DTG data agreed well with the DTA data, suggesting the formation of a new complex.

Table 3.23. Thermo-analytical (TGA, DTG, and DTA) results of Cu(II) complex of cefuroxime axetil.

Compound	Step	Temperature range (°C)	Weight loss (%)	DTG _{max} (T _{DTG})	DTA(T _{DTA})	
					Endo	Exo
Cu(II)-CFU	1 st	25–152	0.7			
	2 nd	152–163.5	6.0			
	3 rd	163– 324	34	201, 307	269.5	312
	4 th	324 - 734	32	340, 369 397, 648, 705	344, 414 493,	377, 439 439
					657, 714	
Total loss			71.3			
Residue			28.7			

Table 3.24. Thermo-analytical (TGA, DTG, and DTA) results of Ni(II) complex of cefuroxime axetil.

Compound	Step	Temperature range (°C)	Weight loss (%)	DTG _{max} (T _{DTG})	DTA(T _{DTA})	
					Endo	Exo
Ni(II)-CFU	1 st	33-199	14	178	200	
	2 nd	199-252	25.3	234		251
	3 rd	252-512	23.5	280, 380	375	
	4 th	512-749	8.3			
	5 th	749-963	7.4			
Total loss			78.5			
Residue			21.5			

3.21. Elemental Analyses of Cefuroxime Axetil with Cu(II) and Ni(II) Metal Ion

The elemental analysis of metal complexes of cefuroxime axetil (CFU) antibiotic was performed and the results are presented in Table 3.25. The results are well-fitted with the proposed molecular formula and agreed to 1:1 ligand to metal stoichiometry.

Table 3.25. Elemental analyses data of metal complexes of cefuroxime axetil (CFU).

Complex	Elemental analysis							
	Carbon %		Hydrogen %		Nitrogen %		Sulphur %	
	Calc.	Found	Calc.	Found	Calc.	Found	Calc.	Found
[Cu(CFU) (H ₂ O) ₂]. H ₂ O	38.24	38.17	4.49	4.41	8.92	8.95	5.10	5.22
[Ni(CFU) (H ₂ O) ₂].7H ₂ O	32.85	32.9	4.76	4.81	7.66	7.76	4.38	4.28

3.22. Proposed Structure of Cefuroxime Axetil with Cu(II) and Ni(II) Metal Ions

Cefuroxime axetil (CFU) is an ester prodrug of cefuroxime, a 2nd-generation cephalosporin antibiotic. The presence of the β -lactam ring in cefuroxime axetil is responsible for its bactericidal activity. Like other cephalosporins, it also has several potential donor atoms to form coordinate bonds with metal ions. So, various spectral techniques like UV-Vis, FT-IR, ¹H NMR, and thermal analyses (TG, DTG and DTA) were used to determine the coordination mode of the CFU antibiotic to the metal ions. Based on all analytical results, it is resolved that the CFU antibiotic formed metal complexes through the participation of the oxygen atom of the β -lactam (C=O) group and the oxygen atom 2° amide group. The

proposed structure of metal complexes of cefuroxime axetil is given in Figure 3.46.

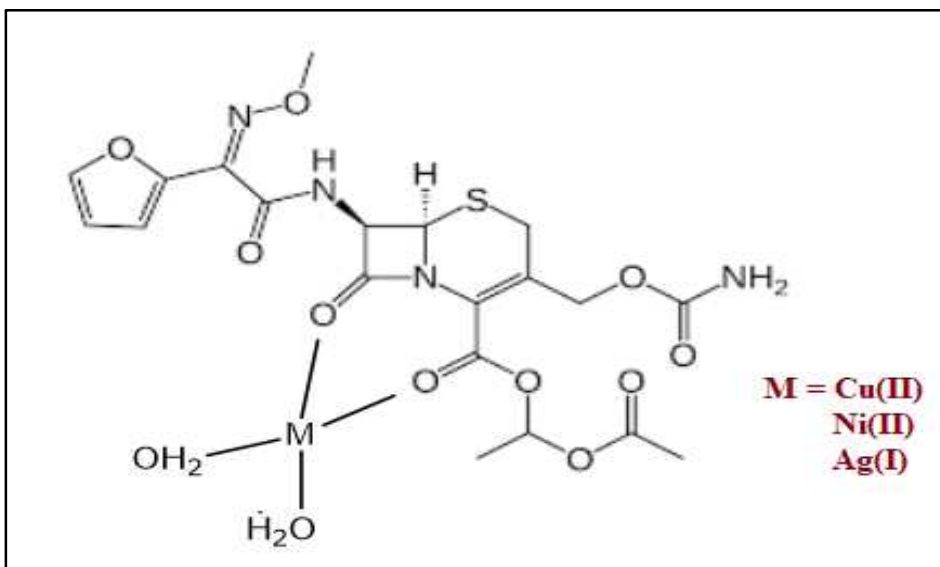


Figure 3.46. Proposed structure of metal complexes cefuroxime axetil antibiotic.

3.23. Biological Activities of Cefuroxime Axetil with Cu(II) and Ni(II) Metal Ions

Cefuroxime axetil is a member of the cephalosporin family, used in the treatment of urinary tract infections, respiratory tract infections, skin, and soft tissue infections. Like other cephalosporins, it is also a bactericidal antibiotic. It kills bacteria in a similar way to penicillin. The bactericidal activity of CFU antibiotic results from the binding of β -lactam ring to the penicillin-binding protein of bacterial cell wall and thus blocks the activity of enzymes and stops the synthesis of cell wall peptidoglycan and the bacteria then die. Because of increasing use of antibiotics, there develops antibiotic resistance. It means that the bacteria causing

infections become resistant to antibiotic treatment. The reason for the resistant mechanism is that the antibiotics not only kill the bacteria causing infection but also kill helpful bacteria which protect human being from infections. As a result, the antibiotic-resistant germs survive and multiply. To combat the resistant issue, there is an urgent need of new therapeutic agents of potent activity. It has been reported that many metal complexes of antibiotics show increased activity towards microbes than the precursor antibiotics [208, 209]. The paper disc diffusion method is used to determine the biological activities as a function of the diameter of the inhibition zone in mm. The microbial strains which are used to determine the bioactivity are: *B. cerus*, *E. coli*, *P. aeruginosa*, *S. aureus*, *S. typhi*, *V. cholerae*, *K.pneumoniae*, *C. freundii*, *E. foecolis*, *E. faecium*. One representative agar plate showing antibacterial activity is given in Figure 3.47.

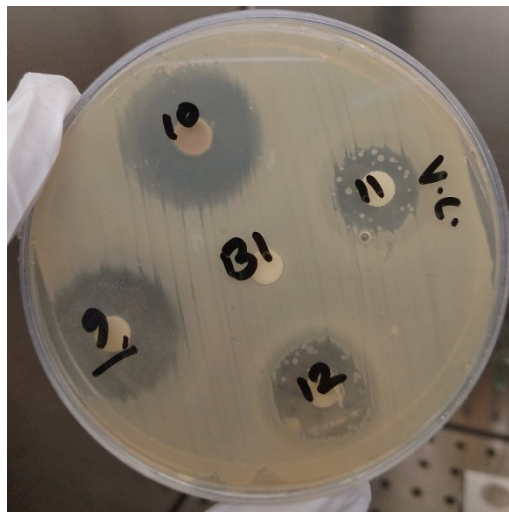


Figure 3.47. An agar plate showing antibacterial activity represented by inhibition zone diameter.

The result of biological activities is concise in Table 3.26.

Table 3.26. The antimicrobial activities of CFU antibiotic and its Cu-complex, represented as inhibition zone diameter values/mm.

Compound	Microbial species												Fungi	
	Bacteria													
	1*	2*	3*	4*	5*	6*	7*	8*	9*	10*	11*	12*	13*	14*
CFU	10	17	14	11	24	17	10	16	15	13	13	16	30	No activity
Cu(II)-CFU	11	17	15	10	24	18	10	19	17	15	15	19	32	6

1* = *B. cerus*; 2* = *E. coli 0157*; 3* = *E. coli*; 4* = *P. aeruginosa*; 5* = *S. aureus*; 6* = *Listeria*; 7* = *S. typhi*; 8* = *V. cholerae*; 9* = *K. pneumoniae*, 10* = *C. freundi*; 11* = *E. foecalis*; 12* = *E. faecium*; 13* = *Candida sp.*; 14 = *A. niger*.

It is found that Cu(II)-complex of CFU antibiotic showed increased activity against most of the bacterial strains and similar activity against *E. coli 0157*, *S. aureus*, and *S. typhi* compared to parent ligand. The complex was also found to be more active against *Candida sp.* and six times active against the *A. niger* fungal strain.

3.24. Physical Properties of Gemifloxacin Mesylate with Cu(II), Ni(II) and Ag(I) Metal Ions

The physical properties of the parent antibiotic and its metal complexes are presented in Table 3.27.

Table 3.27. Physical properties of the parent antibiotic and its metal complexes.

SL No.	Code	Compound	Color	State	M.P. °C	% Yield	Solubility in	
							DMSO	MeOH
1	GMX	Gemifloxacin mesylate	White to light brown	Amorphous	210	-	Soluble	Soluble
2	GMX-Cu	Copper(II)-complex	Black	Crystalline	258	75	Soluble	Soluble
3	GMX-Ni	Nickel(II)-complex	Light brown	Crystalline	313	64	Soluble	Soluble
4	GMX-Ag	Silver(I)-complex	Deep brown	Crystalline	300	76	Soluble	Soluble

The images of the parent antibiotic, antibiotic-metal complexes and their solution are displayed in Figure 3.48.



Figure 3.48. Gemifloxacin mesylate and its Cu(II), Ni(II) and Ag(I) complexes.

3.25. UV-VIS Spectra Analyses of Gemifloxacin Mesylate with Cu(II), Ni(II) and Ag(I) Metal Ions

The electronic (UV) spectra of gemifloxacin mesylate antibiotic and its Cu(II), Ni(II), and Ag(I) complexes are shown in Figure 3.49. The spectral data are summarized in Table 3.28.

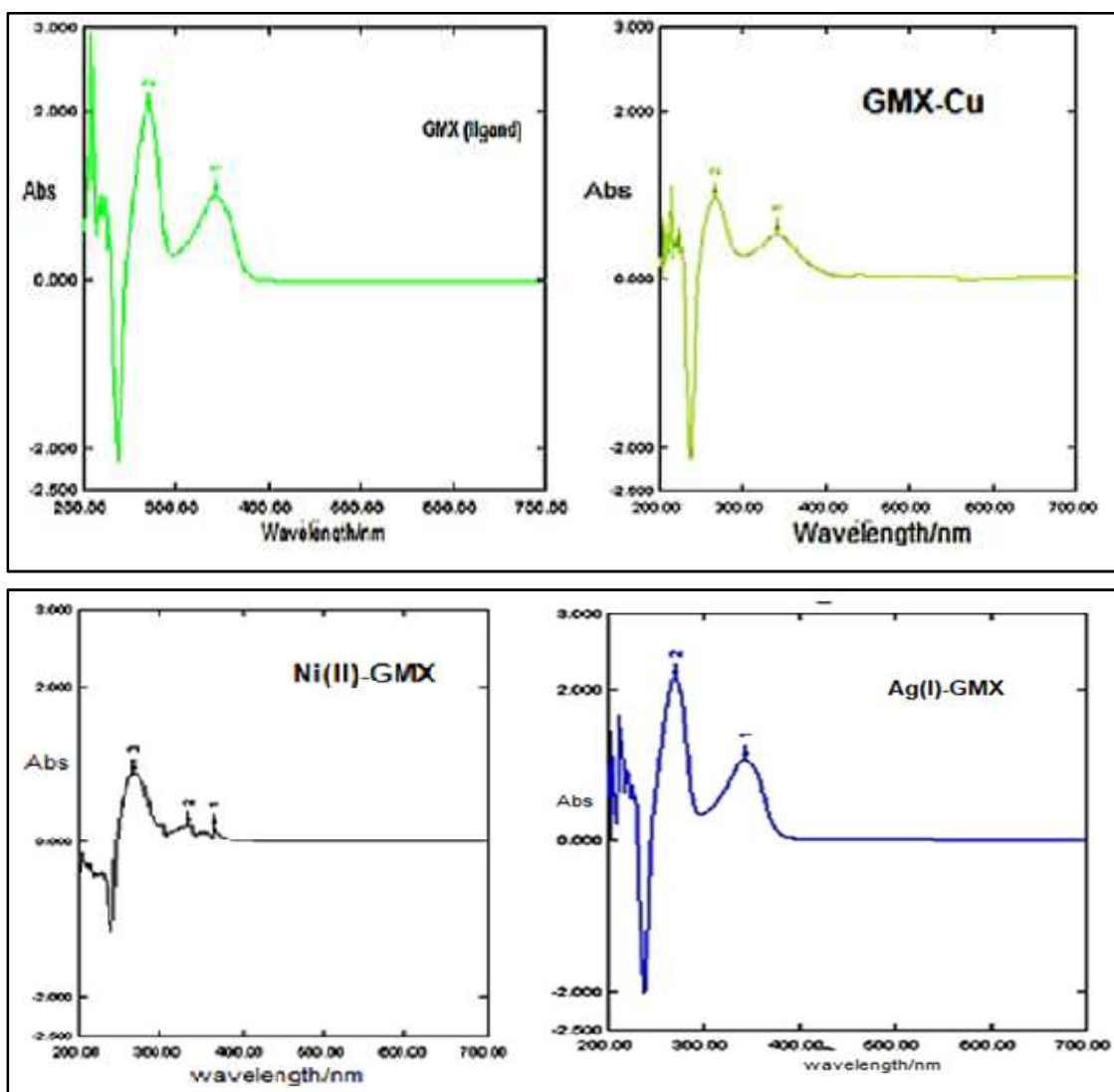


Figure 3.49. Electronic (UV) spectra of parent antibiotic (gemifloxacin mesylate) and its metal complexes.

Table 3.28. UV-Vis spectral data of gemifloxacin mesylate and its complexes.

Compound	The wavelength of electronic transition (nm)
GMX (Parent antibiotic)	342, 270, 296
Cu-GMX	341, 267, 299
Ni-GMX	366, 334, 267
Ag-GMX	342, 269, 296

The absorption bands of free gemifloxacin were found at 342, 270, and 296 nm which are assigned to $n-\pi^*$ and $\pi-\pi^*$ transition. Upon complexation of gemifloxacin mesylate with metal ions, the shifting of absorption bands (λ_{\max}) to lower (hypsochromic) or higher (bathochromic) values occurred, which is attributed to the formation of new coordination complexes. Moreover, the charge-transfer transition occurred. The UV absorption data presented in Table 3.28 are well in agreement with the formation of new metal complexes of gemifloxacin mesylate.

3.26. FT-IR Studies of Gemifloxacin Mesylate with Cu(II), Ni(II) and Ag(I) Metal Ions

FT-IR studies give important information regarding the binding sites of the ligand molecule to metal ions and the elucidation of the structure of new metal complexes [210]. In the formation of metal complexes, the quinolone antibiotic

can behave as a monodentate ligand, bidentate ligand, or bridging ligand. The foremost coordination modes of quinolone antibiotics are depicted in Figure 3.45.

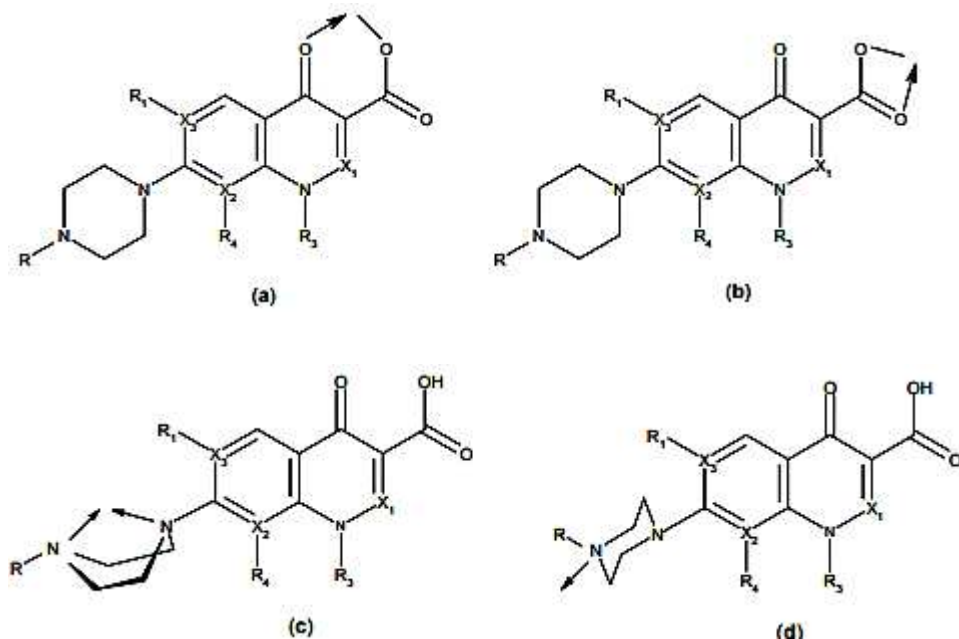


Figure 3.50. Foremost coordination mode of quinolone antibiotics.

Commonly, the quinolone antibiotics bind to metal ions in a bidentate manner through the deprotonated 3-carboxyl group and the 4-oxo group (Figure 3.50a). Hardly, the quinolone antibiotics can behave as a bidentate chelator, chelated *via* two oxygen atoms of the 3-carboxyl group or the two nitrogen atoms of the piperazine ring (Figure 3.50b and 3.50c). Sometimes, the quinolone antibiotics bind to metal ions in a unidentate manner through one of the nitrogen atoms of the piperazine ring (Figure 3.50d).

Gemifloxacin mesylate, a fluoroquinolone antibiotic possesses several binding sites, and the most common binding sites to form metal-coordinated complexes are the 3-carboxyl group and the 4-carbonyl group. Figure 3.51 represents the chemical structure of gemifloxacin mesylate.

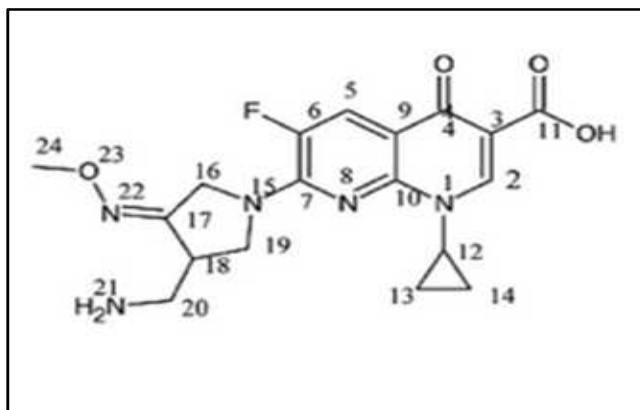


Figure 3.51. Chemical structure of gemifloxacin mesylate.

Generally, the quinolone antibiotics form metal complexes with metal ions in 1:1 [211 -215] or 1:2 (Metal: Ligand) [216-219] stoichiometry. Figure 3.52 represents the common structure of fluoroquinolone chelate where the chelator acts in a bidentate manner. Lomefloxacin, a fluoroquinolone antibiotic coordinates with the metal ions through the oxygen of the carbonyl group and the protonated carboxyl group in a 1:1 (metal: ligand) molar ratio (Figure 3.53) [211]. Norfloxacin is another fluoroquinolone antibiotic that binds to the metal ions through the two carboxyl oxygen atoms in a 1:2 (metal: ligand) mole ratio (Figure 3.54) [217]. On the other hand, gatifloxacin a fourth-generation fluoroquinolone

antibiotic binds to the metal ions through the carbonyl group and the carboxyl group in a 1:2 (metal: ligand) mole ratio (Figure 3.55) [218].

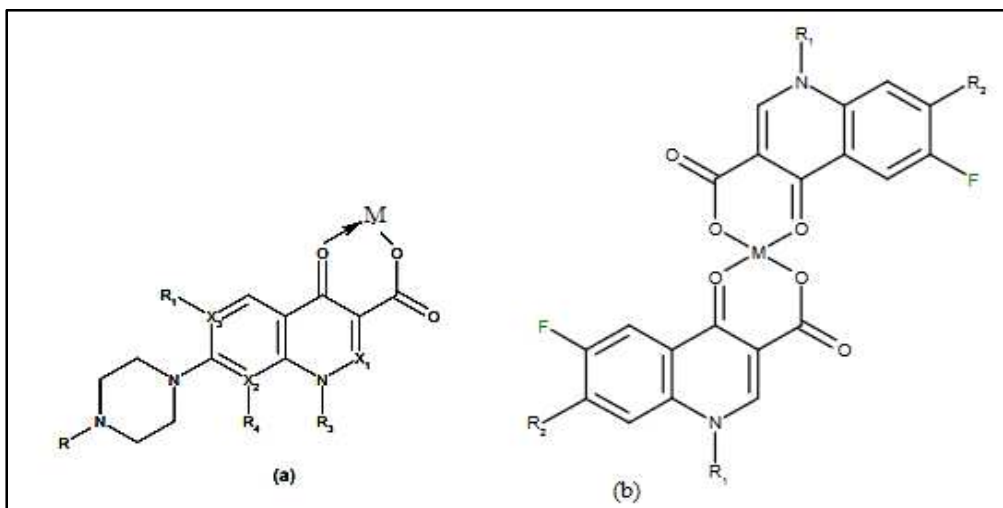


Figure 3.52. The general structure of fluoroquinolone ligand binding to the metal ions in (a) 1:1 and (b) 1:2 (metal: ligand) molar ratio.

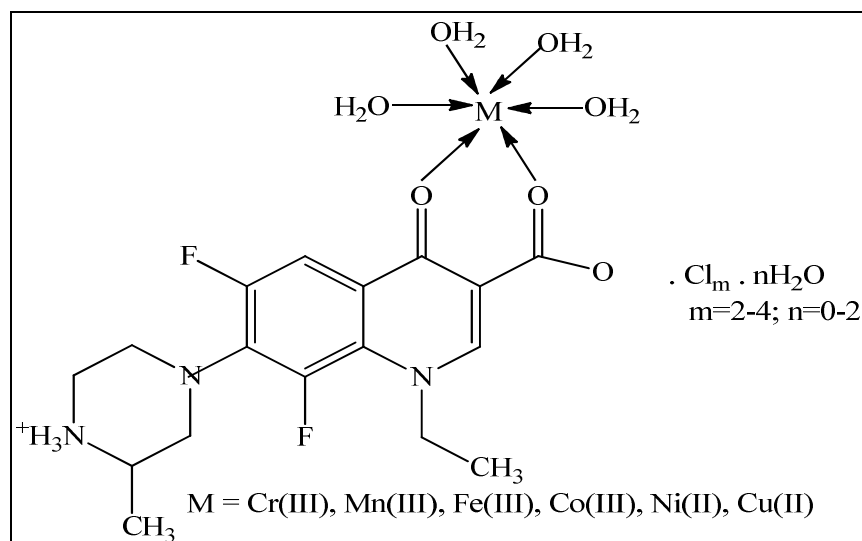


Figure 3.53. Proposed structure of lomefloxacin metal complexes.

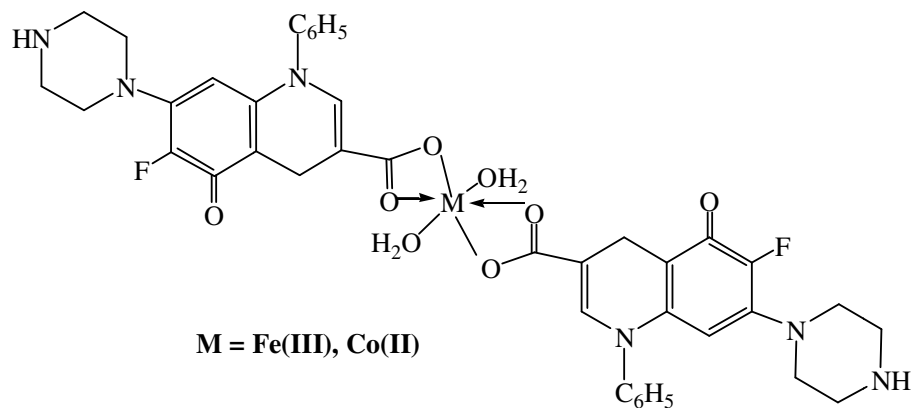


Figure 3.54. Proposed structure of norfloxacin metal complex.

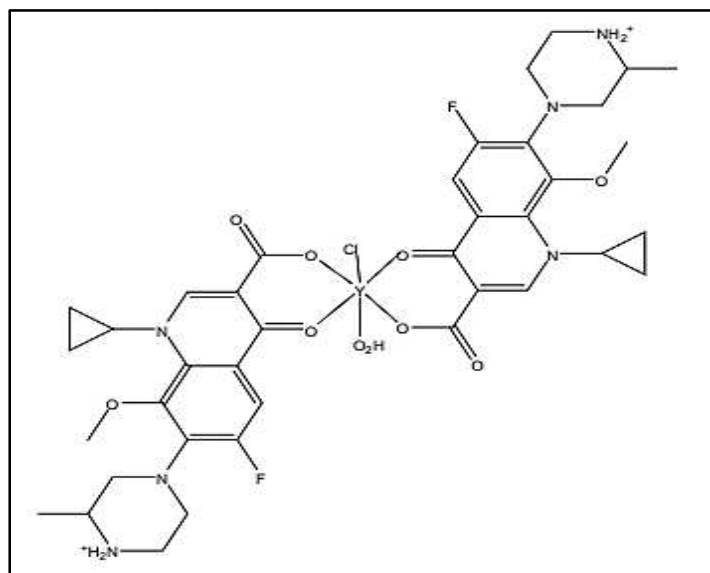


Figure 3.55. Proposed structure of metal complexes of gatifloxacin.

The FT-IR spectra of the precursor antibiotic, gemifloxacin mesylate, and its different metal complexes are depicted in Figures 3.56-3.59, respectively. A

comparison of the FT-IR spectra of the parent antibiotic and its different metal complexes gives proof of the successful interaction of metal ions to the antibiotic (ligand), thus forming new antibiotic-metal complexes. The main vibrational frequencies of the parent ligand and its metal complexes are listed in Table 3.29. The FT-IR spectra of different metal complexes of gemifloxacin mesylate antibiotic are comparable because the same atoms have involved in the formation of new metal complexes. However, the newly formed metal complexes exhibited noteworthy changes in the FT-IR frequencies as compared to the parent antibiotic, thus signifying the successful metal-ligand interaction and formation of new metal complexes.

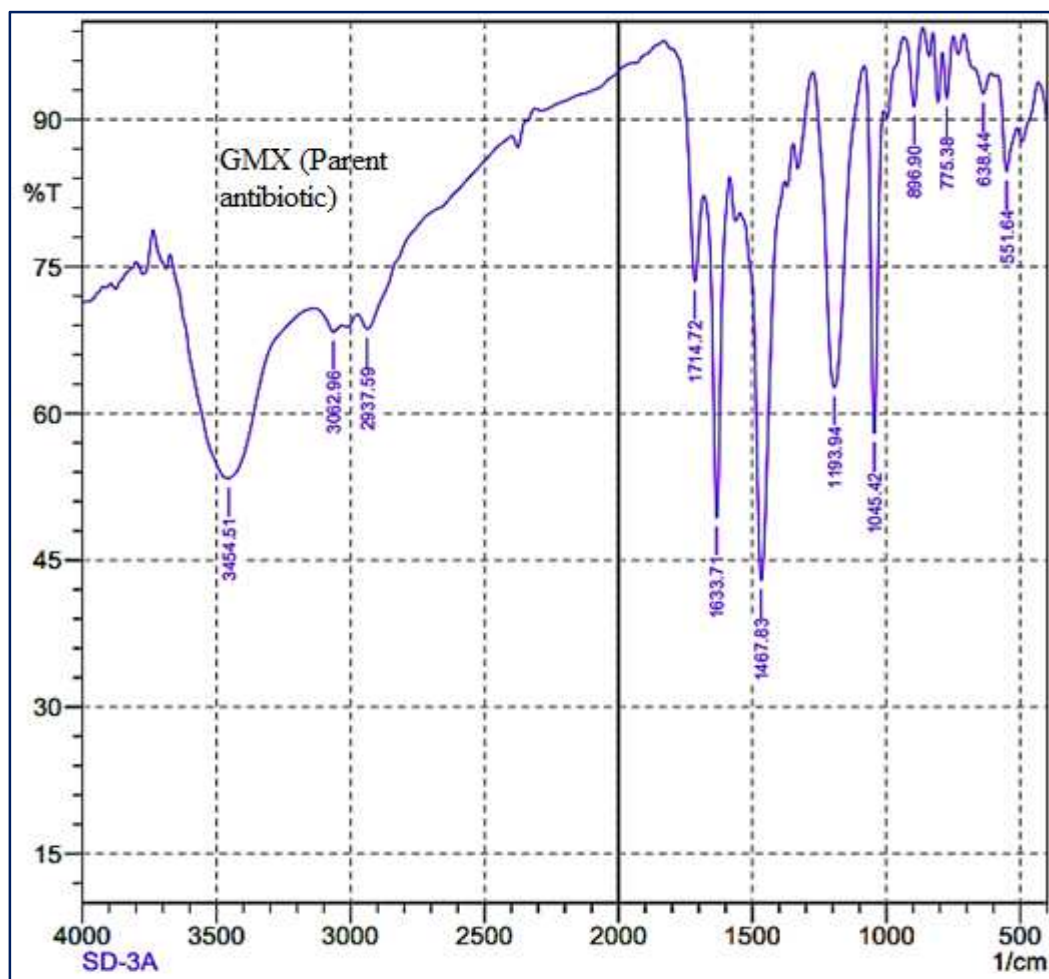


Figure 3.56. FT-IR spectrum of the precursor antibiotic, gemifloxacin mesylate (GMX).

Since most quinolone antibiotics interact with metal ions through the carbonyl group and the carboxyl group of the nearest position, it is important to consider first the group vibration of 3-carboxyl and 4-carbonyl groups.

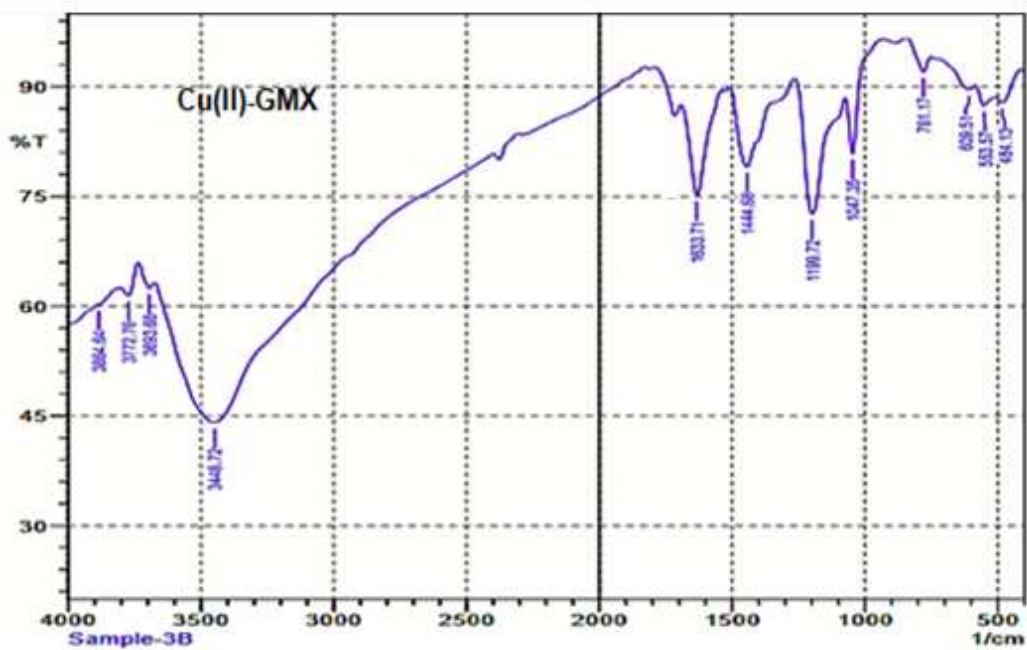


Figure 3.57. FT-IR spectrum of Cu(II)-complex of gemifloxacin mesylate.

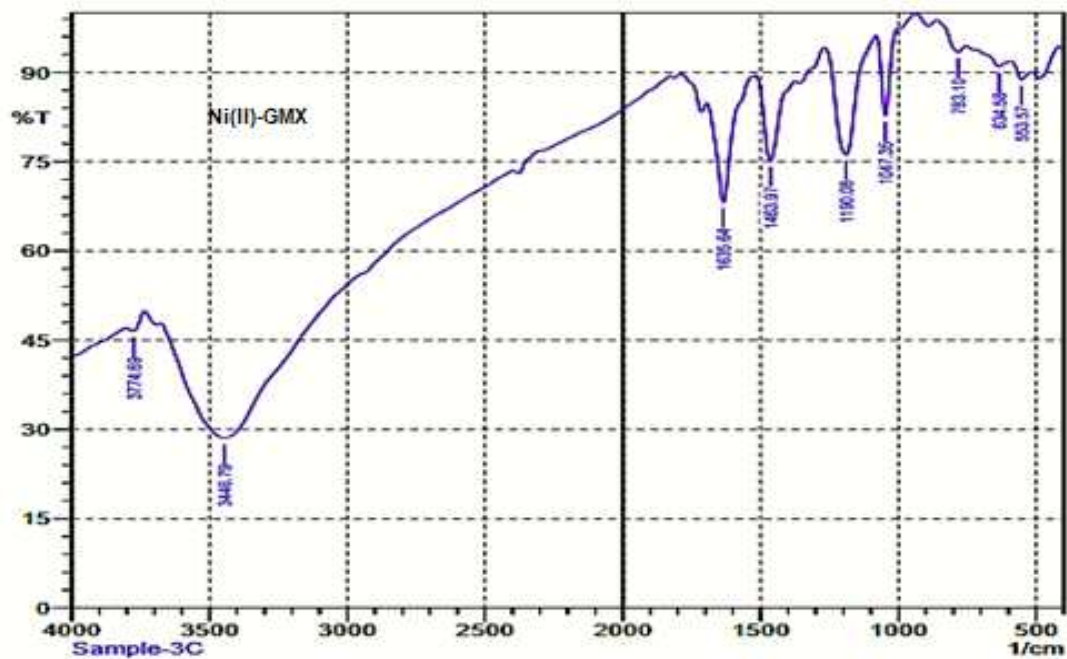


Figure 3.58. FT-IR spectrum of Ni(II)-complex of gemifloxacin mesylate.

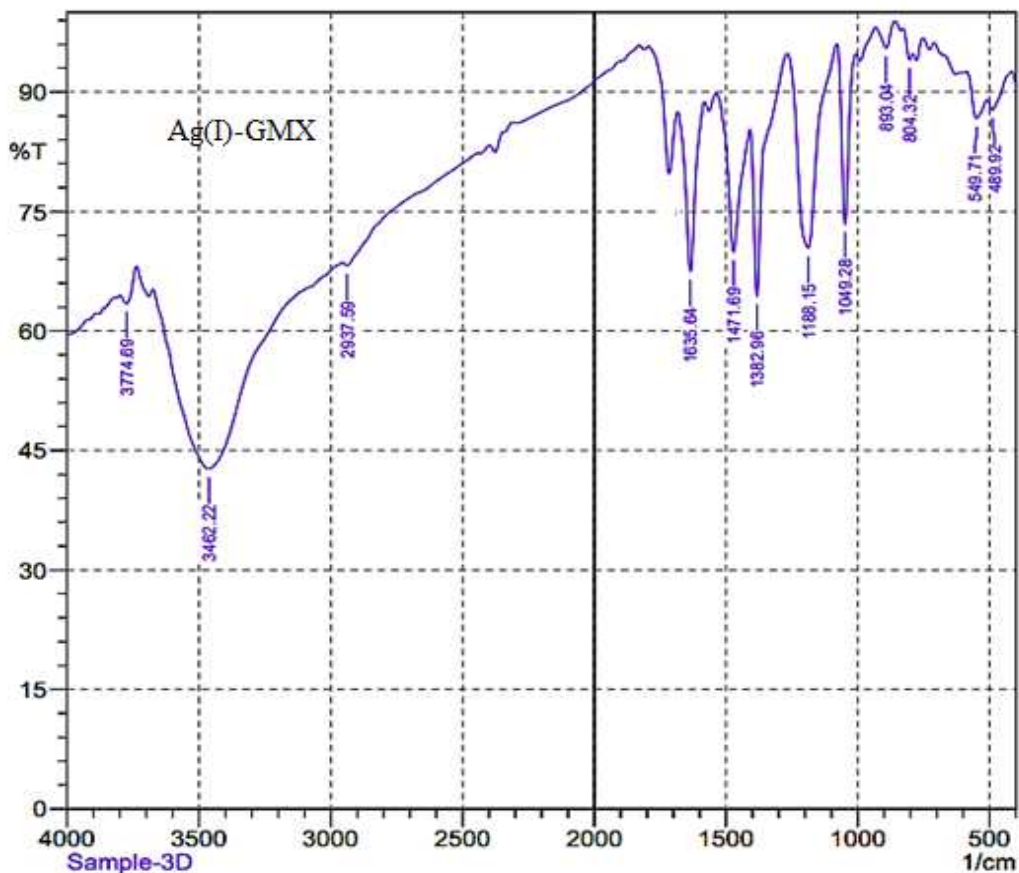


Figure 3.59. FT-IR spectrum of Ag(I)-complex of gemifloxacin mesylate.

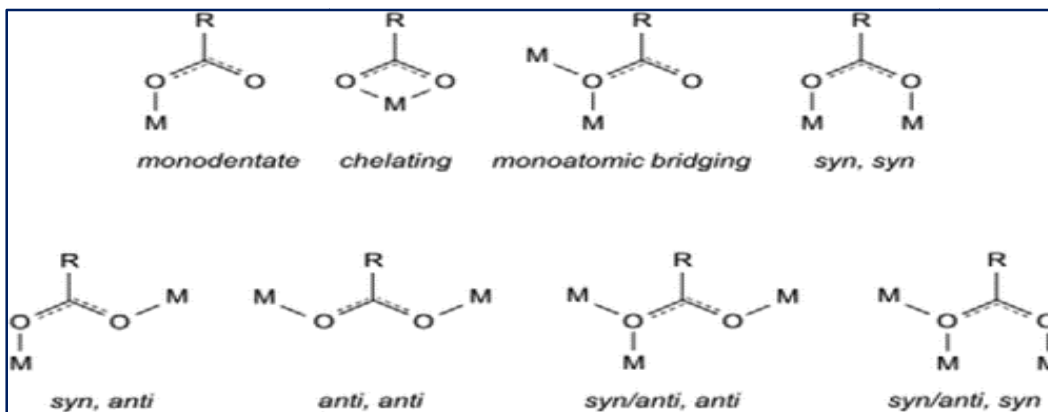
In the FT-IR spectrum of the parent antibiotic, GMX (Figure 3.56), the vibrational bands of the carboxyl stretch, $\nu(\text{C}=\text{O})_c$ and the pyridone stretch, $\nu(\text{C}=\text{O})_p$ were found at 1714 and 1633 cm^{-1} , respectively [218, 221]. On forming the new metal complexes, deprotonation of the carboxyl group occurred and the characteristic band of carboxylic stretching frequency (1714 cm^{-1}) disappeared. This indicates the involvement of the carboxyl group in the formation of new metal complexes. Two characteristic bands were found at around 1635 cm^{-1} and 1450 cm^{-1} which

are designated to the asymmetric, $\nu_a(\text{COO})^-$ and symmetric, $\nu_s(\text{COO})^-$ stretching vibration of the carboxylate group.

Table 3.29. Main vibrational frequencies (cm^{-1}) of gemifloxacin mesylate (GMX) and its metal complexes.

Compound	$\nu(\text{O-H})$	$\nu(\text{CO}), \nu(\text{COOH})$	$\nu_{as}(\text{COO})^-$	$\nu_s(\text{COO})^-$	$\Delta\nu$	$\nu(\text{M-O})^*$
GMX	3454	1714	-	-	-	-
Cu(II)-GMX	3435	-	1631	1444	187	609,585,484
Ni(II)-GMX	3446	-	1635	1463	172	634,553,480
Ag(I)-GMX	3462	-	1635	1471	164	617,549,489

There are different possible ways for coordination of carboxylate group to the metal ions which are presented in **scheme 3.1** [174, 222].



Scheme 3.1. Different options of coordination of carboxylate group.

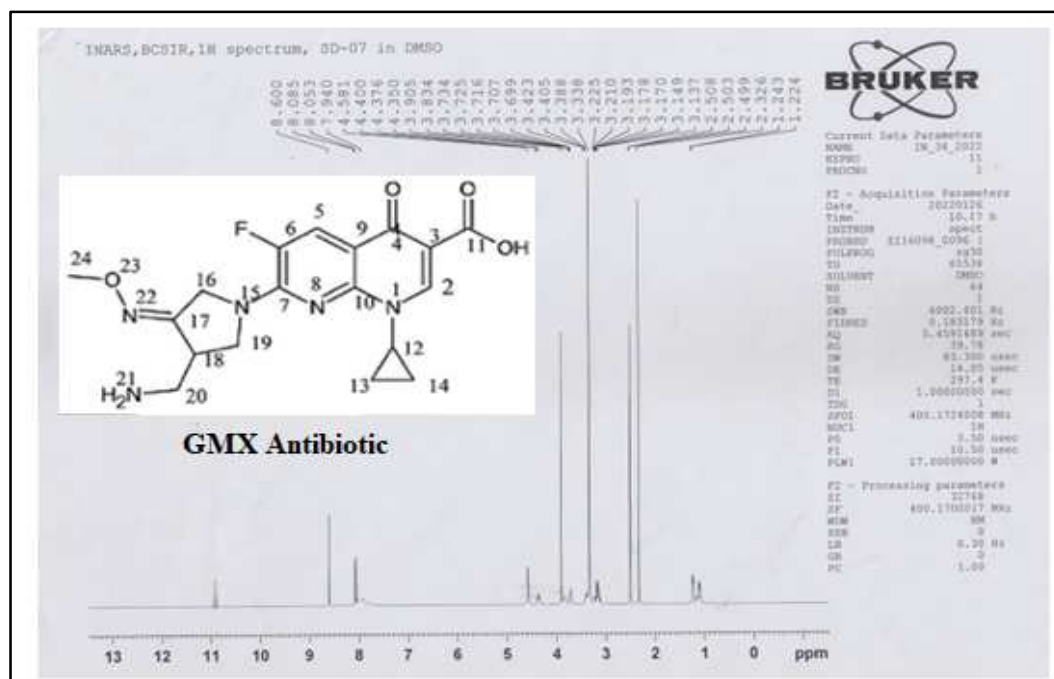
The coordination mode of the carboxylate group can be distinguished by the separation value of the asymmetric and symmetric stretching frequency of the carboxylate group, $\Delta\nu = \nu_{as}(\text{COO})^- - \nu_s(\text{COO})^-$ and the findings were swotted by Deacon and Philipes [175]. It was concluded that the separation value, $\Delta\nu > 180 \text{ cm}^{-1}$ indicates the monodentate coordination mode and $\Delta\nu < 120 \text{ cm}^{-1}$ is indicative of bidentate coordination mode of carboxylate group. On the contrary, the separation value, $\Delta\nu = 170 \pm 10 \text{ cm}^{-1}$ could be related to ionic, bridging or H-bonded monodentate coordination mode of carboxylate group. Usually, a greater separation value of $\Delta\nu > 180$ is observed in case of monodentate coordination mode of carboxylate group where one of the carboxyl oxygens is involved in coordination, because of inequality of two C-O bonds. But whenever the uncoordinated carboxyl oxygen is involved in the formation of strong hydrogen bond with water molecules, the separation value can be decreased [223]. In case of metal complexation of gemifloxacin mesylate, the separation value was found at $170 \pm 10 \text{ cm}^{-1}$ in all the newly formed metal complexes. This suggests the H-bonded monodentate coordination mode of the carboxylate group. Moreover, the characteristic band of ring carbonyl group, $\nu(\text{C=O})_p$ was shifted to lower frequency region due to involvement in coordination with metal ion and appeared as an overlapping peak in the same region of symmetric vibration of carboxylate group. The newly formed metal complexes also showed a broad band in the

region of 3000-3700 cm^{-1} , which corresponds to $\nu(\text{O-H})$ vibration and confirmed the presence of coordinated water in the complexes [224]. The presence of water in the metal complexes of quinolone antibiotics was reported previously by several research groups [225-228]. Also, a group of bands of different intensities ranging from 480-780 cm^{-1} was found in the vibrational spectra of metal complexes of the antibiotic which are assigned to $\nu(\text{M-O})$ [229].

3.27. Interpretation of ^1H NMR of Gemifloxacin Mesylate with Cu(II) , Ni(II) and Ag(I) Metal Ions

NMR is also a common analytical technique to determine the chemical structure.

The ^1H NMR spectrum of the parent antibiotic is given in Figure 3.60.



The interaction of metal ions to the ligand can be determined by observing the significant chemical shifts in the spectra of the metal complexes comparative to that of ligand molecule [230]. A very close similarity was observed in the spectra of the metal complexes compared to its ligand antibiotic, gemifloxacin mesylate. Significant ^1H NMR signals of the precursor antibiotic are concise in Table 3.30.

Table 3.30. Significant ^1H NMR signals of gemifloxacin mesylate (GMX) in DMSO- d_6 .

Chemical shift, δ ppm (Ligand)	No. of protons	Multiplicity	Assignment
1.23	2	Duplet	Cyclopropyl-3-H
3.15-3.22	2	Multiplet	Aminomethyl-H
3.33-3.38	2	Duplet	Pyrrolidiny-2-H
8.60	1	Singlet	Naphthylpyridine-2-H
8.05-8.08	1	Duplet	Naphthylpyridine-5-H
11.01	1	Singlet	Carboxylic-H

The ^1H NMR spectra of Cu(II), Ni(II) and Ag(I)-complexes of gemifloxacin mesylate are presented in the following figures 3.61, 3.62, and 3.63, respectively. The peaks present in the free ligand were found in the spectra of the metal complexes with significant chemical shifts upon complexation with metal ions. From the FT-IR study, it is evident that the coordination of metal ions occurred through the 3-carboxyl group and 4-oxo group. It was found that the proton

signals far from the binding site of the ligand are practically unchanged in the spectra of the metal complexes [219]. In the precursor antibiotic, a sharp peak was found at δ 11.01 ppm, which is due to carboxylic proton.

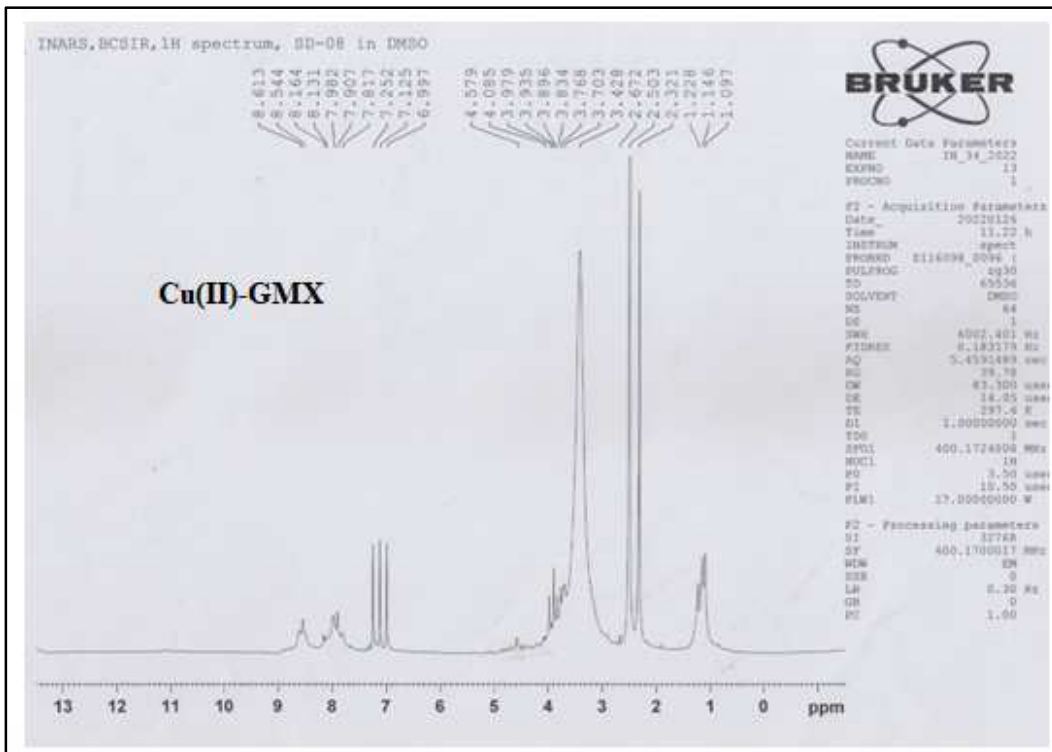


Figure 3.61. ^1H NMR spectrum of Cu(II)-complex of gemifloxacin mesylate.

But the signal due to carboxylic proton disappeared in the spectra of the metal complexes of gemifloxacin mesylate. This indication further suggested the participation of carboxylic proton in the formation of metal complexes [229, 231]. However, the naphthyl pyridine proton at C-2 and C-5 position nearer to binding site of the ligand appeared slightly downfield upon complexation with metal ions.

These changes are indicative of successful interaction of metal ion to ligand through 3-carboxylate and 4-oxygen atom of the carbonyl group. Another peak was observed at δ 4.1 – 4.5 ppm in the spectra of the metal complexes, which may be due to O-H proton, suggesting the presence of water molecule in the complexes.

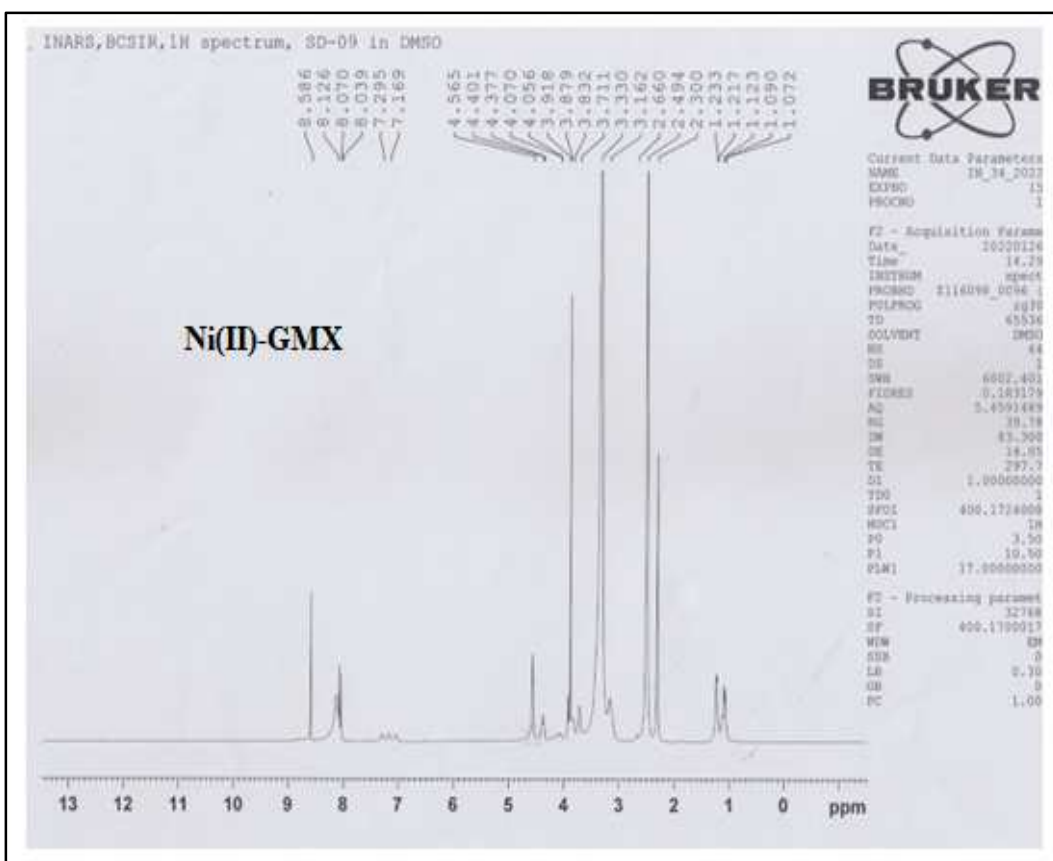


Figure 3.62. ^1H NMR spectrum of Ni(II)-complex of gemifloxacin mesylate.

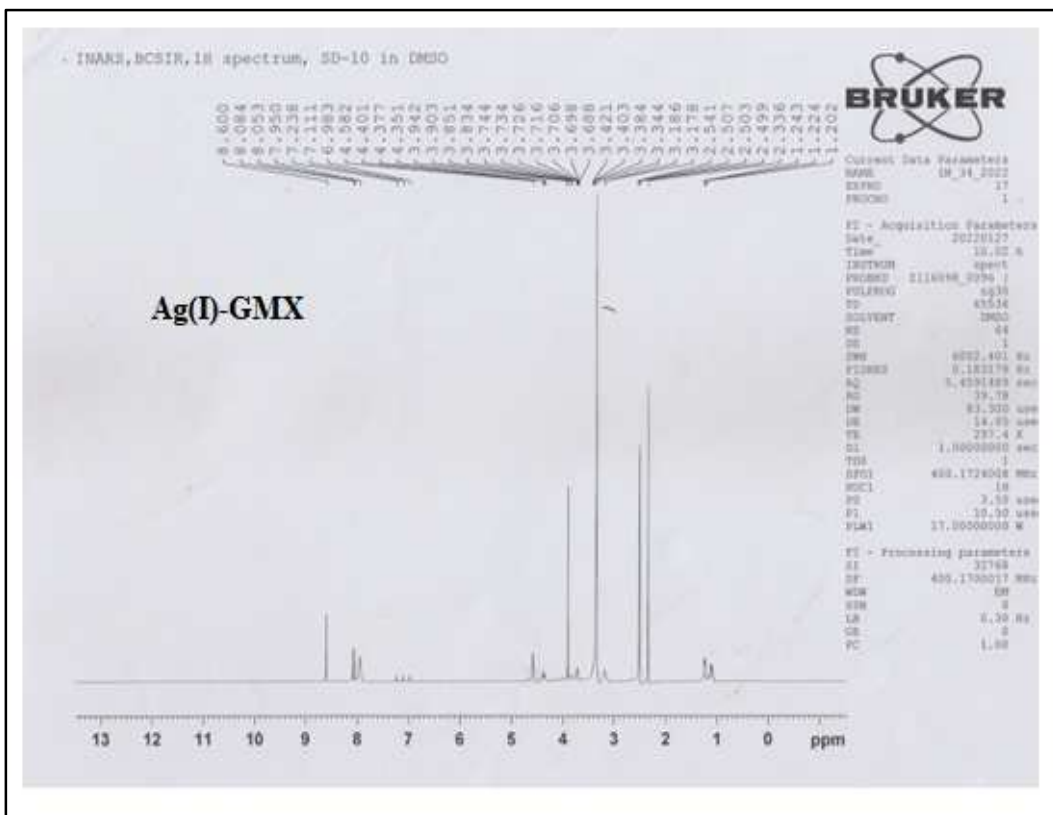


Figure 3.63. ^1H NMR spectrum of Ag(I)-complex of gemifloxacin mesylate.

3.28. Thermal Analyses of Gemifloxacin Mesylate with Cu(II), Ni(II) and Ag(I) Metal Ions

The basic thermal properties of samples can be determined by a group of thermal techniques which include Thermogravimetric analysis (TGA), Derivative thermogravimetric analysis (DTG), Differential thermal analysis (DTA) and Differential Scanning Calorimetry (DSC). In fact, these techniques are used to gather information about the thermal stability of samples, kinetics of decomposition, water content, phase transition, sample purity, melting point and so on [232].

Thus, a comparative analysis of thermograms of the precursor antibiotic and its metal complexes gives confirmation of complex formation as well as the thermal stability of the complexes [233, 234]. The thermal curves of the precursor antibiotic and its metal complexes are shown in Figures 3.64, 3.65, 3.66, and 3.67, respectively.

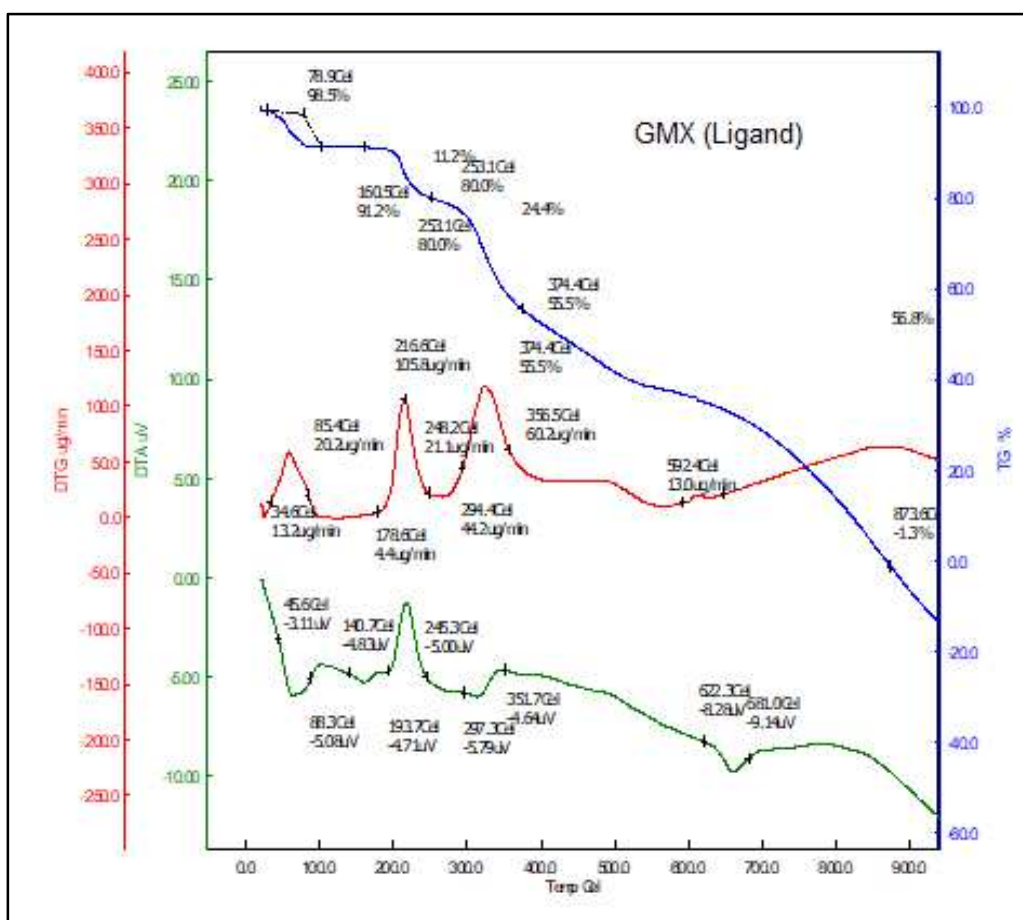


Figure 3.64. TG/DTG/DTA curve of the precursor antibiotic, gemifloxacin mesylate (GMX).

The precursor antibiotic and the newly formed metal complexes followed several thermal decomposition steps where mass changes with increasing temperature. From a close investigation of TG curves, it was found that the precursor antibiotic, gemifloxacin mesylate (GMX) degraded 100% at around 800 °C. While the Cu(II)-GMX, Ni(II)-GMX and Ag(I)-GMX degraded 85.6%, 75% and 69%, respectively even at 1000 °C. So, all the newly synthesized metal complexes of GMX are thermally more stable than the ligand antibiotic itself.

The TG curve of the ligand, GMX was composed of four decomposition steps. The DTG curve showed four overlapping maxima corresponding to overlapping steps in the TG curve. The thermo-analytical results of GMX antibiotic are concise in Table 3.31.

Table 3.31. Thermo-analytical results of the precursor antibiotic, gemifloxacin mesylate (GMX).

Compound	Decom. step	Temperature range (°C)	Weight loss (%)	DTG _{max} (T _{max})	DTA(T _{DTA})	
					Endo	Exo
GMX	1 st	25-160	8.8	59.7	67	
(Ligand)	2 nd	160-253	11.2	216.6	166.5	114.5
	3 rd	255-374	24.4	356.5	324	219
	4 th	374-850	56.8	592.4	651	
Total loss			100			
Residue			-			

The 1st step of decomposition corresponded to weight loss of 8.8% with a DTG_{max} at 59.7 °C which was followed by a weight loss of 11.2% at the temperature range 160-253 °C. In the 3rd step a weight loss of 24.4% was observed at the temperature range of 255-374 °C. Finally, the decomposition (remaining 56.8%) was completed at the temperature range of 374 – 850 °C with a T_{max} at 592.4 °C. There was a sharp endothermic peak at 219 °C which corresponds to melting point of the antibiotic.

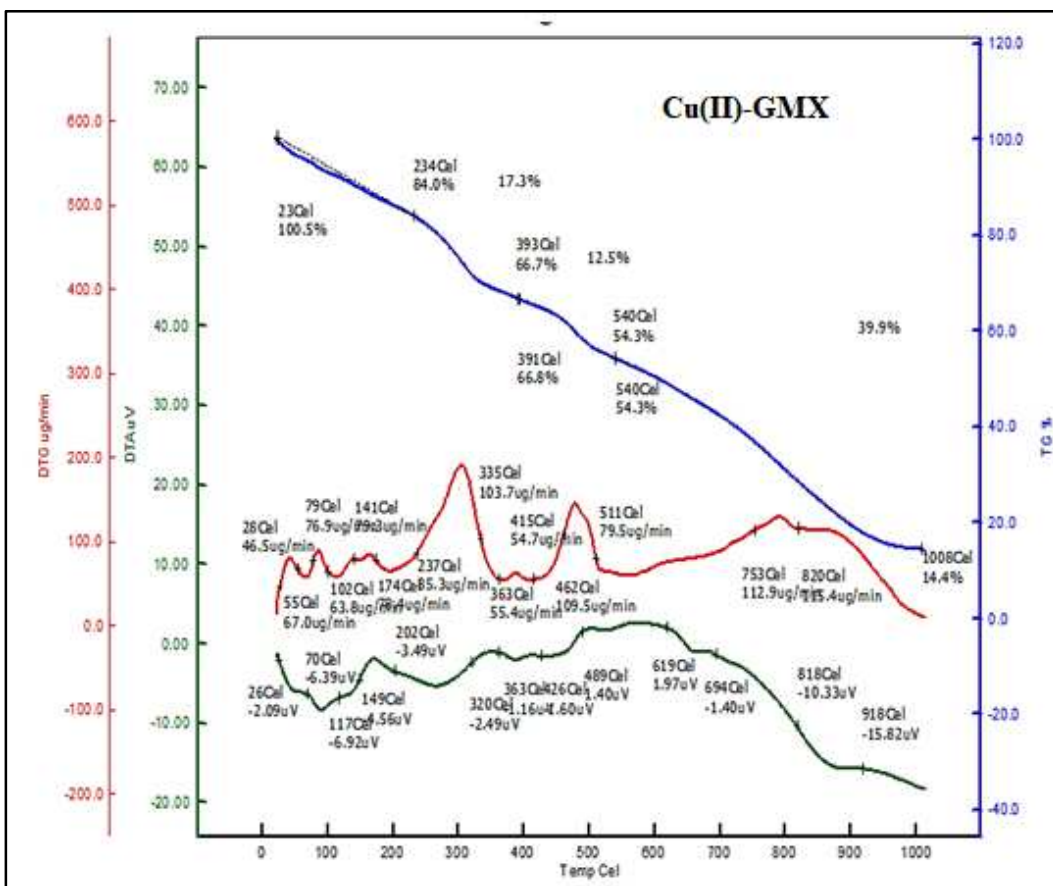


Figure 3.65. TG/DTG/DTA curves of Cu(II)-complex of gemifloxacin mesylate.

Generally, upon heating, the degradation of metal complexes initiates with the removal of water of crystallization which is followed by coordinated water and then disintegration of organic part, lastly leaving metal oxide as residue [235, 236]. The thermo-analytical (TG/DTG/DTA) results of the metal complexes of gemifloxacin mesylate are summarized in Table 3.32.

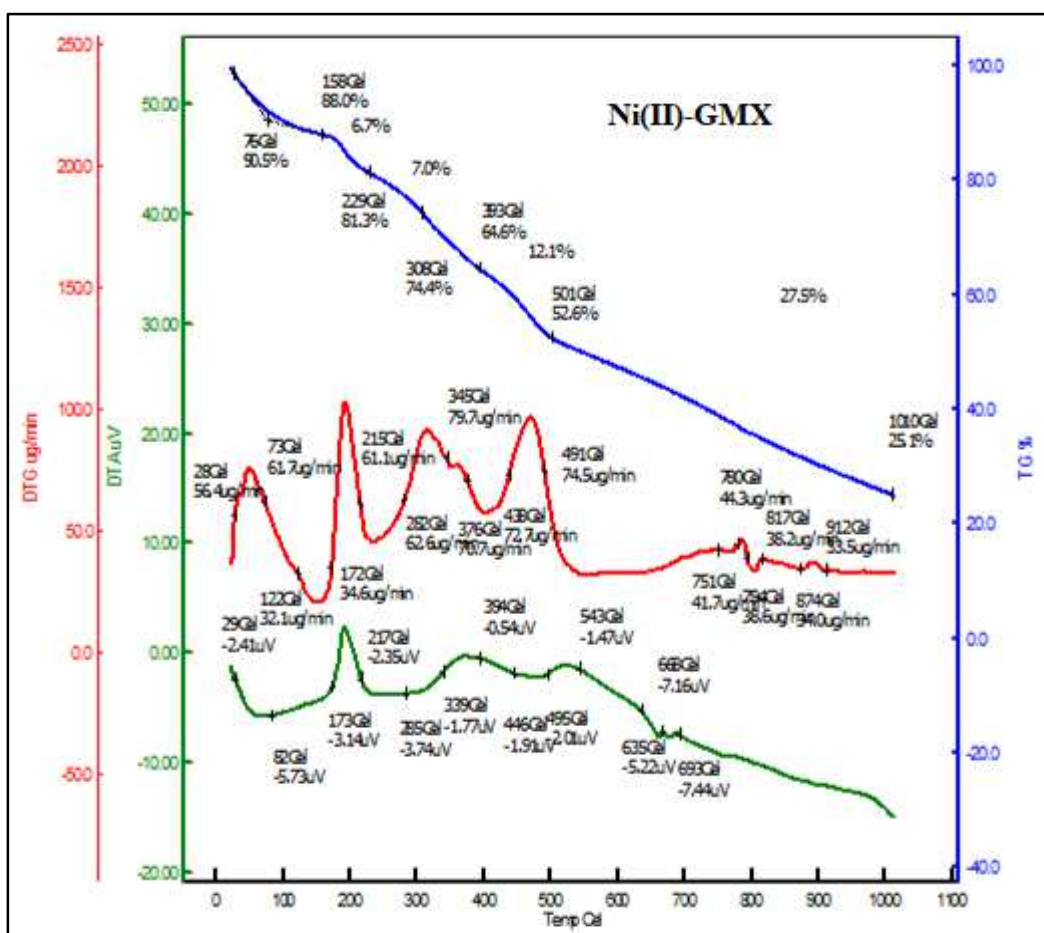


Figure 3.66. Thermograms (TG/DTG/DTA) of Ni(II)-complex of gemifloxacin mesylate.

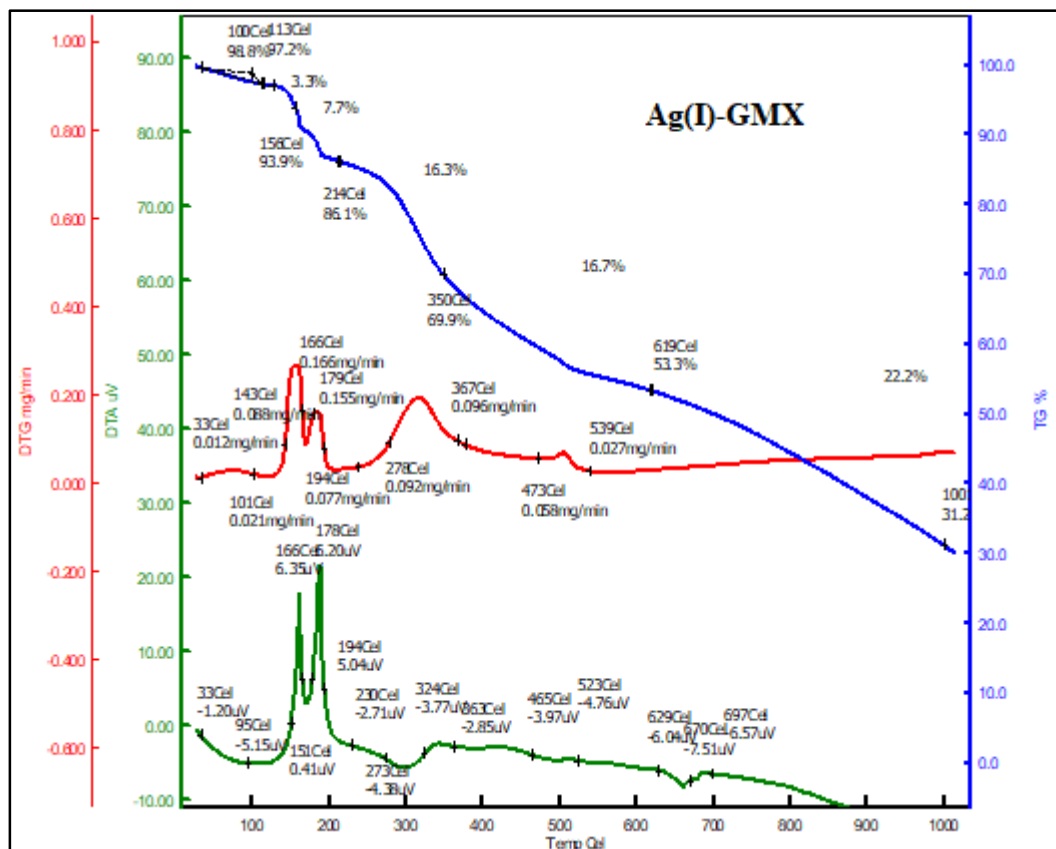


Figure 3.67. Thermograms (TG/DTG/DTA) of Ag(I)-complex of gemifloxacin mesylate.

In the case of Cu(II)-GMX, the degradation started with a 16% weight loss at around 200 °C, which was due to removal of lattice water as well as coordinated water. In the 2nd step, a weight loss of 17.3% was found at the temperature range of 234-393 °C with a T_{max} at 363 °C. In the subsequent steps, 12.5% and 39.9%

weight loss were found at the temperature range of 393 -540 °C and 541-1000 °C, respectively. These losses were due to the degradation of anhydrous complex leaving 14.4% metal oxide as residue. The T_{DTG} and T_{DTA} values are comparable with TG data.

Similarly, in Ni(II)-GMX, the thermal decomposition was composed of four steps at 25-158 °C, 158-229 °C, 229-501 °C, and 501-1010 °C. The 1st step corresponded to 12% weight loss, where the removal of lattice and coordinated water molecule occurred. A stepwise decomposition of the anhydrous metal complex may occur in the 2nd, 3rd and 4th stages leaving metal oxide (25%) as residue. In the DTA curve, a melting endotherm was found at 312 °C which represents the melting temperature of Ni(II)-GMX [237].

The TG curve Ag(I)-GMX consisted of five decomposition steps. The 1st step of decomposition corresponded to a weight loss of 6.1% with T_{max} 67 and 122 °C at the temperature range 25-156 °C. This step is linked with the removal of lattice and coordinated water from the complex. The subsequent steps occurred at the temperature range of 156-214 °C, 214-350 °C, 350-619 °C, and 619-1000 °C, respectively, which are associated with the degradation of anhydrous metal complex. Finally, the complex degraded to 69% even at 1000 °C leaving 31% metal oxide as residue. The DTA data are well agreed with T_{DTG} values and TG

analysis. A sharp endothermic peak at 298.7 °C in the DTA curve of Ag(I)-GMX corresponded to its melting temperature.

Table 3.32. Thermo-analytical (TG/DTG/DTA) results of metal complexes of gemifloxacin mesylate (GMX).

Compound	Decom. step	Temperature range (°C)	Weight loss (%)	DTG _{max} (T _{DTG})	DTA _{max} (T _{DTA})	
					Endo	Exo
Cu(II)- GMX	1 st	25-234	16	41.5, 91	48, 94	175.5
	2 nd	234-393	17.3	286	261	341.5
	3 rd	393-540	12.5	486	457	
	4 th	541-1000	39.9	786.5	658, 868	
Total loss			85.6			
			14.4			
Ni(II)- GMX	1 st	25-158	12	64.5	56	
	2 nd	158-229	6.7	193.5		
	3 rd	229-501	29.2	313, 364	312, 470	366.5
	4 th	501-1010	27.5	787, 893	651, 680	519
Total loss			75			
Residue			25			
Ag(I)- GMX	1 st	25-156	6.1	67, 122	69, 123	
	2 nd	156-214	7.7	166, 179		166,178
	3 rd	214-350	16.3	322.5	298.5	343
	4 th	350-619	16.7	506		
	5 th	619-1000	22.2		663	
Total loss			69.8			
Residue			31.2			

3.29. Elemental Analyses of Gemifloxacin Mesylate (GMX) with Cu(II), Ni(II) and Ag(I) Metal Ions

The percent composition of carbon, hydrogen, nitrogen and sulfur of the precursor antibiotic, GMX and its metal complexes were determined to resolve the correct metal-to-ligand stoichiometry of the metal complexes. The elemental analysis data are listed in Table 3.33.

Table 3.33. Elemental analyses (C, H, N, S) data of the newly synthesized metal complexes.

Complex	Elemental analysis			
	Carbon %	Hydrogen %	Nitrogen %	Sulfur %
	Calc. (Found)	Calc. (Found)	Calc. (Found)	Calc. (Found)
[Cu(GMX) ₂ (H ₂ O) ₂]	32.16	5.68	9.87	6.77
SO ₄ .14H ₂ O	(32.24)	(5.72)	(9.82)	(6,47)
[Ni(GMX) ₂ (H ₂ O)Cl]	34.66	5.51	10.64	4.87
Cl.11H ₂ O	(34.39)	(5.24)	(10.97)	(4.90)
[Ag(GMX) ₂ (H ₂ O) ₂]	37.91	4.60	12.79	5.32
NO ₃ 1.5H ₂ O	(37.69)	(4.41)	(12.76)	(5.21)

The analytical data supported the formation of new metal complexes with a 1:2 metal to ligand stoichiometry. The presence of sulphate, chloride and nitrate ions in the metal complexes as negative counterpart was also confirmed by qualitative determination [238].

3.30. Proposed Structure of Metal Complexes of Gemifloxacin Mesylate with Cu(II), Ni(II) and Ag(I) Metal Ions

The physical properties, spectral characterization, and thermal investigations give shreds of evidence to support the formation of new metal complexes with correct metal-to-ligand stoichiometry. Based on all analytical results, the proposed structure of metal complexes of gemifloxacin mesylate is shown in Figure 3.68.

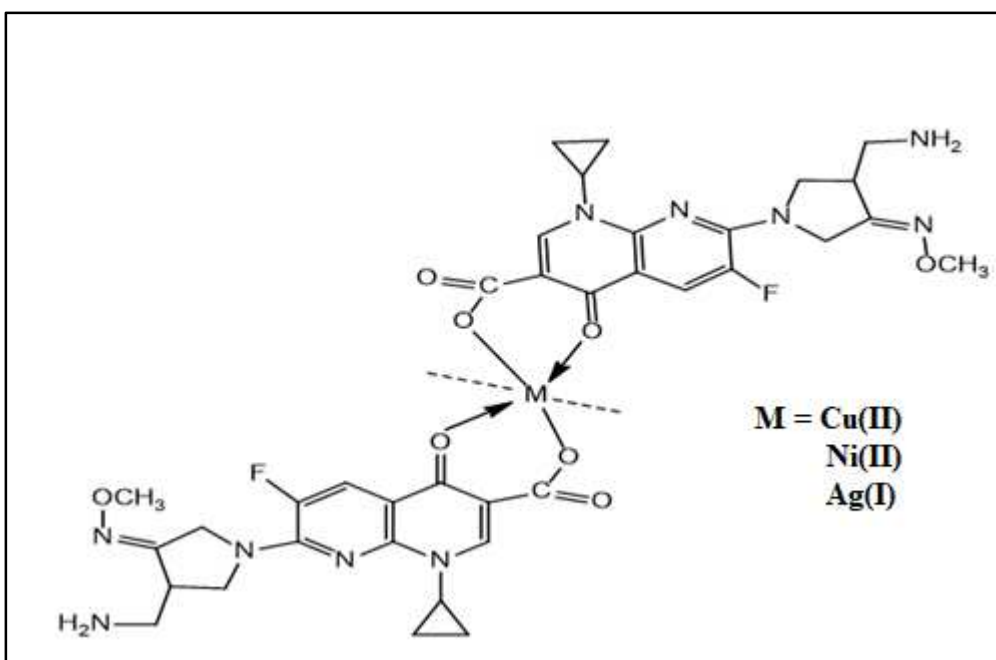


Figure 3.68. The proposed structure of gemifloxacin-metal complexes.

3.31. Biological Activities of Gemifloxacin Mesylate with Cu(II), Ni(II) and Ag(I) Metal Ions

The development of multi-drug resistant is the biggest threat to world economy and mankind as well [239]. Metal-complexes of antibiotics have drawn interest to

scientists in searching of new antibiotics because of their unique electronic and stereochemical properties [240]. Antibiotics, upon coordination with metal ions may increase the biological activity due to increased lipo-solubility of the metal complexes. As a result, the penetration capability of the metal complexes through the lipid membrane is increased and block the protein synthesis which stops the further growth of microorganism [241, 242].

Gemifloxacin mesylate (GMX), a fourth-generation fluoroquinolone antibiotic, is active against a long range of Gram-positive and Gram-negative bacteria. It is used in the treatment of bronchitis and pneumonia caused by bacterial infections. Paper disc-diffusion method was used to study the antimicrobial activity of the parent antibiotic, GMX and its metal complexes. Total 12 bacterial strains including both Gram-positive and Gram-negative and two fungal species were used for this study. The antimicrobial activities of the antibiotic, as well as its metal complexes, were compared by measuring the diameter of the inhibition zone (mm). One of the representative agar plates showing antimicrobial activity is given in Figure 3.69.

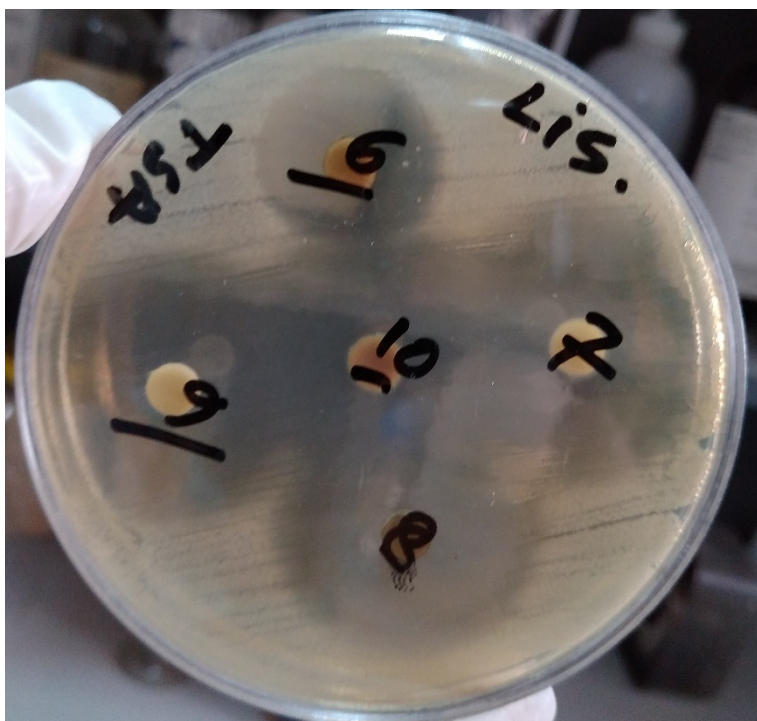


Figure 3.69. A representative agar plate showing the antibacterial activity of GMX antibiotic and its metal complexes.

The results are summarized in Table 3.34.

Table 3.34. The antimicrobial activity of gemifloxacin mesylate (GMX) and its metal complexes, represented as inhibition diameter zone values/mm.

Com- pound	Microbial species													
	Bacteria												Fungi	
	1*	2*	3*	4*	5*	6*	7*	8*	9*	10*	11*	12*	13*	14*
GMX	34	32	34	34	45	33	30	25	28	26	28	32	26	0
Cu(II)- GMX	30	32	33	32	42	33	26	20	25	23	27	28	30	0
Ni(II)- GMX	32	36	34	32	43	33	26	24	28	25	26	30	-	-
Ag(I)- GMX	34	33	40	35	47	34	26	24	28	26	28	30	-	-

The microbial strains which are used to determine biological activity are 1* = *B. cereus*; 2* = *E. coli* 0157; 3* = *E. coli*; 4* = *P. aeruginosa*; 5* = *S. aureus*; 6* = *Listeria*; 7* = *Salmonella typhi*; 8* = *V. cholerae*; 9* = *K. pneumoniae*; 10* = *C. freundii*; 11* = *E. faecalis*; 12* = *E. faecium*; 13* = *Candida sp.*; 14* = *A. niger*.

It was found that the metal complexes of gemifloxacin mesylate showed prominent activity against all the bacterial strains and one of the fungal strains *Candida sp.* Among three complexes, the Ag(I)-GMX was found to show enhanced activity against most of the microbes whereas the Cu(II)-GMX was also found to have enhanced activity against *candida sp* and similar activity against all bacterial strains. The Ni(II)-GMX showed increased activity against *E. coli* 0157 and similar activity against other bacterial strains.

Chapter Four
Conclusion

Antibiotics are chemical agents that either kill bacteria or inhibit the growth of bacteria. They may be natural (aminoglycosides), synthetic (quinolones), and semi-synthetic (cephalosporins). The discovery of the penicillin antibiotic by Alexander Fleming in 1928 opened a new door in the field of medicine which greatly reduced the number of deaths from infections. But, because of overuse and misuse of antibiotics led to antimicrobial resistance and the number of drug-resistant bacteria is increasing day by day. As a result, many curable diseases like tuberculosis, pneumonia, and many other minor infections would become incurable. That's why, antibiotic resistance has become a serious health issue in recent years. Most infectious bacteria are now gaining resistant to at least one of the antibiotics that are usually used to eradicate the infections. This problem persuades the study of new agents that can competently prevent the growth of microbes. Metal and metal-based drugs have a long history in the field of medicine due to their antimicrobial properties. The recent progress of metal complexes in the field of medicinal chemistry is emerging. Many metal complexes are now used in medicine and become successful in the treatment of various life-threatening diseases like cancer, malaria and neurogenerative disorders. Drug metal complexes have already proven as a successful anticancer, anti-diabetic, antacid, antirheumatic and chemotherapeutic agent. Metal-based antimicrobials are less common relative to metal-based anticancer compounds. Recent advances in medicinal chemistry to develop new antimicrobial agents

focused on metal complex-based antimicrobial compounds. Metal complexes of antibiotics with improved bioactivity could be a good solution to treat resistant bacteria. In this regard, complexation of four different antibiotics with three different metals (Cu, Ni & Ag) were done to develop new antibacterial agents with improved bioactivity. The antibiotics were ceftibuten dihydrate (CFT), cefpodoxime proxetil (CFP), cefuroxime axetil (CFU) and gemifloxacin mesylate (GMX). The complexation process was carried out at a definite temperature and at a definite reaction medium keeping the mole ratio of metal to ligand as 1:2. Metal salts were used as a source of metal. Different characterization techniques such as spectral analyses, thermal analyses and elemental analyses were used to establish the structure of metal complexes as well as to confirm the formation of new metal complexes. Based on all analytical results it is found that the proposed structures of metal complexes of three cephalosporin type antibiotics (CFT, CFP and CFU) followed a 1:1 metal-ligand stoichiometry whereas GMX antibiotic-metal complexes followed a 1:2 metal-ligand stoichiometry. After that, *in vitro* biological activities were done against a long range of bacterial strains and fungi by paper disc diffusion method. Metal complexes of antibiotics were found to have increased bioactivity than parent antibiotic itself. This is due to the increased lipo-solubility of metal complexes upon chelation. As a result, the penetration capability of the metal complexes through the lipid membrane of bacterial cell is increased and block the protein synthesis which stop the further growth of

microorganisms and the bacterial cell then die. Among the newly synthesized metal complexes, the Ag(I)- complexes of different antibiotics (CFT, CFP and GMX) were found to be more potent against most of the bacterial strains than the parent antibiotics. The Cu(II)-CFT and Cu(II)-CFU complexes were found to have excellent and enhanced bioactivity than parent ligand. On the contrary, Ni(II)-CFP and Ni(II)-GMX showed similar activity as parent ligand against most of the tested strains and increased activity against one or two strains. So, it is obvious that metal complexes of different antibiotics could hold the place of next-generation antibiotics. Since, antibiotic resistance is the greatest health issue of present time, the development of new antibiotics is a dire need to overcome the crisis. The findings of this study would be a new hope for the development of more potent new antimicrobials. In this regard, metal complexes of different antibiotics with potent bioactivity can play a vital role in the development new antibiotics as well as in the discovery and design of new drugs.

References

1. Waksman, S. A. What is an antibiotic or an antibiotic substance? *Mycologia* **1947**, *39(5)*, 565-569.
2. Calderon C. B, Sabundayo B. P (2007). Antimicrobial classifications: Drugs for bugs. In Schwalbe R, Steele-Moore L, Goodwin AC. Antimicrobial Susceptibility Testing Protocols. CRC Press. Taylor & Frances group. ISBN 978-0-8247-410
3. Chandra, N., Kumar, S. Antibiotics producing soil microorganisms. In: Hashmi, M., Strezov, V., Varma, A. (eds) Antibiotics and Antibiotics Resistance Genes in Soils. Soil Biology, vol 51. Springer, Cham. 2017. https://doi.org/10.1007/978-3-319-66260-2_1
4. Clardy J., Fischbach M. A. Currie, C. R. The natural history of antibiotics. *Current Biology* **2009**, *19(11)*, 437-41.
5. Bérdy, J. Thoughts and facts about antibiotics: Where we are now and where we are heading. *Journal of Antibiotics* **2012**, *65*, 385–395.
6. Kourkouta L. *et al.* History of Antibiotics. *Sumerianz Journal of Medical and Healthcare* **2018**, *1(2)*, 51-54.
7. Vernon, G. Syphilis and Salvarsan. *British Journal of General Practice* **2019**, *69(682)*, 246.
8. Neisser, A. Treatment of syphilis with Ehrlich's preparation 606. *Deutsche Medizinische Wochenschrift* **1910**, *36(1889)*, 1993.
9. Nicholas, C; Lloyd, H. W.; Morgan, P.; Brian, K.; Nicholson, P.; Ronimus, R. S. The Composition of Ehrlich's Salvarsan: Resolution of a Century-Old Debate. *Angewandte Chemie* **2005**, *117(6)*, 963-966.
10. Jeśman, C., Młodzik, A., Cybulska, M. History of antibiotics and sulphonamides discoveries. *Pol Merkur Lekarski* **2011**, *30(179)*, 320-2.

11. Gaynes, R. The discovery of penicillin- New insights after more than 75 years of clinical use. *Emerging Infectious Diseases* **2017**, 23(5), 849–853.
12. Chain, E.; Florey, H. W.; Gardner, N. G.; Heatley, N. G.; Jennings, M. A.; Orr-Ewing, J. *et al.* Penicillin as a chemotherapeutic agent. *Lancet* **1940**, 236, 226-228.
13. Sheehan, J. C.; Henery-Logan, K. R. The total synthesis of penicillin V. *Journal of the American Chemical Society* **1957**, 79(5), 1262–1263.
14. Boundless (2016). Antibiotic Classifications. Boundless microbiology. <https://www.boundless.com/microbiology/textbooks/boundless-microbiology-textbook/antimicrobial-drugs-13/overview-of-antimicrobial-therapy-153/antibiotic-classifications-775-4905/>. Accessed September 13, 2016
15. Waksman, S. A.; Schatz, A.; Reynolds, D. M. Production of antibiotic substances by actinomycetes. *Annals of the New York Academy of Sciences* **2010**, 1213, 112-124.
16. Hutchings, M. I.; Truman, A.W.; Wilkinson, B. Antibiotics: past, present and future. *Current Opinion in Microbiology* **2019**, 51, 72-80.
doi: 10.1016/j.mib.2019.10.008.
17. CVM-MSU (2011) The golden age of antibacterials: Antimicrobial resistance learning site. Michigan State University, East Lansing. <http://amrls.cvm.msu.edu/pharmacology/historical-perspectives/the-golden-age-of-antibacterials>
18. Bbosa, G.; Mwebaza, N.; Odda, J.; Kyegombe, D. and Ntale, M. Antibiotics/antibacterial drug use, their marketing and promotion during the post-antibiotic golden age and their role in the emergence of bacterial resistance. *Health* **2014**, 6, 410-425.
19. (PDF) Antibiotics: Introduction to Classification (researchgate.net)

20. Talaro, K. P. & Chess, B. (2008) Foundations in microbiology; 8th Ed.; McGraw Hill: New York.
21. Wright, G. D. Q & A: Antibiotic resistance: Where does it come from and what can we do about it? *BMC Biology* **2010**, 123.
22. Madigan M. T. & Martinko J. M. (2006) Brock biology of microorganisms; 11th edition; Pearson Prentice Hall Inc.: USA.
23. Reygaert W. C. An overview of the antimicrobial resistance mechanisms of bacteria. *AIMS microbiology* **2018**, 4(3), 482–501. <https://doi.org/10.3934/microbiol.2018.3.482>
24. Ikuma K; Decho A. W.; Lau B. L. When nanoparticles meet biofilms, interactions guiding the environmental fate and accumulation of nanoparticles. *Front Microbiology* **2015**, 6, 591.
25. Dever, L. A.; Dermody, T. S. Mechanisms of Bacterial Resistance to Antibiotics. *Archives of Internal Medicine* **1991**, 151(5), 886–895. doi:10.1001/archinte.1991.00400050040010
26. Dibner, J. J.; Richards, J. D. Antibiotic growth promoters in agriculture: history and mode of action, *Poultry Science* **2005**, 84(4), 634-643.
27. Castanon, J. I. History of the use of antibiotics as growth promoters in European poultry feeds. *Poultry Science* **2007**, 86(11), 2466-24s71. doi: 10.3382/ps.2007-00249.
28. Landers T.F.; Cohen, B.; Wittum, T. E.; *et al.* A review of antibiotic use in food animals: perspective, policy, and potential. *Public Health Reports* **2012**, 127, 4–22.
29. Joint FAO/WHO Expert Committee on Food Additives (JECFA). (1988). Evaluation of certain veterinary drug residues in food. WHO Technical Report Series, 763, 16-33.

30. Joint FAO/WHO Expert Committee on Food Additives (JECFA). (1998a). Toxicological evaluation of certain veterinary drug residues in food: Tetracyclines. WHO Food Additives Series, 41.
31. Joint FAO/WHO Expert Committee on Food Additives (JECFA). (1998b). Toxicological evaluation of certain veterinary drug residues in food: Benzylpenicillin.
<http://www.inchem.org/documents/jecfa/jecmono/v27je05.html>
32. Joint FAO/WHO Expert Committee on Food Additives (JECFA). (1998c). Toxicological evaluation of certain veterinary drug residues in food: Dihydrostreptomycin and streptomycin. WHO Food Additives Series, 39.
33. Joint FAO/WHO Expert Committee on Food Additives (JECFA). (2000a.) Procedures for recommending maximum residue limits-residues of veterinary drugs in food. pp. 43-51.
34. Joint FAO/WHO Expert Committee on Food Additives (JECFA). (2000b). Toxicological evaluation of certain veterinary drug residues in food: Estradiol-17 α , progesterone, and testosterone. WHO Food Additives Series, 43.
35. Joint FAO/WHO Expert Committee on Food Additives (JECFA). (2000c). Toxicological evaluation of certain veterinary drug residues in food: Melengestrol acetate. WHO Food Additives Series, 45.
36. Joint FAO/WHO Expert Committee on Food Additives (JECFA). (2000d). Toxicological evaluation of certain veterinary drug residues in food: Lincomycin. WHO Food Additives Series, 45.
37. Diaz-Sanchez, S.; Doris D.S.; Biswas, D.; Hanning, I. Botanical alternatives to antibiotics for use in organic poultry production. *Poultry Science* **2015**, *94*(6), 1419-1430. <https://doi.org/10.3382/ps/pev014>.
38. Cushnie, T. P.; Cushnie, B., Echeverría, J., Fowsantear, W.; Thammawat, S.; Dodgson, J. L. *et al.* Bioprospecting for antibacterial drugs: a

- multidisciplinary perspective on natural product source material, bioassay selection and avoidable pitfalls. *Pharmaceutical Research* **2020**, *37*(7), 125. doi:10.1007/s11095-020-02849-1.
39. Krauze, M. Phytobiotics, a natural growth promoter for poultry. *Veterinary Medicine and Science*, Intechopen, **2021**, doi: 10.5772/intechopen.99030
 40. <https://www.wattagnet.com/articles/3346-phytobiotics-a-natural-growth-promoter-for-poultry>.
 41. Alghirani, M. M.; Chung, E. L. T.; Jesse, F. F. A.; Sazili, A. Q.; & Loh, T. C. Could phytobiotics replace antibiotics as feed additives to stimulate production performance and health status in poultry? An Overview. *Journal of Advanced Veterinary Research* **2021**, *11*(4), 254-265. <https://advetresearch.com/index.php/AVR/article/view/810>
 42. Saartje M. J. & Nery S.F. Phytogenic feed additives as an alternative to antibiotic growth promoters in poultry nutrition. *Veterinary Medicine and Science* **2021**. doi: 10.5772/intechopen.99401
 43. Aminov, R. I. A brief history of the antibiotic era: lessons learned and challenges for the future. *Frontiers in Microbiology* **2010**, *1*, 134. <https://doi.org/10.3389/fmicb.2010.00134>
 44. CDC. Antibiotic resistance threats in the United States, 2019. Report 2019.
 45. The Journal of global antimicrobial resistance meets the World Health Organization (WHO), *Journal of Global Antimicrobial Resistance* **2019**, *8*, 305-308. <https://doi.org/10.1016/j.jgar.2019.07.022>.
 46. Hoque, R.; Ahmed, S. M.; Naher, N.; Islam, M. A.; Rousham, E. K., Islam BZ, Hassan S. Tackling antimicrobial resistance in Bangladesh: A scoping review of policy and practice in human, animal and environment sectors. *PLoS One*. **2020**, *15*(1), 0227947. doi: 10.1371/journal

47. Asad, M. A.; Khan, U. Global economic impact of antibiotic resistance: A review. *Journal of Global Antimicrobial Resistance* **2019**, *19*, 313-316. <https://doi.org/10.1016/j.jgar.2019.05.024>.
48. Rossiter, S. E.; Fletcher, M. H. and Wuest, W. M. Natural products as platforms to overcome antibiotic resistance. *Chemical Reviews* **2017**, *117* (19), 12415-12474. DOI: 10.1021/acs.chemrev.7b00283
49. Giacomini, E.; Perrone, V.; Alessandrini, D.; Paoli, D.; Nappi, C., Degli Esposti, L. Evidence of antibiotic resistance from population-based studies: A narrative review. *Infect Drug Resist.* **2021**, *14*, 49-858. <https://doi.org/10.2147/IDR.S289741>
50. Edwin, C. C. and Catherine, E. H. Coordination chemistry: the scientific legacy of Alfred Werner. *Chem. Soc. Rev.* **2013**, *42*, 1429-1439.
51. Gupta, S. P. Roles of metals in human health. *MOJ Biorganic & Organic Chemistry*. **2018**, *2*(5), 221–224. DOI: 10.15406/mojboc.2018.02.00085
52. Rebecca, A. A.; Matthew, D. H. and Trevor W. H. The Discovery and development of cisplatin. *Journal of Chemical Education* **2006**, *83*(5), 728. DOI: 10.1021/ed083p728
53. Felson, D. T.; Anderson, J. J.; Meenan, R. F. The comparative efficacy and toxicity of second-line drugs in rheumatoid arthritis. Results of two meta-analyses. *Arthritis Rheum* **1990**, *33*(10), 1449-1461. doi: 10.1002/art.1780331001.
54. Briand, G.G.; Burford, N. Bismuth compounds and preparations with biological or medicinal relevance. *Chem Rev.*, **1999**, *99*(9), 2601-2658. doi: 10.1021/cr980425s.
55. Kelland, L. The resurgence of platinum-based chemotherapy. *Nature Reviews Cancer* **2007**, *7*, 573-584.

56. Dasari, S.; Tchounwou P. B. Cisplatin in cancer therapy: molecular mechanisms of action. *European Journal of Pharmacology* **2014**, *740*, 364-378. doi: 10.1016/j.ejphar.2014.07.025.
57. Weiss, R. B.; Christian, M. C. New cisplatin analogues in development. A review. *Drugs* **1993**, *46*, 360–377.
58. Ghosh, S. Cisplatin: The first metal based anticancer drug. *Bioorganic Chemistry* **2019**, *88*, 102925. <https://doi.org/10.1016/j.bioorg.2019.102925>.
59. Rubio, A.R.; González, R.; Busto, N.; Vaquero, M.; Iglesias, A.L.; Jalón, F.A.; Espino, G.; Rodríguez, A.M.; García, B.; Manzano, B.R. Anticancer activity of half-sandwich Ru, Rh and Ir complexes with chrysin derived ligands: strong effect of the side chain in the ligand and influence of the metal. *Pharmaceutics* **2021**, *13*,1540. <https://doi.org/10.3390/pharmaceutics13101540>
60. Galib, B. M.; Mashru, M.; Jagtap, C.; Patgiri, B. J.; Prajapati, P. K. Therapeutic potentials of metals in ancient India: A review through Charaka Samhita. *J Ayurveda Integr Med.* **2011**, *2*(2), 55-63. doi: 10.4103/0975-9476.82523.
61. Ingle, A. P. *et al.* (2018). Copper in Medicine: Perspectives and Toxicity. In: Rai, M., Ingle, A., Medici, S. (eds) *Biomedical Applications of Metals*. Springer, Cham. https://doi.org/10.1007/978-3-319-74814-6_4
62. Akhidime, I. D.; Saubade, F.; Paul, S.; Benson, P. S.; Butler, J. A.; Olivier, S.; Kelly, P.; Verran, J.; Whitehead, K. A. The antimicrobial effect of metal substrates on food pathogens, *Food and Bioprocess Processing* **2019**, *113*, 68-76. <https://doi.org/10.1016/j.fbp.2018.09.003>.
63. Iakovidis, I.; Delimaris, I.; Piperakis S. M. Copper and its complexes in medicine: a biochemical approach. *Molecular Biology International* **2011**, 594529. doi: 10.4061/2011/594529.

64. Gokhale, N. H.; Padhye, S. S.; Padhye, S. B.; Anson, C. E.; Powell, A. K. Copper complexes of carboxamidrazone derivatives as anticancer agents. 3. Synthesis, characterization and crystal structure of [Cu(appc)Cl₂], (appc=N1-(2-acetylpyridine) pyridine-2-carboxamidrazone). *Inorganica Chimica Acta* **2001**, *319*(1-2), 90–94.
65. Trávníček, Z.; Malon, M.; Šindelář, Z. *et al.* Preparation, physicochemical properties and biological activity of copper(II) complexes with 6-(2-chlorobenzylamino) purine (HL1) or 6-(3-chlorobenzylamino) purine (HL2). The single-crystal X-ray structure of [Cu(H+L2)Cl₃]Cl·2H₂O. *Journal of Inorganic Biochemistry*. **2001**, *84*(1-2), 23–32.
66. Chaviara, A. TH.; Christidis, P. C.; Papageorgiou, A.; Chrysogelou, E.; Hadjipavlou-Litina, D. J. and Bolos, C. A. *In vivo* anticancer, anti-inflammatory, and toxicity studies of mixed-ligand Cu(II) complexes of dien and its Schiff dibases with heterocyclic aldehydes and 2-amino-2-thiazoline. Crystal structure of [Cu(dien)(Br)(2a-2tzn)](Br)(H₂O). *Journal of Inorganic Biochemistry* **2005**, *99*, 11, 2102–2109.
67. Dhar, D. N.; Taploo, C. L. Schiff-bases and their applications. *Journal of Scientific & Industrial Research* **1982**, *41*(8), 501–506.
68. Fatima, A.; Pereira, C. P.; Olímpio, C. R.; Oliveira, B. G. F.; Lucas, L. F.; Silva, P. H. C. Schiff bases and their metal complexes as urease inhibitors – A brief review. *Journal of Advanced Research* **2018**, *13*, 113-126. <https://doi.org/10.1016/j.jare.2018.03.007>.
69. Zhang, Z.; Wang, H.; Yan, M.; Wang, H.; Zhang, C. Novel copper complexes as potential proteasome inhibitors for cancer treatment (Review). *Molecular Medicine Reports* **2017**, *15*(1), 3-11. doi: 10.3892/mmr.2016.6022.
70. Laila H. Abdel-Rahman, Rafat M. El-Khatib, Lobna A.E. Nassr, Ahmed M. Abu-Dief, Mohamed Ismael, Amin Abdou Seleem. Metal based

pharmacologically active agents: Synthesis, structural characterization, molecular modeling, CT-DNA binding studies and in vitro antimicrobial screening of iron(II) bromosalicylidene amino acid chelates, *Spectrochimica Acta Part A: Molecular and Biomolecular Spectroscopy* **2014**, *117*, 366-378. <https://doi.org/10.1016/j.saa.2013.07.056>.

71. Kajal, A.; Bala, S.; Kamboj, S.; Sharma, N. and Saini, V. Schiff Bases: A Versatile Pharmacophore. *Journal of Catalysts* **2013**, *2013*. <https://doi.org/10.1155/2013/893512>
72. Hameed, A.; Rashida, M.; Uroos, M.; Ali, S. A. & Khan, K. M. Schiff bases in medicinal chemistry: a patent review (2010-2015). *Expert Opinion on Therapeutic Patents* **2017**, *27(1)*, 63-79. DOI: 10.1080/13543776.2017.1252752
73. Yu, Z.; Wang, F.; Milacic, V.; Li, X.; Cui, Q. C.; Zhang, B.; Yan, B. and Dou Q. P. Evaluation of copper-dependent proteasome-inhibitory and apoptosis-inducing activities of novel pyrrolidine dithiocarbamate analogues. *Int J Mol Med* **2007**, *20*, 919-925.
74. Wang, F.; Zhai, S.; Liu, X.; Li, L.; Wu, S., Dou, Q. P. and Yan, B. A novel dithiocarbamate analogue with potentially decreased ALDH inhibition has copper-dependent proteasome-inhibitory and apoptosis-inducing activity in human breast cancer cells. *Cancer Lett* **2011**, *300*, 87-95.
75. Daniel, K. G.; Harbach, R. H.; Guida, W. C. and Dou, Q. P. Copper storage diseases: Menkes, Wilson's, and cancer. *FrontBioscience* **2004**, *9*, 2652-2662.
76. Chen, D; Cui, Q. C.; Yang, H. and Dou Q. P. Disulfiram, a clinically used anti-alcoholism drug and copper-binding agent, induces apoptotic cell death in breast cancer cultures and xenografts via inhibition of the proteasome activity. *Cancer Research* **2006**, *66*, 10425-10433.

77. Barillo D. J.; Marx, D. E. Silver in medicine: a brief history BC 335 to present. *Burns* **2014**, *40*, S3-8. doi: 10.1016/j.burns.2014.09.009.
78. Medici, S.; Peana, M.; Guido, C.; Nurchi, V. M.; Lachowicz, J. I.; Remelli, M.; Zoroddu, M. A. Silver coordination compounds: A new horizon in medicine. *Coordination Chemistry Reviews* **2016**, *327*, 349-359. <https://doi.org/10.1016/j.ccr.2016.05.015>.
79. Aleksandra, H.; Paulina, K.; Karolina, K.; Agnieszka, S.; Rowinska-Zyrek Magdalena, R. Z. and Henryk, K. Ag⁺ Complexes as Potential Therapeutic Agents in Medicine and Pharmacy. *Current Medicinal Chemistry* **2019**, *26(4)*, 624-647.
<https://dx.doi.org/10.2174/0929867324666170920125943>
80. Nunes, J. H.; Bergamini, F. R.; Lustri, W. R.; de Paiva P. P.; Ruiz, A. L.; de Carvalho, J. E. *et al.* Synthesis, characterization and in vitro biological assays of a silver (I) complex with 5-fluorouracil: A strategy to overcome multidrug resistant tumor cells. *J Fluor Chem.* **2017**, *195*, 93-101.
81. Banti, C. N.; Hadjikakou, S. K. Anti-proliferative and anti-tumor activity of silver(I) compounds. *Metallomics* **2013**, *5(6)*, 569-596.
82. Raju, S. K.; Karunakaran, A.; Kumar, S.; Sekar, P.; Murugesan, M. & Karthikeyan, M. Silver complexes as anticancer agents: A perspective review. *German Journal of Pharmaceuticals and Biomaterials* **2022**, *1(1)*, 6–28. <https://doi.org/10.5530/gjpb.2022.1.3>
83. Canudo-Barreras, G.; Ortego, L.; Izaga, A.; Marzo, I., Herrera, R. P.; Gimeno, M. C. Synthesis of new thiourea-metal complexes with promising anticancer properties. *Molecules* **2021**, *26(22)*, 6891.
84. Xiao, X.; Liu, E.; Shao, J.; Ge, S. Advances on biodegradable zinc-silver-based alloys for biomedical applications. *Journal of Applied Biomaterials & Functional Materials* **2021**, *19*, 1-11. doi:10.1177/22808000211062407

85. Benedek, T.G. The history of gold therapy for tuberculosis. *J. Hist. Med. Allied Sci.* **2004**, *59*, 50–89. doi: 10.1093/jhmas/jrg042.
86. Medici, S.; Peana, M.; Nurchi, V. M.; Lachowicz, J. I.; Crisponi G.; Zoroddu M. A. Noble metals in medicine: Latest advances. *Coord. Chem. Rev.* **2015**, *284*, 329–350. doi: 10.1016/j.ccr.2014.08.002.
87. <https://www.chem.tamu.edu/rgroup/marcetta/chem489/Presentations/Gold>
88. Yeo, C. I.; Ooi, K. K.; Tiekink, E. R. T. Gold-based medicine: A paradigm shift in anti-cancer therapy? *Molecules* **2018**, *23*(6), 1410. doi: 10.3390/molecules23061410.
89. Ott, I. On the medicinal chemistry of gold complexes as anticancer drugs. *Coordination Chemistry Reviews* 2009, *253*, 1670-1681, <https://doi.org/10.1016/j.ccr.2009.02.019>.
90. Messori, L.; Scaletti, F.; Massai, L.; Cinellu, M. A.; Gabbiani, C.; Vergara, A. and Merlino, A. The mode of action of anticancer gold-based drugs: a structural perspective, *Chem. Commun.*, **2013**, *49*, 10100. DOI:10.1039/C3CC46400H
91. Morones-Ramirez, J. R.; Winkler, J. A.; Spina, C. S.; Collins, J. J. Silver enhances antibiotic activity against gram-negative bacteria. *Sci. Transl. Med.* **2013**, *5*, 1–11.
92. Herisse, M.; Duverger, Y.; Martin-Verstraete, I.; Barras, F.; Ezraty, B. Silver potentiates aminoglycoside toxicity by enhancing their uptake. *Mol. Microbiol.* **2017**, *105*, 115–126.
93. Kim, J.; Pitts, B.; Stewart, P. S.; Camper, A.; Yoon, J. Comparison of the antimicrobial effects of chlorine, silver ion, and tobramycin on biofilm. *Antimicrob. Agents Chemother* **2008**, *52*, 1446–1453.
94. Wan, G.; Ruan, L.; Yin, Y.; Yang, T.; Ge, M.; Cheng, X. Effects of silver nanoparticles in combination with antibiotics on the resistant bacteria *Acinetobacter baumannii*. *Int. J. Nanomed.* **2016**, *11*, 3789–3800.

95. Barras, F.; Aussel, L.; Ezraty, B. Silver and antibiotic, New facts to an old story. *Antibiotics* **2018**, *7*, 79. <https://doi.org/10.3390/antibiotics7030079>
96. Claudel, M.; Schwarte, J. V.; Fromm, K. M. New antimicrobial strategies based on metal complexes. *Chemistry* **2020**, *2*, 849-899. <https://doi.org/10.3390/chemistry2040056>
97. Ramotowska, S.; Wysocka, M.; Brzeski, J.; Chylewska, A.; Makowski, M. A comprehensive approach to the analysis of antibiotic-metal complexes. *TrAC Trends in Analytical Chemistry* **2020**, *123*, 115771. <https://doi.org/10.1016/j.trac.2019.115771>.
98. Miguel, A. Sierra, L. C.; de la Torre, M. C. Bio-organometallic derivatives of antibacterial drugs. *Chem. Eur. J.* **2019**, *25* (30), 7232-7242.
99. Chellan, P. and Sadler, P. J. Enhancing the activity of drugs by conjugation to organometallic fragments. *Chem. Eur. J.* **2020**, *26*, 8676-8688.
100. Top, S.; Vessières, A.; Cabestaing, C.; Laios, I.; Leclercq, G.; Provot, C.; Jaouen, G. Studies on organometallic selective estrogen receptor modulators (SERMs) Dual activity in the hydroxy-ferrocifen series. *J. Organomet. Chem.* **2001**, *637*, 500–506.
101. Top, S.; Vessières, A.; Leclercq, G.; Quivy, J.; Tang, J.; Vaissermann, J.; Huche, M.; Jaouen, G. Synthesis, biochemical properties and molecular modelling studies of organometallic specific estrogen receptor modulators (SERMs), the ferrocifens and hydroxyferrocifens: Evidence for an antiproliferative effect of hydroxyferrocifens on both hormone-dependent and hormone-independent breast cancer cell lines. *Chem. Eur. J.* **2003**, *9*, 5223- 5236.
102. Plazuk, D.; Wiczorek, A.; Ciszewski, W. M.; Kowalczyk, K.; Błauz, A.; Pawleńdzio, S.; Makal, A.; Eurtivong, C.; Arabshahi, H. J.; Reynisson, J.; Hartinger, C. G.; Rychlik, B. Synthesis and *in vitro* biological evaluation

- of ferrocenyl side-chain-functionalized paclitaxel derivatives. *Chem Med Chem* **2017**, *12*, 1882 – 1892.
103. Hathiram, B.T.; Grewal, D.S.; Tankwal, P.; Shah, N.; Agarwal, R. Ceftibuten in ENT infections. *Indian J. Otolary. Head & Neck Surg.* **1999**, *51*, 104-107.
 104. Tomasz, A. The mechanism of the irreversible antimicrobial effects of penicillins: How the beta-lactam antibiotics kill and lyse bacteria. *Annu. Rev. Microbiol.* **1979**, *33*, 113-137.
 105. Watanabe, A.; Oizumi, K.; Motomiya, M.; Yoshida, T.; Ito, T.; Kanayama, H.; Saito, J.; Nakai, Y.; Sato, K. Therapeutic efficacy of ceftibuten in chronic respiratory tract infections. *Jpn. J. Antibiot.* **1990**, *43*, 768-778.
 106. Available at <https://en.wikipedia.org/wiki/Cefpodoxime>.
 107. Fulton, B.; Perry, C. M. Cefpodoxime proxetil: a review of its use in the management of bacterial infections in paediatric patients. *Paediatr Drugs* **2001**, *3(2)*, 137-58. doi: 10.2165/00128072-200103020-00006.
 108. Brogden R. N.; Heel, R. C., Speight, T. M., Avery, G. S. Cefuroxime: a review of its antibacterial activity, pharmacological properties and therapeutic use. *Drugs* **1979**, *17(4)*, 233-66. doi: 10.2165/00003495-197917040-00001.
 109. Shahbaz, K. Cephalosporins: pharmacology and chemistry. *Pharmaceutical and Biological Evaluations* **2017**, *4(6)*, 234-238. DOI: <http://dx.doi.org/10.26510/2394-0859.pbe.2017.36>
 110. Das, N.; Madhavan, J.; Selvi, A.; Das, D. An overview of cephalosporin antibiotics as emerging contaminants: a serious environmental concern. *Biotech.* **2019**, *9(6)*, 231. DOI: 10.1007/s13205-019-1766-9.

111. Padmaja, U. *Pharmacology for Dental and Allied Health Sciences*. **2017**, Jaypee Brothers Medical Publishers (P) Ltd. https://doi.org/10.5005/jp/books/12949_35
112. Rusu, A.; Lungu, I.-A.; Moldovan, O.-L.; Tanase, C.; Hancu, G. Structural characterization of the millennial antibacterial (Fluoro) quinolones—shaping the fifth generation. *Pharmaceutics* **2021**, *13*, 1289. <https://doi.org/10.3390/pharmaceutics13081289>
113. Jomova, K.; Makova, M.; Alomar, S. Y.; Alwasel, S. H.; Nepovimova, E.; Kuca, K.; Rhodes, C. J.; Valko, M. Essential metals in health and disease. *Chemico-Biological Interactions* **2022**, *367*, 110173. <https://doi.org/10.1016/j.cbi.2022.110173>
114. Zoroddu, M. A.; Aaseth, J.; Crisponi, G.; Medici, S.; Peana, M.; Nurchi, V. M. The essential metals for humans: a brief overview, *Journal of Inorganic Biochemistry* **2019**, *195*, 120-129. <https://doi.org/10.1016/j.jinorgbio.2019.03.013>.
115. Duncan, C.; White, A. R. Copper complexes as therapeutic agents. *Metallomics* **2012**, *4*(2), 127–138. <https://doi.org/10.1039/c2mt00174h>
116. Iakovidis, I.; Delimaris, I.; Piperakis, S. M. Copper and its complexes in medicine: A biochemical approach. *Molecular Biology International* **2011**, *2011*, 1-13. <https://doi.org/10.4061/2011/594529>
117. https://en.wikipedia.org/wiki/Nickel_compounds
118. Zdrojewicz, Z.; Popowicz, E.; Winiarski, J. Nickel - role in human organism and toxic effects. *Pol Merkur Lekarski* **2016**, *41*(242), 115-118.
119. Genchi, G.; Carocci, A.; Lauria, G.; Sinicropi, M. S.; Catalano, A. Nickel: Human Health and Environmental Toxicology. *Int J Environ Res Public Health* **2020**, *17*(3), 679. doi: 10.3390/ijerph17030679.
120. El-ghamry, M.A.; Elzawawi, F.M.; Aziz, A.A.A. *et al.* New Schiff base ligand and its novel Cr(III), Mn(II), Co(II), Ni(II), Cu(II), Zn(II)

- complexes: spectral investigation, biological applications, and semiconducting properties. *Sci Rep* **2022**, *12*, 17942. <https://doi.org/10.1038/s41598-022-22713-z>
121. Saiyed, T. A.; Adeyemi, J. O. and Onwudiwe, D. C.. The structural chemistry of zinc(ii) and nickel(ii) dithiocarbamate complexes. *Open Chemistry* **2021**, *19(1)*, 974-986. <https://doi.org/10.1515/chem-2021-0080>
 122. Yankin, A. N & Dmitriev, M. V. Nickel complexes as efficient catalysts in multicomponent synthesis of tetrahydropyridine derivatives, *Synthetic Communications*, **2020**, *50(22)*, 3481-3489. DOI: 10.1080/00397911.2020.1803357
 123. National Center for Biotechnology Information (2022). PubChem Element Summary for AtomicNumber 47, Silver. Retrieved November 4, 2022 from <https://pubchem.ncbi.nlm.nih.gov/element/Silver>.
 124. Barillo, D. J.; Marx, D. E. Silver in medicine: A brief history BC 335 to present, *Burns* **2014**, *40*, S3-S8. <https://doi.org/10.1016/j.burns.2014.09.009>.
 125. Medici, S.; Peana, M.; Crisponi, G.; Nurchi, V. M.; Lachowicz, J. I.; Remelli, M.; Zoroddu, M. A. Silver coordination compounds: A new horizon in medicine. *Coordination Chemistry Reviews* **2016**, *327–328*, 349-359. <https://doi.org/10.1016/j.ccr.2016.05.015>
 126. ClinicalTrials.gov is a Database of Privately and Publicly Funded Clinical Studies Conducted around the World. Available online: www.clinicaltrials.gov (accessed on 5 May 2020).
 127. Möhler, J.S.; Kolmar, T.; Synnatschke, K.; Hergert, M.; Wilson, L.A.; Ramu, S.; Elliott, A.G.; Blaskovich, M.A.T.; Sidjabat, H.E.; Paterson, D.L. et al. Enhancement of antibiotic-activity through complexation with metal ions - Combined ITC, NMR, enzymatic and biological studies. *J. Int. Biochem.* **2017**, *167*, 134–141.

128. Liang, X.; Luan, S.; Zhongqiong, Y.; Min H., Changliang H.; Lizi Y.; Zou, Y.; Yuan, Z.; Li, L.; Xu Song, Chen L.; Zhang, W. Recent advances in the medical use of silver complex. *European Journal of Medicinal Chemistry* **2018**, *157*, 62-68.
<https://doi.org/10.1016/j.ejmech.2018.07.057>.
129. Deore, A. B.; Dhumane, J. R.; Wagh, H.V.; Sonawane, R. B. The Stages of Drug Discovery and Development Process. *Asian Journal of Pharmaceutical Research and Development* **2019**, *7(6)*, 62-67, DOI: <http://dx.doi.org/10>
130. <https://www.pharmacy180.com/article/collaborating-disciplines-2699>
131. Liu, G.; Xie, Y.; Sun, Y. *et al.* Drug research and development opportunities in low- and middle-income countries: accelerating traditional medicine through systematic utilization and comprehensive synergy. *Infect Dis Poverty* **2022**, *11*, 27. <https://doi.org/10.1186/s40249-022-00954-4>
132. Kuhlmann, J. Drug interaction studies during drug development: which, when, how? *Int J Clin Pharmacol Therapeutics* **1994**, *32(6)*, 305-311.
133. Riccardi, L.; Genna, V. & De Vivo, M. Metal–ligand interactions in drug design. *Nat Rev Chem* **2018**, *2*, 100–112. <https://doi.org/10.1038/s41570-018-0018-6>
134. Stapleton, P.D.; Shah S.; Anderson J. C. *et al.* Modulation of beta-lactam resistance in *Staphylococcus aureus* by catechins and gallates. *Int J Antimicrob Agents* **2004**, *23*, 462-467.
135. Boyd N. K.; Teng, C. and Frei C. R. Brief overview of approaches and challenges in new antibiotic development: A focus on drug repurposing. *Front. Cell. Infect. Microbiol.* **2021**, *11*, 684515. doi:10.3389/fcimb.2021.684515.

136. Claudel, M.; Schwarte, J.V.; Fromm, K.M. New antimicrobial strategies based on metal complexes. *Chemistry* **2020**, *2*, 849-899. <https://doi.org/10.3390/chemistry2040056>
137. Katherine J. F. and Metzler-Nolte, N. Introduction: Metals in Medicine, *Chemical Reviews* **2019**, *119*(2), 727-729. DOI: 10.1021/acs.chemrev.8b00685
138. Ndagi, U.; Mhlongo, N. & Soliman, M. E.. Metal complexes in cancer therapy - an update from drug design perspective. *Drug design, development and therapy* **2017**, *11*, 599–616. <https://doi.org/10.2147/DDDT.S119488>
139. Kostova I. Ruthenium complexes as anticancer agents. *Curr Med Chem.* **2006**, *13*(9), 1085–1107.
140. Kar, B.; Roy, N.; Pete, S.; Moharana, P., Paira, P., Ruthenium and iridium based mononuclear and multinuclear complexes: A Breakthrough of Next-Generation anticancer metallopharmaceuticals. *Inorganica Chimica Acta* **2020**, *512*, 119858. <https://doi.org/10.1016/j.ica.2020.119858>.
141. Nareetsile, F. M.; Matshwele, J. T. & Odisitse, S. Metallo-Drugs as Promising Antibacterial Agents and Their Modes of Action. *Journal of Medicinal and Chemical Sciences*, **2022**, *5*(6), 1109-1131. doi: 10.26655/JMCHEMSCI.2022.6.24
142. Korablina, D. D.; et al. Pharmacological Activity of 4,5-Dihydropyrazole Derivatives (Review). *Pharmaceutical Chemistry Journal* **2016**, *50*(5), 281.
143. Vamsikrishna, N.; Kumar, M.P., Tejaswi, S. *et al.* DNA Binding, Cleavage and Antibacterial Activity of Mononuclear Cu(II), Ni(II) and Co(II) Complexes Derived from Novel Benzothiazole Schiff Bases. *J Fluoresc* **2016**, *26*, 1317–1329. <https://doi.org/10.1007/s10895-016-1818-z>

144. Bhadra Sulekha and GajeraAvin, Topical spray of silver sulfadiazine for woundhealing. *Journal of Chemical and Pharmaceutical Research*, **2016**, 8(7), 492-498.
145. Seku, K.; Yamala, A.K.;Kancherla, M. *et al.* Synthesis of moxifloxacin–Au (III) and Ag (I) metal complexes and their biological activities. *Journal of Analytical Science and Technology* **2018**, 9, 14. <https://doi.org/10.1186/s40543-018-0147-z>
146. Leitão, J.H.; Sousa, S.A.; Leite, S.A.; Carvalho, M.F.N.N. Silver camphor imine complexes: novel antibacterial compounds from old medicines. *Antibiotics* **2018**, 7, 65. <https://doi.org/10.3390/antibiotics7030065>
147. Sadeek, S. A.; EI-Shwiniy, W. H.; Zordik, W. A.; EI-Didamony, A. M. Synthetic, spectrotopic, thermal and biologocal activity investigation of new Y(III) and Pd(II) complexes of norfloxacin. *J. Argent. Chem. Soc.*, **2009**, 97(2), 128-148.
148. Shaikh, A. R, Giridhar, R., Yadav, M. R. Bismuth-norfloxacin complex: Synthesis, physicochemical and antimicrobial evaluation. *International journal of Pharmaceutics* 2007, 332(1-2), 24-30.
149. Imran, M., Iqbal, J., Iqbal, S. and Ijaz, N. *In Vitro* antibacterial studies of ciprofloxacin-imines and their complexes with Cu(II),Ni(II),Co(II), and Zn(II). *Turkish Journal of Biology* **2007**, 31(2), 67-72.
150. Guerra, W.; de Andrade Azevedo, E.; de Souza Monteiro, A.R;Bucciarelli-Rodriguez, M.;Chartone-Souza, E.; Nascimento, A. M.; Fontes, A. P.; Le Moyec, L.; Pereira-Maia, E. C. Synthesis, characterization, and antibacterial activity of three palladium(II) complexes of tetracyclines. *J Inorg Biochem.* **2005** 99(12), 2348-54. doi: 10.1016/j.jinorgbio.2005.09.001.

151. Auda, S.H.; Mrestani, Y.; Fetouh, M. I.; Neubert, R. H. H. Characterization and activity of cephalosporin metal complexes. *Pharmazie* **2008**, *63*, 555–561. doi:10.1691/ph.2008.8532
152. Alekseev, V.G. Metal complexes of penicillins and cephalosporins (Review). *Pharmaceutical Chemistry Journal* **2012**, *45*, 679–697. <https://doi.org/10.1007/s11094-012-0703-6>
153. Uivarosi, V. Metal complexes of quinolone antibiotics and their applications: an update. *Molecules* **2013**, *18*(9), 11153–11197. <https://doi.org/10.3390/molecules180911153>
154. Serafin, A.; Stańczak, A. The complexes of metal ions with fluoroquinolones. *Russian Journal of Coordination Chemistry* **2009**, *35*, 81–95. <https://doi.org/10.1134/S1070328409020018>
155. Ascierio, P. A.; Marincola, F.M. Combination therapy: the next opportunity and challenge of medicine. *Journal of Translational Medicine* **2011**, *9*, 115. <https://doi.org/10.1186/1479-5876-9-115>
156. Kumar, M., Sodhi, K. K., Singh, P., Agrawal, P. K. and Singh, D. K. Synthesis and characterization of antibiotic-metal complexes [FeCl₃(L1)₂H₂O and Ni(NO₃)₂(L2)₂H₂O] and enhanced antibacterial activity. *Environ. Nano. Monit. Manga.* 2019. **11**, 100209.
157. Anacona, J. R.; Da Silva, G. Synthesis and antibacterial activity of cefotaxime metal complexes, *J Chilian Chemical Society* **2005**, *50*, 447-450.
158. Anacona, J. R.; Bravo, A.; Lopez, M. E. Antibacterial activity of Cefoperazone Metal Complexes. *Lat. Am. J. Pharm.* **2012**, *31*, 27-31.
159. Nleonu, E. C.; Nnaoma, I. E.; Ojiuko, I. A. Synthesis, characterization and antimicrobial studies of ciprofloxacin complexes with cobalt, copper and iron (II) ions. *World Journal of Pharmaceutical Research* **2020**, *9*(9), 36-43

160. Khalil, T. E.; El-Dissouky, A.; Al-Wahaib, D.; Abrar, N. M.; & El-Sayed, D. S. Synthesis, characterization, antimicrobial activity, 3D-QSAR, DFT, and molecular docking of some ciprofloxacin derivatives and their copper (II) complexes. *Applied Organometallic Chemistry* **2020**, *34*(12), 5998.
161. Sharfalddin, A. A.; Emwas, A. H.; Jaremko, M. and Hussien, M. A. Synthesis and theoretical calculations of metal-antibiotic chelation with thiamphenicol: in vitro DNA and HSA binding molecular docking and cytotoxicity studies. *New J. Chem.* **2021**, *45*(21), 9598-9613.
162. Islam, M. S.; Sikder, K. Y.; Hossain, A. M.; and Faroque, A. Study on the Pattern of Antibiotic Use Including the Resistance Episodes in Bangladesh. *Dhaka University Journal of Pharmaceutical Sciences* **2019**, *18*, 135.
163. Ware, D. C.; Brothers, P. J.; Clark, G. R.; Denny, W. A.; Palmer, B. D.; and Wilson, W. R. Synthesis, structures and hypoxia-selective cytotoxicity of cobalt(III) complexes containing tridentate amine and nitrogen mustard ligands. *J. Chem. Soc., Dalton Trans* **2000**, *6*, 925-932.
164. Iqbal, M. S.; Ahmed, A. R.; Sabir, M.; Asad S. M. Preparation, characterization and biological evaluation of copper(II) and zinc(II) complexes with cephalexin. *J Pharm Pharmacol* **1999**, *51*, 371–375.
165. Bauer, A.W.; Kirby, W. M.; Sherris, J. C.; Turck, M. Antibiotic susceptibility testing by a standardized single disk method. *American Journal of Clinical Pathology* **1966**, *45*(4), 493–496.
166. Barry, A. L.; Garcia, F.; Thrupp, L. D. An Improved Single-disk Method for Testing the Antibiotic Susceptibility of Rapidly-growing Pathogens, *American Journal of Clinical Pathology* **1970**, *53*(2), 49–158, <https://doi.org/10.1093/ajcp/53.2.149>
167. NCCLS. 2002. Performance Standards for Antimicrobial Disk and Dilution Susceptibility Tests for Bacteria Isolated from Animals;

Approved Standard-Second Edition. NCCLS document M31-A2 (ISBN 1-56238-461-9). NCCLS, 940 West Valley Road, Suite 1400, Wayne, Pennsylvania 19087-1898, USA.

168. Pratiwi, R. A.; Nandiyanto, A. B. D. How to read and interpret UV-VIS spectrophotometric results in determining the structure of chemical compounds, *Indonesian Journal of Educational Research and Technology* **2021**, 2 (1), 1-20.
169. Lever, A. B. P. (1984) *Inorganic Electronic Spectroscopy*, Elsevier, Amsterdam, The Netherlands, 2nd edition.
170. Ahmadi, R.A.; Hasanvand, F.; Bruno, G.;Rudbari, H. A.; Amani, S. "Synthesis, Spectroscopy, and Magnetic Characterization of Copper(II) and Cobalt(II) Complexes with 2-Amino-5-bromopyridine as Ligand", *International Scholarly Research Notices*, **2013**, 2013, 1-7. <https://doi.org/10.1155/2013/426712>
171. Khan, S. A.; Khan, S. B.; Khan, L. U.; Farooq, A.; Akhtar, K.; Asiri, A. M. (2018) Fourier Transform Infrared Spectroscopy: Fundamentals and Application in Functional Groups and Nanomaterials Characterization, Handbook of Materials Characterization, Springer International Publishing.
172. Anacona, J. R.; Alvarez, P. Synthesis and antibacterial activity of metal complexes of cefazolin. *Transition Met Chem* **2002**, 27, 856–860.
173. Anacona, J. R.; Rodriguez, J. R. Synthesis and antibacterial activity of cefalexin metal complexes. *Journal of Coordination Chemistry* 2004, 57, 1263–1269.
174. Konstantin, I.; Hadjiivanov, D. A.;Panayotov, M. Y.;Mihaylov, E. Z.; Ivanova, K. K.;Chakarova, S. M. A.; and Nikola L. D. Power of Infrared and Raman Spectroscopies to Characterize Metal-Organic Frameworks

- and Investigate Their Interaction with Guest Molecules, *Chemical Reviews* **2021**, *121* (3), 1286-1424. DOI: 10.1021/acs.chemrev.0c00487
175. Deacon, G.B. and Phillips, R.J. Relationships between the carbon-oxygen stretching frequencies of carboxylate complexes and the type of carboxylate coordination. *Chem. Rev.* **1980**, *33*, 227-250.
 176. Sultana, N.; Arayne, M.S. and Afzal, M. Synthesis and antibacterial activity of cephradine-metal complexes: Part I complexes with magnesium, calcium, chromium and manganese. *Pak. Journal of Pharmaceutical Science* **2003**, *16*, 59-72.
 177. Sultana, N.; Arayne, M. S. and Afzal, M. Synthesis and antibacterial activity of cephradine metal complexes: Part II complexes with cobalt, nickel, copper, zinc and cadmium. *Pak. J. Pharm. Sci.* **2005**, *18*, 36-42.
 178. Aly A. A. M; Osman, A. H.; Abo El-Maali, N., Al-Hazmi, G. A. A. Thermal and photochemical behavior of Zn(II) complexes of some cephalosporins. *J Therm Anal Calorim* **2004**, *75*, 159–168.
 179. Salekin, S., Sharmin, T. and Rahman, M.S. Synthesis, characterization and analgesic activity of cadmium(II) complex of tolfenamic acid. *Dhaka Univ. J. Pharm. Sci.* **2020**, *19*, 59-64.
 180. Tahia, F.; Sultan, M. Z.; Islam, M.; K.; and Rashid, M.A. Thermochemical properties and bioactivity of the metallic complexes of levofloxacin. *Asian J. Org. Med. Chem.* **2019**, *4*, 89-93.
 181. Badea, M.; Olar, R.; Marinescu, D.; Uivarosi, V.; Iacob, D. Thermal decomposition of some biologically active complexes of ruthenium (III) with quinolone derivatives. *Journal of Thermal Analysis and Calorimetry* **2009**, *97*, 735–739.
 182. Ali; S. I., Lei, Z. N.; Ali, M.; Kojima, K.; Ahmed, M.; Peng, R.; Yang, D.H., Haider, S. M.; Ayatollahi, S.A.M.; and Chen, Z.S. Metal(II)

- complexes of fluconazole: Thermal, XRD and cytotoxicity studies. *Iranian J. Pharm. Res.* **2020**, *19*, 171-182.
183. Kavitha, N. and Lakshmi, P.V.A. Synthesis, characterization and thermogravimetric analysis of Co(II), Ni(II), Cu(II) and Zn(II) complexes supported by ONNO tetradentate Schiff base ligand derived from hydrazinobenzoxazine. *J. Saudi Chem. Soc.* **2017**, *21*, S457-S466.
184. El-Tabl, A.S. Synthesis and characterization of Cobalt(II)/(III), Nickel(II) and Copper(II) complexes of new 14, 15 and 16-membered macrocyclic ligands. *Bull. Korean Chem. Soc.* **2004**, *25*, 1757-1763.
185. Zaman, R.; Rehman, W.; Hassan, M.; Khan, M. M.; Anjum, Z.; Shah, S. A. H.; Abbas, S. R. Synthesis, characterization and biological activities of cephalosporin metals complexes; *International Journal of Biosciences*, **2016**, *9(5)*, P163-172.
186. Chohan, Z. H. Synthesis of cobalt(II) and nickel(II) complexes of Cefaclor and preliminary experiments on their antibacterial character. *Chem Pharm Bull* **1991**, *39*, 1578–1580.
187. Bukhari, I. H.; Arif, M.; Akbar, J.; Khan, A. H. Preparation, characterization and Biological Evaluation of Schiff Base Transition Metal Complexes with Cephadrine. *Pakistan journal of Biological Sciences*, **2005**, *8*, 614-617. DOI: 10.3923/pjbs.2005.614.617
188. Tümer, M.; Köksal, H.; Sener, M.K. *et al.* Antimicrobial activity studies of the binuclear metal complexes derived from tridentate Schiff base ligands. *Transition Metal Chemistry* **1999**, *24*, 414–420. <https://doi.org/10.1023/A:1006973823926>
189. Patel, M.N.; Pansuriya, P.B.; Parmar, P.A. *et al.* Synthesis, characterization, and thermal and biocidal aspects of drug-based metal complexes. *Pharm Chem J* **2008**, *42*, 687–692. <https://doi.org/10.1007/s11094-009-0214-2>

190. Vinusha, H. M., Kollur, S. P.; Revanasiddappa, H. D.; Ramu, R.; Prithvi, S.; Shirahatti, M.N.; Prasad, N.; Chandrashekar, S.; Begum, M. Preparation, spectral characterization and biological applications of Schiff base ligand and its transition metal complexes, *Results in Chemistry* **2019**, *1*, 100012, <https://doi.org/10.1016/j.rechem.2019.100012>.
191. Kudrat-E-Zahan, M.; Islam, M.S. & Abul Bashar, M. Synthesis, characteristics, and antimicrobial activity of some complexes of Mn(II), Fe(III), Co(II), Ni(II), Cu(II), and Sb(III) containing bidentate Schiff base of SMDTC. *Russian Journal of General Chemistry* **2015**, *85*, 667–672. <https://doi.org/10.1134/S1070363215030238>
192. Tandon, N.; Tandon, R.; Gupta, R.; Gupta, N. Synthesis and antibacterial activities of metal complexes of ceftiofur, *Rasayan J. Chem.*, **2018**, *11(4)*, 1715-1720. <http://dx.doi.org/10.31788/RJC.2018.1144049>
193. Faraj, R. H.; Salih, S. I. Preparation, characterization and biological activity of some transition metal (II) complexes containing cephalixin and cefotaxime sodium, *Journal of University of Raparine* **2020**, *7(3)*, 1-17. <https://doi.org/10.26750/194>.
194. Nakamoto, K. (1986) *Infrared and Raman Spectra of Inorganic and Coordination Compounds*, 4th ed.; John Wiley: New York, NY, USA.
195. Al-Thubaiti, E.H.; El-Megharbel, S.M.; Albogami, B.; Hamza, R.Z. Synthesis, Spectroscopic, Chemical Characterizations, Anticancer Capacities against HepG-2, Antibacterial and Antioxidant Activities of Cefotaxime Metal Complexes with Ca(II), Cr(III), Zn(II), Cu(II) and Se(IV). *Antibiotics* **2022**, *11*, 967.
196. Pillai, S., PushpaLatha, S. Designing of some novel metallo antibiotics tuning biochemical behaviour towards therapeutics: Synthesis, characterisation and pharmacological studies of metal complexes of cefixime. *Journal of Saudi Chemical Society*, **2016**, *20*, S60-S66.

197. El-Megharbel, S.M.; Qahl, S.H.; Alaryani, F.S.; Hamza, R.Z. Synthesis, Spectroscopic Studies for Five New Mg (II), Fe (III), Cu (II), Zn (II) and Se (IV) Ceftriaxone Antibiotic Drug Complexes and Their Possible Hepatoprotective and Antioxidant Capacities. *Antibiotics* **2022**, *11*, 547. <https://doi.org/10.3390/antibiotics11050547>
198. Chaudhary, R. G.; Juneja, H. D.; Pagadala, R.; Gandhare, N. V.; Gharpure, M. P. Synthesis, characterisation and thermal degradation behaviour of some coordination polymers by using TG–DTG and DTA techniques. *Journal of Saudi Chemical Society* **2015**, *9(4)*, 442-453. <https://doi.org/10.1016/j.jscs.2014.06.002>.
199. Goo K.S.; Sim, T.S. Designing new β -lactams: implications from their targets, resistance factors and synthesizing enzymes. *Curr Comput Aided Drug Des.* **2011**, *7(1)*, 53-80. doi: 10.2174/157340911793743538.
200. Anacona, J. R.; Acosta, F. Synthesis and antibacterial activity of cephadrine metal complexes. *J.Coord. Chem.* **2005**, *59*, 621 – 627.
201. Auda, S.H.; Knütter, I.; Bretschneider, B.; Brandsch, M.; Mrestani, Y.; Große, C.; Neubert, R.H.H. Effect of Different Metal Ions on the Biological Properties of Cefadroxil. *Pharmaceuticals* **2009**, *2*, 184-193. <https://doi.org/10.3390/ph2030184>
202. Lever, A. B. P. (1986) *Inorganic electronic spectroscopy*. Amsterdam, London, New York: Elsevier; p. 454.
203. Bellamy, L. J. (1971) *The Infrared Spectra of Complexes Molecules*, 3rdEdn., John Wiley, New York.
204. Zayed, M. A; Abdallah, S. M. Synthesis, characterization and electronic spectra of cefadroxil complexes of d-block elements. *Spectrochim Acta Part A* **2004**, *60*, 2215–2224.
205. Anacona, J. R.; Gil, C. C. Synthesis and antibacterial activity of cefixime metal complexes. *Transition Met Chem* **2006**, *31*, 227–231.

206. Anacona, J. R.; Rodriguez, A. Synthesis and antibacterial activity of ceftriaxone metal complexes. *Transition Met Chem.* **2005**, *30*, 897–901.
207. Anacona, J.R.; Jose, S. Synthesis and antibacterial activity of metal complexes of cephalothin. *J Coord Chem.* **2003**, *56*, 313–320.
208. Patel, M. N.; Joshi, H. N.; Patel, C.R.; Patel, M. N. Cytotoxic, DNA binding, DNA cleavage and antibacterial studies of ruthenium–fluoroquinolone complexes. *Journal of Chemical Sciences* **2014**, *3*, 739.
209. Naglah, A. M.; Al-Omar, M. A.; Almehezia, A. A.; AlKahtani, H. M.; Bhat, M. A.; Al-Shakliah, N. S.; Belgacem, K.; Majrashi, B. M.; Refat, M. S.; Adam, A. M. A. Synthesis, thermogravimetric, and spectroscopic characterizations of three palladium metal (II) ofloxacin drug and amino acids mixed ligand complexes as advanced antimicrobial materials. *Journal of Molecular Structure* **2020**, *1225*, 129102.
210. Nakamoto, L. Infrared spectra of inorganic and coordination compounds. *J. Chem. Educ.* **1963**, *40*, 501.
211. Abd El-Halim, H.F.; Mohamed, G.G.; El-Dessouky, M.M.I.; Mahmoud, W.H. Ligational behaviour of lomefloxacin drug towards Cr(III), Mn(II), Fe(III), Co(II), Ni(II), Cu(II), Zn(II), Th(IV) and UO₂(VI) ions: Synthesis, structural characterization and biological activity studies. *Spectrochim. Acta A* **2011**, *82*, 8–19.
212. Sagdinc, S.; Bayari, S. Spectroscopic studies on the interaction of ofloxacin with metals. *J. Mol. Struct.* **2004**, *691*, 107–113.
213. Macias, B.; Villa, M.; Rubio, I.; Castineiras, A.; Borrás, J. Complexes of Ni (II) and Cu (II) with ofloxacin. Crystal structure of a new Cu (II) ofloxacin complex. *J. Inorg. Biochem.* **2001**, *84*, 163–170.
214. Xu, M.; Zhang, Y.-C.; Xu, Z.-H.; Zeng, Z.-Z. Crystal structure, biological studies of water-soluble rare earth metal complexes with an ofloxacin derivative. *Inorg. Chim. Acta* **2012**, *384*, 324–332.

215. Gouvea, L.R.; Garcia, L.S.; Lachter, D.R.; Nunes, P.R.; de Castro Pereira, F.; Silveira-Lacerda, E.P.; Louro, S.R.W. Barbeira, P.J.S.; Teixeira, L.R. Atypical fluoroquinolone gold(III) chelates as potential anticancer agents: Relevance of DNA and protein interactions for their mechanism of action. *Eur. J. Med. Chem.* **2012**, *55*, 67–73.
216. Efthimiadou, E.K.; Sanakis, Y.; Katsaros, N.; Karaliota, A.; Psomas G. Transition metal complexes with the quinolone antibacterial agent pipemidic acid: Synthesis, characterization and biological activity. *Polyhedron* **2007**, *26*, 1148–1158.
217. Gao, F.; Yang, P.; Xie, J.; Wang, H. Synthesis, characterization and antibacterial activity of novel Fe(III), Co(II), and Zn(II) complexes with norfloxacin. *J. Inorg. Biochem.* **1995**, *60*, 61–67.
218. Sadeek, S. A., & El-Shwiniy, W. H. Metal complexes of the fourth generation quinolone antimicrobial drug gatifloxacin: Synthesis, structure and biological evaluation. *Journal of Molecular Structure* **2010**, *977*(1-3), 243-253.
219. Efthimiadou, E.K.; Karaliota, A.; Psomas, G. Mononuclear metal complexes of the second-generation quinolone antibacterial agent enrofloxacin: Synthesis, structure, antibacterial activity and interaction with DNA. *Polyhedron* **2008**, *27*, 1729–1738.
220. Sultana, N.; Arayne, M.S.; Rizvi, S.B.S.; Haroon, U.; Mesaik, M.A. Synthesis, spectroscopic, and biological evaluation of some levofloxacin metal complexes. *Med. Chem. Res.* **2013**, *22*, 1371–1377.
221. Sadeek, S. A. Synthesis, thermogravimetric analysis, infrared, electronic and mass spectra of Mn (II), Co (II) and Fe (III) norfloxacin complexes. *Journal of Molecular Structure* **2005**, *753*(1-3), 1-12.
222. Azócar, M. I.; Gómez, G.; Levín, P.; Paez, M.; Muñoz, H. & Nicole Dinamarca, N. Review: Antibacterial behavior of carboxylate silver(I)

- complexes. *Journal of Coordination Chemistry* **2014**, *67*, 3840-3853.
DOI:10.1080/00958972.2014.974582
223. Zelenak, V.; Vargova, Z.; Gyoryova, K. Correlation of Infrared Spectra of Zinc(II) Carboxylates with Their Structures. *Spectrochim. Acta, Part A* **2007**, *66*, 262–272.
224. Anacona, J. R.; Toledo, C. Synthesis and antibacterial activity of metal complexes of ciprofloxacin. *Transition Metal Chemistry* 2001, *26*, 228–231. <https://doi.org/10.1023/A:1007154817081>
225. Tarushi, A.; Psomas, G.; Raptopoulou, C.P.; Kessissoglou, D.P. Zinc complexes of the antibacterial drug oxolinic acid: Structure and DNA-binding properties. *J. Inorg. Biochem.* **2009**, *103*, 898–905.
226. Arayne, S.; Sultana, N.; Haroon, U.; Mesaik, M.A. Synthesis, characterization, antibacterial and anti-inflammatory activities of enoxacin metal complexes. *Bioinorg. Chem. Appl.* **2009**, *2009*, 1-6. doi:10.1155/2009/914105.
227. Batista, D. G. J.; da Silva, P. B.; Stivanin, L.; Lachter, D. R.; Silva, R. S.; Felcman, J.; Louro, S. R. W.; Teixeira, L.R.; de Nazare C. Soeiro, M. Co(II), Mn(II) and Cu(II) complexes of fluoroquinolones: Synthesis, spectroscopical studies and biological evaluation against *Trypanosoma cruzi*. *Polyhedron* **2011**, *30*, 1718–1725.
228. Turel, I.; Šonc, A.; Zupančič, M.; Sepčić, K.; Turk, T. Biological activity of some magnesium(II) complexes of quinolones. *Met. Based Drugs* **2000**, *7*, 101–104.
229. Sadeek A.S., Abd El-Hamid S.M., El-Aasser M.M. Synthesis, characterization, antimicrobial and cytotoxicity studies of some transition metal complexes with gemifloxacin. *Monatsh Chem.* **2015**, *146*, 1967–1982. doi: 10.1007/s00706-015-1507-7.

230. Rusu, A.; Hancu, G.; Imre, S. Essential Guide of Analysis Methods Applied to Silver Complexes with Antibacterial Quinolones, *Adv Pharm Bull.* **2018**, 8(2), 181-189. doi: [10.15171/apb.2018.022](https://doi.org/10.15171/apb.2018.022)
231. Imran, M.; Iqbal, J.; Iqbal, S.; and Ijaz, N. *In vitro* antibacterial studies of ciprofloxacin-imines and their complexes with Cu(II), Ni(II), Co(II), and Zn(II), *Turkish Journal of Biology* **2007**, 31(2), 67–72.
232. Brown, M. E. (2004) Introduction to Thermal Analysis Techniques and Applications. New York: Kluwer Academic Publishers.
233. Debnath, A.; Mogha, N. K; Masram, D.T. Metal complex of the first-generation quinolone antimicrobial drug nalidixic acid: structure and its biological evaluation. *Appl Biochem Biotechnol* **2015**, 175(5), 2659-67. doi: [10.1007/s12010-014-1450-9](https://doi.org/10.1007/s12010-014-1450-9)
234. Giron, D. Application of thermal analysis coupled techniques in pharmaceutical. *J Therm Anal Calorim.* **2002**, 68, 335–57.
235. D. Giron, Applications of thermal analysis in the pharmaceutical industry. *Journal of Pharmaceutical and Biomedical Analysis* **1986**, 4(6), 755-770. [https://doi.org/10.1016/0731-7085\(86\)80086-3](https://doi.org/10.1016/0731-7085(86)80086-3).
236. Mohamed, G. G.; Nour El-Dien, F.A. & El-Gamel, N.E.A. Thermal Behaviour of Metal Complexes of 6-(2-Pyridylazo)-3-acetamidophenol. *Journal of Thermal Analysis and Calorimetry* 2002, 67, 135–146. <https://doi.org/10.1023/A:1013798100065>
237. Elshafie, H. S.; Sadeek, S. A.; Camele, I.; & Mohamed, A. A. Biochemical Characterization of New Gemifloxacin Schiff Base (GMFX-o-phdn) Metal Complexes and Evaluation of Their Antimicrobial Activity against Some Phyto- or Human Pathogens. *International Journal of Molecular Sciences* **2022**, 23(4), 2110.
238. Vogel, A. I (1987) Qualitative Inorganic analysis, 6thedn. Wiley, New York.

239. Frei, A.; Zuegg, J., Elliott, A. G.; Baker, M.; Braese, S.; Brown, C.; Chen, F.; Dowson, C.; Dujardin, G.; Jung, N.; King, A. P.; Mansour, A.M.; Massi, M.; Moat, J.; Mohamed, H.A.; Renfrew, A. K.; Rutledge, P. J.; Sadler, P.J.; Todd M. H; Willans, C. E.; Wilson, J. J.; Cooper, M. A; Blaskovich, M.A.T. Metal complexes as a promising source for new antibiotics. *Chem Sci.* **2020**, *11(10)*, 2627-2639. doi: 10.1039/c9sc06460e
240. Karges, J.; Stokes, R.W.; Cohen, S. M. Metal complexes for therapeutic applications. *Trends Chem.* **2021**, *3(7)*, 523-534. doi: 10.1016/j.trechm.2021.03.006.
241. Rossmore, H. W. (1991): In Disinfection, Sterilization and Preservation, 4th ed.; Block, S.S. Ed.; Lea and Febinger: Philadelphia, p 290,
242. Macias, B. S.; Martinez, C.M.; Sánchez, N. A.; Hurle, A.D. A physico-chemical study of the interaction of ciprofloxacin and ofloxacin with polivalent cations. *Int. J. Pharm.* **1994**, *106*, 229-235.

List of Publications

1. **Shuchismita Dey**, Md. Zakir Sultan and Md. Abdus Salam, Synthesis, Characterization of Ceftibuten-Copper(II) Complex and Prediction of Its Biological Activity. *Asian Journal of Chemistry*, **2021**, 33 (1), 190-194. <https://asianpubs.org/index.php/ajchem/article/view/15143>
2. **Shuchismita Dey**, Md. Zakir Sultan and Md. Abdus Salam, Nickel(II)-Complex of Ceftibuten Dihydrate: Synthesis, Characterization and Thermal Study. *Dhaka Univ. J. Pharm. Sci.* **2021**, 20(2), 219-225. DOI: <https://doi.org/10.3329/dujps.v20i2.57172>
3. **Shuchismita Dey**, Md. Zakir Sultan and Md. Abdus Salam. Essential Divalent Metal (Cu, Ni) Complexes of Gemifloxacin Mesylate: Synthesis, Spectral Characterization, Thermal Behavior and Biological Study, “In Preparation”.